Molecular distributions and hydrogen isotopic compositions of *n*-alkanes from field studies of tree species: applications for paleoclimate studies

Sarah Louise Newberry
September 2013

A thesis submitted to the School of Environmental Sciences
University of East Anglia
In partial fulfilment for the requirements for the degree of
Doctor of Philosophy

Abstract

The compound-specific δD values and molecular distributions of *n*-alkanes preserved in sediment archives are used as paleoclimate proxies. This use is based on two assumptions, 1) *n*-alkane δD values are highly correlated with source water δD values (Sachse 2012), and 2) the δD values of *n*-alkanes within a single site show little variation (Hou 2007). *n*-alkane molecular distributions are also used to infer the dominant source of *n*-alkanes input into sediment archives (Seki 2010). Despite this, paleoclimate reconstructions are being made without full understanding of how the δD values of *n*-alkanes relate to the D isotopic compositions of meteoric waters in the region of synthesis, or how variable *n*-alkanes δD values could be within a single species.

Using an in-depth investigation of Scots pine (*Pinus sylvestris*), significant variations in *n*-alkane molecular distributions and δD values were detected. These results suggest height of sample collection within a natural forest exerts a strong control on both *n*-alkane compositions, and δD values. Furthermore, this investigation indicates evergreen coniferous species synthesize both odd and even-chain-length *n*-alkanes, with high abundances of mid-chain *n*-alkanes, previously a diagnostic of aquatic plants. Both of these conclusions could significantly influence paleoclimate interpretations.

Moreover, *n*-alkane δD values from Scots pine and Salix indicate little control of xylem water δD values on *n*-alkane δD values, suggesting that *n*-alkanes synthesized during spring are more representative of D-enriched stored assimilates. In addition, this study suggests too favourable conditions for photosynthesis could lead to reduced D-enrichment of leaf water, which is subsequently imprinted on the δD values of *n*-alkanes. These data suggest that under-estimations of climatic conditions present during the synthesis of *n*-alkane in sediments could occur if *n*-alkanes from existing plants are synthesized during periods of climatic stress.

"We will not go quietly into the night! We will not vanish without a fight! We're going to live on, we're going to survive."

President Thomas Whitmore

July 4th, 1996

Independence Day (Roland Emmerich, 1996)

Table of contents

4. Water sourcing and leaf water isotopic enrichment of natural Scots pine forests

5. Hydrogen isotopic analysis of *n*-alkanes in Scots pine; variations and fractionations from waters

7. *n*-alkanes *δ*D values; applications for paleoclimate studies and conclusions

List of Figures

List of tables

Acronyms and abbreviations

ACL	Average Chain Length
ACP	Acyl Carrier Protein
ANOVA	Analysis of Variance
BWR	Black Wood of Rannoch
CAM	Crassulacean Acid Metabolism
CPI	Carbon Preference Index
CWMA	Concentration Weighted Mean Alkane
DM	Dried Mass
FAE	Fatty Acid Elongases
FAS	Fatty Acid Synthases
GC-FID	Gas Chromatography- Flame Ionisation Detector
GC-IRMS	Gas Chromatography- Isotope Ratio Mass Spectrometer
GISP	Greenland Ice Sheet Precipitation
GMWL	Global Meteoric Water Line
IAEA	International Atomic Energy Agency
LN_2	Liquid Nitrogen
MAP	Mean Annual Precipitation
Mg	Milligrams
Mv	Millivolts
NADPH	Nicotinamide Adenine Dinucleotide Phosphate
NTW	Norwich Tap Water
PAR	Photosynthetically Active Radiation
PEP	Phosphoenolpyruvate carboxylase
PTV	Programmable temperature vaporization
OIPC	Online Isotopes in Precipitation Calculator
RH	Relative Humidity
Rubisco	Ribulose-1,5-bisophate carboxylase oxygenase
SEM	Standard Error of the Mean
SIL	Stable Isotope Laboratory
SLAP	Standard Light Antarctic Precipitation
Stdev	Standard deviation
TLE	Total Lipid Extract
UEA	the University of East Anglia
VLCFA	Very Long Chained Fatty Acid
VPDB	Vienna Pee Dee Belemnite
VSMOW	Vienna Standard Mean Ocean Water

VSN	Värriö Strict Nature Reserve
WUE	Water Use Efficiency
ε_{app}	Apparent fractionation
ε_{bio}	Biosynthetic fractionation
ΔD Leaf water	Fractionation of leaf water above xylem water
µg	Microgram
µl	Microliter

Acknowledgements

If I was to thank every person that helped me during my PhD, I worry that my acknowledgements would be just as long as my thesis, so I am sorry to those that are not mentioned.

First, I would like to thank Paul Disdle and Paul Dennis, the support I received academically and emotionally from the both of you was the only reason I was able to persevere with my PhD and finish. I will forever be grateful to you both. I would also like to thank Alastair Grant, who may have only come onto my committee during my final year, but was crucial in helping me interpret my data and write up my thesis, without your input I would not have got very far. I would also like to thank Nikolai Pedentchouk for giving me the PhD position at UEA, commenting on my chapters, and giving me the motivation to make my PhD the best it could possibly be. In addition, I would like to thank Anne Grant for all the help and support I received while resolving my PhD issues.

I am a very lucky person to be blessed with so many amazing and supportive friends and I would like to thank Christy for always being there for me and putting up with my frantic phone calls. Christy you are a legend, if you ever need a kidney just give me a call! I would also like to thank Gemma and Lauren for helping me with my fieldwork in Rannoch, you guys gave up your time to help me get samples, without you both I would have no data. I would also like to thank the rest of the Edinburgh crew and the Ireland crew for the banter and support over the years.

I have many friends at UEA that helped me through the problems I encountered during my time here and I would like to thank them all, but a special few deserve honourable mentions. For your support and banter, I would to thank Jenny "ninja" Graham, Christopher-Walker Brown, Sam Royle, Ruth Kirk, Christopher Roberts, Imke Grefe, Christopher Steele, Letty Wickes, Amy Binner, Ben Mills, Phil Underwood, Katy Owen, Alina Mihailova, Yvette Eley, Neill MacKay and Chris Adams- all of you are particularly amazing!

Finally, I would like to thank my family for their support through the ups and downs that were my time here at UEA. My grandma Connie Whelan, always there whenever I need some perspective and wisdom, granny Ida for her amazing cooking and aunty Jacqui for the supportive chats. My Mum and Dad for trying to understand what I was talking about and Jesus Joe, for, well, being Jesus Joe and my boyfriend Matt for getting me through the write up.

I have learnt many things about the world and myself during the four years it took me to write this thesis. I never realised I had such strength and it has taught me to stick to your guns when you know you are right. And, in the words of Alan Partridge "Needless to say, I had the last laugh".

1. Introduction

1.1 Overview

The research presented within the following thesis uses in-depth temporal, spatial, and geographical analysis of individual tree species to determine the level of heterogeneity present in the molecular compositions and δD values of *n*-alkanes within leaf epicuticular wax of forest ecosystems, and how these could influence paleo-environmental reconstructions. In recent times the potential to use *n*-alkanes, synthesised by modern terrestrial vegetation, to make inferences regarding environments of the past has come under intense scrutiny. The very nature of how *n*-alkanes are synthesized, and their specific chemical characteristics, leads to these compounds accumulating in sediment archives across the globe, carrying with them an isotopic signal that is preserved from the moment of biosynthesis.

To date *n*-alkane molecular chain length distribution data is used to infer the dominant source of *n*-alkanes input into a sediment archive (Schwark, Zink et al. 2002, Polissar and Freeman 2010, Seki, Nakatsuka et al. 2010). While the compound-specific hydrogen isotopic compositions are used to make estimations of a plethora of environmental characteristics of the past, including climatic conditions (Rao et al, 2009; Zech et al, 2009; Hren et al 2010), previous vegetation structures (Schwark, Zink et al. 2002, Jansen, Haussmann et al. 2008, Castañeda, Werne et al. 2009, Russell, McCoy et al. 2009), and even altitude (Jia, Wei et al. 2008, Jahren, Byrne et al. 2009, Polissar, Freeman et al. 2009). Despite this, using *n*-alkanes as a paleo-environmental proxy is still in a certain degree of infancy, with many attempts to identify the key processes involved in influencing hydrogen isotopic compositions of *n*-alkanes in living vegetation producing conflicting results. It has therefore become increasingly clear, there are still several issues associated with the basic assumptions of how these compounds are synthesized within living terrestrial vegetation that require investigation.

Most publications to date appear to agree, suggesting the δD values of *n*-alkanes generally mirror those expressed by the regions meteoric water and precipitation δD values over global scales (Sachse 2006, Eglinton 2008, Liu and Yang 2008, Rao 2009, Sachse 2012). However these correlations are based upon crucial assumptions, firstly the δD values of *n*-alkanes synthesized by terrestrial plant species record the region of

synthesis' meteoric water signal with high fidelity (Sachse 2012). Second, the δD values presented by *n*-alkanes within a single site show little variation (Hou 2007), and third, the fractionation of *n*-alkanes above source waters (ε_{app}) is constant for a given species (Tierney, Russell et al. 2008, Polissar, Freeman et al. 2009, Castañeda and Schouten 2011). Therefore, if the hydrogen isotopic composition of *n*-alkanes exhibit significant variation for a single species, at a single site, and ε_{app} is neither constant, nor easily explained, this could cause significant problems for the use of *n*-alkane hydrogen isotopic compositions in paleoclimate reconstructions.

It is already known there are several issues associated with these assumptions. Firstly, research has demonstrated *n*-alkane δD values can be highly variable at a single site (Chikaraishi 2003), and that ε_{app} is certainly not constant across all plant species (Chikaraishi 2003, Liu, Yang et al. 2006, Smith 2006, Liu and Yang 2008, Feakins 2010, Sachse 2012). Furthermore, when the correlations between source water D isotopic compositions and *n*-alkane D isotopic compositions are investigated over smaller spatial scales, they become difficult to relate (Sachse 2009, Sachse 2012). The current problems are identifying how much ε_{app} can vary, and ascertaining what is driving the observed variations in similar plant types at the same location. What is also of concern is it would appear no investigations have conducted an in-depth study of within, and between individual trees of the same species temporally, spatially, and geographically, in conjunction with complete leaf water- xylem water- *n*-alkane D isotopic analyses. Without a study such as this, it is currently impossible to determine how much *n*-alkanes may vary isotopically, as well as in their molecular distributions, within single species. In addition, if any variations detected are greater than the thresholds currently applied in paleo-environmental reconstructions, the variations in δD values within a single individual could overwhelm any signals input into sediment archives.

1.2 Aims and Objectives

The aim of the thesis presented here is to determine the level of molecular distributional and D isotopic heterogeneity present within leaf epicuticular wax *n*-alkanes synthesized by natural forest ecosystems, and how these could influence paleo-environmental reconstructions. Focus falls on how *n*-alkane D isotopic compositions relate to the D isotopic compositions of leaf waters, xylem waters and local meteoric waters. Extensive *n*-alkane abundance and molecular distributional data is also presented to test the diagnostic thresholds applied in the identification of *n*-alkanes within sediment archives. This study represents the first in-depth investigation into the variation of *n*-alkanes across gradients of to 20m in height within, and between, individual trees of the same species in natural environments.

The main objectives are as follows:

1. To determine the level of variation in the molecular distributions of *n*-alkanes over spatial and temporal time scales, how these relate to climatic parameters, and the implications this could have for paleo-environmental reconstructions.

2. To determine the level of variation in the compound-specific D isotopic compositions of *n*-alkanes within, and between, individuals of the same species inhabiting natural forest ecosystems.

3. To examine how the D isotopic compositions of *n*-alkanes are related to both leaf water and xylem water D isotopic compositions, temporally and spatially, in the same species.

4. To identify which hydrogen isotopic source is best represented by *n*-alkanes synthesized in natural forest ecosystems.

5. To ascertain whether the D isotopic compositions of *n*-alkanes are "locked in" at the start of the growth season, and whether leaf water-lipid apparent fractionation factors remain constant over time.

6. Apply the knowledge gained from the data generated within this thesis to that of the current accepted methodologies applied in paleo-environmental studies, and then make recommendations for future research in this area.

1.3 Thesis structure

Chapter 1 gives a general overview of the research conducted within this thesis, providing details of the basic premise of the research, and the fundamental aims and objectives of the project.

Chapter 2 provides the background information relating to the project in general terms, giving details of the isotopic theory that relates to the use of compound-specific D isotopic analyses of leaf wax *n*-alkanes, as well as their abundance and molecular distributions in part 1. Part 2 outlines the methodology used in the current thesis, providing details of the sample sites, sample collection protocols, as well as sample preparation and analyses.

Chapter 3 gives details of an in-depth study of the total abundance and molecular distributions of *n*-alkanes present within, and between, different individuals of Scots pine (*Pinus sylvestris*) with time in both Finnish Lapland and Perthshire, Scotland. The chapter focuses on how variations in microclimate, driven by foliar position within individual trees, influence the *n*-alkanes, and how this varies geographically and temporally.

Chapter 4 describes the meteoric water- plant source water -leaf water relations of the Finnish and Scottish sample sites, within and between the same individuals of Scots pine studied in chapter 3. This chapter is primarily concerned with aiding the interpretations of the compound-specific D isotopic *n*-alkane data presented in the following chapter 5.

Chapter 5 provides the results from compound-specific hydrogen isotopic analyses of *n*-alkanes, synthesised within and between, different sized individuals of Scots pine. The results are discussed in terms of the hydrogen isotopic water data presented in chapter 4, and make inferences regarding the hydrogen isotopic signals that are imprinted on *n*-alkanes of Scots pine, and how these vary in relation to climate.

Chapter 6 outlines a small investigation conducted on a *Salix* (willow) species on the edge of a small lake at UEA, Norwich, UK. This chapter investigates the temporal variation in *n*-alkane abundance, molecular distributions and compound-specific hydrogen isotopic compositions over the course of a growing season. This data is then used in conjunction with water D isotopic compositions and a $\delta^{18}O$ - $\delta^{13}C$ conceptual model to identify how the *n*-alkanes vary with time.

Chapter 7 describes the use of *n*-alkanes in paleo-climate reconstructions and discusses the findings of chapters 3, 4, 5, and 6 with respect to these. This chapter also makes recommendations for future research in this area, as well as outlining the conclusions of this thesis.

2. Compound-specific molecular and δD isotopic analysis of *n*-alkanes in modern terrestrial vegetation: Scientific background and methodology

2.1. Introduction and scope

n-alkanes stand apart from other compounds in sediment records because of their unique chemical properties. They are one of the most abundant, easy to find, easy to extract and purify, molecules preserved in sediments (Cranwell, Eglinton et al. 1987, Sternberg 1988, Poynter, Farrimond et al. 1989, Schimmelmann, Lewan et al. 1999, Eglinton 2008). These compounds consist of saturated hydrocarbon chains (of varying length), with all hydrogen atoms covalently bound to carbon atoms. This results in the hydrogen atoms exchanging with the surrounding environment at much slower rates than other organic compounds (Schimmelmann, Lewan et al. 1999). As a direct result of these chemical characteristics, the longer chain homologues of *n*-alkanes are highly stable, insoluble in water, chemically inert, and display almost no volatility. This allows them to remain intact over significant geological time periods. They will only suffer degradation by high temperatures, radical attack, or highly specific enzymes (Schimmelmann, Lewan et al. 1999, Smith 2006, Eglinton 2008, Polissar, Freeman et al. 2009). In addition, the *n*-alkanes are one of the most abundant lipid molecules synthesized by all plants, algal species, and bacteria (Schimmelmann, Lewan et al. 1999, Chikaraishi 2003, Sachse, Radke et al. 2004, Smith 2006, Sachse 2012).

It is not only the *n*-alkane's resistance to degradation and their sheer abundance that makes them ideal biomarkers. In terrestrial vascular plants, the very nature of how they are synthesized during growth adds to their use. Leaf waxes are critical in the basic functioning of photosynthesis, which results in their biosynthesis, abundance, and composition being an actively regulated process (Post-Beittenmiller 1996). In the last ten years significant amounts of research have gone into understanding what drives the *n*-alkane hydrogen isotopic compositions of modern terrestrial plants to make inferences regarding the climate, vegetation structure, and even the altitude of the past (Chikaraishi and Naraoka 2001). To date, researchers are using the compound-specific hydrogen (δD)

and carbon ($δ^{13}$C) stable isotope compositions, in conjunction with *n*-alkane concentration, and molecular distributions to facilitate this.

2.1.1 *n*-alkanes as a paleoclimate proxy

The use of the hydrogen isotopic compositions of *n*-alkanes as a paleoclimate proxy is based upon two critical assumptions: 1) The compound-specific $δD$ values of *n*-alkanes synthesized by terrestrial plant species are highly correlated to the study region's meteoric water $δD$ values (Sachse 2012). 2) The $δD$ values presented by *n*-alkanes within a single site must show little variation (Hou 2007), and any variability observed must be easily interpreted. Most publications to date appear to agree and suggest that the $δD$ values of *n*-alkanes generally mirror those expressed by the regions meteoric water, with a strong linear positive correlation (figure 2.1) (Sachse 2006, Eglinton 2008, Hou 2008, Liu and Yang 2008, Rao 2009, Sachse 2012).
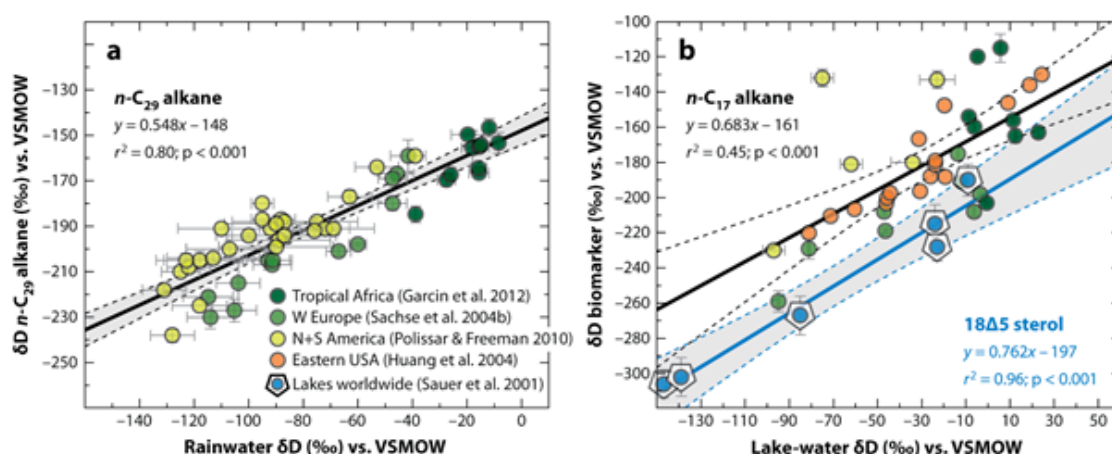
Figure 2.1: Taken from Sachse et al., (2012), showing the strong linear positive correlations between rainwater $δD$ is plot (a) and *n*C$_{29}$ *n*-alkane and *n*C$_{17}$ and lake water in plot (b) for several different species of plant across the globe and the "strong linear correlation" of this relationship.

As research suggests *n*-alkanes are synthesized from water within the leaves (Chikaraishi and Naraoka 2001, Chikaraishi, Naraoka et al. 2004), and because plants obtain this water for growth and biosynthesis, in most cases, from direct absorption from the soil (Dawson, Mambelli et al. 2002). It seems reasonable to assume that variations in the hydrogen isotopic composition of precipitation could be the driving cause of variations in *n*-alkane hydrogen isotopic composition (Sachse 2012). However, as shown in figure 2.1, this strong positive linear correlation does not hold across all samples, with some data points deviating from the linear regression line. This suggests the relationship is not as strong as stated. In addition, the data plotted in figure 2.1 (a) represents *n*-alkanes extracted from sediment archives globally, not *n*-alkanes from modern vegetation.

Therefore the relationship between xylem water, leaf water, and *n*-alkane *δ*D values are not described within this.

Earlier works commonly used *n*-alkanes from sediment archives, and then compared their *δ*D values to that of precipitation. After which, they suggested the *δ*D values of *n*-alkanes synthesized by all modern terrestrial plants track the *δ*D values of precipitation at relatively constant fractionation factors (apparent fractionation, ε_{app}) (Sachse, Radke et al. 2004, Sachse 2006). For example, Schfeß et al (2005) used a ~20 ‰ D-enrichment of the *n*C_{29} alkane extracted from marine sediment archives to infer a period of aridification in equatorial Africa during the Younger Dryas period (Pedentchouk 2008). However, investigation into the signals observed in modern vegetation have suggested that ecosystem and plant physiological processes are not so simple, and when these relationships are investigated over smaller spatial scales, they become much more complex (Sachse 2009, Sachse 2012).

As a constant-averaged ε_{app}, empirically derived from modern living plants, is used in paleo-climatological reconstructions of meteoric water D isotopic composition from *n*-alkanes preserved in ancient sediments around the globe (Yang 2009). The current problem is identifying how much ε_{app} can vary, and ascertaining what is driving the observed variations in similar plant types. It is suggested variations in plant physiology (Hou 2007, Kahmen, Hoffmann et al. 2013, Kahmen, Schefuß et al. 2013), variations in micro-climatic factors (Sachse 2012), or an undetermined combination of both, could have significant effects. Significant inter- and intra-specific variations in the *δ*D values of *n*-alkanes have already been reported, across both temporal and spatial scales; The same publications that have reported significant variations in *n*-alkane *δ*D values have also reported a strong linear relationship between the *δ*D values of the lipids, and that of plant source water (Chikaraishi 2003, Sachse 2006, Hou 2007, Yang 2009). For example, variability of up to ~90 ‰ *δ*D in *n*C_{29}, between different C_3 angiosperms, growing in the same location, has been reported (Chikaraishi 2003).

In recent times, it is becoming clear that addressing the issues of how *n*-alkane *δ*D values relate to those of local meteoric waters cannot be properly investigated without full xylem water – leaf water – *n*-alkane *δ*D isotopic analysis (Sachse 2012, Kahmen, Hoffmann et al. 2013, Kahmen, Schefuß et al. 2013, Tipple 2013). This is due to the observation of large variations in the *δ*D values of *n*-alkanes across a large transect in Australia, when source water isotopic compositions remained relatively constant (Kahmen, Hoffmann et al. 2013). Therefore, recent investigations conducted on living plants suggest that the *δ*D

values of *n*-alkanes are much more complex than initially thought; Where different species, in different geographical locations, may produce *n*-alkanes that carry δD values from completely different sources.

Further to this, when, how often, and from which hydrogen source the biosynthesis of *n*-alkanes occurs is a highly contentious issue. Earlier research suggests *n*-alkanes are continuously synthesized throughout the duration of the growing season (Lockheart, Van Bergen et al. 1997). Where they are synthesised using hydrogen from current leaf waters, which have D isotopic compositions that are enriched through evapotranspiration, in relation to that of soil water D isotopic compositions; therefore, recording seasonal changes in precipitation D isotopic composition, and climate driven seasonal variations of leaf water δD values with time (Pedentchouk 2008, Sachse 2009). These conclusions were drawn because D-depletion in *n*-alkanes has been observed from the beginning of the growing season, in the new spring foliage, to the end of the growing season in autumn (Chikaraishi, Naraoka et al. 2004, Brandes, Wenninger et al. 2007, Pedentchouk 2008). However, more recent publications have suggested the *n*-alkane δD values are "locked in" at the beginning of the growth season, and change very little once leaf expansion has ceased (Sachse 2010, Kahmen 2011, Tipple 2013); where the term "locked in" describes the process where the *n*-alkane D-isotopic composition remains stable for the remainder of the growing season once leaf growth and expansion has ceased after the initial period of leaf flush in spring (Sachse 2010, Kahmen 2011). These debates within current research can significantly influence how *n*-alkanes are interpreted from sediment archives. As how often, and from which hydrogen source *n*-alkanes are synthesized from will significantly influence which δD value is recorded. I.e., if *n*-alkanes represent the D isotopic composition of only spring precipitation, or if *n*-alkanes represent an entire growth season integrated D isotopic composition precipitation signal.

It has therefore become apparent that constraining ε_{app}, within a single species, to improve their use as a paleo-environmental proxy, cannot be achieved without in-depth analyses of the hydrogen isotopic compositions of environmental water-source water-leaf water-*n*-alkanes in future investigations (Sachse 2012). As a result of this, the fractionation of *n*-alkanes above leaf waters (termed biosynthetic fractionation, ε_{bio}), is becoming the focus of much research, with increasing evidence suggesting the levels of leaf water D-enrichment could be just as important as the isotopic signal of source waters (Sachse 2006, Smith 2006, Feakins 2010, Sachse 2010, McInerney 2011, Kahmen, Hoffmann et al. 2013, Kahmen, Schefuß et al. 2013). While variations in the δD values of *n*-alkanes from individual plants have been investigated, little information exists about variations

within an entire forest stand over a growing season; complete with in-depth investigation of the variation within and between individuals of the same species of varying age, a signal that would be much more comparable to a sedimentary record than an individual plant (Sachse 2009). Further to this, although a considerable amount of research has already been conducted, it is currently unknown exactly when, how often, and from which δD source n-alkanes are synthesized from in modern plants (Sachse 2010, McInerney 2011, Sachse 2012, Tipple 2013). Moreover, although n-alkanes are already being used in paleoclimate reconstructions, it is currently unknown which δD signal is imprinted on n-alkanes for the vast majority of modern species, how important leaf water evapotranspirational D-enrichment is in determining n-alkane δD compositions, and whether n-alkanes significantly vary within natural forest stands. Until these issues are fully addressed, significant errors in paleoclimate reconstructions will be made.

To this end, the following chapter will set out the necessary scientific basis and background information for the understanding of the current investigation. This investigation seeks to add more insights into how n-alkanes vary in their abundance, molecular distributions, and compound-specific D isotopic compositions; how these relate to the δD compositions of source water (xylem water) and leaf water, and how these relationships change over time.

2.1.2 Epicuticular leaf wax lipids

The epicuticular leaf wax lipids coat the outer-most part of the leaves of all living modern terrestrial vegetation, serving as protection against environmental stresses (Shepherd and Griffiths 2006). The leaf wax lipids undoubtedly serve to preserve water balance within the plant, and their other protective functions may include minimizing mechanical damage to leaf cells, inhibiting fungal attack, and scattering incoming solar radiation (Eglinton 1967, Post-Beittenmiller 1996, Hietala, Mozes et al. 1997, Shepherd and Griffiths 2006), as well as allowing self-cleaning of the leaves (Barthlott 1990). As a direct result of the epicuticular leaf wax lipids' critical importance in the basic functioning of photosynthetic assimilation, their biosynthesis, abundance, and composition is an actively regulated process (Post-Beittenmiller 1996). The composition and abundance of foliar wax varies from species to species, plant to plant, and even within different organs of the same individual; in conjunction with their stage of development (Eglinton 1967, Dove, Mayes et al. 1996, Post-Beittenmiller 1996, Tipple 2013).

The epicuticular leaf wax lipids are primarily composed of varying combinations of straight-chained *n*-alkanes, fatty acids, alcohols, aldehydes, ketones, esters, triterpenes, sterols, and flavonoids (Kolattukudy 1980, Walton 1990, Kunst and Samuels 2003, Eglinton 2008). The amount of epicuticular wax varies greatly between species, but can be sizeable; it may account for up to 4% green weight of a leaf, and up to 15% dried weight (Eglinton 1967). Of particular interest to plant physiologists and geochemists alike are the *n*-alkanes. Not only are these compounds present in all terrestrial plants (Vogts, Moossen et al. 2009), they are also the products of diagenesis, and highly abundant in algal and bacterial species (Chikaraishi 2003, Eglinton 2008, Sachse 2012).

2.1.2.1 The *n*-alkanes

The *n*-alkanes ($CH_3(CH_2)_nCH_3$) are classed as hydrocarbons as they are composed of hydrogen atoms covalently bound to carbon atoms, in straight chains of 18 to 36 carbons in length (Post-Beittenmiller 1996, Schimmelmann, Lewan et al. 1999, Smith 2006).
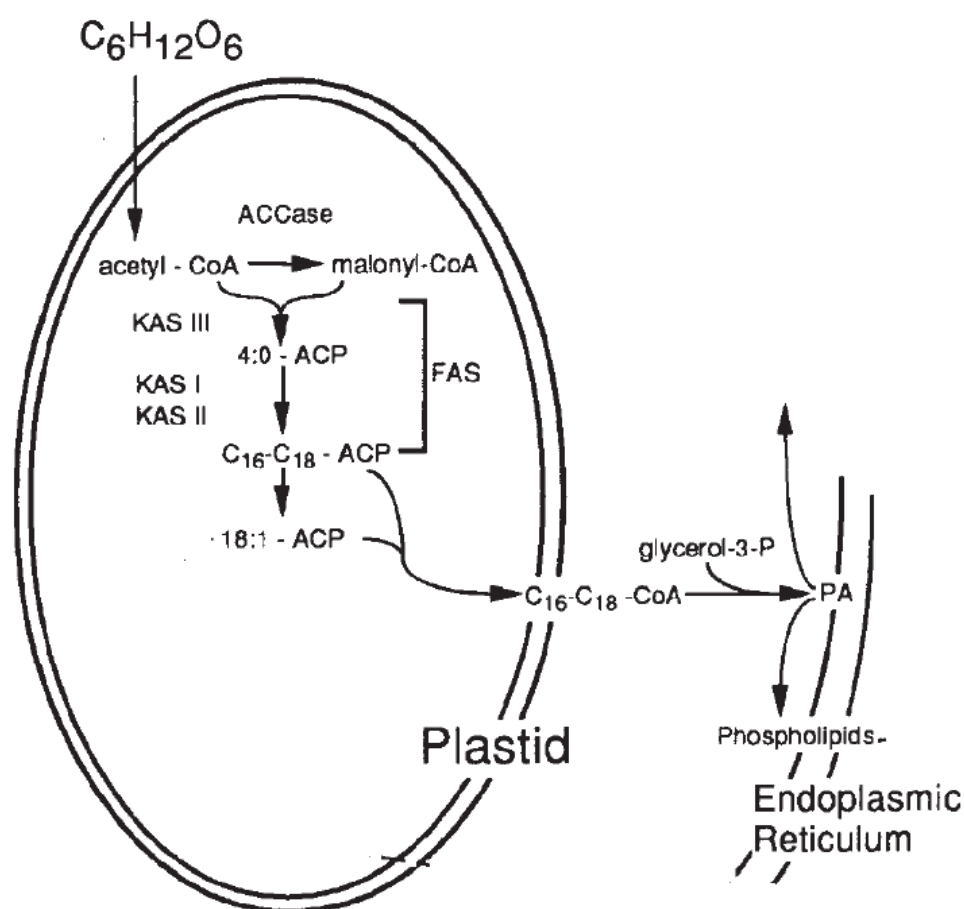
Figure 2.2: A schematic of the processes of *n*-alkane biosynthesis taken and edited from Ohlrogge and Jaworski (1997).

n-alkanes are synthesized via the acetogenic pathway from fatty acid precursors, which themselves are synthesized *de novo* in the plastids (Sessions 1999, Eglinton 2008, Sachse 2012) (figure 2.2). *De novo* fatty acid synthesis begins with the condensation of a malonyl-acyl carrier protein (ACP) with acetyl-CoA, with the subsequent reduction of 3-Ketoacyl-ACP, the dehydration of 3-hydroxyacyl-ACP, and the reduction of Δ^2(E)-2-3—enoyl acyl-ACP. The enzymes that catalyse fatty acid synthesis are packed together in a complex called fatty acid synthase (FAS) (von Wettstein-Knowles 1995, Post-Beittenmiller 1996, Shepherd and Griffiths 2006, von Wettstein-Knowles 2012).

This process of condensation and reduction is repeated, adding two carbons at a time, until C_{16} (Palmitic acid) is produced. This is then transported to the endoplasmic reticulum, where further chain elongation processes occur through Fatty Acid Elongases (FAEs) using NADPH as the reducing agent (Zhang, Gillespie et al. 2009). Each chain elongation cycle produces a two-carbon addition, resulting in multiple elongation cycles to produce fatty acids of longer chain length, termed Very Long Chained Fatty Acids (VLCFA). Typically the VLCFAs lose one carbon through decarbonylation to become *n*-alkanes, a process which is well established, but not very well understood (von Wettstein-Knowles 1995, Post-Beittenmiller 1996, Samuels, Kunst et al. 2008, von Wettstein-Knowles 2012). Due to the loss of one carbon during the fatty acid decarbonylation process, *n*-alkanes typically exhibit an odd-carbon number predominance (Eglinton 2008). This odd-carbon numbered dominance is considered characteristic of *n*-alkanes synthesized by higher terrestrial vascular plants (Cranwell 1982, Jeng 2006), and is often used to distinguish between *n*-alkanes of terrestrial plant origin and those of bacterial and diagenetic origins (Meyers and Ishiwatari 1995, Eglinton 2008).

2.1.2.2 *n*-alkane molecular distributions

Aside from the direct comparison of total *n*-alkane concentrations, there are a number of techniques to quantify the abundance, and distribution, of *n*-alkanes within any sample. Once extraction and analysis has been completed, these are used to infer the major source of *n*-alkanes input into a particular sediment archive (Seki, Meyers et al. 2009). These take the form of calculated formulae, which give a quantitative value describing some specific aspect of the molecular distribution of *n*-alkanes present within a specific sample; this facilitates comparison between different samples and/or different sites. In terms of the current thesis, and due to the nature of the plants under investigation, focus falls upon the Carbon Preference Index (CPI), and the Average Chain Length (ACL) only.

The Carbon Preference Index (CPI), is calculated from equation 2.1 (Allan 1977, Marzi, Torkelson et al. 1993), and describes the odd/even predominance of the carbon number range, this is most applicable in paleoclimate reconstructions.

$$\text{CPI}_{C_{21}-C_{32}} = [(C_{21} - c_{31})_{odd} + (C_{23} - C_{33})_{odd}]/[2 * (C_{22} - C_{32})_{even}]$$

(2.1)

Where $(C_{21}-C_{31})_{odd}$ and $(C_{23}-C_{33})_{odd}$ are the measured abundances of only the odd numbered *n*-alkanes detected within the subscript range, while $(C_{22}-C_{32})_{even}$ represents the measured abundances of only the even-numbered *n*-alkanes detected within the described subscript range. CPI ratios were traditionally used to quantify the level of lipid diagenesis in sediment archives (Meyers and Ishiwatari 1995). However, in more recent times they are used to infer the general source of *n*-alkanes within sediment, and whether significant petrogenic contamination is present (Vogts, Moossen et al. 2009, Vogts, Schefuß et al. 2012). For example, it is widely reported that hydrocarbons of terrestrial vascular land plant origin exhibit a high odd-to-even predominance (OEP) of long-chains (Gearing, Gearing et al. 1976, Farrington and Tripp 1977, Cranwell 1982), typically resulting in CPI ratios greater than 5 (Rielley, Collier et al. 1991, J.I. Hedges 1993, Bi, Sheng et al. 2005, Vogts, Moossen et al. 2009, Vogts, Schefuß et al. 2012). Whereas *n*-alkanes thought to originate from petrogenic contamination, diagenesis, bacterial sources, marine microorganisms, or recycled organic matter, are suggested to display CPI ratios closer to, or less than 3 (Farrington and Tripp 1977, Nishimura and Baker 1986, Jeng 2006, Eglinton 2008).

The second, and most widely applied quantification method to plant physiological and paleoclimate reconstruction studies, is that of Average Chain Length (ACL). This describes the weight-average number of carbon atoms per molecule, equation 2.2 (Poynter 1991).

$$ACL_{C_{21}-C_{33}} =$$
$$\frac{21(nC_{21}) + 22(nC_{22}) + 23(nC_{23}) + 24(nC_{24}) + 25(nC_{25}) + 26(nC_{26}) + 27(nC_{27}) + 28(nC_{28}) + 29(nC_{29}) + 30(nC_{30}) + 31(nC_{31})}{nC_{21} + nC_{22} + nC_{23} + nC_{24} + nC_{25} + nC_{26} + nC_{27} + nC_{28} + nC_{29} + nC_{30} + nC_{31}}$$

(2.2)

Vegetation type is considered to be the dominating influence on ACLs (Cranwell 1973), which has led to specific ranges in ACL ratios being applied as a diagnostic of *n*-alkane source (Seki, Nakatsuka et al. 2010). For example, ACLs less than nC_{20} are indicative of significant bacterial and algal input (Polissar and Freeman 2010), ACLs nC_{20} to nC_{23} suggest significant submerged aquatic plant input, nC_{23} to nC_{25} suggest floating aquatic plants (Ficken, Li et al. 2000, Zech 2009), while nC_{27} to nC_{29} are derived from trees and

shrubs, and nC_{31} and above suggest significant grass inputs (Cranwell 1973, Michener and Lajtha 2008, Zech 2009). However, plant physiological research indicates that it may not necessarily be the variation as a result of species, but rather the prevailing environmental conditions of ecosystems that result in the differences observed. Research suggests temperature, relative humidity (RH), and incoming photosynthetically active radiation (PAR) can influence wax composition (Shepherd and Griffiths 2006). For example, studies have indicated that longer *n*-alkane chain homologues are produced in higher concentrations in warmer climates (Poynter, Farrimond et al. 1989, Castañeda, Werne et al. 2009). This may be because molecular studies have shown higher ACL in conjunction with narrower chain ranges may have higher melting points, resulting in the leaf wax maintaining it's crystalline structure at higher temperatures (Riederer and Schneider 1990). Yet, as light intensity, and stimulation by light, is indicated as a key process in the *de novo* synthesis of leaf wax lipids (Shepherd and Griffiths 2006), the level of incoming PAR can also have a profound effect on the compositions of *n*-alkanes.

Earlier works (Giese 1975; Shepherd 1995, 1997) suggest a shift towards shorter chain homologues under higher irradiation levels (Nødskov Giese 1975, Shepherd, Robertson et al. 1995, Shepherd, Robertson et al. 1997). While contrary to this, it has been suggested that trees with a longer growth season, and greater levels of PAR, synthesise greater chain length *n*-alkanes to protect the leaves from water loss (Sachse 2006). However, an alternative explanation for the observed high ACLs is attributed to the loss of the shorter chain, and less heat stable *n*-alkanes by selective evaporation (Sachse 2006). Furthermore, as temperature, latitude, PAR, water availability, and RH are all closely linked. It is not surprising to find numerous studies linking these parameters to changes in ACL that all appear to report similar trends. For example, ACL was found to decrease with increasing distance from the more humid coastal region for conifer species in Oregon (Oros, Standley et al. 1999), and a correlation between higher annual rainfall and lower carbon chain length *n*-alkanes has also been reported (Dodd, Rafii et al. 1998). In addition, atmospheric dust samples collected along the West African coast were found to contain longer chain homologues when they originated from more arid regions (Huang, Dupont et al. 2000, Schefuß, Ratmeyer et al. 2003).

Unfortunately, all of these variables tend to act at the same time making it very difficult to separate, and disentangle their varying influences. In addition, ACL has also been linked to latitude (Poynter, Farrimond et al. 1989, Poynter 1991), with higher ACLs associated with the lower latitudes (Jeng 2006, Sachse 2006). This relationship appears to hold true when higher temperatures, which are associated with lower latitudes, are considered (i.e.

mean annual temperatures decrease with increasing distance from the equator). For example, populations of *Austrocedrus chilensis* from Argentina and Chile, inhabiting more arid environments with higher annual temperatures, presented higher proportions of the longer chains in their leaf wax *n*-alkanes in comparison to populations growing at the considerably cooler, and more humid rainforest boundary (Dodd, Rafii et al. 1998). As can be seen, the effects of temperature and RH within the aforementioned study could not be separated, making it difficult to ascertain the individual effects of each. In theory, univariate greenhouse controlled growth experiments would be an ideal method for disentangling which climatic factors can influence epicuticular leaf wax molecular composition. However, as the compound-specific hydrogen isotopic composition of the individual lipid compounds is the focus of current research, *n*-alkane molecular distribution data from controlled univariate greenhouse growth experiments is still lacking.

Aside from the issues regarding which climatic and environmental parameters influence the abundance, and molecular compositions, of *n*-alkanes in modern terrestrial higher plants. As mentioned previously, how often *n*-alkanes are synthesized during the life span of a single leaf is the subject of much debate. Greenhouse controlled growth experiments and field studies conducted on barley (Sachse 2010), poplar (Kahmen 2011, Tipple 2013), and grass species of the Great Plains USA (McInerney 2011), have suggested that *n*-alkane synthesis ceases once leaf expansion has stopped. While other research indicates that *n*-alkanes are synthesized throughout the entire growing season in deciduous forest (Pedentchouk 2008, Sachse 2009).

Additional research also suggests *n*-alkanes demonstrate a progressive increase in chain length during successive development from bud to leaves in several deciduous tree species (Piasentier 2000). Furthermore, in depth analysis of *n*-alkane regeneration rates in *Phleum pratense*, a grass species, demonstrated a 2% per hour regeneration rate of nC$_{23}$ between 8am and 3pm, suggesting leaf wax *n*-alkanes are highly dynamic (Gao, Burnier et al. 2012). Similar investigations in *Fraxinus americana*, a deciduous tree species, demonstrated ACLs were dynamic over a 48-hour period, but that *n*-alkane regeneration rates may vary on a species by species basis (Gao, Tsai et al. 2012). Aside from the climatic and environmental variables mentioned previously, there are also a multitude of other factors that could potentially affect the composition of *n*-alkanes in leaf waxes. These include soil nutrient status, genetics, altitude, and pollution (Percy, Cape et al. 1994, Shepherd and Griffiths 2006), however, as is clear, it is very difficult to disentangle all of the various potentially influencing factors.

In addition to the total *n*-alkane abundances and molecular distributional data, it is the compound-specific hydrogen isotopic composition of the *n*-alkanes that holds the most useful information for the reconstruction of climate from *n*-alkanes preserved in sediment archives.

2.1.3 Introduction to stable isotopes

Stable isotopes are different forms of the same chemical element, which have the same number of electrons and protons (i.e. the same atomic number), but different numbers of neutrons within the nucleus (i.e. a different mass number). The different isotopes of the same chemical element have different masses, and it is this mass difference that is the crucial factor in natural abundance stable isotopic analyses, and their subsequent applications.

Table 2.1: The mean relative abundance of the natural stable isotopes of hydrogen, oxygen and carbon, the three elements directly relevant to the current thesis and their respective approximate atomic masses. Data sourced from (Sharp 2007)

Element	Stable Isotope	Atomic mass (u)	Natural abundance (%)
Hydrogen	^{1}H	1	99.985
	^{2}H	2	0.015
Oxygen	^{16}O	15	99.759
	^{17}O	17	0.037
	^{18}O	18	0.2
Carbon	^{12}C	12	98.89
	^{13}C	13	1.11

Concerning plant physiology, and in the context of the current thesis, the three most commonly analysed isotopes include oxygen, hydrogen and carbon. The lightest isotopes of carbon (^{12}C), hydrogen (^{1}H), and oxygen (^{16}O), are present on Earth in the highest abundances, while the heavier isotopes are considerably more rare (table 2.1); this is not always the case for the isotopes of other chemical elements. Therefore, for the chemical elements studied with the current thesis, the difference in the ratio between the common isotope (i.e. lighter), and the rare isotope (i.e. heavier) between two different samples is the basis of natural abundance stable isotopic analyses. Therefore, the natural abundance of different isotopes of the same chemical element, within the same substrate, is calculated as the ratio (R), of the rare isotope, in relation to that of the common isotope (equation 2.3, where an example for hydrogen is given (Coplen 2011)).

$$R(^{1}H/\,^{2}H)_{s} = \left[\frac{N(^{1}H)_{s}}{N(^{2}H)_{s}}\right]$$

(2.3)

Here, the number of lighter isotopes in a sample $(N(^1H)_s)$, is divided by the number of heavier isotopes $(N(^2H)_s)$, with the subscript "s" representing the measured sample. This ratio is then expressed as the relative difference of the two isotope ratios within a sample, to that of a known standard, and is expressed using the "δ" notation. To facilitate this, the ratio of the sample $R(^1H/^2H)_s$ is input into equation 2.4 (Coplen 2011), where it is divided by the ratio of a known standard $(R(^1H/^2H)_{std})$.

$$\delta^2H_{std} = \frac{N\left(^1H\right)_s / N\left(^2H\right)_s}{N\left(^1H\right)_{std} / N\left(^2H\right)_{std}} - 1$$

(2.4)

As the natural abundance of the rare isotopes (in this case heavier) are so low (e.g. 0.015% for ^2H, table 2.1) and the relative differences between the rare and the common isotopes are so small. The δ^2H_{std} values are multiplied by 1000 to make the variations clearer, giving the isotopic composition of the sample under investigation in per mil (‰).

Typically in natural abundance stable isotope research, International Atomic Energy Agency standards (IAEA), such as Vienna Standard Mean Ocean Water (VSMOW), are used in conjunction with individual laboratories own working standards (details of the analytical protocol relevant to the current study is available in section 2.2.3). However, a serious issue associated with the use of stable isotopic analyses is although there are published guidelines and recommendations calling for consistency in the use of isotope nomenclature (Connelly 2005, Coplen 2011); these have not been used in the vast majority of recent publications relevant to the current thesis. Therefore, to make the current thesis consistent with the relevant literature, the δ^2H_{std} term discussed above is instead referred to as δD through out.

In order for anyone to understand how to use natural abundance stable isotope data in any field of research, it is first necessary to understand the basic fundamental principles of isotopic behaviour (Dawson and Siegwolf 2011). As the crux of the current thesis will be in understanding the variation in the δD values of n-alkanes, in order to reconstruct meteoric waters δD values, the following sections outline the basic isotopic theory required to understand the following data chapters.

2.1.3.1 Isotopic fractionation processes

As the number of electrons in an atoms outer shell controls the chemical reactions that atom undergoes, different isotopes of the same chemical element will exhibit the same

chemical behaviours. However, the overall atomic mass dictates the speed at which the element can react and the strength of its bonds (Faure and Mensing 2005). Changes in δD occur in the environment during any chemical, or physical, process involving a source and a product (e.g. evaporation of water), these changes in δD are termed "isotopic fractionation" (Gat 2010). The isotopic fractionation between a source and a product is calculated using equation 2.5 (Coplen 2011), where ε represents the fractionation.

$$\varepsilon({}^{1}H/{}^{2}H)_{s/p} = \alpha_{s/q} - 1$$

(2.5)

$\alpha_{s/p}$ represents the fractionation factor between s (the source), and p (the product), $\alpha_{s/p}$ is calculated from equation 2.6 below (Coplen 2011), Where again, the numerical calculation is multiplied by 1000 to make the small differences much clearer.

$$\alpha_{s/q} = \left[\frac{N({}^{1}H)_{p}/N({}^{2}H)_{p}}{N({}^{1}H)_{s}/N({}^{2}H)_{s}} \right].1000$$

(2.6)

However, as discussed previously, due to the issue of the vast majority of publications relevant to the current thesis using varied isotope terminology, as well as formulae. A variation of equation 2.6 (equation 2.7) is quoted, which is used throughout this thesis. This version of the isotopic fractionation between a source (s), and a product (p), is the most commonly applied version of the isotopic fractionation formula in the scientific publications specific to this field of expertise. Equation 2.7 is used to calculate the hydrogen isotopic fractionation of *n*-alkanes above waters. Outputs of this equation are typically applied to *n*-alkanes extracted from sediment archives to estimate the D isotopic composition of their original source waters (discussed in more detail in chapters 4, 5, 6 and 7).

$$\varepsilon_{s/p} = \left[\frac{(\delta_{p} + 1000)}{(\delta_{s} + 1000)} - 1 \right]$$

(2.7)

These isotopic fractionations are the fundamental basis of the utilization of stable isotopes in scientific research. The isotopic fractionations are a direct result of the slightly different physical and chemical properties caused by the differences in mass, and bond strength, between the light and heavy isotopes. There are three isotopic fractionation processes directly relevant to the current study, these are kinetic fractionation, equilibrium fractionation and transport fractionation.

As the current thesis is concerned with the reconstruction of paleo-climates from the preservation of the deuterium composition (δD) of organic matter, the following will discuss isotopic fractionation effects in terms of hydrogen in meteoric water. Fractionation factors between a source and a product are temperature and rate dependent. If temperature is constant, and the rate of reaction is slow enough, the fractionation factor is simply expressed as the vapour pressure of the lighter isotope relative to the heavy one (Dansgaard 1964), i.e.

$$\propto = \frac{H^1}{H^2}$$

(2.8)

Therefore, if we consider the evaporation of water at 20 °C, the vapour pressure of ^2H_2O is 1.079 at 20 °C, this results in the water vapour being ~80 ‰ D-depleted in relation to the liquid water.

2.1.3.2 Equilibrium fractionation processes

Equilibrium isotopic fractionation processes are reversible and these occur when a reactant and a product are in close contact within a well-mixed system (e.g. as water droplets condense in clouds to form rain) (Yurtsever 1981, Gat 1996, Faure and Mensing 2005). Equilibrium isotopic fractionation is the partial separation of isotopes between two or more substances in chemical equilibrium. This is a mass dependent process, which results from the different vibrational energies of the isotopes taking part in the reaction. An equilibrium exchange reaction can be described as:

$$A^1 + B^2 \leftrightarrow A^2 + B^1$$

(2.9)

Where A and B are the different phases, and the superscripts 1 and 2 are the light isotope and the heavy isotope respectively. Therefore, the equilibrium constant for equation 2.9 may be expressed by equation 2.10, where α_{A-B} represents the equilibrium fractionation factor:

$$K = \frac{(B^1)(A^2)}{(B^2)(A^1)} = \alpha_{A-B}$$

(2.10)

These equilibrium fractionation effects are dominated by the zero-point energies of the binding energies. As the first law of thermodynamics states that energy is always conserved, the vibrational binding energies of the different isotopic molecules can be described by equation 2.11:

$$E = \frac{hv}{2}$$

(2.11)

Where E is the vibrational energy, h is Planck's constant, and v is the fundamental frequency of vibration. Therefore, if the energy of two different molecules containing different isotopes of the same element is equal, the heavier atoms must vibrate more slowly than lighter ones. This lower vibrational energy of the heavier isotopes results in more energy needed to break the bond than that required for a lighter isotope (Bigeleisen, Lee et al. 1973, Gat 1998, Dawson and Siegwolf 2011). This process results in the accumulation of heavier isotopes in the denser phase, which in terms of the condensation of water vapour to rain means the heavier isotopes will accumulate in rain (Gat 1996, Kendall and MacDonnell 1998, Gat 2010).

2.1.3.3 Kinetic isotopic fractionation processes

Kinetic isotopic fractionation processes occur in one direction, and are therefore irreversible. In terms of the current thesis, examples of kinetic isotopic fractionation applicable include fractionation during photosynthetic assimilation and biosynthesis (Gat 1998, Faure and Mensing 2005). Kinetic isotopic fractionation effects are mass dependent and result in the slower reaction of the heavier isotope in relation to the lighter isotope. This is because the first rule of thermodynamics states that energy is always conserved. Therefore, the kinetic energy (KE) of any element is always the same, in the same environment. As KE (equation 2.12) equals half of the mass (m) multiplied by the velocity (v) squared, the heavier isotopes will react more slowly.

$$KE = \frac{1}{2}mv^2$$

(2.12)

Further to this, the mass of the molecules also affects bond strength, where the heavier isotopes are more stable because they vibrate at a lower frequency than the light. Therefore, more energy (Dissociation energy) is required to break the bonds of the heavier isotopes because their zero-point energy is lower, making them more stable (figure 2.3) (Gat 1996, Sharp 2007).
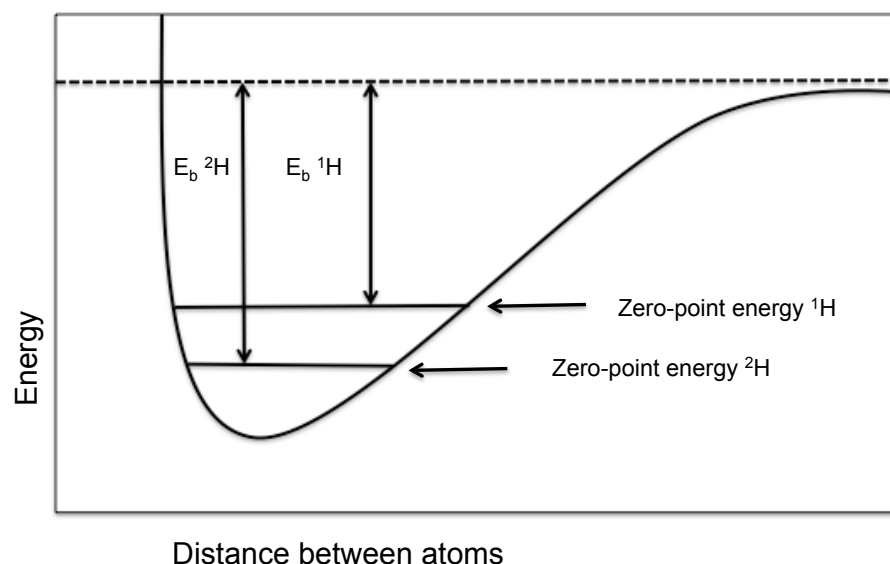
Figure 2.3: A schematic diagram depicting the different zero-point energies of the heavier (2H) and lighter (1H) hydrogen isotopes relevant to the current study. Schematic produced by author, with theory from Sharp (2007).

This mass dependency of the isotopes in any chemical reaction involving a source and a product, also explains why the isotopic fractionations of the light chemical elements are larger. For example, the isotopic fractionations associated with hydrogen are much larger than those of carbon or oxygen; this is because of the relatively large ratio in the differences in mass for hydrogen of 2:1, compared to 18:16 for oxygen, and 12:13 for carbon (Bigeleisen 1965). This is also why in almost any isotopic reaction; the lighter isotopes are preferentially reacted/ evaporated/ lost, over the heavier isotopes. Both kinetic and equilibrium isotopic fractionation effects are temperature dependant and as they are both quantum mechanical effects, the greatest fractionation effects are observed at lower temperatures, and as temperature increases these isotopic effects become less. Mass independent isotopic fractionations do occur, however these are the result of nuclear and/or photochemical reactions (Gat 2010), which are beyond the scope of the current thesis.

2.1.3.4 Isotopic fractionation during transport processes

Previously included under "Kinetic Fractionation Effects", this process is highly mass dependent as it is based on the diffusional properties of the different isotope species (Gat 2010). The process was first identified by Craig (1963), and subsequent experiments have revealed molecular exchange of different isotopes occurs during the evaporation of water under non-equilibrium conditions, and that this was a major influencing factor (Dansgaard 1964, Gat and Craig 1965, Merlivat and Jouzel 1979).

The molecular diffusivities of different isotopes can be calculated from kinetic gas theory (Cappa, Hendricks et al. 2003), where the heavier isotopes diffuse more slowly in relation to the lighter isotopes. Relative humidity also has a large impact on this process as the transport isotopic fractionation is highly dependent upon the concentration gradient between the water in the liquid state, and that in the ambient atmosphere (Gat 2010). Under this rule, water molecules will diffuse from areas of high concentration to areas of low concentration, and as the lighter isotopes diffuse faster, they are preferentially lost. These fluxes can be described using an Ohm's law equivalent (equation 2.13) where:

$$Flux = \frac{conc.\,gradient}{\rho}$$

(2.13)

Where ρ is the transport resistance (Craig and Gordon 1965), and the movement of the water molecules becomes determined by the respective molecular diffusion coefficients, which are themselves affected by mass (Wang, Robinson et al. 1953).

2.1.4 Stable isotopes in plant physiology

The isotopic signatures expressed by plant tissues are affected by a multitude of different interacting factors, these can be categorised into two distinct groups. The first concerns the isotopic compositions of water being directly absorbed by the plant (source water); the second involves the physiological and biochemical aspects of photosynthetic assimilation (Schleucher 1998). Terrestrial higher plants obtain all the hydrogen and oxygen they require for growth through water absorption by roots in the soil; in cases of high ambient relative humidity (RH), water can also be absorbed directly through the stomata (Dawson 1998, Burgess and Dawson 2004). Both of these water sources ultimately originate from meteoric water.

As plants obtain the majority of the oxygen and hydrogen required during photosynthetic assimilation from meteoric water, the isotopic composition of meteoric water is expected to be imprinted, in some capacity, on the isotopic compositions of organic matter synthesized by plants (Martin and Martin 2003). Moreover, because certain geographic and climatic factors influence the isotopic composition of meteoric waters, it is anticipated that these geographic and climatic factors could be reconstructed from the preserved isotopic compositions of plant organic matter (Dawson, Mambelli et al. 2002, Martin and Martin 2003, Dawson and Siegwolf 2011).

2.1.4.1 Meteoric water

The isotopic composition of meteoric water varies strongly over spatial scales. This is because the temperature at which precipitation condenses dictates the level of isotopic fractionation between the different isotope species. This relationship is described via the Clausius-Clapeyron equation and the liquid-vapour relationship between $\delta^{18}O$, δD and temperature (Craig 1961, Dansgaard 1964, Majoube 1971, Yurtsever 1981). Due to the global variations in temperature driven by seasonality, latitude, and altitude, the effects of these different environmental parameters are imprinted on the precipitation. Where precipitation condensing at lower temperatures will be more D-depleted than that falling at higher temperatures (Ehleringer and Dawson 1992, Ehleringer 1993, Gat 2010, Luz and Barkan 2010).

The hydrogen and oxygen isotopes in plant organic matter have a close relationship as both ultimately originate from the same source – meteoric water (Dawson, Mambelli et al. 2002, Martin and Martin 2003, Marshall, Brooks et al. 2007, Dawson and Siegwolf 2011). This relationship between the oxygen and hydrogen isotopes in meteoric water is described by the Global Meteoric Water Line (GMWL, equation 2.14) (Craig 1961).

$$\delta D = 8\delta^{18}O + d$$

(2.14)

Where 8 is the slope of the relationship, and d the intercept, represents the deuterium excess value (Dansgaard 1964). Due to the equilibrium conditions under which the condensation of water vapour occurs to form precipitation, there are no kinetic isotopic fractionation effects. Therefore, the slope of this linear relationship is highly specific, and reflects the equilibrium fractionation factors of δD and $\delta^{18}O$ (Marshall, Brooks et al. 2007, McGuire 2007).

Meteoric water originates in the ocean, where ocean waters are assumed to have an isotopic composition of 0 ‰ for both hydrogen and oxygen. If the isotopic compositions of the ocean were assumed to be 0 ‰, evaporation of water from the ocean must not occur under equilibrium conditions, or the intercept of the GMWL would be 0. Therefore, the evaporation of water does not take place under equilibrium conditions, and kinetic isotopic fractionation effects must have an impact. As the kinetic isotopic fractionation effects of oxygen are larger than the equilibrium effects, while the kinetic and equilibrium effects of hydrogen are very similar; this discrepancy results in the depletion of ^{18}O in water vapour relative to D producing the 10 ‰ intercept (the d-excess) described by the GMWL

(Dansgaard 1964, Craig and Gordon 1965, Yurtsever 1981, Marshall, Brooks et al. 2007, Gat 2010). However, after the initial evaporation of water from the ocean, the water vapour and subsequent precipitation events will fall along the GMWL. This is because the condensation of water vapour to form precipitation occurs under equilibrium conditions, with the temperature during condensation affecting the level of isotopic fractionation (Craig 1961).

Unfortunately, the isotopic compositions of precipitation are not simply affected by temperature during condensation within natural environments. There are also several fundamental processes that occur during the hydrological cycle. These alter the isotopic composition of precipitation as cloud masses are disconnected from their vapour source and move across continents (Craig 1961, Yurtsever 1981, Gat 1996, Gat 1998, Gat 2010). One important factor is that the isotopic compositions of the precipitation, and water vapour, are constantly evolving as precipitation events occur. This is because condensation within clouds occurs under equilibrium conditions, where the heavier isotopes of hydrogen and oxygen accumulate in the denser phase (i.e. rain). Therefore, with every rain event, the remaining water vapour in clouds becomes progressively more depleted in the heavier isotopes. This is a result of the preferential loss of the heavier isotopes in precipitation, and these processes lead to "continentality" and "amount effects".

Rayleigh distillation processes can describe this evolution of precipitation along the GMWL (Yurtsever 1981, Gat 1996, Gat 2010, Dawson and Siegwolf 2011) (equation 2.12):

$$R = R_0 f^{(\alpha - 1)}$$

(2.15)

Where R_0 is the initial isotopic ratio of the phase of interest, R_t is the isotope ratio at time t, α is the fractionation factor between the two isotopes, and ƒ is the fraction of the phase of interest remaining, at time t. This process explains why the isotopic compositions of precipitation become progressively more depleted as cloud masses move across continents. It also explains why greater amounts of precipitation lead to a greater isotopic depletion in the remaining atmospheric water vapour. Therefore, the further a cloud mass travels over land (Ingraham and Taylor 1991, Dawson and Siegwolf 2011), and the greater the frequency, and intensity, of the precipitation it produces, the greater the isotopic depletion in meteoric waters. (Rozanski, Araguás-Araguás et al. 1993, Ingraham 1998).

Although the isotope fractionation processes, which result in the isotopic compositions of precipitation are reasonably easily explained. Once precipitation enters an individual ecosystem the processes involved become much more complex. In addition, although the general theory dictates that the isotopic compositions of meteoric waters are reflected in the isotopic composition of organic compounds synthesized by plants, these processes are also much more complex.

2.1.4.2 Water sourcing

As terrestrial higher plants obtain most of the hydrogen and oxygen that is required for growth through water absorption by roots in the soil. The water absorbed by plants, and subsequently used during photosynthesis and biosynthesis, should be related to the original isotopic values of the precipitation falling on the region, and thus, meteoric water (Epstein, Yapp et al. 1976, Sternberg 1988); however natural forest ecosystems are not so simple. Several processes can occur, which will alter the isotopic compositions of meteoric waters before absorption by the plant happens and issues arise once precipitation enters an individual ecosystem's hydrological cycle. In terms of the current thesis, precipitation falling into a forest ecosystem can be subjected to multiple evaporations before a plant absorbs it. Some examples of this include interception by the canopy (McGuire 2007), and soil water evaporation and mixing processes (Tang and Feng 2001).

These potential evaporation events can result in extensive deviations from the GMWL because once precipitation has fallen it is no longer under equilibrium conditions, and kinetic and transport isotopic fractionation effects will have influence (Gat 2010). Once removed from the cloud, water droplets are subjected to evaporation and exchange with environmental water vapour (Dansgaard 1964). These effects of kinetic and transport isotopic fractionations result in a reduction of the slope of the GMWL, which alters the d-excess value (Gat 1996, Gat 1998, McGuire, McDonnell et al. 2007, Gat 2010). This can often make it very difficult to relate the water directly absorbed by the plant to the original isotopic composition of the meteoric water. These issues can be overcome by direct isotopic measurement of extracted plant xylem waters, which has been shown to be a direct proxy for the water absorbed by the plant (except in saline conditions) (Ehleringer, Phillips et al. 1991, Feakins 2010). However, it still presents the issue that the plants could be absorbing water with an isotopic composition that is far-removed from the isotopic compositions of the meteoric water, which originally fell upon the region of study (Gat 1996, Sachse 2009, Feakins 2010).

Source water issues aside, the water absorbed by the plant travels to the foliage to facilitate photosynthesis. It is here that additional isotopic fractionation occurs during photosynthetic assimilation and biosynthesis, which can make it even more difficult to relate the isotopic compositions of plant organic matter to that of meteoric waters.

2.1.4.2 Isotopic enrichment of leaf water

The isotopic enrichment of leaf water with ^{18}O was first observed in 1965 (Gonfiantini, Gratziu et al. 1965), and the enrichment with deuterium in 1966 (Wershaw, Friedman et al. 1966). It was at the same time that Craig & Gordon (1965) modelled the isotopic effects of evaporation from an open water surface, and from this seminal work they were able to demonstrate that the water remaining after evaporation is isotopically enriched. Through the application of these principles the theoretical basis of leaf water isotopic enrichment was derived (Dongmann, Nürnberg et al. 1974, Farquhar, Hubick et al. 1989, Flanagan, Comstock et al. 1991, Farquhar, Cernusak et al. 2007). Since then, many attempts have been made to model the evaporative isotopic enrichment of leaf water, and although modelling ^{18}O enrichment has been relatively successful, attempts to model D-enrichment have proved more difficult (Shu, Feng et al. 2008, Shu, Feng et al. 2008).

Nevertheless, ascertaining the physiological and climatic drivers of the transpiration of a single leaf can be complex. This is because these two are often interrelated, as leaf water isotopic enrichment varies strongly due to fluctuations in climate, leaf physiology, and the isotopic composition of water vapour surrounding the leaf (Craig and Gordon 1965, Kahmen, Hoffmann et al. 2013). Despite this, the level of D-enrichment within an individual leaf is accepted to be driven by RH, boundary layer dynamics, the level of photosynthetically active radiation (PAR), the water status of the entire plant, the isotopic composition of the water vapour surrounding the leaf (Smith 2006, Hou 2008, Shu, Feng et al. 2008, Yang 2009), and species specific physiological parameters (Kahmen, Simonin et al. 2008, Shu, Feng et al. 2008, Shu, Feng et al. 2008). In most cases, apart from those where the leaves have directly absorbed significantly D-depleted atmospheric water vapour through the stomata (Dawson 1998, Burgess and Dawson 2004), leaf waters are D-enriched in relation to xylem waters (Leaney, Osmond et al. 1985, Yakir, DeNiro et al. 1990, Wang and Yakir 1995). It is well established that transpiration, i.e. the evaporation of water out of the leaf through stomata, is what drives this enrichment of leaf water and xylem water transport during photosynthesis (Farquhar, Cernusak et al. 2007, Shu, Feng et al. 2008).

During evapotranspiration, water leaving the leaf is subject to equilibrium, kinetic, and transport isotopic fractionation processes (Craig and Gordon 1965, Flanagan, Comstock et al. 1991). The mechanisms of which, are described previously in sections 2.1.2.2, 2.1.2.3 and 2.1.2.4 of this chapter. The RH of the ambient atmosphere surrounding the leaf is the main influence on the level of isotopic enrichment of leaf waters. Where RH creates a water vapour gradient between the water within the leaf, and the water vapour in the atmosphere (Brandes, Wenninger et al. 2007). This is because xylem water isotopic composition is out of equilibrium with the isotopic composition of atmospheric water vapour (Farquhar and Cernusak 2005, Farquhar, Cernusak et al. 2007). Evidence of this effect has been extensively documented in natural field conditions, as well as in laboratory experiments (Helliker and Griffiths 2007, Reye-GarcÍa, Mejia-Chang et al. 2008, Welp, Lee et al. 2008, Kim and Lee 2011). Under this principle, a concentration gradient between the leaf water and the ambient atmosphere drives leaf water evaporation. Where, water moves from the high concentration conditions within the leaf to the low concentration conditions outside the leaf; due to the binary diffusivity of the heavier isotopes in water being slower than that of the lighter isotopes, the lighter isotopes are preferentially evaporated (Farquhar, Cernusak et al. 2007, Gat 2010).

Yet, when the ambient air surrounding a leaf becomes saturated with water vapour, isotopic equilibrium conditions are reached, the diffusional gradient breaks down and no evaporation can occur (Farquhar, Barbour et al. 1998, Gat 1998). This can be further exacerbated by a stagnant air pocket that can form around a leaf called the "boundary layer". This boundary layer is species specific and the extent of it is affected by how well the shape of an individual leaf is coupled to the atmosphere, and how turbulent the air surrounding the leaf is (Allison, Gat et al. 1985, Kahmen, Simonin et al. 2008, Gat 2010). Therefore, under low wind conditions significant boundary layers can build up around a leaf, which will restrict evaporative leaf water isotopic enrichment. While under windy conditions, where the air is more turbulent, the boundary layer is continuously removed and greater levels of evaporative leaf water isotopic enrichment occur (Brandes, Wenninger et al. 2007, Powers, Pregitzer et al. 2008).

In addition to a reduction in evaporative isotopic enrichment of leaf water under high RH conditions. Another process can occur at this time, which can lead to leaf water that is isotopically depleted in relation to xylem water. If RH conditions surrounding the leaf are so great that dew formation on the leaf surface occurs, this dew water can block the stomata and alter the efficiency of gas diffusion (Kim and Lee 2011). Under these conditions, it has been demonstrated that diffusion of the lighter isotopes, into the

relatively isotopically enriched leaf water, from the isotopically depleted water surrounding the leaf can occur, even though there is no net flux of water itself (Welp, Lee et al. 2008, Kim and Lee 2011), this process is of particular relevance in chapter 4.

There are also other physiological issues that can affect the isotopic composition of leaf water. These include; the overall distance the water has to travel within a plant to the site of evaporation, the interveinal distance of a leaf, and the Péclet effect (Kahmen, Simonin et al. 2008, Shu, Feng et al. 2008, Shu, Feng et al. 2008). The Péclet effect describes the advection and back-diffusion that occurs between isotopically enriched leaf water and un-enriched xylem water (Yakir, Berry et al. 1994). This effect was responsible for the over-estimation of leaf water isotopic enrichment in the earlier attempts to model leaf water evapotranspirational enrichment (Farquhar and Lloyd 1993). Given these issues, and speaking in general terms, provided water to the sites of evaporation is not a limiting factor, higher PAR levels, higher temperatures, a more dynamic boundary layer, with lower RH, should typically result in more isotopically enriched leaf waters. As leaf water is the ultimate source of hydrogen and oxygen for all subsequent biosynthates (Leaney, Osmond et al. 1985, Marshall, Brooks et al. 2007), the isotopic composition of the this may be imprinted on the subsequently synthesized organic matter.

2.1.4.3 Carbon isotopes in plant physiology

Plants obtain all the carbon they require for growth through the fixation of carbon absorbed as CO_2 from the atmosphere through the stomata (Sharkey 1982). Regardless of environmental conditions, different levels of carbon isotopic fractionation are expressed during carbon fixation with respect to the different photosynthetic mechanisms (C_3, C_4 and CAM). C_3 plants utilise the most primitive photosynthetic pathway known as the Calvin-Benson cycle, where atmospheric CO_2 diffuses into the leaf through the stomata, where it is fixed to ribulose 1,5-bisphosphate by the carboxylating enzyme Rubisco (O'Leary 1981, Farquhar 1982). When CO_2 supply to the sites of fixation is not limiting, there is a constant fractionation factor of ~27 ‰, caused by the active discrimination of the primary C_3 carboxylating enzyme (Farquhar 1980, O'Leary 1988). Even though Rubisco is a carboxylase, under certain conditions, such as high light intensity and aridity, Rubisco can react with diatomic oxygen; this is termed photorespiration and can reduce net primary production (O'Leary 1981, Farquhar 1982, Farquhar and Richards 1984).

Due to this photorespiration issue, the C_4 pathway evolved to allow more efficient photosynthetic assimilation in drier, warmer environments. Plants that utilise the C_4

pathway have the different primary carboxylating enzyme phosphoenol-pyruvate carboxylase (PEP), which has a significantly smaller fractionation factor of ~-2.2 ‰ (O'Leary 1988, Fogel and Cifuentes 1993, O'Leary, Ehleringer et al. 1993). PEP carboxylase does not react with diatomic oxygen, which prevents photorespiration, and the fixed CO_2 is transported in the form of aspartate or malate into internal bundle sheath cells. Within the bundle sheath cells, CO_2 is decarboxylated and then proceeds to a carbon fixation pathway that is analogous to that used in C_3 plants, where it is fixed by Rubisco. In the bundle sheath cells, the majority of CO_2 is fixed into organic matter because they are almost a closed system, and no further isotopic fractionations can occur (Fogel and Cifuentes 1993). As a direct result of these differences, C_4 plants have $\delta^{13}C$ values that range -6 to -23 ‰, while C_3 plants range -23 to -34 ‰, showing no overlap. This means the carbon isotope value fixed, via the two different pathways, can always be differentiated (Faure and Mensing 2005).

In addition to their invaluable use in differentiating C_3 and C_4 species, the isotopic carbon analyses of a single leaf can provide insights into the dominating environmental conditions that a particular leaf experienced during formation, growth, and photosynthetic assimilation (O'Leary 1988, Fogel and Cifuentes 1993). Significant variations in bulk foliar $\delta^{13}C$ have been observed within the same environment, between different specimens of the same species, and even at different points in the same plant (Farquhar 1989, Vogel 1993, Scartazza 1998). Variations in bulk foliar $\delta^{13}C$ are generally considered to be a function of photosynthetic capacity, or changes in the ratio of internal to ambient CO_2 (Farquhar 1989), both of which are effected by stomatal aperture (Brugnoli 1998). In a typical C_3 plant, the stomata are open during the day allowing ambient CO_2 to diffuse into the leaf for fixation, and water to transpire out (Farquhar 1980, Farquhar 1989, Vogel 1993). Therefore, when the stomata are closed, the photosynthetic fixation system must utilize whatever CO_2 is inside the leaf, regardless of molecular mass.

The functioning of stomatal aperture however is highly dependent on environmental factors. Farquhar et al., (1982) first proposed the relationship between carbon isotopic composition and water use in C_3 plants. C_3 plants that fix more carbon per unit water transpired show enrichment in ^{13}C of their tissues, i.e. water use efficiency (WUE) is negatively correlated with ^{13}C isotopic enrichment (Farquhar and Richards 1984, Farquhar, Hubick et al. 1989, Marshall 1993, Scartazza 1998). However, light intensity, temperature, water availability, and salinity all influence stomatal aperture (Farquhar 1982). This further complicates the interpretation of bulk foliar $\delta^{13}C$ values, as it is often very difficult to disentangle these variables. Despite these issues, it is now possible to use

$\delta^{13}C$ values, in conjunction with other isotopic analyses, to disentangle some of the variables. One analysis, which is of particular use, is the $\delta^{18}O$ values of the associated organic matter or leaf waters.

2.1.4.4 The isotopic oxygen versus carbon conceptual model

Both ^{18}O and ^{13}C isotopic compositions of leaf material are affected by the level of stomatal aperture, while ^{13}C is also affected by photosynthetic capacity. As a result of this, an oxygen-carbon isotope conceptual model has been proposed (Scheidegger 2000). The application of this conceptual model can facilitate the distinction between changes in photosynthetic capacity and changes in stomatal aperture (Farquhar, Barbour et al. 1998, Cernusak, Farquhar et al. 2005).

Under this conceptual model if $\delta^{18}O$ and $\delta^{13}C$ values exhibit a positive correlation, it indicates a stomatal reaction (i.e. stomatal aperture is the limiting factor). This is because the level of leaf water evapotranspiration, which is controlled only by stomatal aperture, affects the $\delta^{18}O$ value. While the $\delta^{13}C$ value is affected by the absorption of CO_2, which is also controlled by stomatal aperture. However, if there is no correlation between $\delta^{18}O$ and $\delta^{13}C$ values, where $\delta^{18}O$ values are variable, but $\delta^{13}C$ values are relatively constant, this indicates that stomatal aperture is not affected and some aspect of photosynthetic capacity is (Saurer 1997, Scheidegger 2000). The application of this conceptual model has proved to be very useful in aiding the interpretation of plant water relations with respect to photosynthesis (Yakir and Wang 1996, Riley, Still et al. 2002). Furthermore, its application may help elucidate whether photosynthetic capacity, or stomatal aperture, is the controlling mechanism in determining the isotopic composition of organic matter.

2.2: Methodology

2.2.1 Field sampling

Samples for the following thesis were collected from Scots pine trees (*Pinus Sylvestris*) inhabiting the Blackwood of Rannoch, Scotland, and Värriö Strict Nature Reserve, Finland, during the 2010-growing season. Additional samples were collected from willow (*Salix*) inhabiting the University Broad, Norwich, UK, during the 2012-growing season (figure 2.4).

Figure 2.4: Google Earth© satellite image showing the locations of the three different study sites investigated within the current thesis.

These sites were chosen due to the author's familiarity with the forests under question and also due to the convenience of the location; elevation and GPS data is provided in table 2.2.

Table 2.2: Details of the GPS positions and elevations of the three sample sites investigated in the current study.

Location	Latitude	Longitude	Elevation (m, asl)
Värriö Strict Nature Reserve, Finnish Lapland	N 67°45'01.0"	E 29°39'0.6.4"	341
Black Wood of Rannoch, Perthshire, Scotland	N56°40'26.2"	W 04°19'47.7"	91
The University Broad, UEA, Norwich, England	N52°37'5.10"	E01°14'23.45"	11

Photographs of each sample site for comparison are provided in figure 2.5.

Figure 2.5: Photographs (S.Newberry) of the three different sample forests investigated, (a) shows Scots pine forest in Värriö Strict Nature Reserve located in North-Eastern Finnish Lapland, (b) shows riparian Salix (Willow) trees located around the University Broad at the University of East Anglia, Norfolk, Norwich, England and (c) shows Scots pine forest within the Black Wood of Rannoch, Perthshire, Scotland.

The OIPC estimations of precipitation oxygen and hydrogen isotope compositions for each of the sample sites are provided in table 2.3.

Table 2.3: OIPC estimations of mean annual precipitation (MAP) and monthly averages (Bowen 2013), for the Black Wood of Rannoch Scotland (BWR), Värriö Strict Nature Reserve Finland (VSN) and Norwich (NRW). All values are quoted in per mil (‰) relative to VSMOW.

	Annual average	Jan	Feb	Mar	Apr	May	Jun	Jul	Aug	Sept	Oct	Nov	Dec
BWR δD	-68	-80	-71	-75	-72	-60	-56	-55	-53	-56	-67	-75	-79
BWR $\delta^{18}O$	-9.6	-11.1	-10.2	-10.1	-9.9	-8.6	-8	-6.9	-7.5	-8.2	-9.7	-10.9	-11.1
VSN δD	-99	-126	-109	-126	-98	-88	-88	-82	-79	-86	-105	-121	-130
VSN $\delta^{18}O$	-13.4	-16.9	-14.9	-16.8	-13.5	-12.3	-11.6	-10.5	-10.6	-11.9	-14.5	-16.3	-17.7
NRW δD	-57	-70	-65	-62	-62	-52	-48	-44	-43	-47	-56	-67	-70
NRW $\delta^{18}O$	-8.3	-9.9	-9.4	-8.6	-8.8	-7.5	-7	-6.1	-6.3	-7.2	-8.5	-9.7	-10

2.2.1.2 Värriö Strict Nature Reserve, Finnish Lapland

Värriö Strict Nature Reserve is located 900 km north of Helsinki, 250km north of the Arctic Circle, and the eastern boundary of the park is the Russian border (Figure 2.4, 2.5 (a), table 2.2). The climate of the region is characterised by a short growing season that varies from 100 to 140 days on a year-to-year basis, an extensive period of which experiences 24-hour low angle incoming solar radiation (FMI, 2009). Mean annual precipitation of the area is around 600mm and the average mean annual temperature is -1 °C. Värriö Strict Nature Reserve (figure 2.6) was established in 1981: under Finnish conservation law, strict nature reserves are areas, which have been designated for scientific purposes only, and as a result they are not, under normal circumstances, open to the public.
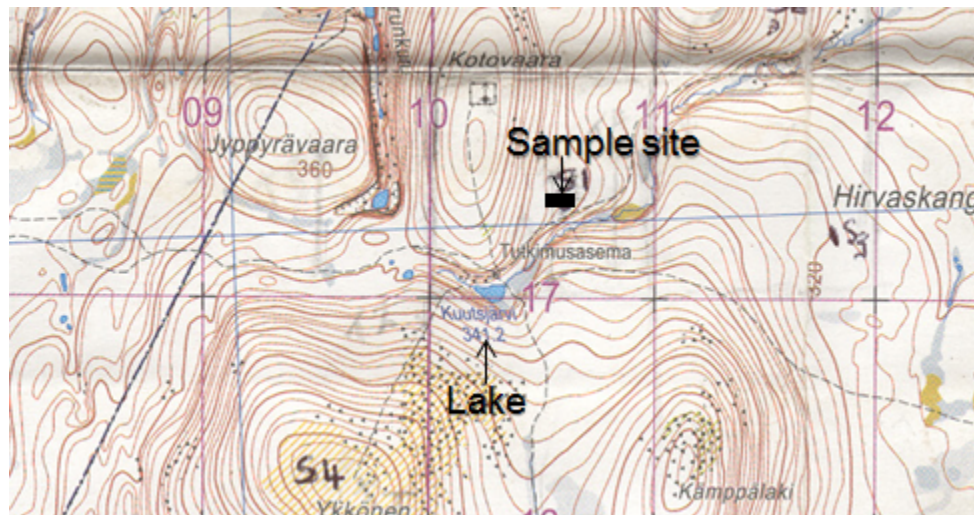
Figure 2.6: Topographic map of the region in Finnish Lapland where sample collection took place, the black square indicates the sample collection site and the small lake close to the sample site is indicated. Map copyright by the Finnish National Land Survey.

The closest major road to the reserve is 100km away and there are negligible sources of pollutants, due to a lack of industry or urban conurbation in the immediate area (Hari 1994, Kulmala 2000, Ruuskanen 2003). Although the area is sparsely populated, and hunting within the reserve is completely banned, the forest is still used by Sámi reindeer (*Rangifer tarandus* L.) herders. The reindeer are found in relatively high densities; nevertheless the anthropogenic impact on the forest ecosystem is still minimal.

The forest is dominated by natural stands of Scots pine (*Pinus sylvestris*) of varying age and size, but also has considerable pockets of Norway spruce (*Picea abies*), as well as birch species (*Betula spp*.). As can be seen in figure 2.5(a), the forest exhibits a low stand density and the forest floor typically has ground coverage of wild European blueberry (*Vaccinium myrtillus*), mosses and lichens.

2.2.1.3 The Black Wood of Rannoch, Perthshire, Scotland

The Black wood of Rannoch is one of the largest remaining remnants of ancient Caledonian pine forest, which has covered the highlands of Scotland since the end of the last ice age 10,000 years ago; it is designated as a Site of Special Scientific Interest (SSSI) (figure 2.4, 2.5(c) and table 2.2). The wood is approximately 83% Scots pine and 9% deciduous broad-leaved woodland. The site is managed primarily by the Scottish Forestry Commission for conservation because of the important communities of old pine-wood indicator species such as lichen and fungi (McLeod 2013). The forest is open to the public for recreation purposes, however, these only include walking and cycling on pre-existing pathways, and therefore disturbance to the forest itself is kept to a minimum.

Figure 2.7: Google Earth© satellite image showing the locations of the Black Wood of Rannoch in Perthshire Scotland, where Scots pine samples were collected during 2010. Loch Rannoch, the closest water body, is labelled in yellow.

The lowest temperatures experienced by the forest occur during December, January, and February. However, the mean monthly-recorded temperature for these months is never below 0 °C. The site can experience up to 18-hours sunlight during peak summer, but it does not experience a 24-hour photoperiod (climatic data from the nearest weather station to the site, Ardtalnaig weather station) (Eliassen 2012). Individual trees, which are thought to be over 400 years old, inhabit this wood (as can be seen in figure 2.5(c)). As this forest is almost completely undisturbed, it consists of individuals of varying size and age. The wood is located on the northern shore of Loch Rannoch in Perthshire, and is

approximately 80km from the nearest urban conurbation (figure 2.7). As detailed, the wood is dominated by Scots pine, and the forest floor is characterized by dense ground coverage of *Sphagnum spp*. moss and wild European blueberry (*Vaccinium myrtillus*).

2.2.1.4 Sample collection protocol Finland and Scotland

The same sampling protocol was applied in both field campaigns, one in Finnish Lapland, and the second in the Black Wood of Rannoch, Scotland. This sampling campaign was specifically designed to use the well-established gradients in microclimatic variables within natural forest canopies. These were used to investigate the potential variations in epicuticular leaf wax *n*-alkane isotopic, and molecular compositions, within and between, different sized individual Scots pine trees. These gradients of microclimatic variables occur with height in natural forest stands, where PAR levels increase with increasing height off the forest floor (Le Roux, Bariac et al. 2001), and wind speed (which influences boundary layer dynamics), and RH vary in relation to canopy position (Garten Jr and Taylor Jr 1992, Broadmeadow 1993, Niinemets, Kull et al. 1999, Niinemets, Sonninen et al. 2004, Woodruff, Meinzer et al. 2008, Woodruff, Meinzer et al. 2009) (See figure 2.8).
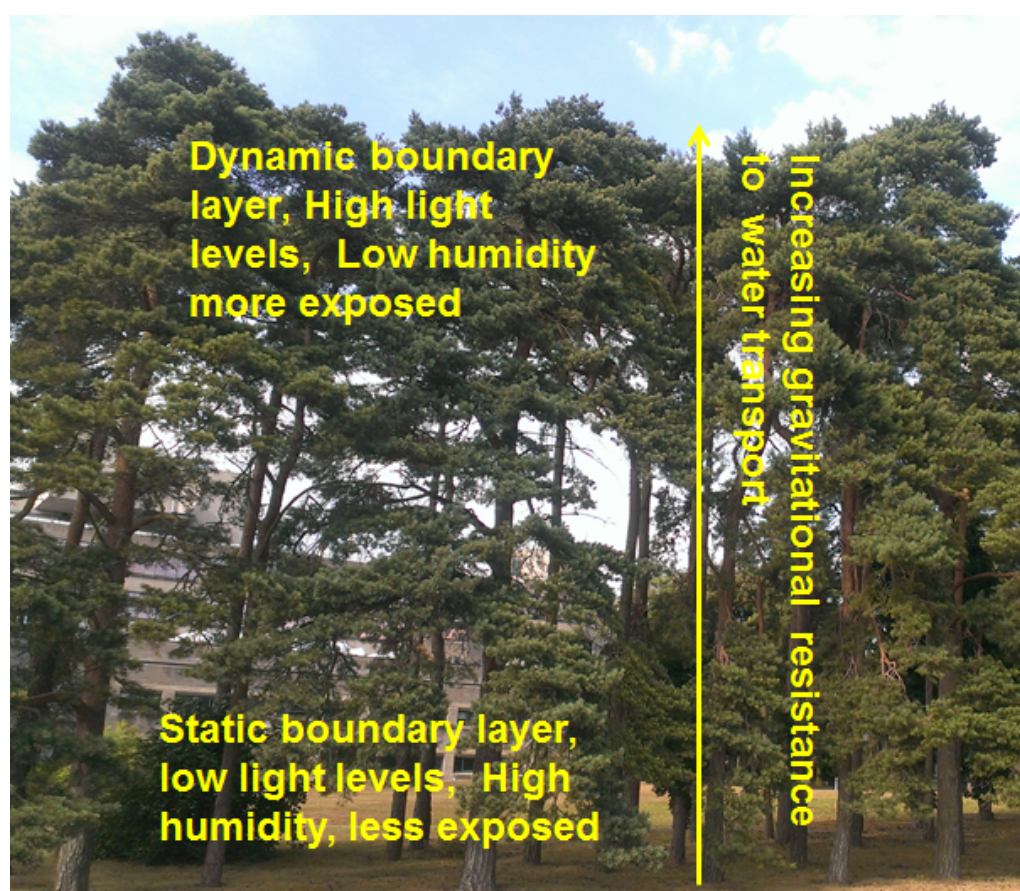
Figure 2.8: Photograph (S.Newberry), a schematic diagram for clarification of how microclimatic variables can vary within natural forest stands.

One could hypothesize that the natural variations in these parameters, which are reported to influence leaf water isotopic enrichment, would result in different levels of D-enriched leaf water at different positions in the canopy. These principles have already been used to demonstrate significant variations in bulk foliar $\delta^{13}C$ values with height within large individual trees in natural forest stands (Garten Jr and Taylor Jr 1992, Broadmeadow 1993, Duursma and Marshall 2006). In these studies bulk foliar $\delta^{13}C$ has been positively correlated with height of sample collection (Ometto, Flanagan et al. 2002, McDowell, Licata et al. 2005), therefore, observing similar trends in the D isotopic compositions in leaf wax *n*-alkanes is a very likely possibility. As the level of isotopic enrichment in leaf waters may be imprinted on subsequently synthesized organic matter, isotopically analysing these could provide information regarding the climatic conditions during which the organic matter was synthesized (Sauer, Eglinton et al. 2001, Sachse 2006).

Figure 2.9: Photograph (S.Newberry) showing apical growth on a branch of Scots pine and how current years and previous year's growth needles are identified.

Using this hypothesis at each sampling site, 2 large Scots pines (> 20m), 2 small (8-15m), and 4 saplings (< 4m) were randomly selected for investigation. Current year's growth needles (i.e. Year 0) (which are easily identified because of the way in which Scots pine grows new needles each growth season on apical stems (figure 2.9), were collected for analysis, along with a small section of the stem that feeds water to these needles. From the large trees and small trees samples were collected from the bottom, middle, and top of the north and south facing side of 5 trees. This resulted in 6 samples per tree: 3 samples from the upper, middle and lower crown from the north facing needles, and 3 samples from the upper, middle and lower crown from south facing foliage. To do this, single-rope

canopy access tree climbing techniques were used. At the same time saplings were sampled, however these were only sampled at one height (2m) from south facing foliage. This sampling strategy resulted in a total of 28 sample points for each time period in each location, i.e. 28 in July for Finland, and 28 in September, and the same for each collection period in Scotland.

In addition to the foliar and xylem material sampled, attempts were made to sample soil waters. This was with the aim of quantifying hydrogen and oxygen isotopic variation with depth in the soil profile in order to investigate whether different sized/aged individual trees relied on water extraction from different depths. This phenomenon has been previously documented and has the potential to produce heterogeneous *n*-alkane D isotopic compositions within adjacent vegetation. This is because soil water isotopic composition has been shown to significantly vary with depth due to soil water evaporation, transport and mixing processes (Gat 1998, Tang and Feng 2001, Brooks 2010). Despite this, and as discussed in the following sections, soil water sampling was not possible at most of the sample locations. Further to this, when soil water sampling was possible, unfortunately the laboratory water extraction methods were not developed enough to extract reliable samples.

To prevent contamination of the epicuticular leaf wax lipids from human skin lipids, needle materials, and the stem that fed the foliage with water, were cut approximately 20cm before the foliage. These were tagged with a masking tape label by the cut end, and dropped for processing on the ground. Due to restrictions on sample analysis time, as well as expense, needles were collected for leaf water analysis once a day between 12:00 and 15:00 hours, as it was assumed that this would be the period of time when D-enrichment of leaf waters would be at their greatest (Cernusak, Pate et al. 2002, Sachse 2010).

All needle and stem samples were processed for storage and subsequent transport back to the laboratory using the same sample protocol. Y0 needles were split into two different samples, the first for *n*-alkane extraction, and the second for leaf water extraction. Needles for *n*-alkane extraction were carefully removed with tweezers and placed in labelled paper envelopes. These were gently dried at 30 °C in an oven to prevent decay. Samples for water extraction and analysis were placed in separate, labelled, exetainer glass gas sample tubes, sealed with Parafilm©, and refrigerated until water was extracted in the laboratory. While samples were collected, the overall height from the forest floor of each sample point was measured, along with the overall height of each tree. In conjunction with the needle and stem material, samples of local water sources were also

collected. In Finland these were collected from a small lake less than 200m from the sample site (figure 2.6), and from Loch Rannoch (figure 2.7) in Scotland. These water samples were stored in glass exetainers, sealed with Parafilm©, and refrigerated until analysis. The same sampling protocol outlined above was carried out at the beginning and end of the growth season in each location. This includes July and September for Finland, and April and October for Scotland.

2.2.1.5 Salix study, UEA, Norwich

A small temporal study was conducted on 3 Salix trees, located in close proximity to each other, on the edge of the University Broad within the campus grounds of The University of East Anglia, Norwich, UK (figure 2.4, 2.5(b) and table 2.2). The Broad is a manmade lake which was originally a large pit dug for gravel and sand extraction during the building of The University of East Anglia between 1973 and 1978. Over time, it filled with water (figure 2.10), and has since become a site of great biodiversity, although it is heavily managed for recreational purposes (Rhodes 2012).

The average weather of the region is mild, with annual mean temperatures varying between 3 °C and 22 °C and rarely drop below -2 °C. The warm season spans June to September, and the cold season November to March. The longest day of the year during June is almost 18-hours long (Diebel 2013), so the vegetation in the region is not subject to a 24-hour photoperiod.
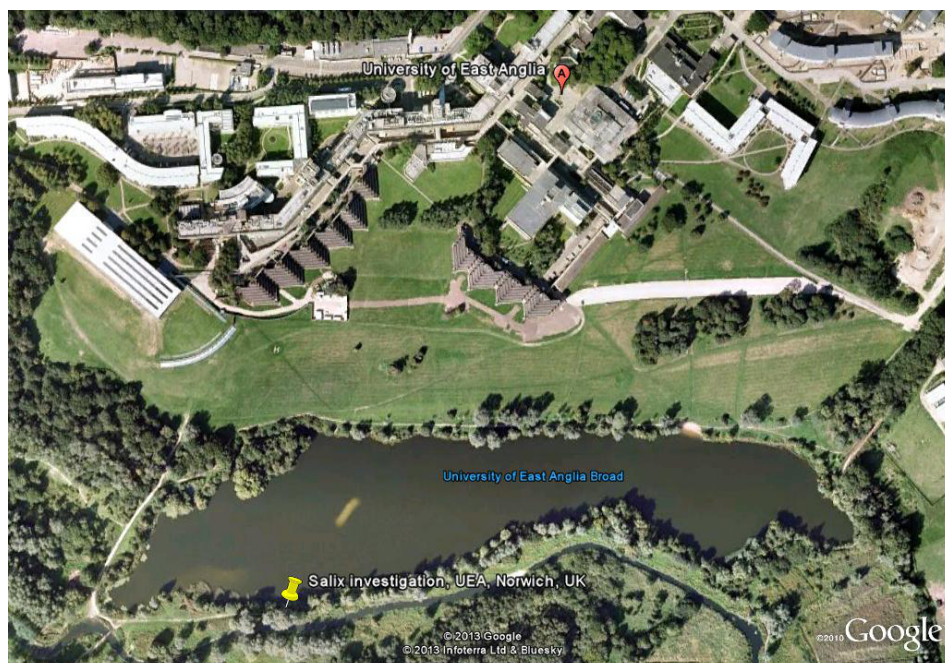
Figure 2.10: Google Earth© satellite image showing the UEA Broad, with the yellow pin marking the site of the 3 Salix trees studied.

Samples were collected during the growing season of 2012, beginning on the 8th of April 2012 (when the new season's leaves were of significant enough size to be sampled, ~2cm in length), and collected again on the 26th of April, the 28th of May, 15th of June, 12th of July, 17th of August, and the 25th of September. 3 Salix individuals, 5m in height, in close proximity to each other, were randomly selected and marked with yellow string. All 3 individuals had leaf and xylem material collected in duplicate, using similar sample collection protocol to that adopted in the Scottish and Finnish sites. However, during this Salix study, only one height from the forest floor was investigated. Sections of stem and leaves were placed in separate, labelled exetainer glass gas sample tubes (Labco Exetainer©, Lampeter, UK), sealed with Parafilm© (Sigma-Aldrich, Gillingham, UK), and refrigerated until water was extracted in the laboratory. An additional leaf sample for *n*-alkane extraction was collected using tweezers and placed in a labelled paper envelope.

In a similar manner to the Finnish and Scottish sample collection campaigns, needle material was collected between 12:00 and 15:00 hours, as it was assumed that this would be the period of time at which D-enrichment of leaf waters would be at their greatest (Cernusak, Pate et al. 2002, Sachse 2010). In addition, during each sample collection day, a sample of water from the University Broad (figure 2.9) was also collected, sealed in an Exetainer, and refrigerated analysis.

2.2.2. Sample preparation
2.2.2.1 *n*-alkane extractions

Needle samples for *n*-alkane extraction were freeze-dried for 48-hours, then weighed to obtain the dried mass (DM) immediately prior extraction. The needles were sonicated in laboratory grade hexane (15mins x 2) to obtain the total lipid extract (TLE). For *n*-alkane quantification, 5µl of 5α-Androstane ($C_{19}H_{32}$) (sigma-Aldrich, Gillingham, UK) (0.56g/l concentration) was added as the internal standard, prior to the concentration of the TLE to 1ml using a TurboVap II Concentration Evaporator Workstation (Zymark Corp., Hopkinton, MA, USA), using laboratory grade nitrogen gas. It is very difficult to quantify exactly what percentage of the "true total epicuticular wax" is dissolved in the solvent during the sonication procedure for a particular given sample. During the TLE procedure one assumes 100% of the epicuticular wax is recovered for subsequent purification and analysis, however at this time there is no method for guaranteeing this. In addition, grinding of foliar material and/or additional sonication is not recommended as this can lead to the release of lipids and other compounds from internal leaf cells (Cromier In prep). These internal lipids and compounds can interfere with the GC analysis, producing

"dirty chromatograms" where the peaks of interest are difficult to identify as many different compounds coelute at the same time. As a result, the *n*-alkanes extracted and analysed within the current thesis, as well as the concentration data discussed in chapter 3, represents the "extracted epicuticular leaf waxes" and not the "true total epicuticular wax".

Once concentrated to 1ml, the TLE was transferred to 4ml glass vials with the TurboVap concentration tube rinsed with hexane to fill the 4ml vial, this limits the amount of sample residue left behind. The TLE was then concentrated to ~500µl under a stream of laboratory grade nitrogen gas in preparation for column chromatography. For column chromatography, the highly concentrated TLE was passed through glass Pasteur pipettes (145 x 9mm) packed with activated silica gel (0.063-0.200nm, Sigma-Aldrich, Gillingham, UK) and eluted with laboratory grade hexane to separate the *n*-alkane fraction. The *n*-alkane fraction was concentrated to ~50µl under a stream of high grade nitrogen gas and transferred into a 250µl glass insert vial. The previous 4ml vial was rinsed with hexane to minimise sample residue being left behind to make the extract up 250µl. This was then concentrated to ~125µl under laboratory grade nitrogen gas for subsequent analysis on a GC-FID. Unfortunately we did not complete a total procedure blank to document the level of *n*-alkane contamination during the TLE extraction and purification procedure. This would be a significant recommendation for future research. However, as the samples under investigation did not come into contact with plastics, and all equipment used was either single use, or cleaned and dry ashed at 400°C. We anticipate and assume *n*-alkane contamination from external sources during the TLE procedure was negligible.

This methodology was applied to every *n*-alkane extraction using brand new pipettes, glass vials, and dry ashed at 400 °C glassware to avoid cross-contamination of samples.

2.2.2.2 Cryogenic vacuum distillation of leaf and xylem waters

To extract water from the leaves and xylems for oxygen and hydrogen isotopic analysis, the samples were cryogenically vacuum-distilled. To facilitate the process, a custom cryogenic vacuum distillation line was constructed in the Stable Isotope Laboratory (figure 2.11) (Sarah Newberry, Paul Disdle, Paul Dennis, SIL, UEA Norwich, UK). The apparatus consisted of 6 custom-made glass units sealed with Swagelok© Ultrator 12mm Cajons (Swagelok©, Solon, OH, USA) to a glass manifold. Each glass unit was made up of a collection tube, and an extraction tube, where each individual unit could be isolated from the manifold by a Louwers 9mm vacuum tap (Hapert, NL). Each sample collection tube could also be isolated from the rest of the vacuum line by a Louwers 9mm vacuum tap

(Hapert, NL). The glass manifold was connected to an Edwards Ltd. E2MY.5 dual stage vacuum pump (Crawley, England), via an Edwards Pre10K gauge head (Crawley, England), which was also connected to an Edwards Pirani Vacuum Gauge (Crawely, England).

Figure 2.11: Photograph of the cryogenic vacuum distillation line set up used to extract water from leaves and xylems for hydrogen and oxygen isotope analysis, photograph (S.Newberry).

To extract water from a sample, sealed exetainers containing material for extraction were pre-frozen in liquid nitrogen (LN$_2$) for 15 minutes. The caps were removed and the open exetainers were placed in the extraction tube and connected to the glass unit. The extraction tube was then submerged in LN$_2$ to keep the sample frozen, and the Louwers 9mm vacuum tap was opened to pump the unit down to 8×10^{-2}mBar, when the Louwers 9mm vacuum tap was closed again. The extraction tube was then placed in a 5l beaker of hot water, kept near boiling with electronic hotplates, and the collection tube, with the Louwers 9mm vacuum tap open, was submerged in LN$_2$ (figures 2.11).

Extraction times varied significantly depending upon what kind of substrate was being extracted (up to 5 hours for large pine needle samples). To identify when extraction was complete, cotton swabs dipped in LN$_2$ were pressed against the glass tube between the extraction tube and the collection tube. If water vapour did not condense on the inside of the glass, the distillation was deemed complete. This method seemed appropriate as a method devised by West et al., (2006), indicates after ~30 minutes of cryogenic vacuum distillation, over 98% of water is recovered from pine needles. In addition, 100% water extraction is not absolutely necessary as the precision of instrumental isotopic analysis of both hydrogen and oxygen is less than 2% (West, Patrickson et al. 2006). Once extraction was complete, the sample collection tube was sealed from the rest of the line by a

Louwers 9mm vacuum tap, and the water inside allowed to defrost at room temperature. The sample extraction tube was removed, the extracted sample disposed of, and the remainder of the line placed back under vacuum to prevent cross-contamination of samples. The extracted water was transferred to a 2ml vial, sealed with Parafilm©, and refrigerated until subsequent analysis. The sample collection tube was then reconnected to the rest of the vacuum line to remove any remnants of water left behind. A new sample was not run until the entire glass unit has reached pre-extraction vacuum levels (8×10^{-2} mBar). This process was repeated for every water sample extracted.

2.2.2.3 Bulk foliar $\delta^{13}C$ sample preparation

Foliar material which was previously freeze-dried for 48-hours were individually ball milled in small plastic containers, with added glass balls, into a fine powder using a SPEX Sample Prep 8000M mixer/mill (4mins, SPEX, Metcuchen, NJ, USA). 0.5±0.02 mg of dried powdered leaf material was carefully weighed and placed in tin capsules, which were then compressed into a small pellet.

2.2.3. Sample analysis

2.2.3.1. *n*-alkane quantification and molecular distributions

Processed *n*-alkane extracts were analysed on a HP Agilent 7820A Gas Chromatograph (Agilent Technologies Inc., Washington, USA) with a flame ionisation detector (FID). 1µl of sample was injected using a split/splitless injector at 300 °C in splitless mode, with helium as the carrier gas at a flow rate of 1.2 ml/min, and the GC equipped with a DB-5 capillary column (30m x 0.32mm x 0.25µm) (Agilent Technologies Inc., Santa Clara, USA). The temperature programme for the GC oven was as follows, programmed from 50 °C (held 1min), increased at 20 °C/min to 150 °C, and then increased at 8 °C/min to 320 °C and then held for 10 min with the detector at 280 °C.

Individual *n*-alkane chains were identified through comparison of the elution times with a known standard mixture of 15 *n*-alkanes ranging nC_{16} to nC_{30} (Dr Arndt Schimmelmann; Department of Geological Sciences, Indiana University, USA), and the area of each individual *n*-alkane peak was calculated using chemstation software (Agilent Technologies Inc., Wilmington, USA). *n*-alkane concentration was calculated under the assumption of a response factor of 1, using equation 2.16. Where, $Conc_{nCn}$ is the concentration of the *n*-alkane chain under investigation, and $Conc_{standard}$ is the known concentration of added standard.

$$Conc_{nCn} = Conc_{standard} \times \left(\frac{peak\ area\ of\ sample}{peak\ area\ of\ standard} \right)$$

(2.16)

To obtain the total *n*-alkane concentration of the "extracted epicuticular leaf waxes" (from here on referred to as the "total *n*-alkane concentration), each *n*-alkane chain calculated as above is summed and then expressed as total *n*-alkane concentration Dried Mass (DM), using the weight data measured prior to extraction. The individual *n*-alkane chain peak areas were also input into equations 2.1 (CPI) and 2.2 (ACL) to calculate the Carbon Preference Index, and Average Chain Length of each sample.

2.2.3.2. Compound specific *n*-alkane *δ*D analysis

After GC-FID analysis, the *n*-alkane extracts were analysed for their compound-specific hydrogen isotopic composition using a Delta V Advantage Isotope Ratio Mass Spectrometer interfaced with GC-Isolink Trace Ultra GC Combustion, and High Temperature conversion system (GC-IRMS) (Thermo Scientific, Bremen, Germany). 2µl of sample was injected using a programmable temperature vaporization (PTV) injector, in splitless mode at 280 °C, with analytical grade helium as the carrier gas at a flow rate of 1.0 ml/min. The *n*-alkanes were separated using a DB-5 capillary column (30mx0.32mmx0.25µm). The temperature programme of the GC oven was as follows: from 50 °C (held for 1 min), increased at a rate of 20 °C/min to 150 °C, then increased again at a rate of 8 °C/min to 320 °C, where is was held at temperature for 10 min. Pyrolytic conversion of the individual *n*-alkane chains to H_2 gas was conducted at 1420 °C.

Prior to every analysis run, an instrument background scan was completed, along with the determination of an H3+ factor. Once these were deemed to be within a suitable range for reliable analysis, the composition of the H_2 working gas was determined against VSMOW, using a known laboratory standard. This standard (Dr Arndt Schimmelmann; Department of Geological Sciences, Indiana University, USA available from http://mypage.iu.edu/~aschimme/compounds.html), consists of a mixture of 15 *n*-alkanes ranging nC_{16} to nC_{30}, each of which have a known hydrogen isotopic composition (table 2.5).

Table 2.4: A list of the defined δD value, with errors, for each of the 15 individual *n*-alkane chains present within the Schimmelmann GC-IRMS standard used during compound-specific δD analyses of all *n*-alkanes present within the following thesis (http://mypage.iu.edu/~aschimme/files/list%20of%20n-alkanes.pdf).

	δD value (‰, VSMOW)	Error (±, ‰)		δD value (‰, VSMOW)	Error (±, ‰)
			nC_{23}	-48.8	1.4
nC_{16}	-9.1	1.8	nC_{24}	-53	1.6
nC_{17}	-117.9	2.3	nC_{25}	-254.1	1.5
nC_{18}	-53.8	2.1	nC_{26}	-45.9	1.0
nC_{19}	-56.3	1.0	nC_{27}	-172.8	1.6
nC_{20}	-52.6	0.8	nC_{28}	-49	1.5
nC_{21}	-214.7	2.0	nC_{29}	-179.3	2.7
nC_{22}	-62.8	1.6	nC_{30}	-213.6	2.4

To calibrate the working gas, the known standard was analysed 3 times in succession and the "measured" δD values are scrutinized in two steps. First, the "measured" δD value of each individual *n*-alkane chain is compared to that of the previous measurements, and provided there is no significant difference (i.e. an absolute difference of less than ±5 %), analysis proceeded. Second, the absolute error of the 3 replicate measurements themselves must be below ±5 %, once these criteria are met, the published values (table 2.5) of the standard are then used to "correct" the "measured" δD value of the working gas. If the reproducibility of the standard, or the "measured" δD values of each chain length, fell below the required error threshold, standard operating procedure diagnostics, and maintenance, was undertaken until instrument precision returned.

All samples were analysed in duplicate, with the standard analysed every 10 samples. In order to convert the "measured" δD data to the "true" δD data, the following data processing methodology was applied. Firstly the chromatograms produced on the GC-IRMS where compared to those produced on the GC-FID to ensure the output was sufficiently similar, after which individual *n*-alkane peaks above 1000mv were processed using Isodat software 3.0 (Thermo Scientific, Bremen, Germany). The "measured" values were converted to "true" values based on the δD composition of the working gas. The isotopic composition of the working gas was re-calibrated every 10 samples via re-analysis of the known standard. The δD composition of the duplicate analyses were averaged, and only averages of duplicate analyses with an absolute difference of less than 5% were included within the following thesis.

2.2.3.3 Oxygen and hydrogen isotopic analysis of leaf and xylem waters

After cryogenic vacuum distillation, the extracted water samples were analysed for their oxygen and hydrogen isotopic compositions using a Delta XP with a TECA and AS 300 Triplus autosampler (Thermo Scientific, Bremen, Germany). Water samples for hydrogen

isotopic analysis were pyrolysed at 1400 °C in an alumina reactor, with a graphite tube insert filled with graphite chips. The GC oven was programmed at 85 °C, with analytical grade helium as the carrier gas, at a flow rate of 1.3 ml/min, producing H_2 gas. Water samples for oxygen analyses were analysed using the same helium carrier gas, and the same alumina reactor with a graphite tube insert filled with graphite chips. However, the samples were pyrolysed at 1450 °C, producing CO, and the GC oven was programmed to 90 °C.

To ensure the data produced during analysis was comparable to that of published research, the following protocols were adhered to. Prior to each analysis run a background scan was completed, the H3+ factor was determined, and the stability of the working gas (zero-enrichment) was completed through standard-on-offs. Once these protocols were completed, and the results obtained deemed to be within the accepted range for accurate analysis, sample analysis was undertaken.

For the hydrogen isotopic analysis of waters, raw data was obtained through the measurement of the samples relative to the δD composition of an analytical grade H_2 working gas that was calibrated against VSMOW. Each sample was injected and analysed 6 times in succession with NTW (Norwich Tap Water) reference material (table 2.4) every 30 injections to ensure instrument precision.

Table 2.5: The standards used in the oxygen and hydrogen isotopic analysis of leaf and xylem waters with their respective IAEA values and the internal laboratory reference material NTW, in all cases apart from VSMOW; all values are quoted with reference to VSMOW.

Standard	$\delta^{18}O$ ‰ (±SD)	δD ‰ (±SD)
VSMOW (IAEA)	0	0
GISP (IAEA)	-24.76 ± 0.009	-189.5 ± 1.2
USGS64444 (IAEA)	-51.14 ±	-399.1 ±
SLAP (IAEA)	-55.50 ± 0.02	-427.5 ± 0.3
NTW (Internal reference)	-7.25 ± 0.12	-47 ± 1.40

The raw data was then scale normalized using a two-point correction with VSMOW and SLAP (table 2.4), together which produce a total range of 427.5 ‰ δD, as the end members of this scale. The linear equation produced via the two-point correction scale was then used to convert the raw measurements to "true" measurements using equation 2.17 (Paul 2007).

$$\delta D_{true} = m \cdot \delta D_{measured} + y$$

(2.17)

Only the "true" measured values of the last 3 injections of each sample were used during the subsequent data processing procedures as within laboratory tests have indicated that this reduces the possibility of sample memory effects. Especially when waters of highly variable isotopic composition are being analysed within the same sequence. These 3 injections were averaged, and if the standard deviation (Stdev) of this was above 2 ‰, the measurements were rejected and re-analysed. Only "true" δD measurements with a Stdev below 2 were included within the following thesis.

The δ^{18}O composition of the CO was measured relative to analytical grade CO working gas, which was calibrated to VSMOW. The sample sequences were the same as for the hydrogen isotopic analyses, with 6 injections per sample, and internal reference material NTW (table 2.4) every 30 injections to monitor instrument precision. The raw data was normalized to the VSMOW-SLAP scale using the method described previously (equation 2.17) (Paul 2007), and only the last 3 injections of each sample were used to remove potential memory effects. An average of the last 3 injections was then calculated and only "true" data with a standard deviation below 0.2‰ were used within the following thesis. Any measurements that fell outside of this range were rejected and re-analysed.

2.2.3.4 Bulk foliar δ^{13}C sample analysis

After sample preparation leaf samples were analysed for bulk carbon isotopic composition using a Delta XP (Thermo Scientific, Bremen, Germany) with a Costech ECS 4010 Elemental Analyser (Costech, Valencia, CA, USA) and zero blank autosampler (Costech, Valencia, CA, USA). Each sample was dropped and flash combusted at 1020 °C in a reactor packed with chromium oxide and silvered copper oxide. Using laboratory grade helium as the carrier gas, the sample was carried through a reduced copper reduction reactor at 650 °C. The flow then continued through a water trap (magnesium perchlorate) and the sample was then measured with respect to a laboratory grade CO_2 working gas that was calibrated to VPDB. Each sample was run in duplicate, with two internal reference standards, bovine casein and collagen, run every 14 samples to ensure instrument precision. An average of the two sample analyses was calculated and if the stdev of this was above 0.3, the measurements were disregarded and re-analysed.

Table 2.6: The standards used in the bulk carbon isotopic analysis of leaf material all values are quoted with reference to VPDB except of the IAEA standard VPDB.

Standard	δ^{13}C ‰
VPDB (IAEA)	0
Bovine casein (Internal ref)	-23.37
Collagen (Internal ref)	-17.98

2.2.3.5 Statistical Analysis

All data was processed in R (GNU Project, GNU General Public Licence, available for download at http://www.r-project.org/) and Microsoft Excel© (Microsoft, Redmond, WA, USA). Standard error of the mean (SEM), simple linear regression analyses, and paired t-tests were conducted using Microsoft Excel©, and two-way Analysis of Variance (ANOVA) were conducted using R.

3. n-alkane concentrations and chain length distributions

3.1 Concentration and molecular distribution of *n*-alkanes, a literature review

3.1.1 Introduction

As *n*-alkanes are increasingly applied as paleo-climate proxies, many recent publications have sought to utilize the chain length distributions, and concentrations, of these from modern existing vegetation to aid in the interpretation of *n*–alkanes extracted from the sediment record. Few published data exist on the lipid composition of coniferous plants, with the epicuticular waxes only being studied for the most economically important species (Riederer 1989). Recent work from a paleo-environmental perspective has reported negligible concentrations, or a complete lack, of *n*-alkanes within conifer epicuticular waxes (Riederer 1989, Sachse, Radke et al. 2004, Sachse 2006). However, studies addressing the structure and composition of conifer epicuticular wax from a plant physiological perspective exist and provide contradictory results, where appreciable abundances of *n*-alkanes within conifer epicuticular leaf waxes is reported (Prügel, Loosveldt et al. 1994, Prügel and Lognay 1996, Oros, Standley et al. 1999).

Coniferous species are the major constituent of the boreal forest, which spans the northern-most part of three continents and covers 11% of the Earth's terrestrial surface (Bonan 1989). They are also present in high densities in alpine regions of much lower latitudes; therefore investigating the potential of conifers to contribute to sedimentary *n*-alkanes is of high importance.

3.1.2 *n*-alkane concentrations

There are several methods of numerically quantifying variations in the molecular distributions of *n*-alkanes within an individual sample; the first and most obvious is direct comparison of the total *n*-alkane content. Deciduous species are reported to contain the greatest amount of extractable *n*-alkanes (Sachse 2006), while conifer species are reported to have higher concentrations of primary and secondary alcohols, and fatty acids (Prügel and Lognay 1996), with only minor amounts or a complete lack in *n*-alkanes

(Riederer 1989, Sachse, Radke et al. 2004, Pedentchouk 2008). Furthermore, concentrations are reported to increase with leaf age (Piasentier 2000, Kahmen 2011), along with large variations in total *n*-alkane concentration being reported as a result of latitude, with decreasing north to south gradients in *n*-alkane content (Prügel, Loosveldt et al. 1994). Few studies have directly addressed exactly which physiological and/or environmental factors affect *n*-alkane concentrations within conifer species, however it is known that temperature, relative humidity (RH), and irradiance (PAR), can influence leaf wax morphology in other plant species (Shepherd and Griffiths 2006). Unfortunately, due to the complex protective chemical properties of *n*-alkanes in relation to carbon number, and the mixture of individual *n*-alkane homologues that are typically present within epicuticular leaf waxes, total *n*-alkane concentration data alone is usually not enough to draw definitive conclusions of the general climate of origin for paleo-climate reconstructions.

This has resulted in the application of numerical quantifications of *n*-alkane chain length distribution characteristics within individual samples; these ascertain which *n*-alkane homologues are most predominant, and the carbon number characteristics of these. The two most commonly applied *n*-alkane distribution quantification techniques used are Carbon Preference Index (CPI), and Average Chain Length (ACL).

3.1.3 Average Chain Length

The average chain length (ACL) describes the average number of carbon atoms per molecule based on the abundance of the odd-carbon-numbered higher plant *n*-alkanes (Poynter 1991), this is calculated from equation 2.2 (chapter 2, section 2.1.2.2). The formula used to calculate ACL can been adapted to fit the range of compounds detected within a particular *n*-alkane extract, and in terms of the current study, the formula was adapted to calculate ACL for chains ranging from nC_{21} to nC_{33}, as this was the total range of *n*-alkane chains detected. This numerical ratio representation of the molecular distribution and abundance of individual *n*-alkane chains (Vogts, Schefuß et al. 2012) is the most widely applied quantification technique when *n*-alkane samples extracted from preserved sediments are compared to living modern vegetation.

The extensive available literature utilizing ACLs in the interpretation of preserved sedimentary *n*-alkanes is a result of the suggested characteristic molecular distributional differences reported for the different organisms which synthesize them (Seki, Nakatsuka et al. 2010). For example, Cranwell (1973) suggested vegetation type was the major

influence on chain length, and it has since been reported that ACLs nC_{17} to nC_{21} are indicative of algae and bacterial sources (Polissar and Freeman 2010), ACLs below nC_{23} are primarily produced by submerged aquatic plants, nC_{23} to nC_{25} are indicative of floating aquatic plants (Ficken, Li et al. 2000, Zech 2009), nC_{27} to nC_{29} are generally derived from trees and shrubs, and nC_{31} to nC_{33} are major constituents of grasses (Cranwell 1973, Michener and Lajtha 2008, Zech 2009).

In terms of the current thesis, and focusing on modern vegetation, it has also been hypothesized that the distributions observed within an individual are the result of the plants environment (Ficken, Li et al. 2000). For example, Cranwell (1973) reported the ACL for grassland species was on average greater than lipids derived from forest plants. This finding was further corroborated by Vogts et al., (2012), where similar differences were observed in ACL between savanna and rainforest species. Although this is a valid interpretation, taking a plant physiological approach, it may not be the variation as a result of species, but the prevailing environmental conditions of these two ecosystems that result in the differences observed. This conclusion appears to be valid as there is extensive literature detailing the potential influence of temperature, relative humidity (RH), and incoming photosynthetically active radiation (PAR), on the abundance and molecular distributions of leaf waxes (Shepherd and Griffiths 2006). Unfortunately, in natural ecosystems all of these variables act at the same time making it very difficult to separate and disentangle all their varying influences (Sachse 2006, Shepherd and Griffiths 2006). In addition, another factor that complicates matters further is exactly when and how often *n*-alkanes are synthesized during the ontogeny of a leaf.

Whether *n*-alkanes are continuously synthesized throughout the entire life of a leaf is currently a highly debated topic. Field observations have indicated continuous *n*-alkane synthesis throughout the growth season for deciduous tree species (Piasentier 2000, Sachse 2006, Pedentchouk 2008, Sachse 2009, Gao, Tsai et al. 2012). Mature fully expanded leaves have also shown substantial changes in their *n*-alkane concentrations and compositions with time (Prügel, Loosveldt et al. 1994, Shepherd and Griffiths 2006, Gao, Tsai et al. 2012). However, observations from controlled greenhouse growth experiments conducted on *Populus trichocarpa* seedlings indicate *n*-alkanes are not continuously synthesized throughout the growth period of an individual during the normal ontogeny of the plant (Kahmen 2011).

Nevertheless, environmental stresses are suggested to be a crucial trigger in the *de novo* synthesis of new *n*-alkanes within the leaf waxes (Shepherd and Griffiths 2006, Gao,

Burnier et al. 2012), as significant amounts of wax removal have been observed as a result of washing by rain, as well as wind ablation (Baker and Hunt 1986, Gao, Burnier et al. 2012). The reported lack of continuous *n*-alkane synthesis in *Populus* seedlings (Kahmen 2011), may be due to the lack of a natural "Environmental stressor" in the controlled growth experiments, and this highlights the need for in-depth field investigations within natural ecosystems.

3.1.4 Environmental and climatic effects on ACL

As mentioned previously, there is extensive literature available detailing the potential influence of various climatic factors on leaf wax morphology from a plant physiological perspective (Shepherd and Griffiths 2006), as well as a paleo-environmental proxy perspective (Eglinton 2008).

Variations in ACLs have been linked to variations in latitude, temperature, RH, PAR levels, precipitation, and even altitude. As temperature and light intensity are known to vary with latitude, and water availability and RH are closely linked, it is not surprising to find numerous studies linking these parameters to changes in ACL that all appear to be in agreement. For example, higher ACLs have been associated with the lower latitudes (Poynter, Farrimond et al. 1989, Poynter 1991, Sachse 2006), with estimated shifts in ACL ratios of 0.04 for a 1-degree change in latitude (Jeng 2006).

It has also been suggested that the longer chain homologues are produced in higher concentrations in warmer climates (Poynter, Farrimond et al. 1989, Castañeda, Werne et al. 2009), and morphological studies have shown waxes with higher ACLs, in conjunction with narrower chain ranges, may have a higher melting point as they maintain their crystalline structure at higher temperatures (Riederer and Schneider 1990). In addition, populations of *Austrocedrus chilensis* from Argentina and Chile, inhabiting more arid environments with higher annual temperatures, presented higher proportions of the longer chains within their waxes when compared to populations growing at the considerably cooler, and more humid rainforest boundary (Dodd, Rafii et al. 1998). Furthermore, more recent research has indicated an increase in ACL from rainforest species to savannah species (Vogts, Moossen et al. 2009). Despite these findings, it is important to note the extensive inconsistencies in the sampling methodology for the aforementioned investigation (Vogts, Moossen et al. 2009), with leaves collected at varying stages of development, different times in the growth season, and over a 13 year period all being compared.

It can be seen that these studies not only make comparisons between extremes in temperature, but also varying RH and water availability regimes, proving once again that these variables are inherently linked. For example, ACL was found to decrease with increasing distance from the more humid coastal region for conifer species in Oregon (Oros, Standley et al. 1999), and a greater correlation between higher annual rainfall and lower carbon chain lengths have also been reported (Dodd, Rafii et al. 1998). Furthermore, atmospheric dust samples collected along the West African coast were found to contain longer chain homologues when they originated from more arid regions (Huang, Dupont et al. 2000, Schefuß, Ratmeyer et al. 2003). However, it is important to note, there is currently no information available on the independent effects of temperature, RH, and/ or PAR, making it difficult to disentangle which variables have greatest influence.

In addition to the climatic variables mentioned previously, light intensity and stimulation by light is thought to be a key process in the *de novo* synthesis of leaf wax lipids (Shepherd and Griffiths 2006); yet, the research to date on this subject is somewhat contradictory. Earlier works (Nødskov Giese 1975, Shepherd, Robertson et al. 1995, Shepherd, Robertson et al. 1997) suggest a shift towards shorter chain homologues under higher irradiation levels, while an increased abundance in shorter chains was associated with a high intensity of UV-B light for *Nicotiana tabacum* (Barnes, Percy et al. 1996). Contrary to this, Sachse et al (2006) have suggested that trees with a longer growth season, and greater levels of incoming solar radiation, synthesize greater chain length *n*-alkanes to protect the leaves from water loss. It should be noted they also put forward an alternate potential explanation for the observed high ACLs, where they attribute the loss of the shorter chained, and less heat stable, *n*-alkanes to selective evaporation (Sachse 2006).

Aside from the climatic variables mentioned previously, there are a multitude of other factors that could potentially affect the composition of *n*-alkanes in leaf waxes, such as soil nutrient status, genetics, altitude, and pollution (Percy, Cape et al. 1994, Shepherd and Griffiths 2006). Currently, there is a lack of available literature dealing with these aspects in any great detail. However, there has been a suggestion of a strong genetic influence for the adaption of hydrocarbons to environmental parameters for species of the *Cupressaceae* family (Dodd and Afzal-Rafii 2000), this is despite the limited amount of literature available detailing the many genes involved and their various functions (Shepherd and Griffiths 2006).

As can be seen by the vast number of interacting factors, it is clear that more research is needed to disentangle all the possible influencing parameters. The influence of these

factors, and how they work in combination, or isolation, is reflected in the relative abundance and composition of the synthesized *n*-alkanes chains. How these fast turnover compounds are influenced by these factors are closely associated with the controls of biosynthesis, and as a result, how they change with time, in relation to the changing stresses, may provide insight into the biochemical processes within the plants themselves.

3.1.5 Carbon Preference Index

The Carbon Preference Index (CPI) calculates the odd/even predominance of carbon number range, it is generally most applicable to paleo-reconstructions, and is described by equation 2.1 (chapter 2, section 2.1.2.2) (Allan 1977, Marzi, Torkelson et al. 1993). In a manner similar to the equation 2.2, the range of *n*-alkanes for which this was calculated (nC_{21} to nC_{33}) was chosen as a result of the range of *n*-alkanes detected within the *n*-alkane extracts of this study.

Traditionally in organic geochemistry, CPIs are used as a numerical indicator of the levels of lipid diagenesis within the sediment record (Meyers and Ishiwatari 1995). CPIs are also applied to sediments to identify the level of petrogenic contamination (Vogts, Moossen et al. 2009, Vogts, Schefuß et al. 2012), and/or the maturity level of oils (Marzi, Torkelson et al. 1993). Nevertheless, in more recent times, and in the context of the current thesis, CPIs have been applied to hydrocarbons extracted from preserved sediments as a tool to determine *n*-alkane source (Rielley, Collier et al. 1991, Jeng 2006) during paleo-environmental reconstructions. For example, a study detailing the molecular distributions of 26 different plant species, including a range of photosynthetic pathways and plant types, reported CPI ratios ranging from 2.3 to 54.3 (Bi, Sheng et al. 2005). Where, within Paleo-environmental reconstructions, CPI ratios less than 3 are reported to indicate petrogenic contamination within the sediments and/or a greater sediment input from marine/aquatic organisms (Farrington and Tripp 1977, Jeng 2006, Eglinton 2008, Vogts, Moossen et al. 2009, Vogts, Schefuß et al. 2012), while CPIs greater than 5 indicate significant contribution from terrestrial plant material (Rielley, Collier et al. 1991, J.I. Hedges 1993, Bi, Sheng et al. 2005, Vogts, Moossen et al. 2009, Vogts, Schefuß et al. 2012).

In addition to using CPIs to identify the level of contamination within a particular sediment sample, several recent publications have tried to relate CPIs to aspects of climate. For example, investigations conducted on a deep-sea sediment transect off South-West Africa report a shift in CPI from ~4 in the north, to ~7 further south (Vogts, Schefuß et al. 2012).

After mass spectral investigation of the extracted samples, they found similarly small amounts of 17-hopane; an indication of petrogenic contamination, across all of their samples, suggesting petrogenic contamination was not an issue. However, they did not find a corresponding shift in CPIs within the existing terrestrial vegetation adjacent to the transect, and suggest the most likely cause of this was due to the extent of degradation of the wax carrying components (Vogts, Moossen et al. 2009).

Other publications have also suggested a link between plant environment and CPI ratios. For example, a study conducted on 45 soil surface samples spanning 18°N- 50°N in Eastern China reported higher CPIs in the colder, drier, areas when to compared to the warmer tropical regions (Rao 2009). It is suggested this trend is due to moisture levels in the warmer tropical regions facilitating more rapid microbial breakdown of *n*-alkanes in sediments (Rao 2009, Vogts, Schefuß et al. 2012), however, there is no information on CPI ratios from the corresponding vegetation available for comparison.

3.2. Aims

The interpretation of *n*-alkanes extracted from sediment records for paleoclimate reconstructions is based upon bulk extractions of *n*-alkanes from multiple potential sources. It would appear that diagnostic molecular distribution techniques, such as CPI and ACL, are being applied to identify the major sources of *n*-alkanes within sediments without a clear understanding of how these can vary within existing vegetation, in natural environments. There also seems to be a complete lack of field studies addressing the potential compositional variations in *n*-alkanes within, and between, individuals of the same species.

This current study utilized the documented variations in environmental parameters within the crown of large trees, as well as several individuals of varying size, to investigate how the molecular distributions and total concentrations of *n*-alkanes vary spatially, and temporally, in relation to environmental conditions. Variations in climatic variables with height in the canopies of natural forest ecosystems are a well-established concept. Where significant gradients of PAR, RH, temperature, and wind speed can exist. Typically, with increased light and wind speed with increasing height from the forest floor (Niinemets, Kull et al. 1999, Niinemets, Sonninen et al. 2004, Duursma and Marshall 2006). As RH, PAR, and temperature have been suggested to be key parameters in influencing the concentration and molecular composition of *n*-alkanes, it is hoped that natural variations in these parameters, in the crowns of large trees, will be reflected in the composition of the *n*-alkanes synthesized in these areas.

To this end Scots pine (*Pinus sylvestris)* needles from multiple individuals of varying age, and in different geographical locations, were sampled during multiple field campaigns with the aim of addressing the following questions:

1. Can a conifer species significantly contribute to the sediment record?
2. How do the molecular distributions of conifers compare to other species?
3. What is the level of variation in *n*-alkane concentration and molecular distributions within natural forest ecosystems? Are these constant across individuals and with time?
4. Do sample collection height, and/or aspect, have any effect on total *n*-alkane concentrations and/or molecular distributions?

3.3. Methods

In brief, samples of needle material collected from Värriö Strict Nature Reserve, North-Eastern Finnish Lapland, and the Black Wood of Rannoch, Perthshire, Scotland have been subject to comparison (full site descriptions available in chapter 2 sections 2.2.1 to 2.2.1.4). Samples were collected at the beginning and end of the 2010 growth season, during April and October for the Scottish site, and during July and September for the Finnish site.

The current year's growth of needles, i.e. Y0 needles, were collected from the top, middle and lower crown on the north and south facing sides of Scots pine trees (*Pinus sylvestris*) of varying size and age. Samples were collected from large trees (25-30m), medium trees (15-25m), small trees (5-15m), and saplings (<3m), with saplings sampled at only one south facing point at 2m high. A total of 28 samples were collected in both October and April from Scotland, and 28 samples collected in both July and September from Finland. In total, 4 saplings, 2 medium trees, and 2 large trees were sampled from the Scottish and Finnish sites respectively.

Samples were prepared and *n*-alkanes extracted for each sample point, in each geographical location, at the beginning and end of the growth season. For full sampling and analytical details and methodology please refer to chapter 2, section 2.2.2. All data presented within the following chapter was processed in Microsoft Excel® and R, where result of statistical tests producing a P value < 0.05, and an adjusted R^2 value above 0.25 are considered statistically significant. These thresholds were deemed appropriate due to the heterogeneous nature of the natural environments under investigation.

3.4. Results

3.4.1. Finland *n*-alkane abundances

The total *n*-alkane concentrations, from the 28 samples collected during July 2010 in Finland, display a range of 1.52 - 13.34 µg/g DM (Dried mass). While the repeated sampling of the same locations during September, yielded a range in total *n*-alkane concentrations of 2.62 – 76.76 µg/g DM. The mean *n*-alkane concentration for July was 8.06 ± 2.21 µg/g DM (SEM, n=28), while the mean concentration for September was 25.14 ± 4.58 µg/g DM (SEM, n=28). This indicates a statistically significant increase in the total *n*-alkane concentration of the Finnish Scots pine during the course of the 2010 growth season (paired t-test, t=-4.26, P=0.0002, n=28) (complete raw data is available in table 1 in the appendix).

This trend can be clearly observed in the gas chromatogram examples. Figure 3.1 is the GC-FID output of the Very large tree south top sample collected in July, while figure 3.2 is the same sample collected in September.

Figure 3.1: Gas chromatogram of the very large tree south top July 2010 *n*-alkane extract, the individual *n*-alkanes are marked by their respective carbon number below the x-axis. The numbers depicted at the tip of each peak represent the retention times of each compound and the peak eluting at 15.481 represents Androstane which was a standard added during the extraction in order to quantify *n*-alkane concentrations.

It can be seen that although roughly the same amount of foliar material was extracted, there is a clear shift in the relative peak sizes of the individual plant synthesized *n*-alkanes in relation to the added standard (Androstane), which elutes at 15,481 minutes in figure 3.1 and 15.451 minutes in figure 3.2. This significant shift in the ratio of added standard to *n*-alkanes detected within the hexane extracts, with the standard peak displaying much lower intensity in relation to the *n*-alkanes in September in comparison to July, shows the

significant increase in concentrations, and is a consistently observed among all other samples.
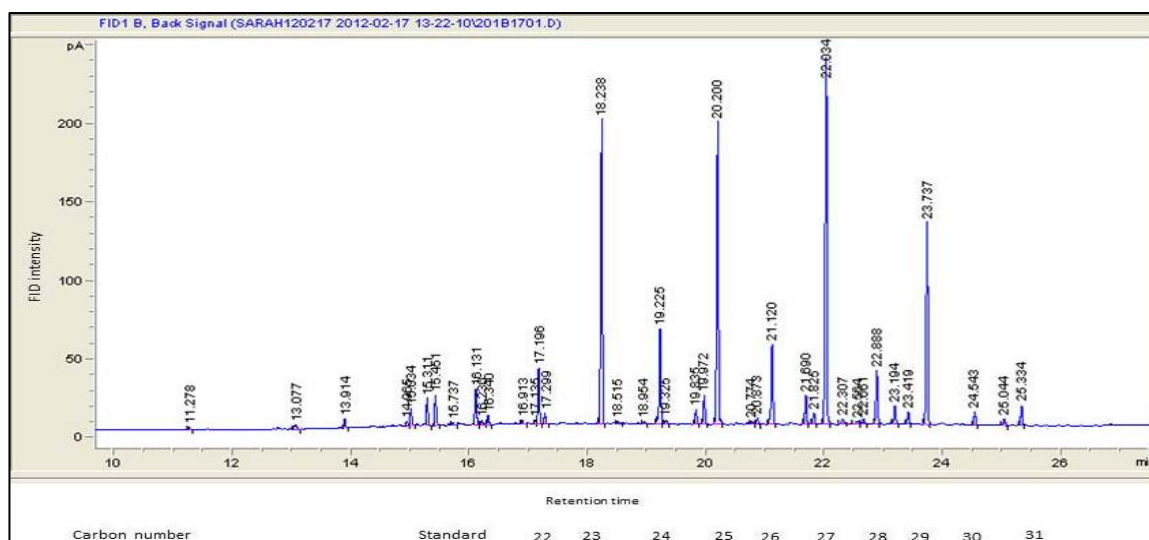
Figure 3.2: Gas chromatogram of the very large tree south top September 2010 *n*-alkane extract, the individual *n*-alkanes are marked by their respective carbon number below the x-axis. The numbers depicted at the tip of each peak represent the retention times of each compound and the peak eluting at 15.451 represents Androstane which was a standard added during the extraction in order to quantify *n*-alkane concentrations.

The mean total *n*-alkane content increases from July to September across all the different size/aged trees investigated (figure 3.3). Not only does the *n*-alkane content increase in September, but the variability in total *n*-alkane concentrations (depicted by the error bars which represent SEM) also increases.
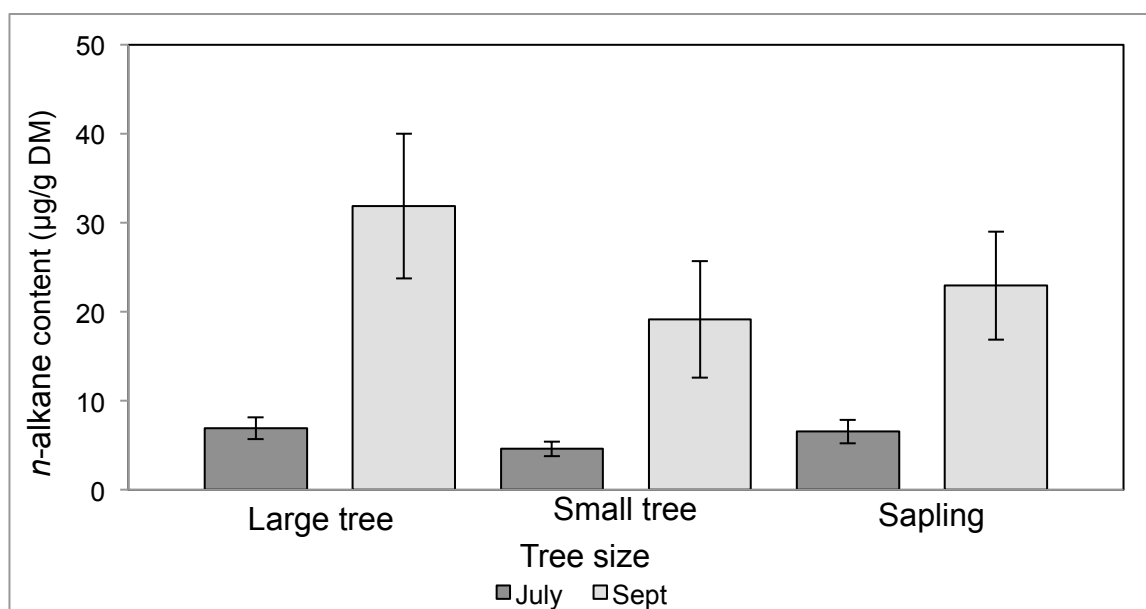
Figure 3.3: Mean total *n*-alkane concentration (µg/g DM) by tree type for the Finnish data. Dark bars show July 2010 data, while light grey depict September 2010 values. Error bars represent the standard error of the mean (SEM).

To test the effect of each of the sample locational variables on total *n*-alkane concentration during the Finnish sample campaigns, the data set was subjected to Two-

way ANOVAs (table 3.1). Two-way ANOVA, with individual tree size and relative height in the crown as categorical factors, and total *n*-alkane concentrations as the continuous factor, failed to detected significant variation in total *n*-alkane concentrations as a result of different size/aged individual trees during July or September (table 3.1). This suggests *n*-alkane concentrations are not driven by individual tree size/age in the Finnish Site. Total *n*-alkane concentrations also show clear increases between July and September for all relative heights within the crown (figure 3.4), with September data showing much greater variation than July (SEM error bars, figure 3.4).

Table 3.1: Summary of two-way ANOVAs applied to the total n-alkane concentration data (µg/g DM) for the Finnish sample sites. Total n-alkane concentration was the continuous factor and individual tree size/age and relative height in the crown were the categorical factors.

Time	Source	DF	F	P
	Tree Size	2	1.31	0.29
	Relative height	2	0.48	0.62
	Interaction	2	0.8	0.46
July	Residuals	21		
	Tree Size	2	0.86	0.44
	Relative height	2	0.29	0.75
	Interaction	2	2	0.16
Sept	Residuals	21		
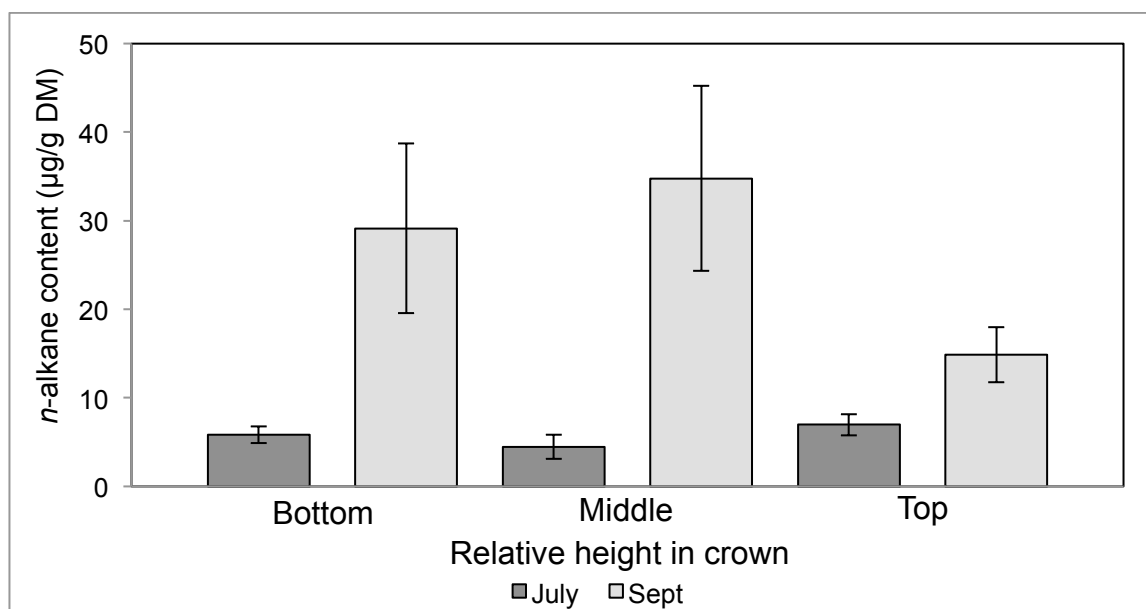
Figure 3.4: mean total *n*-alkane concentrations (µg/g DM) by relative height within the crown for the Finnish data, dark bars represent July 2010 and light grey bars show September 2010. Error bars show the standard error of the mean.

The largest increase in total *n*-alkane concentration was observed in the middle of the crown. However, two-way ANOVA failed to attribute any significant variation in concentrations as a result of relative height in the crown during July, or September (table 3.1). In addition, no significant variation as a result of the interaction between individual

tree size and relative height within the crown for each sample period was reported (table 3.1).

3.4.2. Scotland *n*-alkane abundances

The findings of the Finnish sample site are in contrast to the observations from the Scottish sample sites. Scottish Scots pine total *n*-alkane content, observed across all tree categories, sample locations, and time in the growth season, is much lower than the Finnish sample sites (Full sample descriptions and raw data appendix table 2). Total *n*-alkane concentrations for April 2010 ranged 2.68 – 15.95 µg/g DM, while a range of 3.6 – 7.62 µg/g DM was observed in October 2010. In addition, mean total *n*-alkane concentrations were 6.91 ± 0.53 µg/g DM (SEM, n=28) in April 2010, and 6.68 ± 0.57 µg/g DM (SEM, n=28) in October, and show no statistically significant difference (paired t-test, t= 0.30, P=0.77). There is no clear trend in total *n*-alkane concentrations between April and October across the different sized/aged trees studied in Scotland (figure 3.5), along with no systematic increase in variation (SEM, error bars, figure 3.5). Two-way ANOVAs (table 3.2), with tree size and relative height in the crown as categorical factors, and total *n*-alkane concentration as the continuous factor did not detect a statistically significant amount of variation as a result of tree size/age during April, or October.
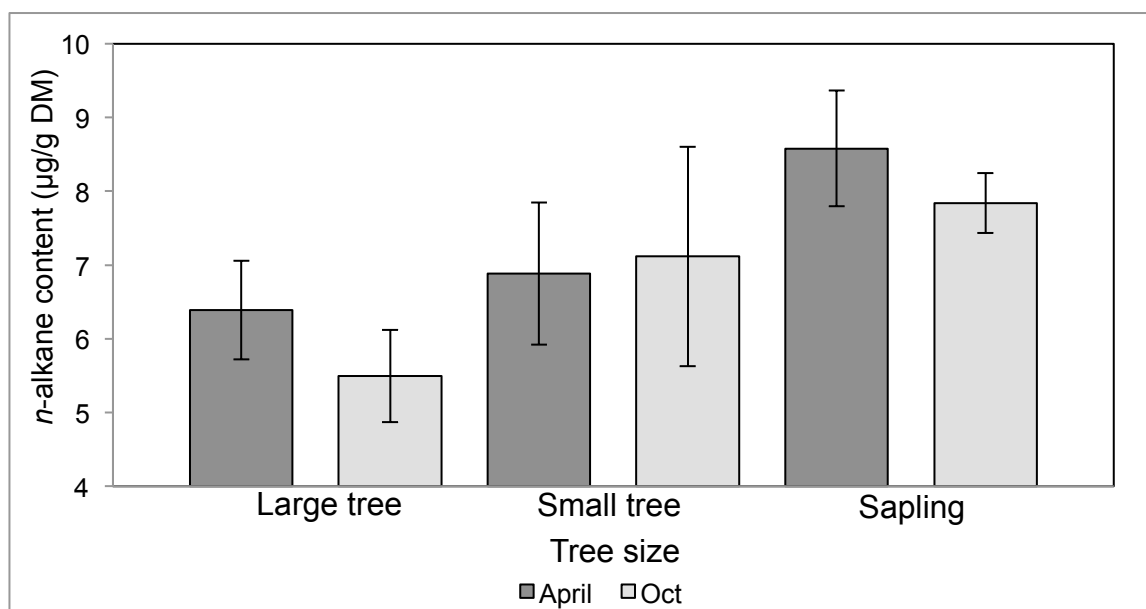
Figure 3.5: Mean total *n*-alkane concentration (µg/g DM) by tree type for the Scottish data. Dark bars show April 2010 data, while light grey depict October 2010 values. Error bars represent the standard error of the mean (SEM).

Total *n*-alkane concentrations also showed no consistent trends between April and October for all relative heights within the crown in Scotland (figure 3.6). Two-way ANOVAs (table 3.2) found no significant variation as a result of relative height in the crown during

April; however, a statistically significant relationship was detected during October (F=5.12, P=0.02).

Table 3.2: Summary of two-way ANOVAs applied to the Scottish Scots pine total n-alkane concentration data. Total n-alkane concentration (µg/g DM) is the continuous factor and individual tree size and relative height in the crown are the categorical factors. Significant results are marked with "*".

Time	Source	DF	F	P
	Tree Size	2	0.99	0.39
	Relative height	2	1.74	0.20
	Interaction	2	1.27	0.30
April	Residuals	21		
	Tree Size	2	1.78	0.19
	Relative height	2	5.12	0.02 *
	Interaction	2	1.40	0.27
Oct	Residuals	21		

These findings suggest position within the crown causes significant variation in total *n*-alkane concentrations during October across all trees sampled. However, no statistically significant variation is detected as a result of the interaction between tree size, and relative height in the crown during April or October (table 3.2).
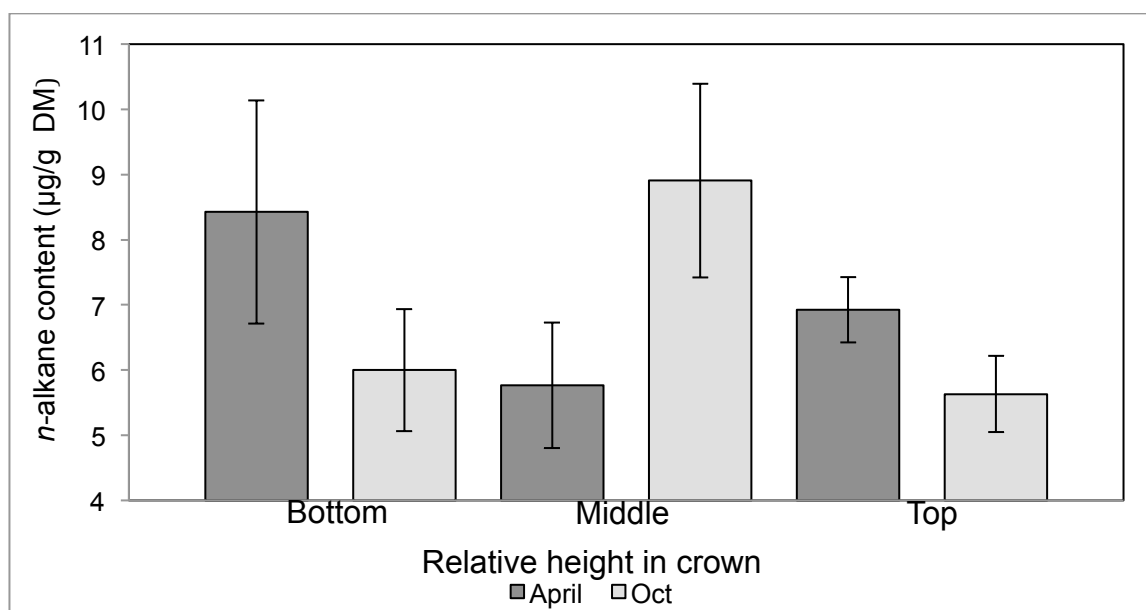
Figure 3.6: mean total *n*-alkane concentrations (µg/g DM) by relative height within the crown for the Scottish data, dark bars represent April 2010 and light grey bars show October 2010. Error bars show the standard error of the mean.

3.4.3 The effect of sample position on total *n*-alkane concentration

3.4.3.1. Finland

Examination of the relationship between total *n*-alkane concentration and height of sample appear to show strong positive correlations during September, but little correlation during July (figure 3.7). Simple linear regression analyses (table 3.3) failed to detect statistically significant correlations between height of sample and north facing needles during July, and height of sample and south facing needles during July (table 3.3).

Table 3.3: Summary of the simple linear regression analyses applied to the Finnish data, where "North" and "South" represent northern and southern aspect needles.

Time	x,y	Equation	Adjusted R^2	F	P
	Height vs. North	Y=0.2841x + 2.6718	0.18	3.94	0.07
July	Height vs. South	Y=0.2401x + 4.7615	0.11	2.63	0.13
	Height vs. North	Y=1.5933x + 8.50	0.03	1.46	0.25
Sept	Height vs. South	Y=1.3718x + 17.351	0.12	2.70	0.13
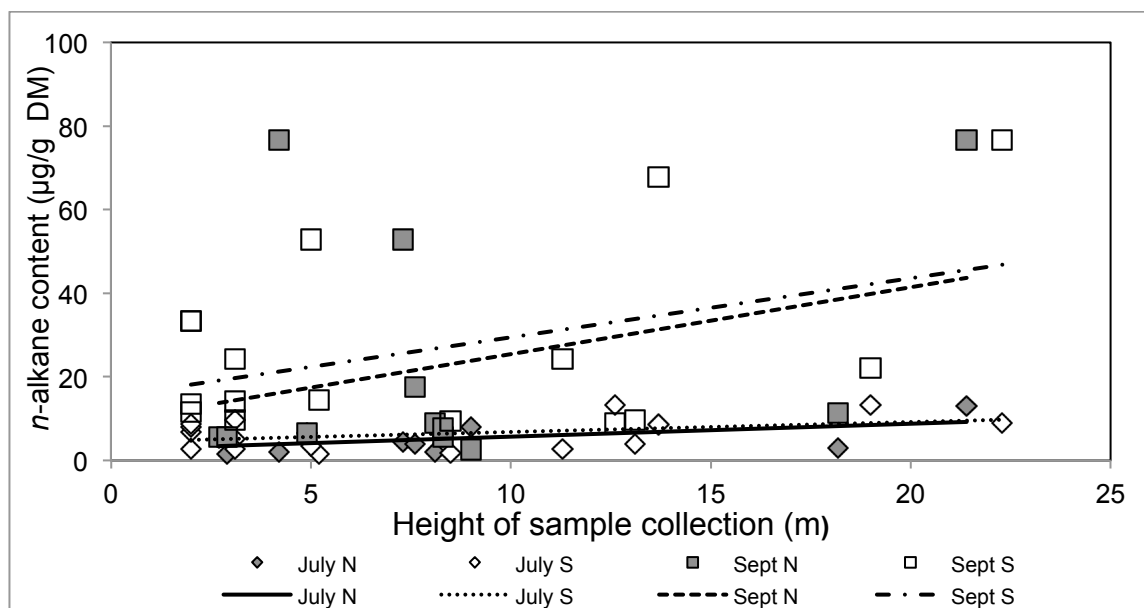
Figure 3.7: The total *n*-alkane concentration in µg/g DM against measured height (m) of sample collection for the whole Finnish data set. Dark diamonds represent July 2010 north aspect data, while light diamonds July 2010 South aspect data. Dark squares are September 2010 north aspect data and white squares September south aspect data. Trend lines show the results of simple linear regressions.

However, a two-way ANOVA (table 3.4), with height of sample and aspect as categorical factors, and total *n*-alkane concentration as the continuous factor, did attribute a statistically significant amount of variation in total *n*-alkane concentration to height of sample during July (F=6.26, P=0.02), with no statistically significant variation as a result of aspect, or the interaction of height and aspect (table 3.4).

Table 3.4: Two-way ANOVA summary for the Finnish Scots pine data set where height of sample collection (m), and aspect are the categorical factors and total *n*-alkane concentration (µg/g DM) as the continuous factor. Significant results are depicted with a "*".

Time	Source	DF	F	P
	Height	2	6.26	0.02 *
	Aspect	2	1.93	0.18
	Interaction	2	1.01	0.33
July	Residuals	21		
	Height	2	3.90	0.06
	Aspect	2	0.62	0.44
	Interaction	2	0.52	0.48
Sept	Residuals	21		

Additionally, although figure 3.7 suggests strong positive correlations between height of sample and concentration for both north and south facing needles during September, simple linear regression analyses do not support this finding (table 3.3). No statistically significant correlation was observed between both north facing needles and height, and south facing needles and height. Two-way ANOVA also failed to detect statistically significant variation as a result of height of sample, aspect, or the interaction between height and aspect in the September data (table 3.4). These data suggests that height of sample affects the *n*-alkane concentrations of scots pine needles during July only.

3.4.3.2. Scotland

The Scottish data shows no statistically significant relationship between height of sample collection and *n*-alkane concentration for either north or south facing needles during April (figure 3.8, table 3.5). In addition, no relationship is observed between height of sample and total *n*-alkane concentration for either north, or south facing needles during October (figure 3.8, table 3.5).

Table 3.5: Summary of simple linear regression analyses applied to the Scottish Scots pine data, the "x,y" column indicates which variables are subject to the correlation, statistically significant results are marked with "*".

Time	x,y	Equation	Adjusted R^2	F	P
	Height vs. North	Y=0.06901x +6.347	-0.09	0.11	0.75
April	Height vs. South	Y=-0.0483x+7.1245	-0.06	0.14	0.71
	Height vs. North	Y=0.1111x + 5.297	-0.10	0.11	0.74
Oct	Height vs. South	Y=0.1217x+4.30075	0.13	3.23	0.09
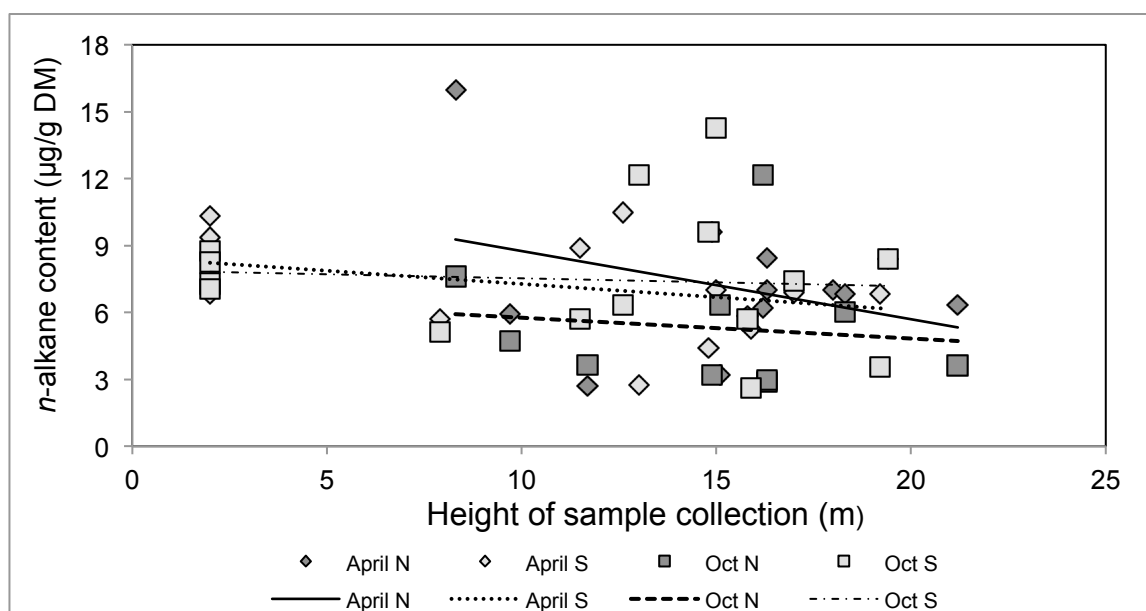
Figure 3.8: The total *n*-alkane concentration in μg/g DM against the measured height (m) of sample collection. Dark diamonds represent April 2010 north aspect data, while light diamonds April 2010 South aspect data. Dark squares are October 2010 north aspect data and white squares October south aspect data. The trend lines depict simple linear regressions.

Both simple linear regressions, and two-way ANOVAs (table 3.6), do not report any statistically significant variation as a result of height, or aspect, in the total *n*-alkane concentrations observed in Scotland during either April or October.

Table 3.6: Results summary of two-way ANOVAs applied to the Scottish Scots pine data sets, where height and aspect are categorical factors and total n-alkane concentration (μg/g DM) is the continuous factor. Statistically significant results are marked with "*".

Time	Source	DF	F	P
	Height	2	0.00	0.99
	Aspect	2	1.08	0.38
	Interaction	2	0.12	0.73
April	Residuals	21		
	Height	2	2.21	0.15
	Aspect	2	0.13	0.94
	Interaction	2	0.07	0.80
Oct	Residuals	21		

3.4.4 Average chain length

The Average Chain Length (ACL) for the *n*-alkane chains ranging nC_{23} to nC_{33} (equation 2.2), modified from (Poynter 1991), are reported for the Finnish and Scottish sample sites (raw data table 1 appendix). It should be noted that in a few cases poor compound separation on the GC-FID column resulted in missing measurements, as individual peak areas could not be easily and reliably quantified. Therefore, in the statistical data reported within the following sections, in any case where n= less than 28, this is due to unobtainable peak area data.

3.4.4.1. Finland Average Chain Length

ACL data from the Finnish site are in the range of 22.58 – 26.03 for July, with a mean of 23.69 ± 0.15 (SEM, n=26). While September ACLs range 22.08 – 26.15, with a mean of 24.69 ± 0.23 (SEM, n=24), giving a statistically significant increase in mean ACL of 1.0 from the Beginning (July) to the end (September) of the 2010 Finnish growth season (paired t-test, t=-5.37, P=2.52E^{-05}).
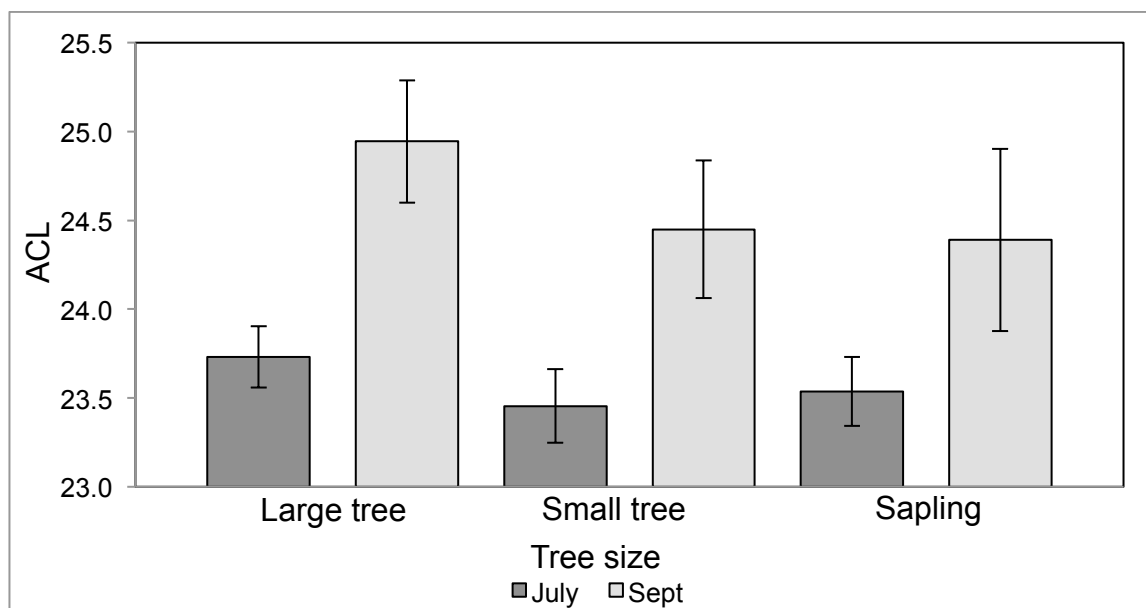
Figure 3.9: Mean average chain length (ACL) by tree type for the Finnish data. Dark bars show July 2010 data, while light grey depict September 2010 ratios. Error bars represent the standard error of the mean (SEM).

Mean ACLs show a clear increase between July and September for each tree size/age category examined (figure 3.9). Two-way ANOVA (table 3.7), with individual tree size/age and relative height in the crown as categorical factors, and ACL as the continuous factor, did not detect statistically significant variation as a result of tree category during July or September (table 3.7). This suggests individual tree size/age is not a major influencing factor on ACLs within Finnish Scots pine at any time during the growth season.

Table 3.7: Summary of a two-way ANOVA of Finnish ACL as the continuous factor and individual tree size and relative height in the crown as the categorical factors.

Time	Source	DF	F	P
	Tree Size	2	0.52	0.60
	Relative height	2	0.07	0.94
	Interaction	2	0.65	0.64
July	Residuals	21		
	Tree Size	2	0.58	0.57
	Relative height	2	0.28	0.76
	Interaction	2	1.00	0.44
Sept	Residuals	21		

In addition, ACLs averaged by relative height in the canopy, i.e. top, middle, and bottom of the individual tree crown, also show clear increases in ACL between July and September (figure 3.10); with relatively consistent ACLs, exhibiting little variation (SEM, error bars, figure 3.10) in each position within the crown during July. However, during September, the middle of the tree crowns exhibit the highest ACLs, with the September data set showing much greater overall variation (SEM, error bars, figure 3.10). Nevertheless, two-way ANOVA (table 3.7) does not attribute a statistically significant amount of variation in ACL to be the result of relative height within the crown during July, or September. Furthermore, no significant variation as a result of the interaction between individual tree size, and relative height in the crown is observed during both July and September
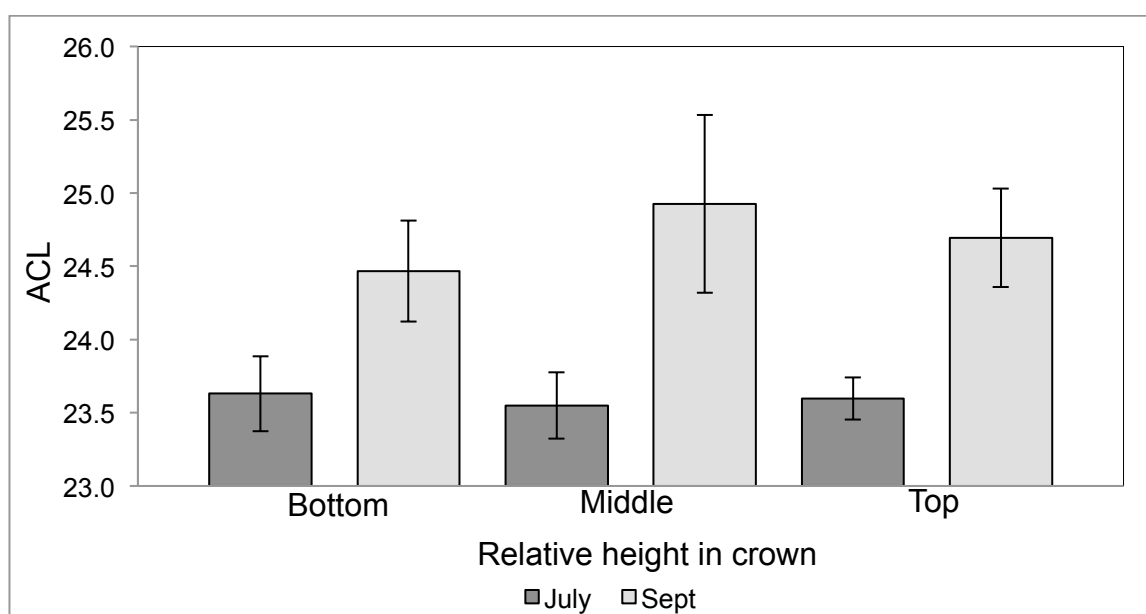
Figure 3.10: Mean average chain length (ACL) by relative height within the crown for the Finnish data, dark bars represent July 2010 and light grey bars show September 2010. Error bars show the standard error of the mean.

3.4.4.2. Scotland Average Chain Length

The ACL data from the Scottish field site exhibits different trends to the Finnish observations (raw data, table 2 in the appendix). The nC$_{23}$ n-alkane chain length homologue is the most common, and in the highest concentrations across all samples and times in growth season. However, the mean ACL across all samples collected in April 2010 is 24.9 ± 0.17 (SEM, n=28), while October mean ACL is 24.17 ± 0.16 (SEM, n=28). This shows a statistically significant decrease in mean ACL of 0.73 with time in the growth season (paired t-test, t=3.082, P=0.0047).
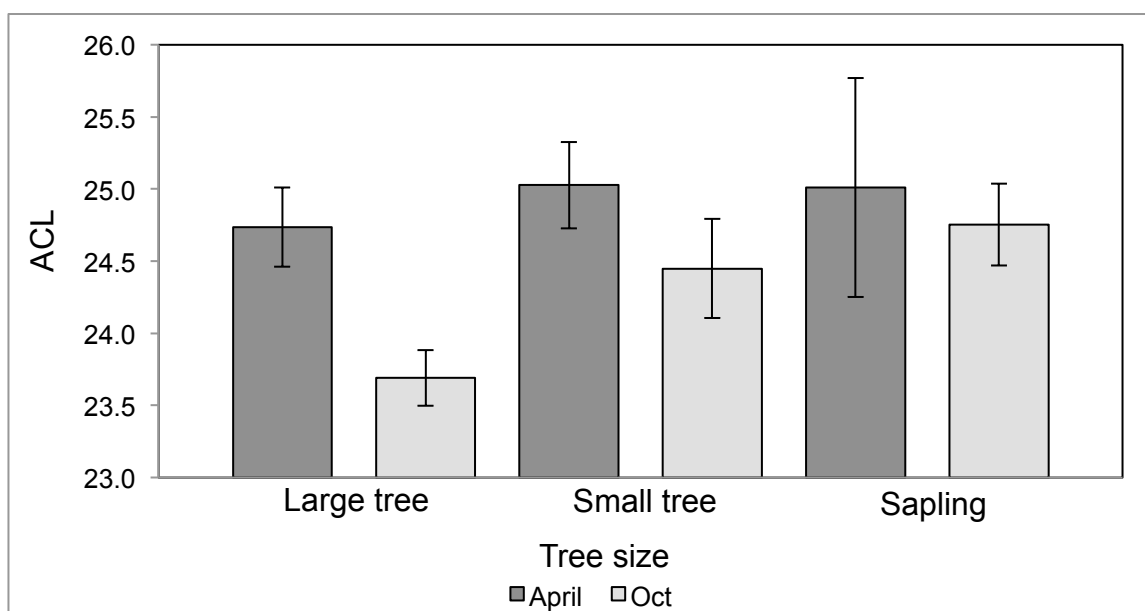
Figure 3.11: Mean average chain length (ACL) by tree type for the Scottish data. Dark bars show April 2010 data, while light grey depict October 2010 ratios. Error bars represent the standard error of the mean (SEM).

Mean ACL decreased across all tree size/age categories with time in the growth season (figure 3.11), and similar applications of a two-way ANOVA (table 3.8) show no statistically significant variation as a result of individual tree size/age during April.

Table 3.8: Two-way ANOVA summary of Scottish Scots pine ACL data from April and October 2010. ACL is the continuous factor while individual tree size and relative height in the canopy are the categorical factors, significant results are marked "*".

Time	Source	DF	F	P
	Tree Size	2	0.32	0.73
	Relative height	2	0.55	0.59
	Interaction	2	1.15	0.34
April	Residuals	21		
	Tree Size	2	4.33	0.03*
	Relative height	2	0.53	0.50
	Interaction	2	0.55	0.58
Oct	Residuals	21		

Yet, a statistically significant variation as a result of individual tree size/age is reported for October (F=4.33, P=0.03). This indicates that individual tree size can affect the ACLs at the end of the Scottish growth season, with increasing ACL with decreasing tree age/size. ACLs also show a clear decrease between April and October for all relative heights within the tree crown (figure 3.12). However, two-way ANOVA (table 3.8) failed to detected statistically significant variation as a result of relative height within the crown during both April and October. No significant effect of the interaction between individual tree size and relative height in the crown was also reported during April or October (table 3.8).
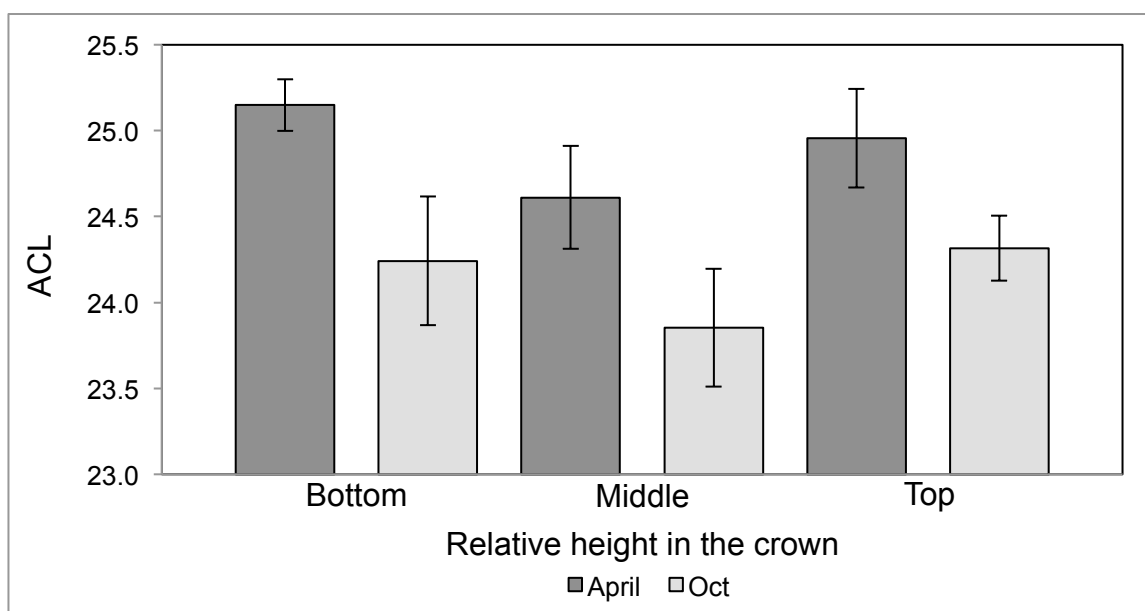
Figure 3.12: Mean average chain length (ACL) by relative height within the crown for the Scottish data, dark bars represents April 2010 and light grey bars show October 2010. Error bars show the standard error of the mean.

3.4.5 The effect of sample position on Average Chain Length

3.4.5.1 Finland

Investigations into the effects of sample collection height, and aspect, on the ACLs of Scots pine inhabiting Finnish Lapland (figure 3.13) appear to show strong positive correlations between height of sample and south facing needles during both July and September. Although simple linear regressions report a high statistical significance of these correlations with adjusted R^2=0.26, F=6.12, P=0.03 observed during July, and, adjusted R^2=0.38, F=8.85, P=0.01 during September (table 3.9).

Table 3.9: Summary table of simple linear regression analyses conducted on the Finnish Scots pine ACL data for each sample period. The "x,y" depicts the two variables subject to correlation where "north" and "south" refer to the aspect of the vegetation. Significant results are marked with "*".

Time	x,y	Equation	Adjusted R^2	F	P
	Height vs. North	Y=-0.0004x+23.502	-0.10	0.00	0.99
July	Height vs. South	Y=0.0495x+23.2	0.26	6.12	0.03*
	Height vs. North	Y=0.0374x+23.823	-0.08	0.32	0.59
Sept	Height vs. South	Y=0.101x+23.953	0.38	8.85	0.01*

Two-way ANOVAs (table 3.10), with height of sample collection and aspect as categorical factors, and ACL as the continuous factor, did not detect significant variation as a result of sample collection height during July or September. In addition, no significant effect of aspect, or the interaction between height and aspect, was observed during July or September (table 3.10).

Table 3:10: Summary table of two-way ANOVAs applied to the Finnish ACL data sets, where ACL is the continuous variable and height of sample collection (m) and Aspect are the categorical variables. Significant results are marked "*".

Time	Source	DF	F	P
	Height	2	1.92	0.18
	Aspect	2	0.09	0.77
	Interaction	2	4.16	0.05*
July	Residuals	21		
	Height	2	3.37	0.08
	Aspect	2	2.11	0.16
	Interaction	2	1.57	0.22
Sept	Residuals	21		
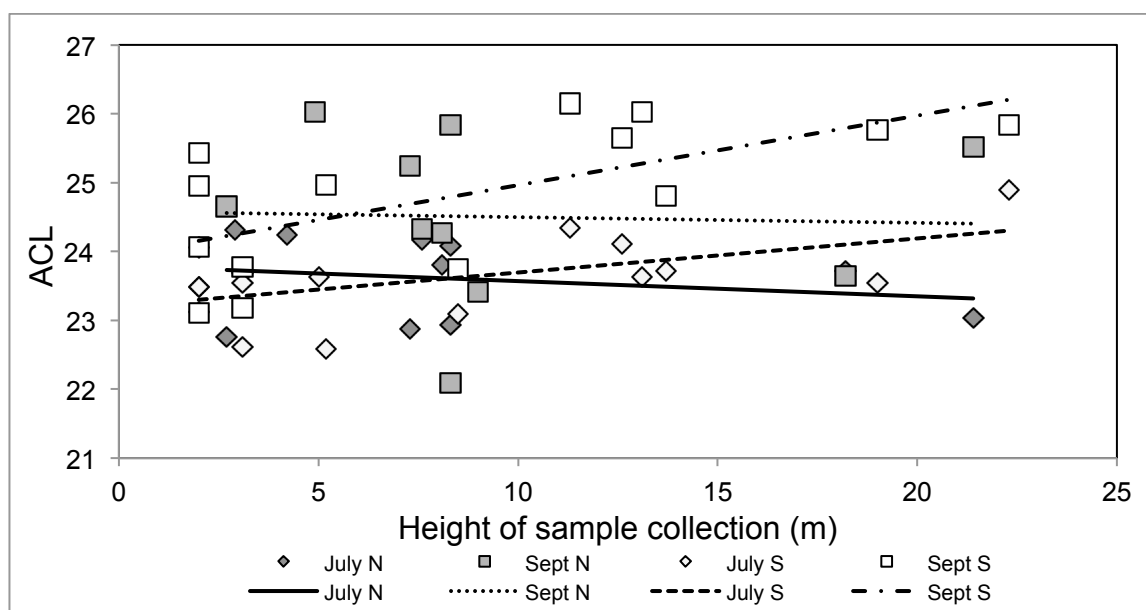
Figure 3.13: Average chain length (ACL) against the measured height (m) of sample collection. Dark diamonds represent July 2010 north aspect data, while light diamonds July 2010 South aspect data. Dark squares are September 2010 north aspect data and white squares September south aspect data. Trend lines show simple linear regressions.

These findings suggest that aspect and height of sample collection can affect ACLs during July, with higher ACLs in south facing needles; although a statistically significant positive correlation is observed for south facing needles during September, two-way ANOVA (table 3.10) does not support this result.

3.4.5.2 Scotland

Investigation into the effects of sample collection height and aspect on ACLs from Scotland (figure 3.14) show no clear trends in ACL as a result of sample collection height during both April and October, with no clear observable difference between aspects. Both simple linear regression analysis (table 3.11), and two-way ANOVAs (table 3.12), detects no statistically significant correlations, or variations, as a result of height, aspect, or the interaction between sample collection height and aspect during either April or October in the Scottish samples.
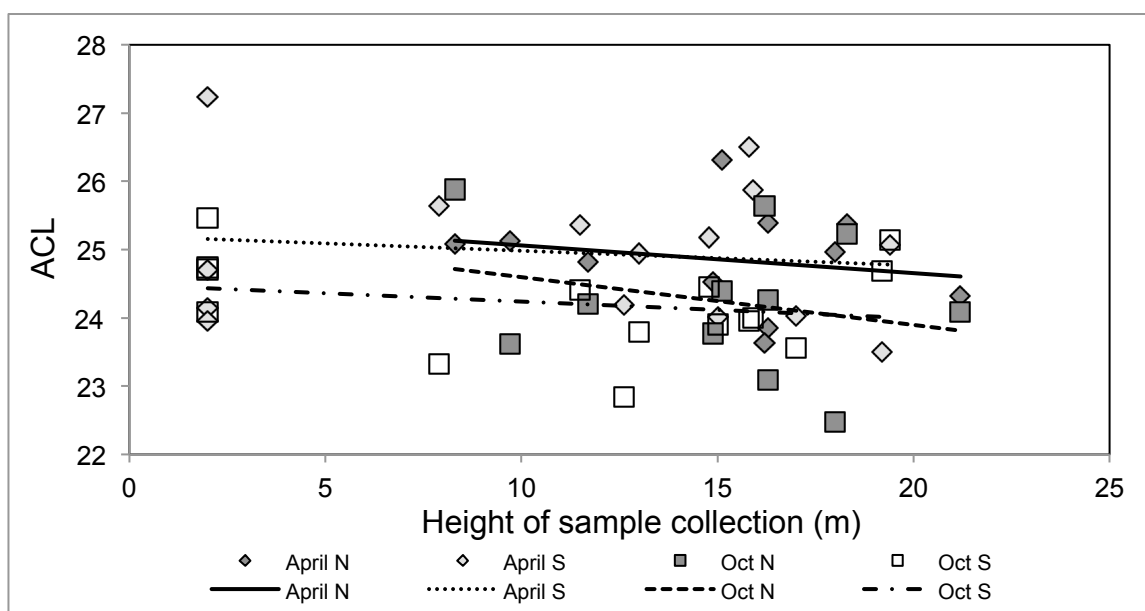
Figure 3.14: The average chain length data against the measured height (m) of sample collection. Dark diamonds represent April 2010 north aspect data, while light diamonds April 2010 South aspect data. Dark squares are October 2010 north aspect data and white squares October south aspect data. The trend lines are simple linear regressions.

Table 3.11: Summary table of simple linear regression analyses applied to the Scottish Scots pine ACL data, where "x,y" represents the variables treated.

Time	x,y	Equation	Adjusted R^2	F	P
	Height vs. North	Y=-0.041x+25.51	-0.05	0.44	0.52
April	Height vs. South	Y=-0.0268x+25.215	-0.04	0.40	0.53
	Height vs. North	Y=-0.0684x+25.21	-0.03	0.66	0.44
Oct	Height vs. South	Y=0.02886x+24.496	0.00	1.05	0.32

Table 3.12: Two-way ANOVA summary for the Scottish ACL data, where ACL is the continuous factor and Height of sample collection and aspect are the categorical factors.

Time	Source	DF	F	P
	Height	2	0.66	0.43
	Aspect	2	0.27	0.85
	Interaction	2	0.05	0.83
April	Residuals	21		
	Height	2	1.19	0.29
	Aspect	2	0.43	0.74
	Interaction	2	0.33	0.57
Oct	Residuals	21		

3.4.6 Carbon Preference Index

The Carbon Preference Index (CPI) ratios, calculated using equation 2.1(Allan 1977, Marzi, Torkelson et al. 1993), describe the odd/even dominance of the hydrocarbon chains present within individual samples of extracted *n*-alkanes. Total raw data, with details of sample collection are available in tables 1 and 2 in the appendix, where in a similar manner to the previous section, poor compound separation on the GC column

prevented reliable peak area measurements for CPI ratio calculation. As result, where stated n= less than 28, this is because CPI data was not obtainable.

3.4.6.1 Finland Carbon Preference Index

The mean CPI across all samples from July 2010 was 1.79 ± 0.09 (SEM, n=26), while the mean CPI in September 2010 was 2.93 ± 0.27 (SEM, n=25). This gives a statistically significant increase in mean CPI of 1.14 between the beginning and end of the 2010 Finnish growth season (paired t-test, t=3.55, P=0.002). The range in CPIs observed during July is also lower than September, with ratios of 0.35 – 2.53 for July, while September ratios are within the 0.50 – 6.32 range (SEM error bars, figure 3.15). This shift in CPIs can clearly be seen in the example chromatograms, with figure 3.1, GC-FID output of large tree south top from July, showing significantly higher proportions of even *n*-alkanes within its extract in comparison to figure 3.2, showing the molecular distribution of the *n*-alkanes extracted from the same sample in September.
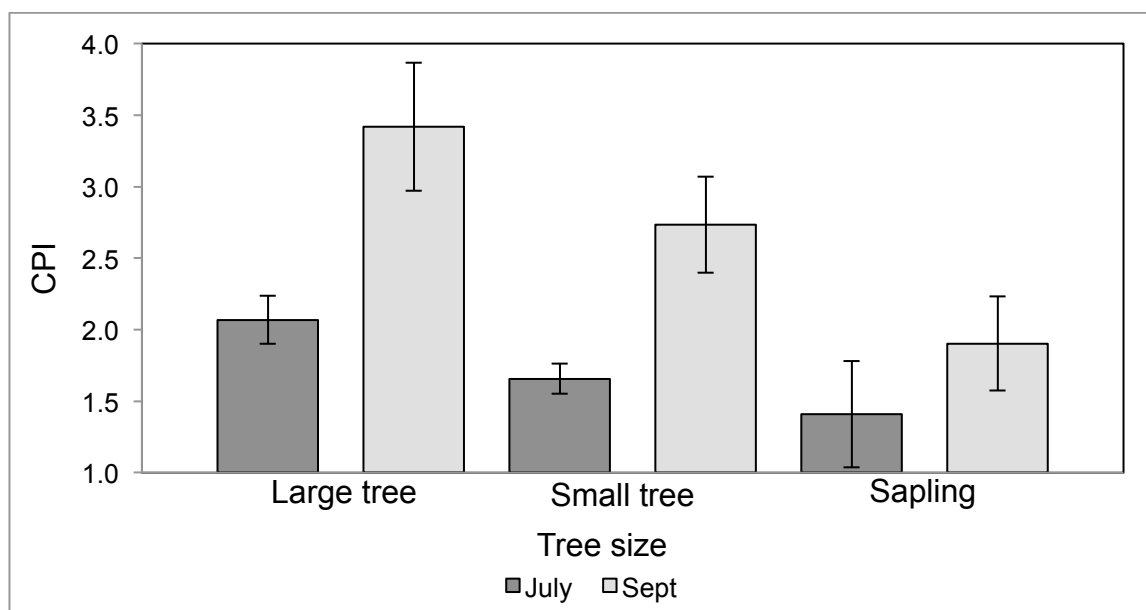
Figure 3.15: Mean Carbon preference index (CPI) by tree type for the Finnish data. Dark bars show July 2010 data, while light grey depict September 2010 ratios. Error bars represent the standard error of the mean (SEM).

Although the data appears to show CPI ratios decreasing from the large trees studied to saplings during both July and September (figure 3.15). Two-way ANOVAs (table 3.12), with individual tree size and relative height in the crown as categorical factors, and CPI as the continuous factors, only indicate statistically significant variation due to individual tree size/age during July (F=3.88, P=0.04), and not September.

Table 3.13: Summary of two-way ANOVAs applied to the Finnish CPI data, where CPI ratio is the continuous variable, while individual tree size and relative height in the crown are the categorical variables. Significant results are marked with "*".

Time	Source	DF	F	P
	Tree Size	2	3.88	0.04*
	Relative height	2	0.03	0.97
	Interaction	2	0.07	0.93
July	Residuals	21		
	Tree Size	2	2.26	0.13
	Relative height	2	0.28	0.75
	Interaction	2	1.63	0.22
Sept	Residuals	21		

In addition, the relative heights within the tree crown also show clear increases in both mean CPI, and variation in the CPIs observed between July and September (figure 3.16, SEM error bars). The mean CPI ratios appear relatively uniform across all relative heights within the crown during both July and September (figure 3.16); two-way ANOVAs confirm statistically significant variations cannot be found as a result of crown position during either July, or September (table 3.12). Furthermore, no significant effect of the interaction between individual tree size, and relative height in the crown during July or September is observed. These data suggests that crown position had no effect on CPI ratios at any time for the Finnish Scots pine studied, and individual tree size/age can influence CPI ratios, but only during July.
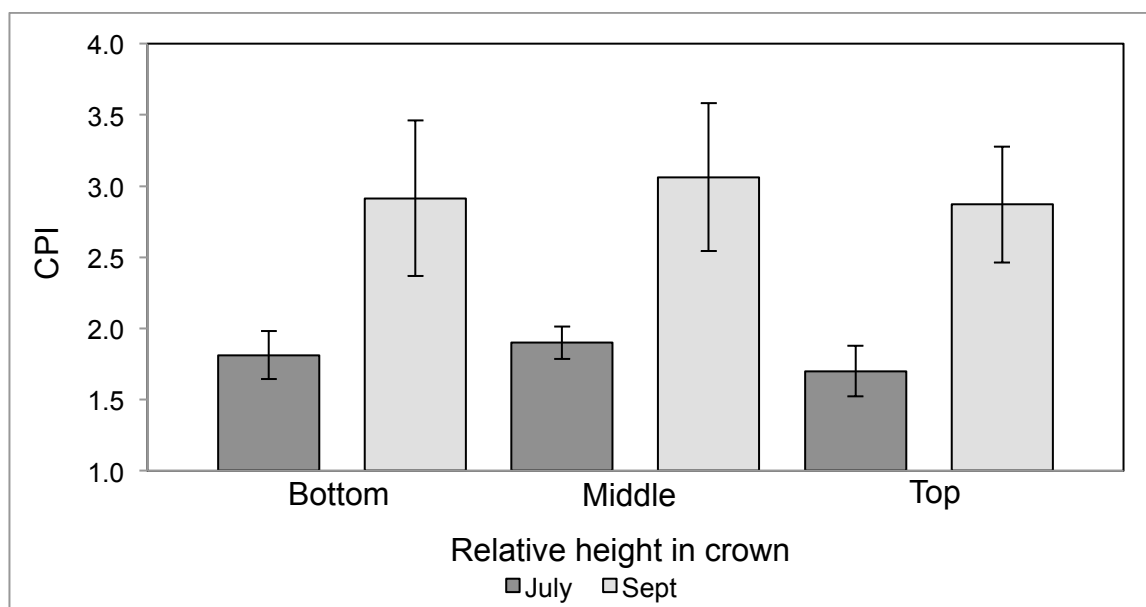
Figure 3.16: mean Carbon preference indexes (CPI) by relative height within the crown for the Finnish data, dark bars represent July 2010 and light grey bars show September 2010. Error bars show the standard error of the mean.

3.4.6.2 Scotland Carbon Preference Index

The total mean CPI data for the Scottish site shows a slight, but not significant decrease with time during the growth season (paired t-test, t =1.63, P=0.11), with 1.84 ± 0.14 (SEM, n=28) observed for April, while October ratios averaged 1.43 ± 0.10 (SEM, n=28). The CPIs during April have a greater range of 0.44 – 4.29 when compared to October ratios of 0.51 – 2.72, shown by the smaller SEM error bars (figure 3.17).
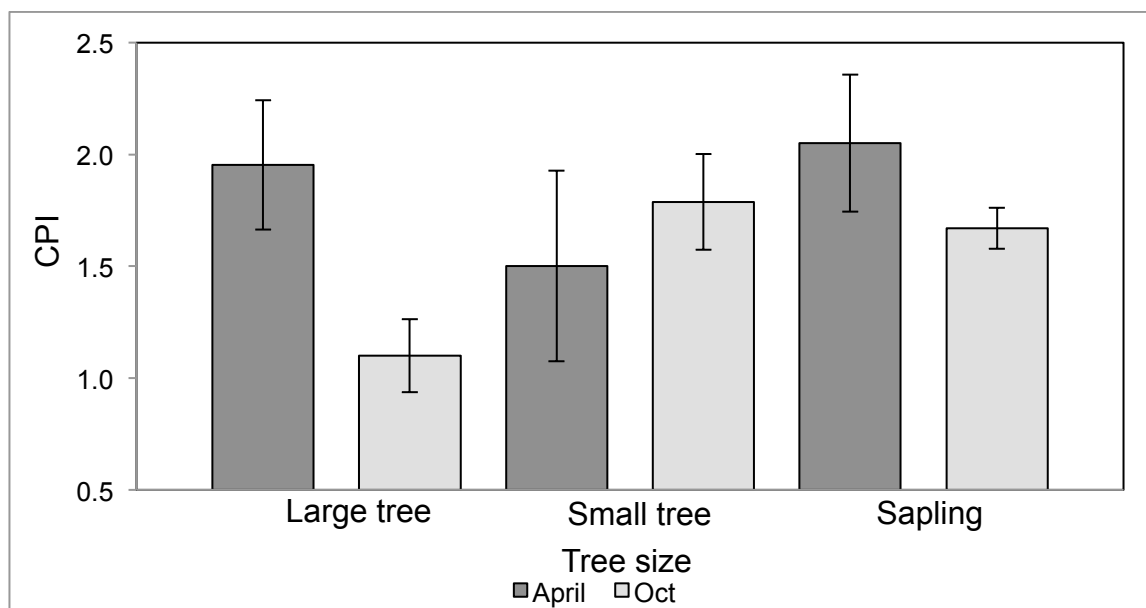
Figure 3.17: Mean Carbon preference indexes (CPI) by relative height within the crown for the Scottish data, dark bars represent April 2010 and light grey bars show October 2010. Error bars show the standard error of the mean.

In addition, mean CPI by individual size/age tree category shows no consistent trends with time during the growth season; for example, both large trees and Saplings exhibit a decrease in CPI with time, while small trees increase (figure 3.17). However, a two-way ANOVA (table 3.13), with individual tree size and relative height in the crown as categorical factors, and CPI as the continuous factor, detected statistically significant variation in CPI as a result of individual tree size/age during October (F=6.69, P=0.006), but not during April.

Table 3.14: Two-way ANOVA summary of the Scottish CPI data, were individual tree size and relative height in the crown are categorical factors and CPI ratio is the continuous factor. Significant results are marked "*".

Time	Source	DF	F	P
	Tree Size	2	1.35	0.28
	Relative height	2	0.33	0.72
	Interaction	2	2.32	0.12
April	Residuals	21		
	Tree Size	2	6.69	0.006*
	Relative height	2	1.02	0.38
	Interaction	2	1.11	0.35
Oct	Residuals	21		

Examination of the effect of crown position on CPIs show modest decreases in CPI in the bottom and top of tree crowns between April and October, with a much larger decrease shown in the middle of the crown (figure 3.18).
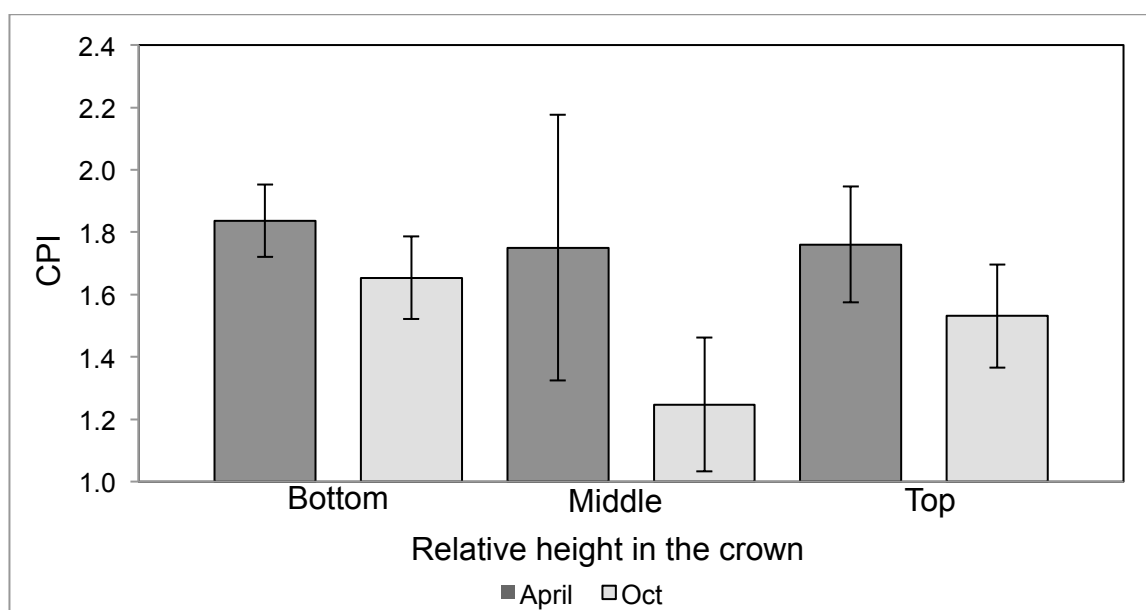
Figure 3.18: Mean Carbon preference index (CPI) by tree type for the Scottish data. Dark bars show April 2010 data, while light grey depict October 2010 ratios. Error bars represent the standard error of the mean (SEM).

Nevertheless, a two-way ANOVA (table 3.13) does not find statistically significant variation as a result of relative height in the crown during both April and October, with no significant variation as a result of the interaction between individual tree size and relative height in during April or October either. These data suggest tree size can affect CPI during October only.

3.4.7 The effect of sample position on Carbon Preference Index

3.4.7.1 Finland

Investigation into the effect of sample collection height and aspect on the CPI ratios of the Finnish Scots pine (figure 3.19) indicates a statistically significant, and strong positive correlation between height of sample and CPI for south facing needles during September (adjusted R^2= 0.62, F= 23.54, P=0.0003) (table 3.14).

Table 3.15: summary of simple linear regression analyses performed on the Finnish CPI ratio data sets, the "x,y" column shows the variables that have been subject to the correlations. Significant results are marked "*".

Time	x,y	Equation	Adjusted R^2	F	P
	Height vs. North	Y=0.029x+1.653	0.17	3.22	0.10
July	Height vs. South	Y=0.0378x+1.401	0.11	2.53	0.14
	Height vs. North	Y=0.059+1.857	-0.02	0.86	0.38
Sept	Height vs. South	Y=0.1798x+1.5403	0.62	23.54	0.0003*
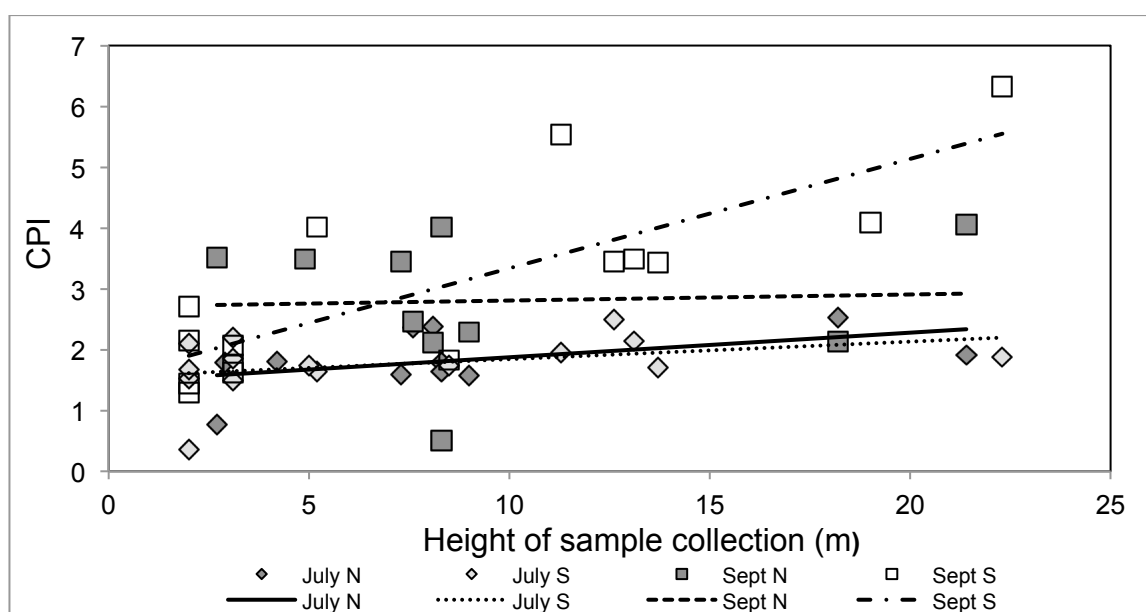
Figure 3.19: CPI against the measured height (m) of sample collection. Dark diamonds represent July 2010 north aspect data, while light diamonds July 2010 South aspect data. Dark squares are September 2010 north aspect data and white squares September south aspect data. Trend lines depict simple linear regressions.

However, two-way ANOVA (table 3.15), with sample collection height and aspect as categorical factors, and CPI as the continuous factor, suggests that a statistically significant amount of variation during July can be explained by sample collection height (F=4.62, P=0.04). No significant effect is reported as a result of aspect (F=0.04, P=0.84), and no effect of the interaction between height and aspect (F=0.04, P=0.85).

Table 3.16: Summary of two-way ANOVAs applied to the Finnish CPI data sets, where CPI is the continuous variable and height of sample collection and aspect are the categorical variables. Significant results are marked "*".

Time	Source	DF	F	P
	Height	2	4.62	0.04*
	Aspect	2	0.04	0.84
	Interaction	2	0.04	0.85
July	Residuals	21		
	Height	2	13.57	0.001*
	Aspect	2	2.24	0.15
	Interaction	2	4.56	0.04*
Sept	Residuals	21		

Two-way ANOVA also further confirmed the statistically significant positive correlation of only south facing needles with height during September (table 3.15). Reporting statistically significant variation as a result of sample collection height (F=13.57, P=0.001), and the interaction between height of sample collection and aspect (F=4.56, P=0.04), but no effect of aspect itself (F=2.24, P=0.15).

3.4.7.2 Scotland

CPI ratios from the Scottish Scots pine showed no statistically significant correlations with height of sample during April and October (figure 3.20) through simple linear regression analysis (table 3.16).
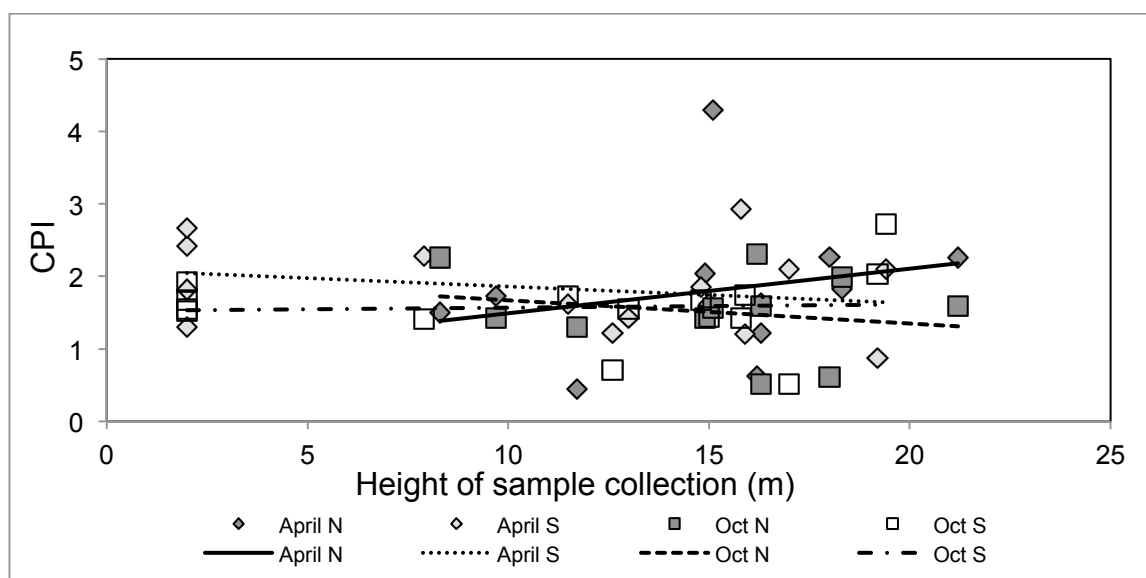
Figure 3.20: The Carbon Preference Index (CPI) data against the measured height (m) of sample collection. Dark diamonds represent April 2010 north aspect data, while light diamonds April 2010 South aspect data. Dark squares are October 2010 north aspect data and white squares October south aspect data. The trend lines show the results of simple linear regressions.

Table 3.17: Summary of the simple linear regression analyses applied to the Scottish CPI data sets. The "X,Y" column describes the two variables subject to comparison.

Time	x,y	Equation	Adjusted R^2	F	P
	Height vs. North	Y=0.03138x+0.889	-0.04	0.56	0.47
April	Height vs. South	Y=-0.0268+25.215	0.04	1.54	0.23
	Height vs. North	Y=-0.03x+1.889	-0.66	0.35	0.57
Oct	Height vs. South	Y=-0.0289x+24.496	0.00	1.05	0.32

In addition, no significant difference as a result of aspect during either sample collection period was detected. These findings are further supported by two-way ANOVA (table 3.17).

Table 3.18: Summary of two-way ANOVAs conducted on the Scottish CPI data, where CPI is the continuous variable and height of sample collection and aspect are the categorical variables.

Time	Source	DF	F	P
	Height	2	0.16	0.69
	Aspect	2	0.87	0.47
	Interaction	2	1.31	0.29
April	Residuals	21		
	Height	2	0.28	0.60
	Aspect	2	1.86	0.17
	Interaction	2	0.50	0.49
Oct	Residuals	21		

3.5. Discussion

3.5.1 *n*-alkane concentrations

Despite suggestions from paleo-environmental studies that *n*-alkanes are found in only minor concentrations within the epicuticular waxes of coniferous needles (Riederer 1989, Sachse, Radke et al. 2004, Sachse 2006), the results of the current study indicate that this may not always be the case. In agreement with the plant physiological studies (Prügel, Loosveldt et al. 1994, Prügel and Lognay 1996, Oros, Standley et al. 1999), the concentrations observed for the total *n*-alkane content of Scots pine are generally lower than those reported for other conifer species, where concentrations of up to 1mg/g DM are observed in *Picea abies* (Prügel, Loosveldt et al. 1994). However, they are still within the range previously reported during other investigations into deciduous tree and grass species; within the whole data set, total *n*-alkane concentrations range 1.52 – 76.76 µg/g DM (table 1 and 2 appendix). These concentrations are within the range of those from previous publications, which have investigated species considered to contain large concentrations of *n*-alkanes within their leaf waxes. For example, a max concentration of *n*-alkanes in the epicuticular leaf waxes in barley of 50 µg/g DM (Sachse 2010), and a total range of 7.4 – 2770 µg/g DM, in 45 Savanna and 24 rainforest species (Vogts, Schefuß et al. 2012) have been reported.

Nevertheless, there are marked differences in the total *n*-alkane concentrations of the leaf waxes of Scots pine between the two geographical locations (Figures 3.3 and 3.5). Concentrations are similar early in the growth season with 2.68-15.95 µg/g DM (April 2010) in Scotland, and 1.52- 13.34 µg/g DM (July 2010) in Finland. However, over the course of the growth season the behavior of the two geographical locations deviates, with a significant and large increase in total *n*-alkane concentrations in Finland during September, while a slight decrease in total *n*-alkane concentrations is observed during October in Scotland.

The concentrations from April and October in Scotland, and July in Finland, would agree with the general consensus of paleoclimate literature, where coniferous species are suggested to contain too low concentrations of *n*-alkanes to make a detectable contribution to the sediment record (Riederer 1989, Sachse, Radke et al. 2004, Sachse 2006). However, September concentrations in Sub-Arctic Scots pine (figures 3.3 and 3.4) could significantly contribute to sediment records towards the end of the growth season within this region, in direct contrast to previous paleo-climate literature. One previous study investigating the *n*-alkane concentrations of Scots pine inhabiting Siberia, where the

trees experienced environmental conditions not too dissimilar to those in Finland, indicated that Scots pine contains very low total concentrations of *n*-alkanes within its leaf waxes (Tarasov, Müller et al. 2013). Yet, it is important to consider Tarasov et al., (2013) collected samples for analysis during the summer, which, as is shown within the current study, is when total *n*-alkane concentrations are very low in Finnish Scots pine. As a result, analysis of Scots pine needles from a variety of locations across the Boreal zone, towards the end of the growth season in September, would be a significant recommendation for future research. As the current investigation is the first in-depth study investigating the composition of leaf wax lipids from a single tree species (and conifer), with variations within and between individuals, as well as variation with time during the growing season from field locations within the boreal forest zone. This may also be why this is the first report of a coniferous tree species possessing the abilities to synthesize significantly high enough *n*-alkane concentrations to impact sediment records.

To see such a significant variation in the observed total *n*-alkane concentrations within a single species, over a large geographical range, suggests an ecosystem/environment-specific response in the epicuticular wax composition, and total concentration of *n*-alkanes within a single species. The findings suggest low and homogenous concentrations of *n*-alkanes are synthesized in Scots pine as a species, as part of the normal ontogenty of the plant at the beginning of the growing season. I.e. just enough *n*-alkanes are synthesized during leaf flush to protect the needle. However, the significantly increased concentrations displayed in Finnish September samples, along with the greater level of variation in concentrations observed suggest, 1) Scots pine in Scotland utilize different epicuticular wax constituents as the primary component of their waxes, such as fatty acids and alcohols (Prügel and Lognay 1996), and 2) the different, and much harsher environment of the sub-arctic may be driving the increased synthesis of *n*-alkanes within Finland.

The growth environment of North-Eastern Finnish Lapland is very harsh, with a mean annual temperature of -1°C, and winter temperatures that frequently drop below -40°C. The relatively short growing season, in the region of 100 – 140 days, is characterized by a period of 24-hour sunlight (Institute 2009). In addition, the sub-arctic boreal forest sampled within this study is considered to be the limit of the arctic timberline, and the Scots pine in Värriö have been shown to be growing at their geographical northern limit (Grace 2002), and on very nitrogen limited soils (Ste-Marie 1999). This is in direct contrast to the Scottish sample site where the environment is less harsh, with a mean annual temperature of 8.5°C (Met office, 2013), no 24-hour photoperiod, and where the Scots pine are growing well within their geographical limits. It has also been extensively

documented that Scots pine inhabiting sub-arctic areas retain their needles for multiple years to conserve nutrients (Sen'kina 2002). During sample collection, needle retention of up to 8 years was observed, whereas maximum needle retention of 3 years was observed in the Scottish sites. The combination of these factors suggests the significant increase in total *n*-alkane concentration towards the end of the Finnish growth season is to facilitate the preservation of needles over the long harsh winter months for the next growth season. This finding is consistent with a previous investigation where it was suggested that *n*-alkane abundances are generally higher within longer lived foliage (Diefendorf, Freeman et al. 2011); however this hypothesis has not been demonstrated under controlled growth experiment conditions, this would be a significant recommendation for future research.

These findings also suggest that *n*-alkanes are continuously synthesized during the course of the growth season in Finnish Lapland, in response to natural environmental cues. This is in agreement with previous research conducted using controlled growth experiments (Gao, Burnier et al. 2012, Gao, Tsai et al. 2012), as well as in field investigations (Pedentchouk 2008, Sachse 2009). As *n*-alkanes are not continuously synthesized throughout the growth season for Scottish Scots pine, this suggests *n*-alkane synthesis is ecosystem specific, and not species specific.

3.5.2. Average Chain Length

The ACL data from the current study provides the first analysis of *n*-alkane molecular distributions of Scots pine across a large geographical range, as well as the first in-depth analysis of the potential molecular variation in *n*-alkanes within, and between, a single species in a natural forest environment. To date, the majority of publications have focused on controlled growth experiments of saplings (Yang 2009, Kahmen 2011), or pooled samples from a constant height and aspect analysis of mature individuals (Hou 2008, Pedentchouk 2008, Sachse 2009), with few studies investigating boreal species either in-situ or altogether (Yang 2009). Therefore, these data sets provide novel insights into the molecular distributions of Scots pine, and evergreen coniferous species as a whole.

The overall ACL ratios observed for the entire data set are substantially lower than expected. ACLs ranging 22.08- 27.13 are reported with nC$_{23}$ found as the most dominant occurring *n*-alkane homologue, across all of the data, with 24.69 ± 0.23 (SEM, n=24, Finland, September) as the highest observed ACL value. Previous literature indicates ACLs below nC$_{23}$ are indicative of submerged aquatic plants and/or bacteria, nC$_{23}$ to nC$_{25}$ indicates floating aquatic plants, and nC$_{27}$ to nC$_{29}$ indicates trees and shrubs (Ficken, Li et

al. 2000, Zech 2009), while nC$_{23}$ has emerged as a proxy for significant Sphagnum mosses (Pancost, Baas et al. 2002, Bush and McInerney 2013). However, as Sachse et al (2006) have reported high concentrations of nC$_{23}$ in Betula spp., even though it was not the dominant compound and considered an anomaly, this is not the first report of high concentrations of nC$_{23}$ within the epicuticular waxes of a tree species. To find such large concentrations of nC$_{23}$, consistently across all samples, could have potentially serious impacts for the paleo-environmental interpretations of the sediment records (which will be discussed in greater depth in chapter 7).

The overall level of variation observed in ACLs for Scots pine, across all samples is highly extensive. In an area of research where shifts in ACL of ~0.5 are considered significant (Vogts, Moossen et al. 2009, Gao, Burnier et al. 2012, Vogts, Schefuß et al. 2012), the total range of 5.15 ACLs observed in the current study, for the same species of tree, is quite dramatic. Shifts in ACL of this magnitude have been previously documented (Bi, Sheng et al. 2005, Sachse 2006), and attributed to either latitude, with lower latitudes associated with higher ACLs (Poynter, Farrimond et al. 1989, Poynter 1991, Jeng 2006) or differences in plant type (Cranwell 1973, Ficken, Li et al. 2000, Zech 2009). However, variation of 3.44 ACLs is observed at different heights and aspects within the crown of the same individual, sampled at the same time, in the same geographical location (VLT Finland, September appendix Table1). This is a greater variation than those commonly observed in paleoclimate studies. This finding alone is significant as it shows how extensive the variation in ACLs can be within a single individual, this is particularly significant when it is considered that vegetation type has long been suggested as the greatest influence on ACLs (Cranwell 1973). Especially as these variations are occurring when differences in species, water availability, nutrient status, and genetics are completely removed.

Comparisons of the range in mean ACLs observed from Scotland and Finland have produced contradictory results. The significant increase in ACL of 1.0 between July and September for Finland is expected, and predicted, as increases in ACL during the course of the growing season have been previously documented (Piasentier 2000, Sachse 2009). In addition, as the *n*-alkane concentration data shows a significant increase in total *n*-alkane concentration during the same period, the data suggest *n*-alkanes are continuously synthesized during the growing season in Finnish Scots pine. However, the significant decrease in mean ACL of 0.73 between April and October in Scotland is in direct contrast to the Finnish data, and in agreement with the total *n*-alkane concentration data from this

site, suggests *n*-alkanes are not continuously synthesized, or a significant component of Scots pine epicuticular wax within this region.

3.5.3. Carbon Preference Index

The mean CPI data across all of the samples is much lower than published observations with a total range of 0.35 – 6.32. Based on the current available literature, this suggests significant sample contamination with even *n*-alkane chains from petrochemical substances, human skin lipids, bacterial/algal/fungal inputs, or all of the above (CPIs less than 5) (Nishimura and Baker 1986, Elias, Simoneit et al. 1997, Jeng 2006, Sachse 2006, Eglinton 2008). Great care was taken during sample collection, preparation, and extraction to minimize contamination from human sources, and at no point did the samples or extracts come into contact with hydrocarbon-based products such as plastic. As the samples represent only vegetation extracts, contamination from aquatic organisms can be completely ruled out (CPI ratios less than 3) (Farrington and Tripp 1977, Jeng 2006, Eglinton 2008, Vogts, Schefuß et al. 2012). Furthermore, the Scottish and Finnish sample sites are located in remote areas; The Blackwood of Rannoch is over 80km away from the nearest city, while Värriö Strict nature reserve in Finland is 100km away from the closest major road, therefore, sources of pollutants are negligible (Hari 1994, Kulmala 2000, Ruuskanen 2003).

Eliminating potential sample contamination from external sources, bacteria/fungi growing on the needles themselves could have contributed to the presence of high abundances of even-number *n*-alkane chains. For example, high abundances of nC$_{18}$ to nC$_{24}$ in recent marine sediments were attributed to bacterial residues (Nishimura and Baker 1986). Moreover, there have been several reports of high abundances of even *n*-alkanes present in sediments archives around the globe, including the Amazon shelf (Elias, Simoneit et al. 1997), marine surface sediments from the Gulf of Mexico, the Davis Strait and Smith Sound (Nishimura and Baker 1986), lake surface sediments from northern Europe (Sachse, Radke et al. 2004), and Lacustrine sediments in Linxia Basin, NE Tibetan Plateau (Wang, Fang et al. 2010). In all of these publications, the predominance of even *n*-alkanes was attributed to algal inputs and/or bacterial degradation.

Within the current study, not only are there very low to negligible abundances of these short chains characteristic of bacterial and fungal inputs (<C$_{20}$) (Weete 1976, Harwood and Russell 1984), there is also no presence of nC$_{17}$, an indicator for bacteria (Polissar and Freeman 2010). In addition, there are also significant concentrations of nC$_{26,}$ nC$_{28,}$

and nC$_{30}$, which can be easily identified (e.g. figures 3.1 and 3.2), and have been consistently found across all the analyzed sample extracts. This suggests the high levels of even n-alkane chains present within Scots pine are indeed synthesized by the plant itself, and not representative of some form of external contamination. Moreover, given the small masses of material extracted for analysis (see tables 1 and 2, appendix), for a bacteria/fungi to contribute even n-alkane chain abundances in similar concentrations as the odd-numbered n-alkanes, it is assumed that a bacterial or fungal film would be visible on the needle surfaces. This was not observed on any samples analyzed. Low CPIs in terrestrial vegetation have been reported previously, with Bi et al (2005) reporting ratios as low as 2.3 for a range of vegetation. Observations of very low CPIs made by Vogts et al (2009) from several rainforest species were attributed to the level of leaf senescence at the time of sampling. However, as great care was taken to ensure only the current year's growth were sampled within the present study, significant leaf wax degradation as a result of this is unlikely.

The few publications available, specifically addressing the molecular distributions of living modern conifer leaf wax n-alkanes, have also reported unusually low CPIs similar to those found in the current study. n-alkanes extracted from *Pinus strobes* and *P. taeda* showed variable n-alkane compositions, displaying both odd and even n-alkane chains within their leaf waxes (Tipple 2012). Additional evidence from Serbian spruce (*Picea omorika*) also show uncharacteristically low CPIs for terrestrial vegetation, with a range of 0.34 - 4.78, a mean of 2.48, and significant contributions from nC$_{26,}$ nC$_{28}$, and nC$_{30}$ (Nikolic, Tesevic et al. 2009), in agreement with the data presented here. Therefore, all data presented here indicates conifer species may synthesize different distributions of n-alkanes, with high abundances of even length chain n-alkanes a large component of their waxes. This presents a significant issue for the use of CPI as a tool for differentiating n-alkane source, as well as the level of sediment maturity and petrogenic contamination, which is discussed in greater detail in chapter 7.

Aside from the unusually low CPI ratios, the CPI data from the two regions show different changes in CPI across the growing season. Mean CPI significantly increases by 1.14 between July and September in Finland, yet they decrease by 0.41 between April and October in Scotland. The increase in CPI between July and September in Finland is consistent across all tree size/age categories (figure 3.15), while there are no consistent patterns in CPI observed across all tree size/age categories studied in Scotland (figure 3.17). The increased CPI, increased total n-alkane concentration, and increased ACL, observed across all samples in Finland during September suggest continuous n-alkane

synthesis during the growth season, with greater proportions of longer odd-numbered-chains being synthesized with time. While no significant differences in *n*-alkane concentrations, a significant decrease in ACL, and no significant difference in CPI between April and October in Scotland suggest that *n*-alkanes are not a significant component of epicuticular waxes at this location, and as a result, do not respond to environmental influences in the same manner as the Finnish Scots pine.

3.5.4. The effect of sample position on *n*-alkane concentration, ACL and CPI

Investigation into sample position within and between different size/aged individual Scots pine trees has revealed contradictory behavior between the two geographically different sample locations. Although micro-climatic variables were not measured in-situ, due to the well-established gradients of temperature, RH, wind speed, and PAR in natural forest canopies (See figure 2.7, Chapter 2, section 2.2.1.4 for explanatory schematic), different sample collection position parameters have been used as proxies for variations of these. The following sections cannot conclusively prove which climatic parameters significantly influence the concentration and molecular compositions of *n*-alkanes in natural ecosystems. However, inferences can be made, which will provide insight into the key climatic parameters that should be the focus of future research.

3.5.4.1 Finland

The epicuticular wax of Finnish Scots pine during September has a significantly different composition to that observed during July, exhibiting significantly increased total *n*-alkane concentrations, ACLs, and CPIs. Although increases in ACL and CPI alone do not prove continuous *n*-alkane synthesis with time, as preferential removal of shorter *n*-alkane chains, as well as even-numbered chains could affect ACL and CPI in the same manner (Sachse 2006). The combination of significant increases in total *n*-alkane concentration, with the significant increases in ACLs and CPI, suggest continuous *n*-alkane synthesis with time in the growth season, with increased synthesis of longer *n*-alkane chains, and higher abundances of the odd-numbered chains.

Collation of concentration, ACL and CPI data from the Finnish site indicates a significant influence of sample position on *n*-alkane compositions within these epicuticular waxes. Using height above ground, relative position in the crown, and aspect of sample collection as proxies for PAR, RH and temperature. Under the assumption that south facing needles will receive more PAR than north facing, increasing PAR and temperature with increasing

height off the forest floor, and decreasing RH with height (Niinemets, Kull et al. 1999, Niinemets, Sonninen et al. 2004, Duursma and Marshall 2006), the influence of PAR, temperature and RH on *n*-alkane compositions can be elucidated. These data suggest that different sample position locational parameters can affect different aspects of *n*-alkane molecular compositions within the epicuticular wax in different ways at different points in the Finnish growth season. Despite recent research suggesting *n*-alkane abundance and composition does not significantly vary with canopy position within large individual trees (Bush and McInerney 2013), the current study clearly shows that this is not the case. The reason for the discrepancy between the current study and that of Bush and McInerney (2013), may be because gradients in height of 2m to 22m were investigated within natural field forest conditions; while Bush and McInerney (2013) examined north versus south aspects, at one height of 3m, in isolated trees growing in botanical gardens. The data presented here however, suggest height of sample from the forest floor is a major driver of *n*-alkane concentration during July, with a positive correlation with height. While ACL is significantly affected by aspect, with increased ACL for south facing leaves, and CPI is driven by both tree size and height of sample during July. However, during September, height of sample and aspect affect CPIs, and there are no significant variations in total *n*-alkane concentration or ACL.

The data suggest increased total *n*-alkane concentrations with height during July are a factor of decreased RH, increased PAR, and increased temperature. Indicating higher total *n*-alkane concentrations to protect the needles from increased evaporative water loss. As height of sample collection has no effect on concentrations or ACL during September, when PAR levels and temperature are much lower, but RH is much higher, PAR and temperature would appear to exert greater influence on concentrations than RH. Furthermore, as ACL is affected by aspect, with higher chain lengths present in south facing leaves, but not height of sample collection, this would suggest ACL is sensitive to PAR levels but not RH and temperature.

Previous literature has indicated the importance of light for the expression of many genes involved in leaf wax synthesis (Van Gardingen and Grace 1991), and higher proportions of longer chains being synthesized in response to increased light levels are also extensively reported (Eglinton 1967, Poynter, Farrimond et al. 1989, Poynter 1991, Shepherd and Griffiths 2006). It is therefore not surprising to see a strong impact of light intensity on ACLs during July in Finland. Although increased temperature is suggested to cause increases in ACL (Poynter, Farrimond et al. 1989, Jeng 2006, Sachse 2006), the current study reports no effect of sample height on ACLs, indicating the higher ACLs

observed in warmer climates, and lower latitudes, are the result of increased light, rather than increased temperatures.

The CPI data proves more difficult to interpret, as the results indicate CPI is affected by tree size/age and height of sample during July, and by height of sample and aspect during September. Attempts to correlate variations in CPI to variations in environmental parameters are not new concepts. However, these studies draw their conclusions from the amount of wax degradation occurring as a result of environmental conditions (Rao 2009, Vogts, Schefuß et al. 2012), rather than the potential for environmental conditions to affect the CPI ratios of *n*-alkanes during biosynthesis. For example, higher CPIs observed from a north to south transect of soil surface samples from Eastern China were attributed to more rapid microbial breakdown of samples in the south due to higher moisture levels (Rao 2009). As bacterial degradation and contamination have been ruled out within the current study, shifts in CPI must been driven by shifts in the relative abundance of even-numbered and odd-numbered *n*-alkane chains.

Older/larger trees exhibited higher CPIs, and higher CPIs were expressed with increasing height during July. This suggests greater abundances of odd-numbered *n*-alkane chains with height of sample and age/size in Finland during July. CPIs also significantly increased between July and September, along with a significant positive correlation with height of sample, which is stronger in south facing needles than north. These findings suggest that greater abundances of odd-numbered *n*-alkane chains are synthesized to protect against the increased light intensity and temperature experienced in these locations, or that even-chains are preferentially eroded by this (Sachse 2006). The significant increase in total *n*-alkane concentration and CPI observed during September, in conjunction with the strong positive correlation of CPI with height, which is more significant for south facing needles, indicates higher concentrations of odd-numbered *n*-alkane chains in response to higher PAR levels.

These data show that total *n*-alkane concentration, ACL and CPI are all significantly affected by height of sample collection during July in Finland. This suggests that PAR levels may be a crucial driving factor, especially for ACL, as this significantly varies due to aspect during the 24-hour photoperiod. Future research should focus upon repeating the results found here, complete with in-situ PAR measurements.

3.5.4.2 Scotland

The *n*-alkane compositions of the Scottish Scots pine were more difficult to interpret as there are no clear and consistent trends between April and October. There is no significant change in total *n*-alkane concentration, or CPI, with time in the growth season, and yet there is a significant decrease in ACL. None of the sample collection parameters show any significant effect on total *n*-alkane concentrations, CPI or ACL during April, however an effect is detected during October.

Both ACL and CPI significantly vary in relation to individual tree size/age at the end of the growth season in October, and total *n*-alkane concentration significantly varies in relation to relative height in the crown. It is therefore difficult to draw any clear information from the Scottish data sets, as it appears *n*-alkanes are not a major component of the epicuticular waxes in this region. These findings are consistent with the hypothesis that *n*-alkanes are not a significant constituent of the epicuticular waxes of temperate conifer species; this is because the data suggests no significant re-synthesis of *n*-alkanes has occurred over the course of the growth season. ACL also shows no correlation with height of sample for either April or October, with no difference between north and south facing needles within the Scottish Scots pine sampled (figure 3.14). The lack of an increase in total *n*-alkane concentration, in conjunction with the overall decrease in ACL shown for this location, indicates that continuous *n*-alkane synthesis does not occur in Scottish Scots pine.

3.5.4.3 Summary

The results of the current study highlight the need for ecosystem-specific investigations into the total concentrations, ACLs, and CPIs of *n*-alkanes within individual plant species. Significant variation in the behavior of the same species geographically, spatially, and temporally, is observed and until this phenomenon is fully investigated, these findings could have significant impacts for the use of *n*-alkanes as a paleo-climate proxy (discussed in detail, chapter 7). Scots pine inhabiting Sub-arctic Finland and Scotland exhibit significantly different *n*-alkane characteristics within their leaf waxes, which the current investigation concludes is mainly climate driven. Nevertheless, until full in-situ measurements of how climatic variables have changed with time, in conjunction with regular *n*-alkane sampling is undertaken, the major drivers of variation in total *n*-alkane concentrations, ACLs and CPIs can only be inferred.

3.6. Conclusions

1. *n*-alkanes are synthesized in high enough concentrations to significantly contribute to the sediment records of Sub-Arctic pine forest, but not temperate pine forest.

2. Coniferous species synthesize both odd-and-even length *n*-alkane chains.

3. Scots pine trees synthesize high concentrations of nC$_{23}$, a compound previously assumed to be characteristic of submerged aquatic plants or Sphagnum moss.

4. Significant variation in *n*-alkane concentrations, ACLs, and CPIs were found within, and between individuals of the same species, inhabiting the same region, sampled at the same time.

5. Height of sample is significantly positively correlated with total *n*-alkane concentration, ACL, and CPI during July in Finnish Lapland.

6. The largest trees studied showed the greatest within canopy variation, suggesting stand structure, and age of a forest could have a significant impact on the *n*-alkane signal input into regional sediments.

4. Water sourcing and leaf water isotopic enrichment of natural Scots pine forests

4.1. Forest isotopic hydrology and leaf water D-enrichment: a literature review

4.1.1 Introduction

The isotopic compositions of plant tissues are affected by many different factors that can be categorised into two distinct groups. The first concerns the isotopic composition of the water being directly absorbed by the plant (source water), and the second involves the physiological, and biochemical, aspects of photosynthetic assimilation (Schleucher 1998). Hydrogen and oxygen isotopes in plant organic matter have a close relationship as both ultimately originate from the same source – meteoric water (Craig 1961, Ehleringer and Dawson 1992, Marshall, Brooks et al. 2007). This relationship is being exploited by using n-alkanes extracted from sediment records, where the preserved δD values of n-alkanes are used to reconstruct the δD values of meteoric waters from the past (Eglinton 2008, Castañeda and Schouten 2011, Sachse 2012). As the crux of this current work is in investigating how the compound-specific δD values of n-alkanes synthesized by natural forest ecosystems vary, and what could be driving these variations. This chapter discusses the water sourcing and leaf water isotopic behaviour of the forests under investigation. The data presented within this chapter is then used to try to understand what is driving the hydrogen isotopic compositions of the n-alkanes, which are discussed in Chapter 5.

4.1.2. Meteoric waters

Meteoric water originates in the oceans, where clouds and precipitation is generated through evaporation. Due to mass and kinetic isotope effects, i.e. the water molecules containing the lighter isotopes of both oxygen and hydrogen require less energy to evaporate than the heavier ones, clouds and precipitation are depleted in the heavier isotopes relative to water in the ocean (Dansgaard 1964). As clouds migrate over landmasses, and precipitation events occur, the atmospheric moisture is disconnected from its vapour source. This results in the depletion of the heavier isotopes with time as

the heavier isotopes of both oxygen and hydrogen are preferentially lost through Rayleigh distillation; the so called "rain-out effect" (Dansgaard 1964, Gat 1996, Gat 1998, Marshall, Brooks et al. 2007, Gat 2010). The change in isotopic composition of precipitation as a result of Rayleigh distillation is closely linked to temperature via the Clausius-Clapeyron equation, and the liquid-vapour phase boundary for water. As a result, there is a strong linear relationship between $\delta^{18}O$, δD and temperature (Majoube 1971, Yurtsever 1981). This level of depletion is generally a function of geographical variables, with greater depletion in isotopic composition with increasing latitude, altitude, and distance inland. Aspects of seasonality, in conjunction with "amount effects", also have influence with winter precipitation showing more D-depletion in relation to summer, and heavier precipitation events resulting in further depletion (Gat 2010). The fractionations that occur during these processes facilitate the use of the isotopic values of oxygen and hydrogen in waters for paleoclimate reconstructions. This is because temperature is generally the major driver of these fractionations (Craig 1961, Dansgaard 1964) (discussed in greater detail chapter 2, section 2.1.4.1).

Annual Average precipitation at temperate latitudes will have an oxygen and hydrogen isotopic composition, which is correlated and described by the Global Meteoric Water Line (GWML), where $\delta D = 8\delta^{18}O + 10$ ‰ (Craig 1961). As terrestrial higher plants obtain most of the hydrogen they require through water absorption by roots in the soil, water absorbed by plants, and subsequently used in photosynthesis and biosynthesis, should be related to the original isotopic composition of the precipitation falling on the region of study, and thus meteoric water (Epstein, Yapp et al. 1976, Sternberg 1988). Unfortunately, natural forest ecosystems are not so simple and several processes can occur, which will alter the isotopic compositions of meteoric water before the plant can absorb it. Unless these processes are fully investigated and quantified on an ecosystem specific basis, prior to using the hydrogen isotopic compositions of plant organic matter, significant errors could be made in the reconstructions of meteoric water.

4.1.3. Water sourcing

Once precipitation enters an individual ecosystem's hydrological cycle, several processes operate that can significantly alter it's isotopic composition. Precipitation falling on a forest canopy can be subject to evaporative enrichment through interception by the canopy, which can alter the deuterium signal (McGuire, McDonnell et al. 2007). Once precipitation enters the soil further alterations can also occur, which are a function of soil structure,

hydrological processes, climatic processes, or a mixture of all three (Tang and Feng 2001).

Water in the top layers of the soil profile can become D-enriched due to evaporative enrichment, with the level of enrichment usually positively correlated with temperature, and negatively correlated with relative humidity (RH) (Zimmermann, Ehhalt et al. 1968). Subsequent rain events can result in this enriched water signal being flushed into deeper soil layers (Gat 1998) where mixing can occur. The levels of mixing, and the speed and efficiency of water transport through the profile, are a function of precipitation frequency, intensity, and soil structure (Yurtsever 1981, Dawson and Ehleringer 1998, Gat 1998, Tang and Feng 2001). As a result of this, and the variability in precipitation intensity, the soil profile can often contain water from multiple precipitation events. This has led Tang and Feng (2001) to introduce the concept of soil water reset.

In an investigation Tang and Feng (2001) measured the isotopic composition of precipitation, soil water, and xylem water biweekly for an entire growth season. They concluded that for the sandy loam soils in Hanover, USA, soil water in the early part of the growth season maintains an isotopic composition close to that of winter precipitation, even in the deeper horizons. As the growth season progresses, this signal gradually shifts towards that of summer precipitation with evaporative enrichment signals superimposed on top of this in the shallow soil layers (20cm depth). Yet it is not until there is a significant precipitation event, in this case a rain event of approx. 100mm during a two-week period that the deeper soil horizon (50cm depth) shifts towards the summer signal. This may result in only part of the seasonal isotopic composition of precipitation being utilized, and recorded, in leaf waters and subsequently synthesised organic matter (Yurtsever 1981). This is also in agreement with recent evidence from a Mediterranean forest, where it was observed trees uptake water from pools within the soil that are recharged every autumn after the summer dry period (Brooks 2010). These processes are clearly region and climate specific, and may not be applicable to other areas. For example, due to a closed canopy and a 1-2 cm thick humic layer on top of the forest floor surface, soil water evaporation was demonstrated to be heavily restricted (Sachse 2009). This was confirmed by the minimal variation in δD values with depth in the soil profile under investigation in this study. In similar terms, if the forest floor has a dense coverage of ground vegetation, especially a water absorbent species such as *Sphagnum* moss. Precipitation may not even enter the soil profile in significant volumes; potentially further disconnecting the water source absorbed by trees from local precipitation events.

The situation can be further complicated when the vegetation structure is considered as a whole. If an entire forest stand is being investigated, different species will have different habitat preferences, as well as root structures (Tang and Feng 2001). As a result, different species could source water from different depths in the soil profile. This may result in further complication of isotopic signals when investigations attempt to make comparisons involving many different species. Moreover, even if a single species is under investigation, individuals of different ages may extract water from the soil profile at varying depths (Tang and Feng 2001). Studies indicate that older, and subsequently larger trees could have access to deeper soil water pools that they can sometimes create themselves through a process termed hydraulic lift. This process can result in additional integration of water from multiple precipitation events, and of variable degrees of evaporation (Dawson and Pate 1996, Dawson and Ehleringer 1998). Consequently, mixing and evaporation processes vary from year to year. This can result in the isotopic composition of a plant's source water showing little reflection of the inter-annual variability of temperature carried by meteoric water (Tang and Feng 2001).

One method of removing the issues associated with a lack of knowledge of the source water isotopic composition is to isotopically analyse the plant's xylem water. This has been shown to be a direct proxy for the water being up taken by the plant (Feakins 2010). It has also been argued that the deviation of xylem water isotopic composition from that of meteoric waters, through evaporation, may also provide information about RH (Tang and Feng 2001).

4.1.4 Leaf water D-enrichment

The water absorbed by the plant travels to the foliage to facilitate photosynthetic assimilation; it is here that additional fractionation occurs during photosynthesis, carbon fixation, and subsequent biosynthesis. This is where it can become difficult to relate the isotopic signal expressed by organic matter to the signal of the water absorbed.

The isotopic enrichment of leaf water with ^{18}O was first observed in 1965 (Gonfiantini, Gratziu et al. 1965) and the enrichment with deuterium in 1966 (Wershaw, Friedman et al. 1966). It was at the same time that Craig & Gordon (1965) modelled the isotopic effects of evaporation from an open water surface. In this seminal work they were able to demonstrate that the water remaining after evaporation is isotopically enriched. Through the application of these principles the theoretical basis of leaf water isotopic enrichment was derived (Dongmann, Nürnberg et al. 1974, Farquhar, Hubick et al. 1989, Flanagan,

Comstock et al. 1991, Farquhar, Cernusak et al. 2007), and is discussed in greater detail in chapter 2 section 2.1.4.2. Due to the focus of hydrogen isotopes within the current thesis, following on from here the isotopic enrichment of leaf water will mainly be discussed for hydrogen isotopes only, although in general the same principles apply to oxygen.

In most cases, apart from those where leaves have taken up significantly D-depleted atmospheric water vapour directly through the stomata (Dawson 1998, Burgess and Dawson 2004), leaf waters are D-enriched in relation to xylem waters (Leaney, Osmond et al. 1985, Yakir, DeNiro et al. 1990, Wang and Yakir 1995). It is well established that transpiration, i.e. the evaporation of water out of the leaf through stomata, is what drives both the enrichment of leaf water and xylem water transport (Farquhar, Cernusak et al. 2007, Shu, Feng et al. 2008), and often results in peak enrichment in the afternoon (Kim and Lee 2011).

Nevertheless, ascertaining the physiological and climatic drivers of the transpiration of a single leaf can be complex as these two are often interrelated. This is because leaf water isotopic enrichment varies strongly as a result of fluctuating climate, leaf physiology, and the isotopic composition of water vapour surrounding the leaf (Craig and Gordon 1965, Kahmen, Hoffmann et al. 2013). However, the level of D-enrichment within an individual leaf is accepted to be the result of RH, boundary layer dynamics, the level of photosynthetically active radiation (PAR), the water status of the entire plant, and the isotopic composition of the water vapour surrounding the leaf (Smith 2006, Hou 2008, Shu, Feng et al. 2008, Yang 2009).

Where, in general terms, lower RH outside the leaf, where there is a lower partial pressure of water vapour in the atmosphere compared to partial pressure within, will drive a diffusional gradient of water out of the leaf; this results in greater levels of leaf water D-enrichment. In a similar manner, differences in the isotopic composition of water vapour surrounding the leaf and that inside will drive isotopic diffusional gradients. These gradients occur in relation to whether atmospheric water vapour is D-enriched or depleted in relation to leaf water, further driving changes in leaf water isotopic composition (Gat 1996, Helliker and Griffiths 2007, Reye-GarcÍa, Mejia-Chang et al. 2008, Welp, Lee et al. 2008, Gat 2010). In addition, higher incoming PAR levels and a more dynamic boundary layer are also associated with greater leaf transpiration and thus leaf water D-enrichment (Brandes, Wenninger et al. 2007, Powers, Pregitzer et al. 2008).

Utilizing the well documented gradients in micro-climatic variables with height in natural forest stands, where PAR increases with height off the forest floor (Le Roux, Bariac et al. 2001), and wind speed (which influences boundary layer dynamics) and RH varies in relation to canopy position (Niinemets, Kull et al. 1999, Niinemets, Sonninen et al. 2004, Woodruff, Meinzer et al. 2008, Woodruff, Meinzer et al. 2009) (see chapter 2, section 2.2.1.4, figure 2.7). One could hypothesize that the natural variations in these parameters, which are reported to influence leaf water isotopic enrichment, would result in different levels of D-enriched leaf water at different positions in the canopy. As the level of D-enrichment of leaf waters is indicated to be imprinted on subsequently synthesized organic matter, isotopically analysing this could provide information regarding the climatic conditions during which the organic matter was synthesized (Sauer, Eglinton et al. 2001, Sachse 2006).

Therefore, this chapter is directly concerned with ascertaining the behaviour of hydrogen isotopes through the natural forest ecosystems under investigation in order to aid in understanding the hydrogen isotopic signatures of *n*-alkanes synthesized within these. Understanding issues relating to the modelling of the D-enrichment of leaf waters is not directly relevant here. Instead the following investigation focuses on the water sourcing behaviour of natural Scots pine (*Pinus sylvestris L*.) stands and the mechanisms of leaf water isotopic D-enrichment in order to interpret the *n*-alkane isotopic compositions discussed in chapter 5.

4.2   Aims

In this chapter I characterize how the δD compositions of xylem and leaf waters vary spatially and temporally, within and between individuals of the same species of tree, and how these relate to the meteoric water of the regions under study. The results of this are then used in the understanding of the *n*-alkane isotopic compositions presented in chapter 5.

Hydrogen isotopic measurements of meteoric water, xylem water and leaf waters were made within and between individuals of Scots pine (*Pinus sylvestris L.*). This was to characterize the hydrology of two distinctly different natural forest ecosystems, in two different geographical areas. As one species is investigated in detail, aspects of leaf morphology and differing physiology can be omitted (Smith 2006, Kahmen, Simonin et al. 2008). Instead aspects of within individual physiology, and/or the effects of microclimate can be focussed upon. Identifying the dominant water source for the forests under investigation will also test whether the application of a single averaged value to characterize an entire forest stand is a valid technique.

Specifically I address the following questions;

1. Do different size/aged trees source water with differing isotopic compositions?
2. Do the trees studied extract a constant soil water source with time in the growth season?
3. Do xylem water δD values significantly vary within individuals?
4. Do leaf water δD values significantly vary within and between individuals?
5. Which climatic and/or physiological mechanisms are the dominant drivers of the leaf water hydrogen isotopic compositions observed?

4.3   Methods

As the current thesis is concerned with investigating the potential variation in epicuticular leaf wax *n*-alkanes, needle and stem material for cryogenic vacuum water extraction were collected at the same times, and in the same locations, as the needle material collected for *n*-alkane extraction and analysis. As described in chapter 2, sections 2.2.1, 2.2.1.2, 2.2.1.3 and chapter 3 section 3.3, this study was conducted in Värriö Strict Nature Reserve, North-Eastern Finnish Lapland and the Black Wood of Rannoch, Perthshire, Scotland (full site descriptions available in chapter 2 sections, 2.2.1, 2.2.1.2 and 2.2.1.3). With samples collected at the beginning and end of the 2010 growth season, during April and October for the Scottish site, and July and September for the Finnish site.

The current year's growth of needles, and a small section of the immediately preceding xylem were collected from the top, middle and lower crown of the north and south facing sides of Scots pine trees of varying size and age. Samples were collected from large trees (25-30m), medium trees (15-25m), small trees (5-15m), and saplings (<3m), with saplings sampled at only one 2m-high south facing point. A total of 28 samples were collected for leaf water extraction and analysis in both October and April from Scotland, and 28 samples in both July and September from Finland; with the same sampling protocol applied to the xylem sample collection. Overall, 4 saplings, 2 medium trees, and 2 large trees were sampled from the Scottish and Finnish sites respectively. Due to the destructive sampling techniques, and the costly and time-consuming sample preparation and analyses, there are no replicates for each data collection point.

Bulk Leaf and xylem waters were extracted via cryogenic vacuum distillation and measured via Delta XP TCEA as described in chapter 2 sections 2.2.2.2 and 2.2.3.3. However, it is important to note that in some cases not all 28 data points are available for leaf water and xylem water isotopic data due to incomplete cryogenic vacuum distillation; as a result, n=less than 28 is sometimes given. Fractionation of leaf water above xylem water was calculated using equation 2.7 (chapter 2, section 2.1.2.1), and the data generated was processed and subject to simple linear regressions using Microsoft Excel, and two-way ANOVA using R. Furthermore, as discussed in previous sections, only statistical tests with a P value < 0.05 are considered statistically significant, and in the case of simple linear regressions, only if the adjusted R^2 value is above 0.25. For full sampling and analytical details and methodology please refer to chapter 2, sections 2.2.1.4, 2.2.2.2, 2.2.3.3 and 2.2.3.5.

4.4. Results

4.4.1. Värriö Strict Nature Reserve, Finland

Data for the oxygen and hydrogen isotopic compositions of xylem, leaf, and local surface waters from Finland have been plotted as δD versus $\delta^{18}O$ in figure 4.1. Xylem water isotopic composition, measured for both July and September 2010, fall slightly to the right of the global meteoric water line (GMWL, red line- figure 4.1) (blue diamonds for July and red squares for September, figure 4.1.). This suggests these trees are sourcing waters which have been subject to only slight isotopic enrichment with respect to the local annual precipitation isotopic compositions (Brandes, Wenninger et al. 2007) (full raw data available table 3, appendix).
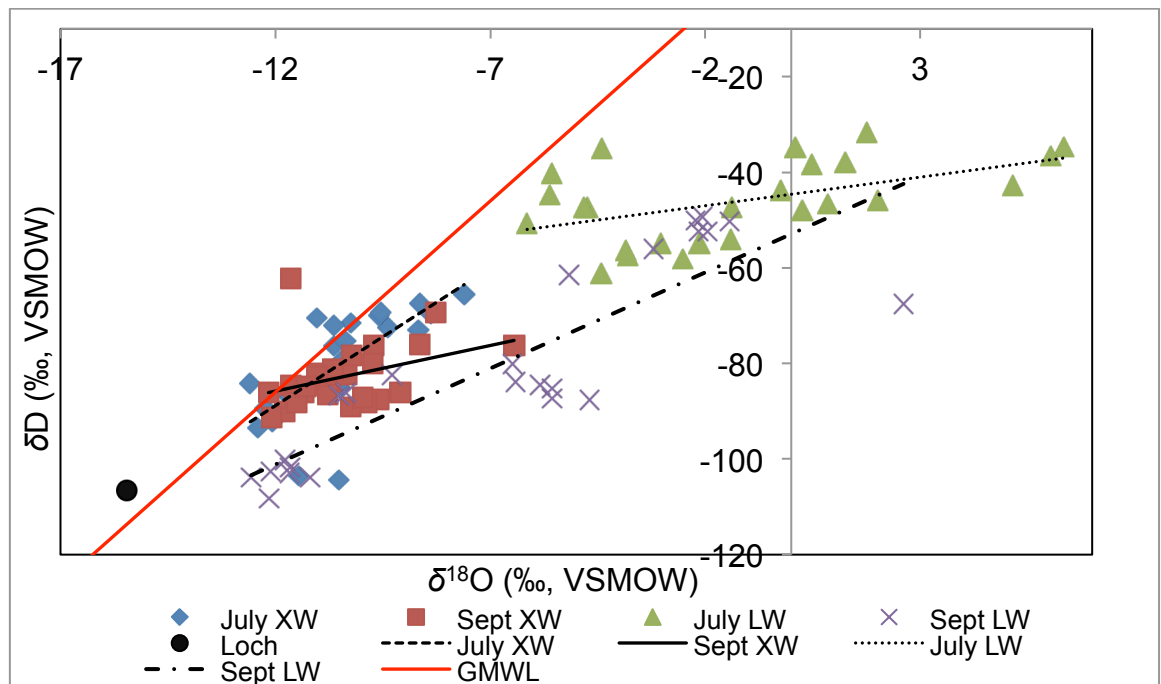
Figure 4.1: $\delta^{18}O$ versus δD scatter plot of all environmental waters analysed in Finland during the 2010 growth season, where XW = xylem water and LW = leaf water. The red line shows the global meteoric water line (GMWL, $\delta D=8\delta^{18}O+10$) and the different dashed trend lines indicate the local meteoric water lines.

The data also indicate summer precipitation values are more important for the trees than winter precipitation. Although precipitation was not measured on site, using the Online Isotopes in Precipitation Calculator (OIPC) (Bowen 2013), where annual precipitation δD values range from -130 ‰ in December to -79 ‰ δD in August (chapter 2, section 2.2.1, table 2.3). Estimations of precipitation during July approximate -82 ‰ δD, which is very similar to mean xylem water values for both July (δD -78.72±3.11 ‰ SEM, n=22) and September (δD -82.84±1.21 ‰ SEM, n=28). Furthermore, measured lake water, a proxy for mean annual precipitation (MAP) (black dot, figure 4.1), is more D-depleted (-102 ‰

δD). This indicates that significantly D-depleted snow melt water from winter precipitation impacts the local ground waters, but is not a significant water source for scots pine within this region.

The July leaf water oxygen and hydrogen isotopic data (green triangles figure 4.1) fall to the right of the GMWL, on a local meteoric water line (LMWL) of y=1.1961x-44.606. This indicates evaporative D-enrichment of leaf waters in relation to xylem waters. The September leaf water data however (purple crosses, figure 4.1), is much more complex and appears to be separated in three distinct groups on a LMWL of y=4.0172x-52.915 (Sept LW trend line). Where one group shares a similar level of D-enrichment to the July leaf water isotopic enrichments, the second has hydrogen isotopic values, which are similar to xylem water but with a more enriched $\delta^{18}O$ signature. While the third group appear significantly depleted in both oxygen and hydrogen in relation to the associated xylem waters.

4.4.2. Black Wood of Rannoch, Perthshire, Scotland

Xylem water data is not available for the Scottish sample site during April 2010. This results from the fact that this was the first attempt to extract xylem water within the whole study and the method was not correct. As a result of this, a different, more robust, and correct method was applied when extracting xylem water for the subsequent samples.
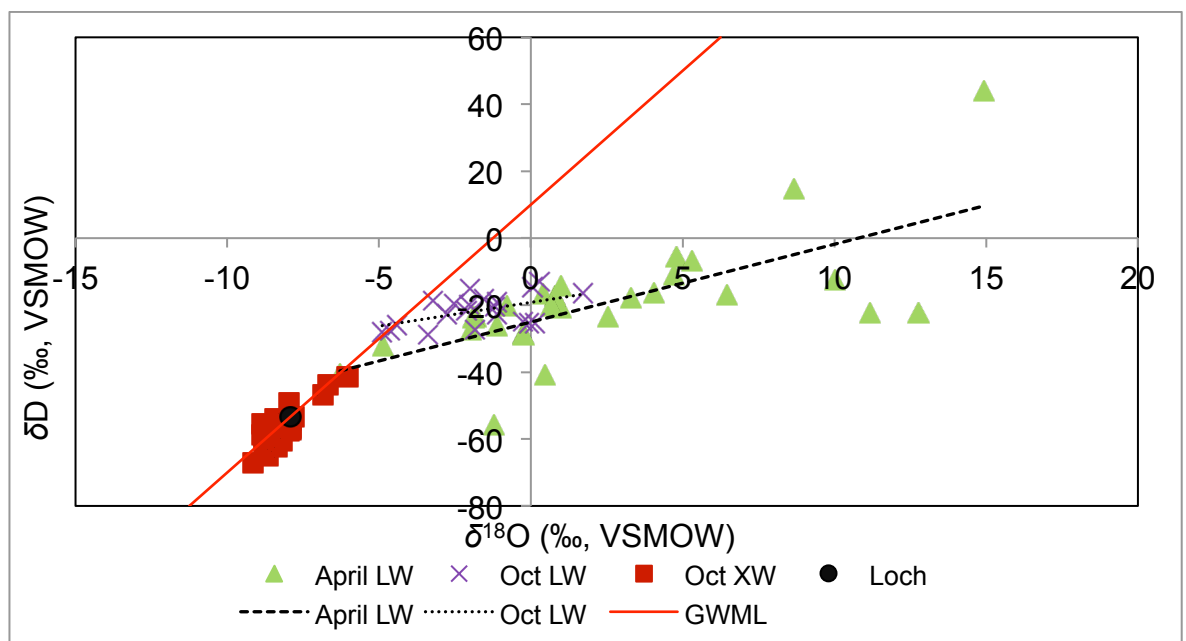
Figure 4.2: $\delta^{18}O$ versus δD scatter plot of all environmental waters analysed in Scotland during the 2010 growth season where XW = xylem water and LW=leaf water. The red line shows the global meteoric water line (GMWL, $\delta D=8\delta^{18}O+10$). No April xylem water analyses were undertaken.

The October xylem water data falls directly on the GMWL (red squares, figure 4.2.) with a mean δD value of -56.05±1.41 ‰ (SEM, n=23). As measured local Loch water δD, a proxy for MAP is -53.9 ‰ δD, with δD measurements of small streams crossing the sample site exhibiting δD values of -56.08 and -59.27 ‰ δD respectively. These data suggest that MAP is a more dominant water source for the Scots pine within this region than local growth season precipitation (full raw data, table 4, appendix). In a similar manner to the Finnish site, and although local precipitation was not measured in situ, estimations from the OIPC (Bowen 2013) indicate precipitation to be in the region of -71 ‰ and -66 ‰ δD for April and October respectively. As these values are more D-depleted, this further suggests MAP is a more important water source for the Scots pine growing in Scotland. However, a complete April 2010 xylem water δD data set would be needed to fully confirm this hypothesis.

The April leaf water data (green triangles, figure 4.2) falls to the right of the GMWL, on a LMWL of y=2.3244x-25.066. This indicates significant leaf water evaporative D-enrichment, which also show high levels of variability. The October leaf water data displays much different behaviour (purple crosses, figure 4.2) to that measured in April. Although the leaf water data falls to the right of the GMWL, on a LMWL of y=1.4205x-19.188, indicating evaporative enrichment. The data is much closer to the GMWL and more tightly clustered, this suggests less variation and less evaporative D-enrichment than leaf waters measured in April at the same location.

4.4.3. Finland xylem water; effects of tree size and canopy position

Mean xylem water δD values appear relatively consistent between July and September in Finland (figure 4.3), with -78.72±3.11 ‰ (SEM, n=22) observed in July and -82.84±1.21 ‰ (SEM, n=24) during September. A paired t-test does not detect a significant difference in mean xylem water δD values between July and September (t=1.44, P=0.16). In addition, two-way ANOVA (table 4.1), with individual tree size/age and relative height in the crown as categorical factors, and xylem water δD values as the continuous factor, does not detect significant variation as a result of individual tree-size during July or September. This suggests tree size/age does not significantly influence the δD signatures of xylem waters in Finnish Scots pine.
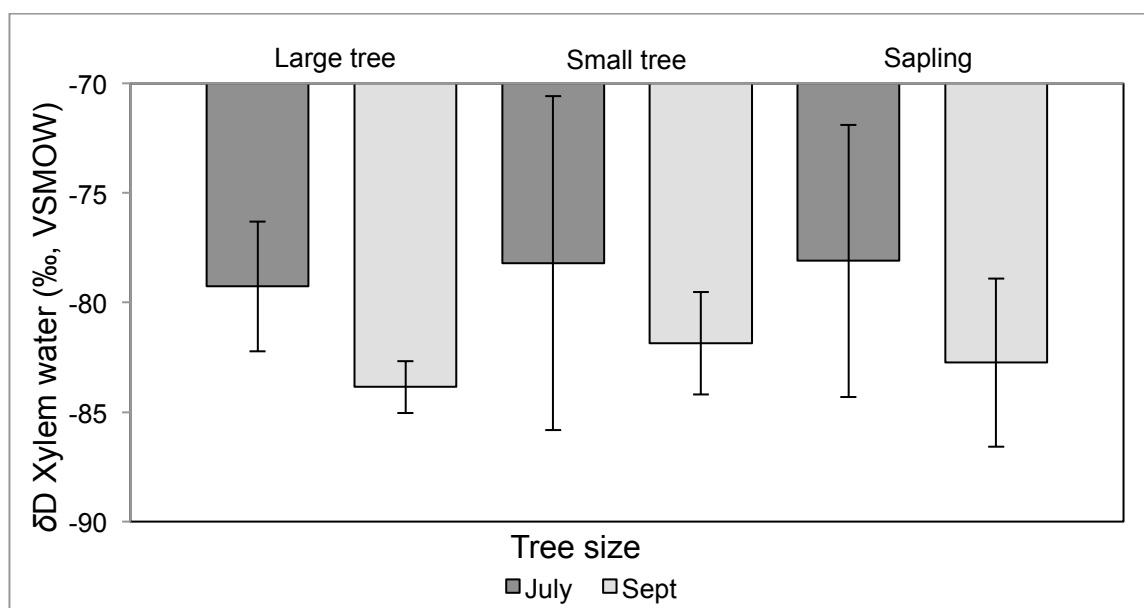
Figure 4.3: Mean xylem water δD (‰, VSMOW) by tree type for the Finnish data. Dark bars show July 2010 data, while light grey depict September 2010 values. Error bars represent the standard error of the mean (SEM).

Table 4.1: Summary of the two-way ANOVAs applied to the Finnish xylem water δD values, where tree size and relative height in the crown are the categorical factors and δD xylem water is the continuous factor. Statistically significant results are marked "*",

Time	Source	DF	F	P
	Tree Size	2	0.02	0.98
	Relative height	2	1.48	0.26
	Interaction	2	4.39	0.03*
July	Residuals	21		
	Tree Size	2	0.34	0.72
	Relative height	2	2.03	0.16
	Interaction	2	0.50	0.61
Sept	Residuals	21		

Furthermore, two-way ANOVAs do not detect significant variation in xylem water δD values as a result of relative height within the crown during July or September, but a significant variation is detected as a result of the interaction between individual tree-size and relative height in the crown during July only (F=4.39, P=0.03). This suggests the relative position in the canopy, i.e. top, middle or lower foliar position, can impact the δD value of xylem water within an individual tree during July. Examination of xylem water δD values in relation to canopy position (figure 4.4) suggests greater D-depletion of xylem waters in the upper (top) and lower (bottom) canopy sections of the trees studied at this time.

These data therefore suggest the Finnish Scots pine under investigation have a consistent xylem water D isotopic composition across individuals, and with time in the growing season.
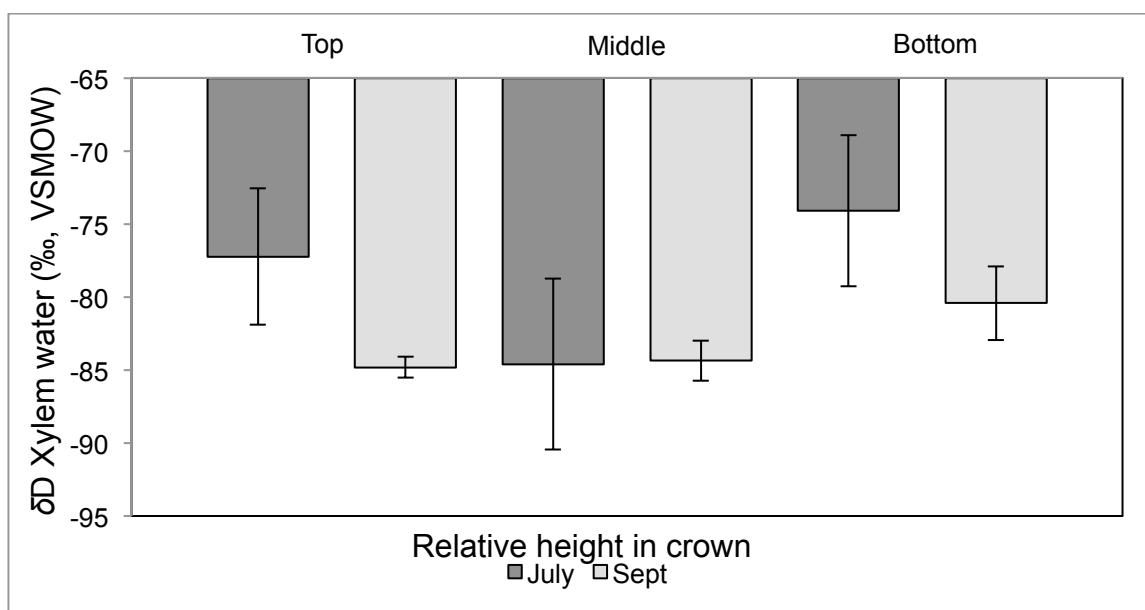
Figure 4.4: Mean xylem water δD (‰, VSMOW) by relative height within the crown for the Finnish data, dark bars represent July 2010 and light grey bars show September 2010. Error bars show the standard error of the mean.

4.4.4. Finland leaf water; effects of tree size and canopy position

The leaf water δD values from the Finnish sample site reveal a significant D-depletion in leaf water between the July and September sample collections (paired t-test, t=5.93, P=5.68E^{-06}). Giving a mean δD leaf water value during July of -46.28±1.57 ‰ (SEM, n=27) and -80.28±4.14 ‰ (SEM, n=24) during September. The total range of leaf water δD values during July of -31.63 to -61.17 ‰ is much less than the range of -49.28 to -108.24 ‰ δD observed during September (figure 4.5).

Table 4.2: Summary of the two-way ANOVAs applied to the Finnish leaf water δD values, where tree size and relative height in the crown are categorical factors and δD leaf is the continuous factor. Statistically significant results are marked "*".

Time	Source	DF	F	P
	Tree Size	2	4.14	0.03*
	Relative height	2	1.13	0.30
	Interaction	2	0.28	0.60
July	Residuals	21		
	Tree Size	2	6.15	0.009*
	Relative height	2	0.07	0.79
	Interaction	2	0.09	0.76
Sept	Residuals	21		

Investigation into the effect of individual tree size/age on the leaf water δD values (figure 4.5.) indicates a clear D-depletion across all the different tree-size categories between July and September 2010. In addition, although it would appear from figure 4.5 that there are no clear trends in D-depletion in relation to individual tree-size within each sample collection period. Two-way ANOVA (table 4.2) with individual tree-size and relative height

in the crown as categorical factors, and leaf water δD values as the continuous factor, reveals there is a significant effect of size/age on the D-enrichment of leaf waters during both July (F=3.81, P=0.04) and September (F=5.49, P=0.01).
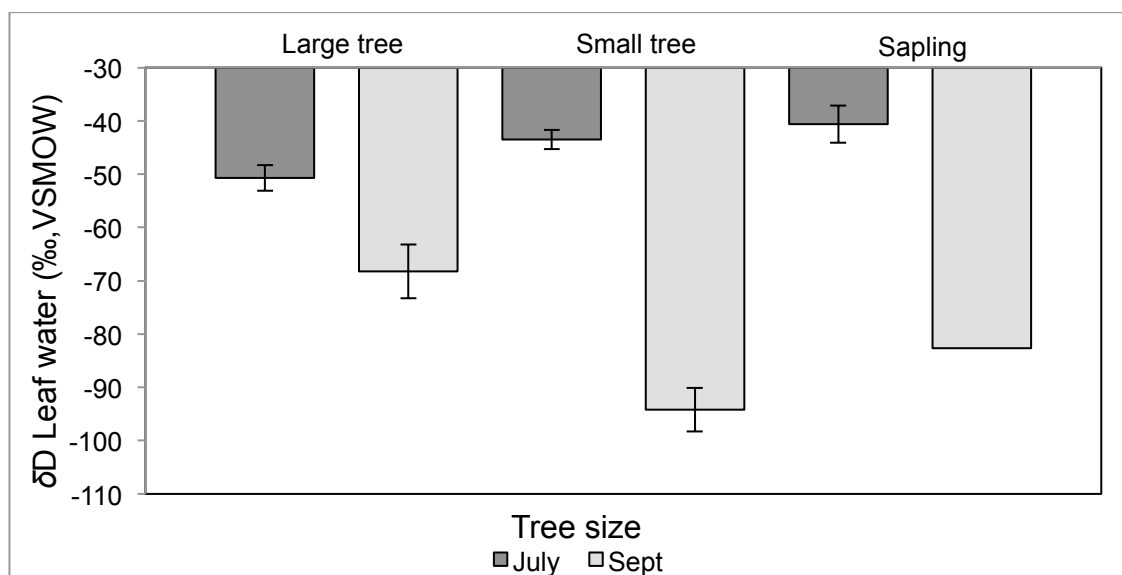
Figure 4.5: Mean leaf water δD (‰, VSMOW) by tree type for the Finnish data. Dark bars show July 2010 data, while light grey depict September 2010 values. Error bars represent the standard error of the mean (SEM), n=6 except for the Sapling category during Sept were too few measurements were possible and n=2.

Break down of mean leaf water δD values by relative height in the tree crown (figure 4.6) reveals significant D-depletion in leaf waters across all locations with time in the growth season. However, two-way ANOVA (table 4.2) does not detect significant variation as a result of canopy position during July or September. As well as no significant effect of the interaction between relative height in the crown and individual tree-size, this indicates these parameters does not influence leaf water δD values.
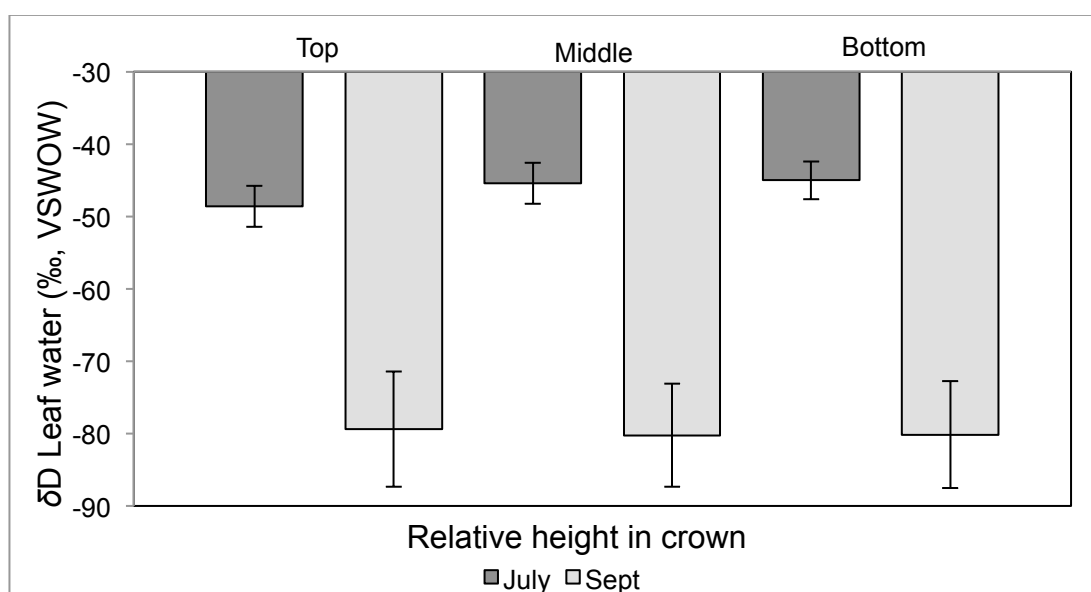
Figure 4.6: mean leaf water δD (‰, VSMOW) by relative height within the crown for the Finnish data, dark bars represent July 2010 and light grey bars show September 2010. Error bars show the standard error of the mean.

4.4.5. Finland leaf water fractionation above xylem water

As the fractionation of a "product water pool" above a "source water pool" is calculated using the same equation as that used in calculating the apparent fractionation of n-alkanes above waters; the fractionation of leaf water above xylem water (ΔD leaf water) is calculated using equation 2.7:

$$\varepsilon_{s/p} = 1000 \times \left[\frac{(\delta_p + 1000)}{(\delta_s + 1000)} - 1 \right]$$

(2.7)

Where, δ_p is the hydrogen isotopic composition of the leaf water and δ_s is the isotopic composition of the xylem water. This data indicates significantly different behaviour within the Finnish Scots pine between July and September. Mean ΔD leaf water exhibits a significant reduction between July and September with 38.18±2.67 ‰ (SEM, n=21) and 4.00±4.32 ‰ (SEM, n=25) observed respectively (paired t-test, t=5.59, P=2.15E^{-05}). This significantly different behaviour can be clearly seen across all the different sized/aged trees sampled in Finland (figure 4.7), and in the δD versus δ^{18}O plot (figure 4.1). Two-way ANOVAs (table 4.3), with individual tree size and relative height in the crown as categorical factors, and ΔD leaf water as the continuous factor, indicate a significant effect of individual tree size/age on ΔD leaf water during July (F=10.09, P=0.002) and September (F=6.71, P=0.007). This suggests individual tree size has a significant influence on the fractionation of leaf waters above xylem waters.
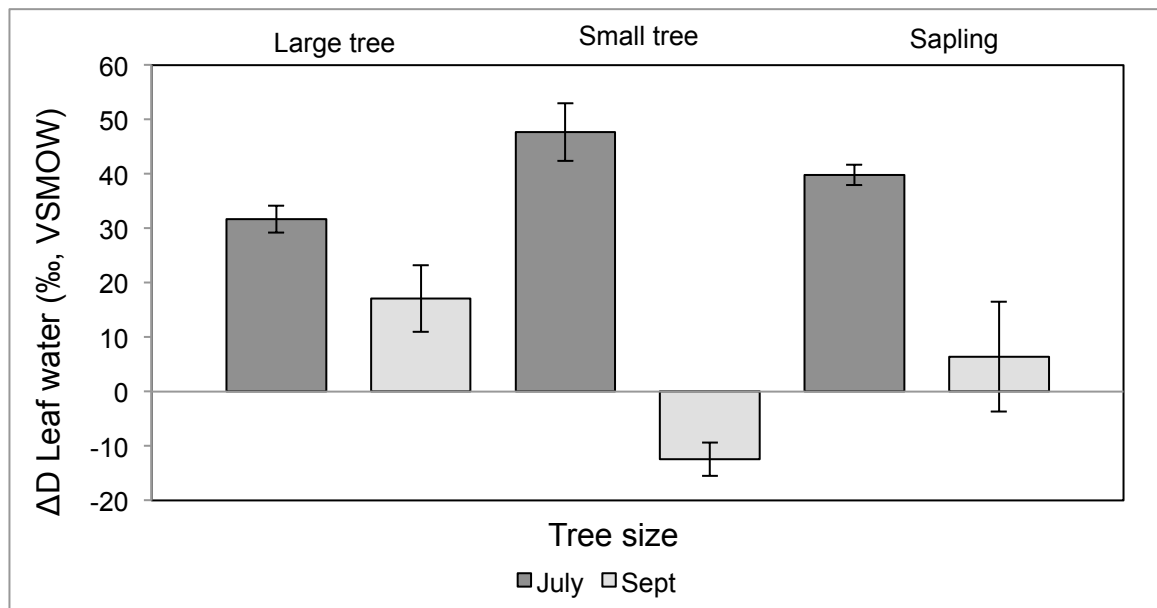
Figure 4.7: Mean fractionation of leaf water above xylem water (‰, VSMOW) by tree type for the Finnish data. Dark bars show July 2010 data, while light grey depict September 2010 values. Error bars represent the standard error of the mean (SEM).

Table 4.3: Summary results of the two-way ANOVAs the Finnish ΔD leaf water data were subject to, where tree size and relative height were categorical factors and ΔD leaf water was the continuous factor. Statistically significant results are marked "*".

Time	Source	DF	F	P
	Tree Size	2	10.09	0.002*
	Relative height	2	0.34	0.06
	Interaction	2	6.70	0.009*
July	Residuals	21		
	Tree Size	2	6.71	0.007*
	Relative height	2	0.16	0.85
	Interaction	2	0.02	0.98
Sept	Residuals	21		

Examination of the effect of relative canopy position on ΔD leaf water between July and September (figure 4.8) further highlights the significant difference in ΔD leaf water with time in the growth season. For example, two-way ANOVAs (table 4.3) suggest a significant amount of variation within individual trees is driven by relative canopy position during July (F=6.70, P=0.009) with no similar effect observed during September. No significant effect of the interaction between individual tree size and relative height in the crown is observed during July or September. These data suggest that relative canopy position within individual trees is an important factor in determining the level of leaf water D-enrichment above xylem water during July only in Finland.
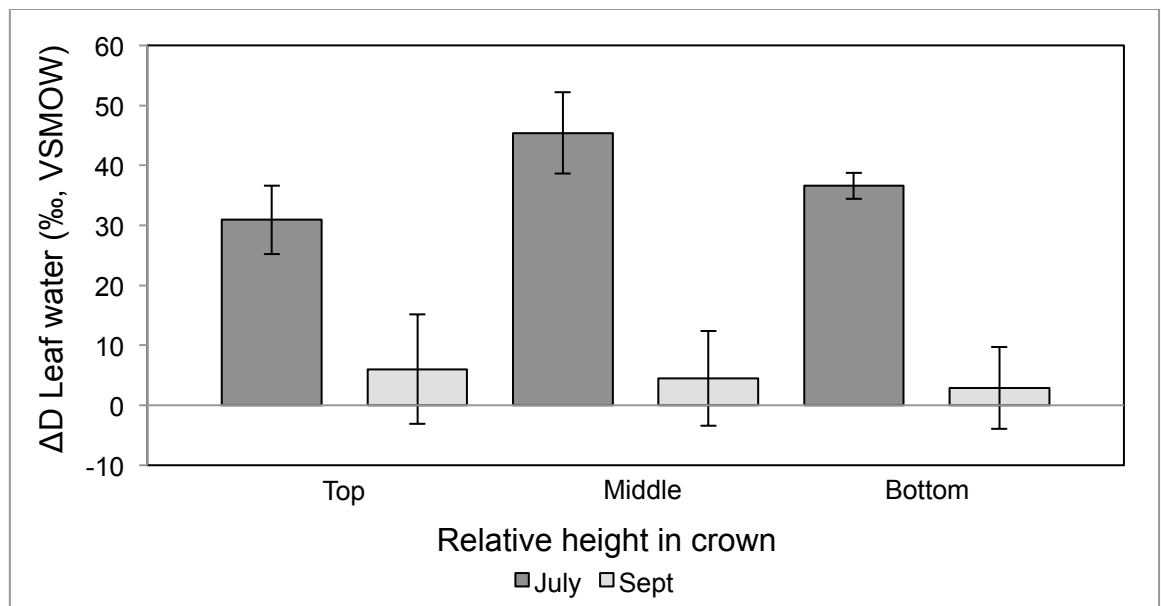
Figure 4.8: mean fractionation of leaf water above xylem water (‰, VSMOW) by relative height within the crown for the Finnish data, dark bars represent July 2010 and light grey bars show September 2010. Error bars show the standard error of the mean.

4.4.6. Scotland leaf water; effects of tree size and canopy position

Due to the lack of complete xylem water δD data sets for the Scottish sampling site during both April and October, the breakdown of this data by tree size/age category, and relative height within the tree crown is not shown, however it is available in table 4 included in the appendix.

Two-way ANOVA (table 4.4) with individual tree-size and relative height in the crown as categorical factors, and xylem water δD value as the continuous factor, does not detect significant variation in xylem water δD values during October as a result of individual tree size/age, relative height within the crown, or the interaction of individual tree size and relative height in the crown.

Table 4.4: Summary of the two-way ANOVA the Scottish leaf water δD values were subjected to, where tree size and relative height are categorical factors and δD leaf water was the continuous factor.

Time	Source	DF	F	P
	Tree Size	2	1.79	0.20
	Relative height	2	1.99	0.17
	Interaction	2	0.47	0.63
Oct	Residuals	21		

The total range of leaf water isotopic composition observed during April of -55.70 to 10.75 ‰ δD, is larger than that observed during October of -44.0 to -13.02 ‰ δD. However, total mean leaf water δD shows no significant difference between the April and October sample collections in Scotland (paired t-test, t=0.25, P=0.81), with -19.08±3.35 ‰ δD (SEM, n=28) observed in April and -22.88±1.33 ‰ δD (SEM, n=24) in October.

Investigation into the effect of individual tree-size on the level of leaf water D-enrichment (figure 4.9) shows relatively consistent leaf water δD values. With the exception of April leaf water in the sapling category, which appears much more D-depleted in comparison to the other tree size/age categories. This observation is further supported by two-way ANOVA (table 4.5), with individual tree-size and relative height in the crown as categorical factors, and leaf water δD values as the continuous factor. Where, a significant level of variation in leaf water δD values is observed as a result of individual tree-size during April (F=4.42, P=0.03), and not October. These data suggest individual tree size can affect leaf water δD values during April only.
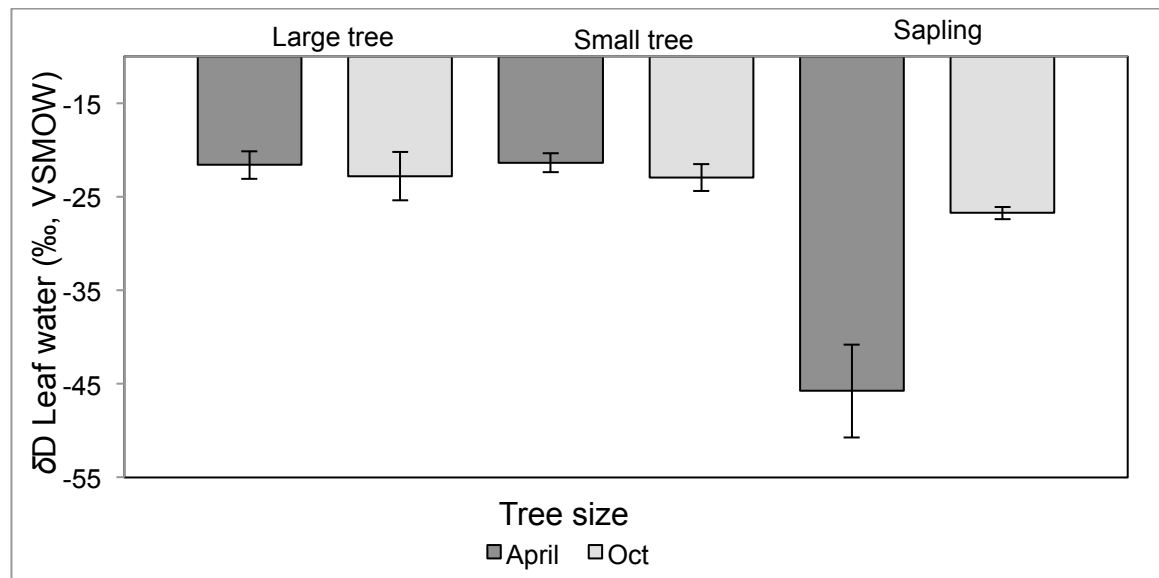
Figure 4.9: Mean leaf water δD (‰, VSMOW) by tree type for the Scottish data. Dark bars show April 2010 data, while light grey depict October 2010 values. Error bars represent the standard error of the mean (SEM).

Table 4.5: Summary table of the results of two-way ANOVAs the Scottish leaf water δD values were subjected to. Tree size and relative height were the categorical factors and δD leaf water the continuous factor, statistically significant results are marked "*".

Time	Source	DF	F	P
	Tree Size	2	4.42	0.03*
	Relative height	2	1.30	0.30
	Interaction	2	3.29	0.06
April	Residuals	21		
	Tree Size	2	2.82	0.09
	Relative height	2	0.18	0.84
	Interaction	2	0.23	0.79
Oct	Residuals	21		

Further investigation into the effect of relative canopy position on leaf water δD values (figure 4.10) indicates relative canopy position, or the interaction of canopy position and individual tree-size, has no significant influence on the D isotopic compositions of leaf waters during either April or October within the Scottish Scots pine (table 4.5).

Chapter 4: Water sourcing and leaf water isotopic enrichment of
natural Scots pine forests
| 107
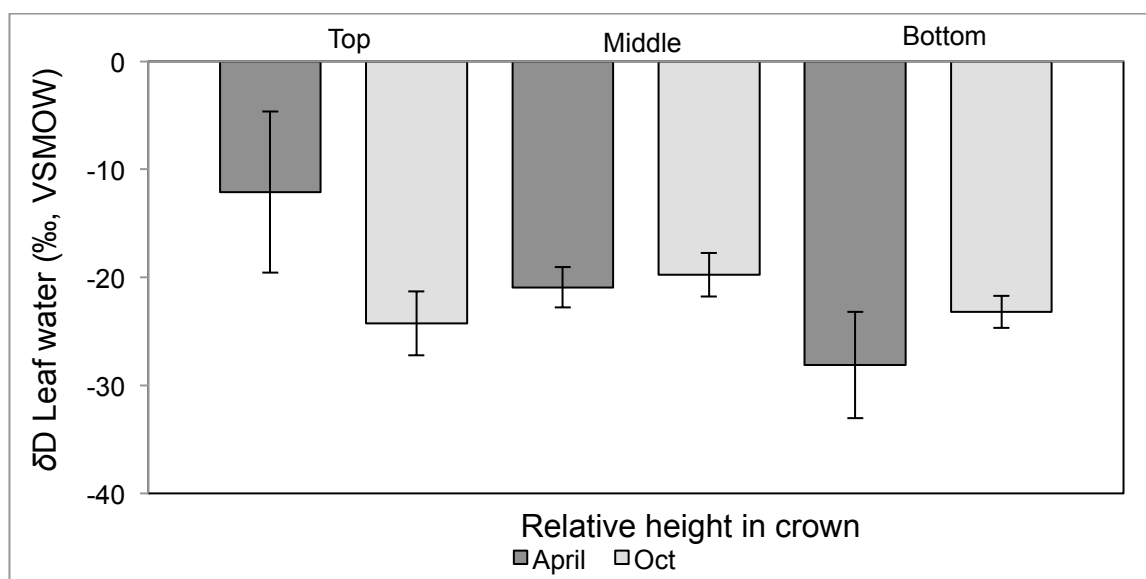
Figure 4.10: Mean leaf water δD (‰, VSMOW) by relative height within the crown for the Scottish data. Dark bars show April 2010 data, while light grey depict October 2010 values. Error bars represent the standard error of the mean (SEM).

4.4.7 Finland trends with height

As variations in height from the forest floor can drive variations in micro-climatic variables in natural forest stands (Niinemets, Kull et al. 1999, Le Roux, Bariac et al. 2001, Woodruff, Meinzer et al. 2009), the impact of height of sample collection was investigated in the data sets. Correlation of xylem water δD values against height of sample collection, during July and September from Finnish Scots pine, suggest no relationship between these variables (figure 4.11). This finding is further supported by simple linear regression analysis (table 4.6), where no significant correlation between height of sample and xylem water δD values was detected. Furthermore, two-way ANOVA with height of sample collection (m) and aspect as categorical factors, and xylem water δD values as the continuous factor, did not detect significant variation as a result of sample collection height, aspect, or the interaction of height and aspect during July or September (table 4.7).

Table 4.6: summary of the simple linear regression analyses applied to the Finnish xylem water δD values (XW δD) plotted versus height of sample collection (m).

Time	x,y	Equation	Adjusted R^2	F	P
July	XW δD vs Height	Y=0.1312x-81.95	-0.05	0.10	0.75
Sept	XW δD vs Height	Y=-0.288x-80.404	0.04	2.07	0.16
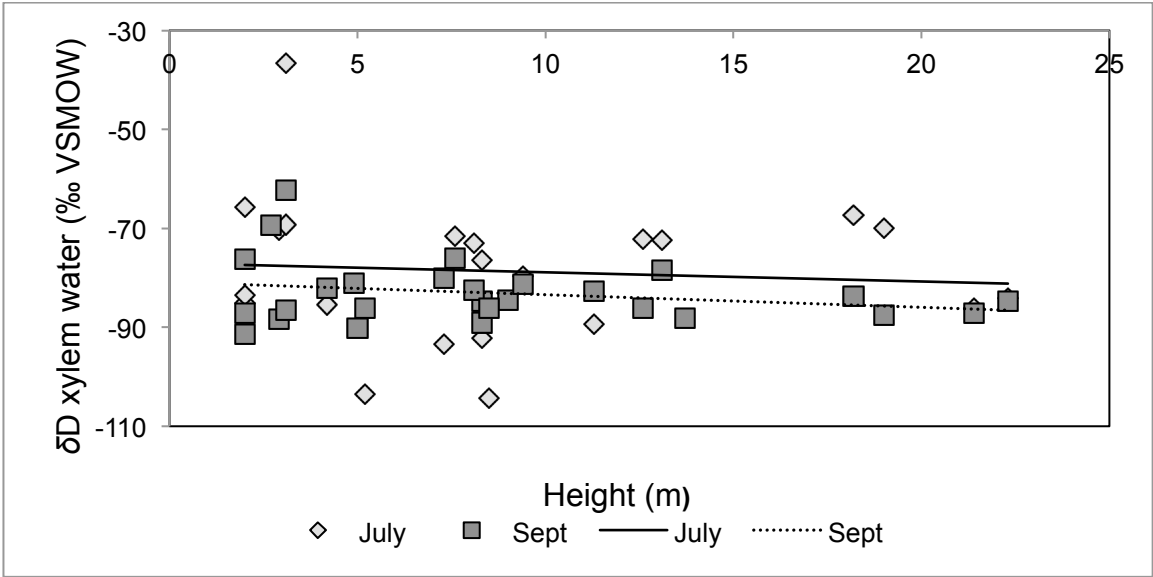
Figure 4.11: Scatter plot with simple linear regression lines for height of sample collection (m) versus xylem water δD (measured in ‰ VSMOW) for July and September 2010 in Finland. Light diamonds represent July data and dark squares depict September data.

Table 4.7: Summary of two-way ANOVA outputs from the Finnish xylem water δD data, where height and aspect are categorical factors and xylem water δD value is the continuous factor.

Time	Source	DF	F	P
	Height	2	0.12	0.73
	Aspect	2	0.08	0.78
	Interaction	2	0.11	0.75
July	Residuals	21		
	Height	2	2.20	0.15
	Aspect	2	0.10	0.75
	Interaction	2	0.02	0.89
Sept	Residuals	21		

Despite these findings, the leaf water δD data from the Finnish site reveal significantly different trends. Not only are there the previously mentioned significant difference in mean leaf water δD values between July and September, there also appears to be significantly different correlations with height of sample collection between July and September (figure 4.12).
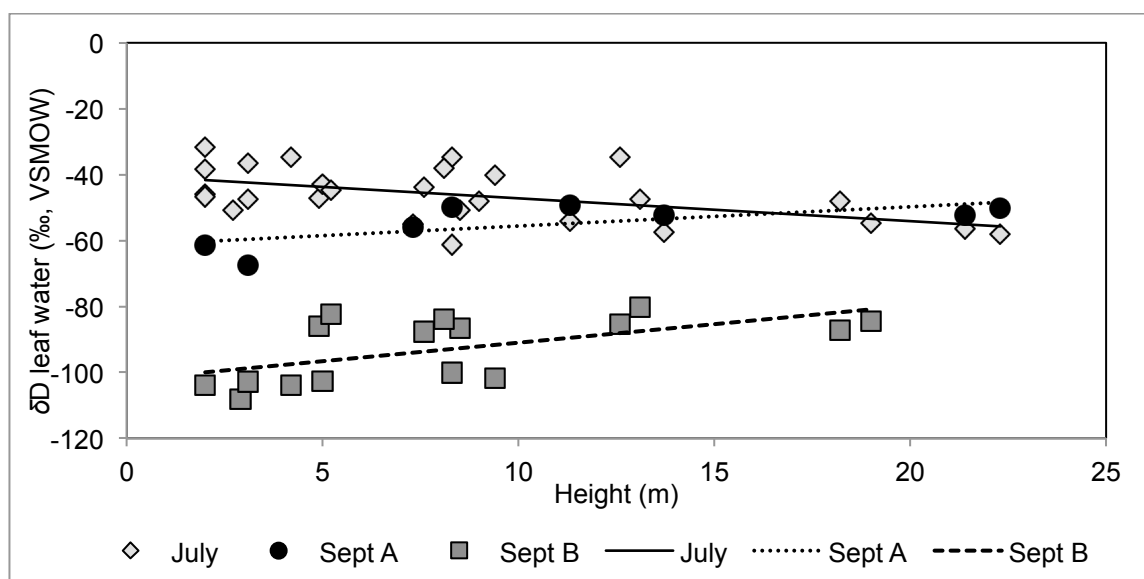
Figure 4.12: Scatter plot with simple linear regression lines for height of sample collection (m) versus leaf water δD (measured in ‰) for July and separated September 2010 in Finland (Sept A and Sept B). Light diamonds represent July data black circles show September A and dark squares depict September B data.

Simple linear regression analysis of height of sample collection versus leaf water δD values (table 4.8) indicates a significant, moderate, negative correlation with height of sample collection during July (R^2=0.21, F=7.6, P=0.011); while much different processes are at work during September. Upon inspection of the δD versus $δ^{18}O$ plot (figure 4.1), it was deemed necessary to separate the September Finnish leaf water δD data into two separate components, Sept A and Sept B. This was because the two different data sets exhibit two completely different linear regressions. It was therefore assumed that because Sept A and Sept B samples were collected on two different days, two different processes affected the leaf water D-enrichment on each day (figure 4.12). Independent simple linear regression analyses of the Sept A and Sept B indicated no significant relationship between height of sample collection and Sept A leaf water, while Sept B data exhibits a strong, statistically positive, correlation between height of sample collection and leaf water δD values (table 4.8, R^2=0.31, F=7.66, P=0.02).

Table 4.8: Summary table of the simple linear regression analyses applied to the Finnish leaf water data sets, where leaf water δD values (LW δD) has been plotted against height of sample collection. Statistically significant results are marked "*".

Time	x,y	Equation	Adjusted R^2	F	P
July	LW δD vs Height	Y=-0.692x-40.27	0.23	8.89	0.006*
Sept A	LW δD vs Height	Y=0.364x-57.60	0.26	3.29	0.13
Sept B	LW δD vs Height	Y=1.12x-102.24	0.31	7.67	0.02*

Two-way ANOVAs further support these findings (table 4.9), with significant levels of variation detected in leaf water δD values as a result of sample collection height during both July (F=8.32, P=0.008) and September (F=5.30, P=0.03). No significant effect of

aspect, or the interaction between height and aspect was detected during either sample collection period.

Table 4.9: summary of the two-way ANOVA tests using the Finnish leaf water δD values, where height and aspect were the categorical factors and δD leaf water the continuous factor. Statistically significant results are marked "*".

Time	Source	DF	F	P
	Height	2	3.32	0.008*
	Aspect	2	0.27	0.61
	Interaction	2	0.08	0.77
July	Residuals	21		
	Height	2	5.30	0.03*
	Aspect	2	0.21	0.65
	Interaction	2	0.57	0.46
Sept	Residuals	21		

Investigation into the effect of sample collection height on the fractionation of leaf waters above xylem waters (ΔD leaf water, figure 4.13) reveals very similar trends to the leaf water δD values (figure 4.12). Simple linear regressions (table 4.10) indicate a significant, weak-negative, correlation between sample collection height and ΔD leaf water during July (R^2= 0.21, F=6.4, P=0.02). Sept A data has no statistically significant correlation between ΔD leaf water and height of sample collection, while Sept B data exhibits a significant, moderately positive, correlation with height of sample collection (table 4.10, R^2=0.26, F=6.30, P=0.02) (figure 4.13).

Table 4.10: Summary of the simple linear regression statistical analyses the Finnish ΔD leaf water data (ΔD LW) was subjected to, significant results are marked "*".

Time	x,y	Equation	Adjusted R^2	F	P
July	ΔD LW vs height	Y=-0.965x-47.23	0.21	6.40	0.02*
Sept A	ΔD LW vs height	Y=0.81x+23.82	0.29	3.51	0.12
Sept B	ΔD LW vs height	Y=1.043x-17.85	0.26	6.30	0.02*

Application of two-way ANOVAs (table 4.11) also reports significant variation due to height of sample collection on ΔD leaf water during both July (F=5.85, P=0.03) and September (F=6.33, P=0.02), with no variation due to aspect.

Table 4.11: Two-way ANOVA summary for the ΔD leaf water data from Finland, where height and aspect are the categorical factors and ΔD leaf water the continuous factor. Statistically significant results are marked "*".

Time	Source	DF	F	P
	Height	2	5.85	0.03*
	Aspect	2	0.11	0.75
	Interaction	2	0.26	0.62
July	Residuals	21		
	Height	2	6.33	0.02*
	Aspect	2	0.35	0.56
	Interaction	2	0.72	0.41
Sept	Residuals	21		
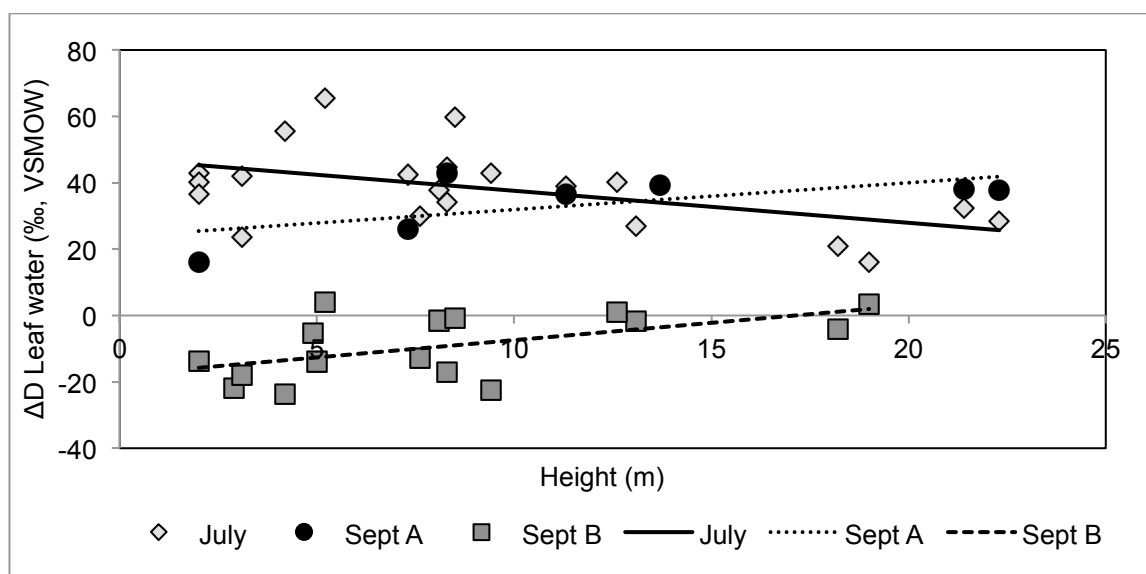
Figure 4.13: Scatter plot with simple linear regression lines for height of sample collection (m) versus fractionation of leaf water above xylem water (measured in ‰) for July and separated September 2010 in Finland. Light diamonds represent July data, black circles show September A and dark squares depict September B data.

In addition to the aforementioned findings, the ΔD leaf water data from September further highlight the anomalous leaf water D isotopic measurements observed in Finland. Where Sept B samples, collected between approximately 10 to 20m heights, have leaf water δD values which roughly equal xylem water δD values (figure 4.13, where several data points sit directly on the x-axis suggesting zero fractionation of leaf water from xylem water), while several sample collection points below 10m have leaf water δD values, which are D-depleted in relation to xylem water. The Sept A samples however, exhibit no trend with height of sample collection, but do exhibit the expected D-enriched leaf water above xylem waters reported during isotopic analyses of waters in plants. Therefore, the September ΔD leaf water data indicates some different hydrological process must be influencing the leaf water D isotopic compositions of the Sept B data in the Finnish forest at the time of sample collection.

4.4.8. Trends with height Scotland

Both simple linear regression analysis (Y=0.1312x-81.95, adjusted R2= -0.05, F=10, P=0.75), and two-way ANOVAs (table 4.12), failed to indicate significant variation in xylem water δD values with height of sample collection, as a result of aspect, or as a result of the interaction between height of sample collection and aspect (figure 4.14).

Table 4.12: Two.way ANOVA where δD xlylem water from October in Scotland is the continuous variable and height and aspect of sample collection are the categorical factors.

Time	Source	DF	F	P
	Height	2	1.15	0.29
	Aspect	2	0.01	0.93
	Interaction	2	0.09	0.78
Oct	Residuals	21		
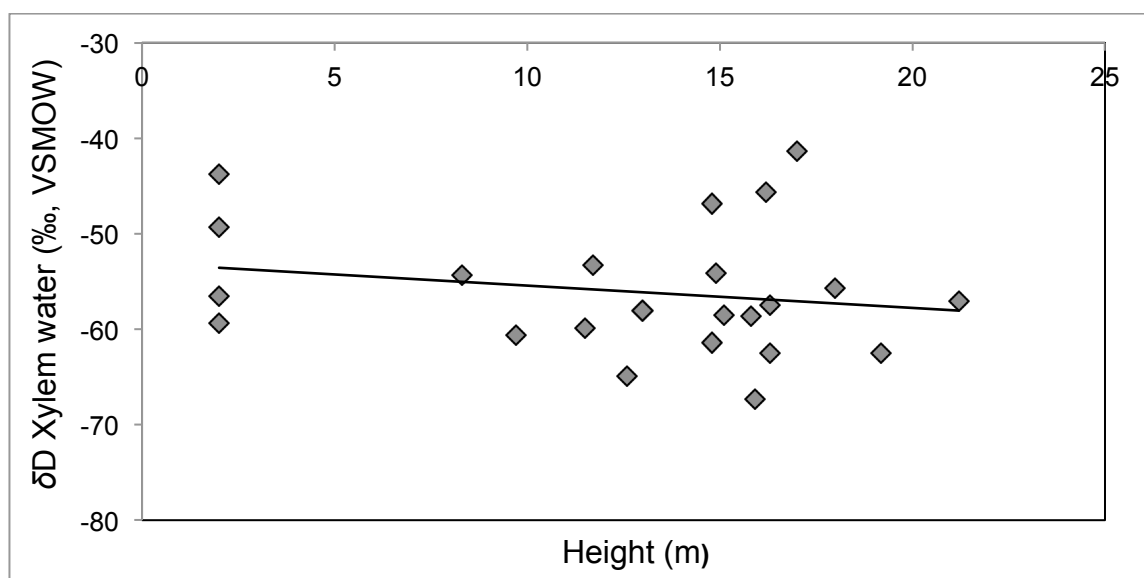
Figure 4.14: Scatter plot with simple linear regression line for height of sample collection (m) versus xylem water δD (measured in ‰) for October 2010 in Scotland.

Although no significant difference in mean leaf water δD values is observed between April and October (t-test, t=-0.25, P=0.81), simple linear regressions report a significant moderate, positive correlation between height of sample collection and leaf water δD values during April (R^2=0.34, F=13.30, P=0.001). No similar relationship is observed for the same samples collected during October (R^2=0.03, F=1.60, P=0.23) (figure 4.15, table 4.13).

Table 4.13: summary of the simple linear regression analyses of leaf water δD values (LW δD) versus height of sample collection (m) from the Scottish sample sites. Statistically significant results are marked "*".

Time	x,y	Equation	Adjusted R^2	F	P
April	LW δD vs Height	Y=1.261x-35.57	0.34	13.30	0.001*
October	LW δD vs Height	Y=0.284x-26.53	0.03	1.60	0.23
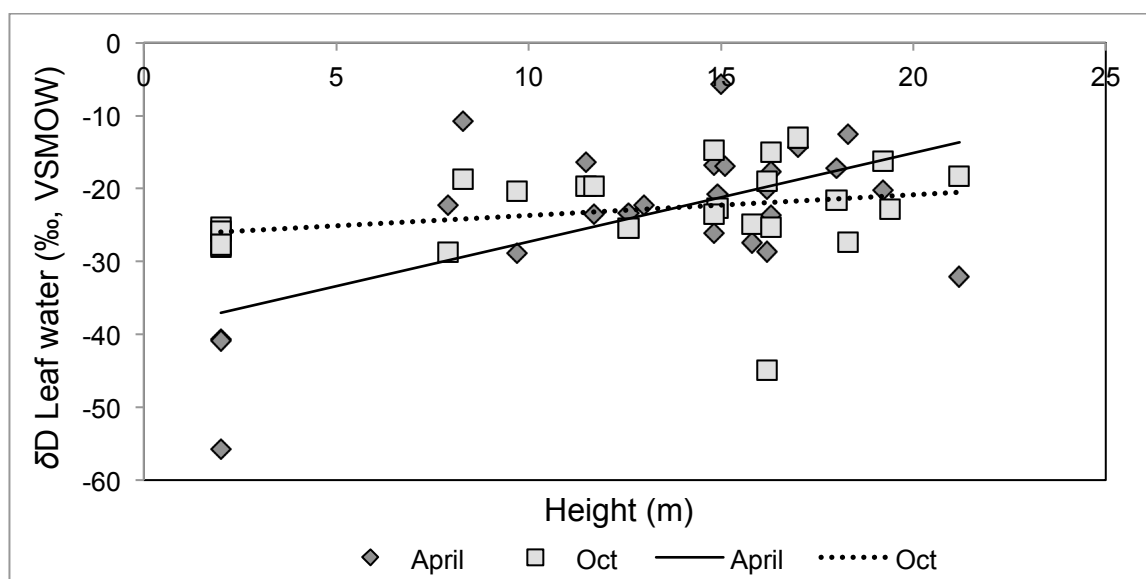
Figure 4.15: Scatter plot with simple linear regression lines for height of sample collection (m) versus leaf water δD (measured in ‰) for April and October 2010 in Scotland. Light diamonds represent April data and dark squares depict October data.

Nevertheless, two-way ANOVAs with height of sample collection and aspect as categorical factors, and leaf water δD values as a continuous factor (table 4.14), detect significant variation due to sample collection height during both April (F=5.39, P=0.03) and October (F=7.78, P=0.01). These ANOVAs indicate no effect of aspect, or the interaction between height and aspect during both April and October. These data suggest that leaf water δD values significantly, and positively, correlate with height of sample during April, and although leaf water significantly varies with height of sample collection during October, this variation is not a simple linear correlation.

Table 4.14: Summary of the Scottish leaf water δD two-way ANOVAs, where height of sample collection and aspect were the categorical factors and δD leaf water was the continuous factor, statistically significant results are marked "*".

Time	Source	DF	F	P
	Height	2	5.39	0.03*
	Aspect	2	2.26	0.15
	Interaction	2	2.76	0.11
April	Residuals	21		
	Height	2	7.78	0.01*
	Aspect	2	0.00	0.95
	Interaction	2	3.55	0.08
Oct	Residuals	21		

4.5. Discussion

The water sourcing behaviour of a natural forest stand can display significant variation between individual trees, even when a single species is investigated. As the aim of the current study is to characterise the isotope hydrology of natural Scots pine forests in two separate geographical locations. Detailed within and between individual tree isotopic analyses of xylem and leaf waters are presented, were the key drivers of trends within and between individuals are identified.

4.5.1. Forest water sourcing Finland

The whole forest isotope hydrology δD versus δ^{18}O plot (figure 4.1) suggests the Finnish Scots pine uptake water that carries an isotopic signature that is very slightly D-enriched in relation to meteoric waters. This falls to the right of the GMWL, indicating these waters have been subject to small levels of evaporative D-enrichment (Brandes, Wenninger et al. 2007). As mean xylem water δD values demonstrate no significant difference between July (-78.82±3.11 ‰, SEM, n=22) and September (-82.84±1.21 ‰, SEM, n=28), along with no significant variation attributable to individual tree size/age (figure 4.3), these data indicate Finnish Scots pine have consistent xylem water δD values that do not significantly vary between individuals, or with time in the growth season. In addition, the consistent xylem water isotopic composition, across all individuals, and with time the in growth season, suggest that this forest is not water limited (Hu, Moore et al. 2010). Therefore, the utilization of an averaged xylem water isotopic composition within this sample site would appear to be a valid technique in describing whole forest stand water sourcing behaviour within this region. Not-with-standing the observation that the data for xylem water δD values plotted in figure 4.1 shows a limited range of variation along a trajectory suggesting some degree of evaporative isotopic enrichment has occurred; the spread in isotopic composition is narrow, and does not invalidate the conclusion that the mean xylem water isotopic composition represents a good average of the forest stand.

Isotopic measurements of a small lake in the immediate vicinity of the sample site (figure 2.5, chapter 2, section 2.2.1.2) exhibits a D-depleted hydrogen isotopic signature of -102 ‰ δD, when compared to the mean xylem water δD values of ~80 ‰. As local lake and stream water is often a proxy for MAP (Feakins 2010), this suggests the trees are utilizing a different, and more D-enriched, water source. These findings, in conjunction with estimations of local precipitation from the OIPC (Bowen and Revenaugh 2003, Bowen

2013), where July precipitation is estimated at -82 ‰ δD, with a total growth season range of -79 to -86 ‰ δD, indicate summer precipitation is the dominant isotopic signature exhibited by the xylem waters of Scots pine in Finland. Furthermore, the lake water measurements indicate that winter precipitation signatures, estimated in the region of -121 to -130 ‰ δD (Bowen 2013), may influence the isotopic composition of the local MAP, but as the Scots pine under investigation do not access this water source during the growth season, the MAP signal will not be recorded in the organic matter subsequently synthesized by the trees under investigation.

These data therefore demonstrate a consistent xylem water D isotopic composition across all individuals and time in Finnish Lapland. However, the xylem water travels to the leaf, where transpiration during photosynthetic assimilation further alters the isotopic composition of this water. Therefore, a consistent xylem water isotopic composition, in terms of the current thesis, may be of little importance as this could be overwhelmed by leaf water isotopic fractionation. As research suggests it is the leaf water δD signal that is imprinted on subsequently synthesized organic matter (Leaney, Osmond et al. 1985, Marshall, Brooks et al. 2007), the δD values of *n*-alkanes may not be easily related to the isotopic composition of source waters, regardless of how consistent xylem waters may be temporally or spatially.

4.5.2. Leaf water D-enrichment Finland

Although there is a statistically consistent xylem water D isotopic composition within the Finnish forest, mean July leaf water δD values are significantly D-enriched in comparison to mean September leaf water, exhibiting a difference of ~34 ‰ δD. As the xylem water D-signals for the same samples demonstrate consistent δD values, while mean fractionation of leaf water above xylem water (ΔD leaf water) are significantly different between July and September (figure 4.7). The observed differences in leaf water δD values with time in the growth season are not driven by source water, and instead should be driven by differing levels of leaf water evaporative D-enrichment. Due to the more favourable conditions for photosynthesis during early summer in comparison to autumn, increased transpiration is generally anticipated to be the driving cause of this.

Not only is there a significant difference in the δD composition leaf waters between July and September, the within and between individuals δD data has produced some interesting trends. For example, individual tree size/age has a significant influence on leaf water δD values during July and September (figure 4.5, table 4.2), while height of sample

collection also has a significant effect on leaf water isotopic composition during July and September (table 4.9). However, the trends observed are completely opposing during the two different sample campaigns (figure 4.12).

As is demonstrated through simple linear regression analysis (figure 4.12, table 4.8), leaf water δD values are significantly negatively correlated with height of sample during July, while September Sept B leaf water δD values are significantly positively correlated. Under the assumption of increasingly favourable conditions for photosynthesis with increasing height in a forest canopy (Niinemets, Kull et al. 1999, Duursma and Marshall 2006, Powers, Pregitzer et al. 2008), one would anticipate increased leaf water D-enrichment with increasing height of sample collection. Nevertheless, as is shown, this trend is observed during September but not July.

Examination of the leaf water δD data alone would suggest leaf transpiration decreases with height during July, while leaf transpiration increases with height during September in Sept B data. Given the 24-hour photoperiod experienced by the Finnish forest during July, a positive correlation between leaf transpiration and height of sample would have been anticipated at this time. Nevertheless, leaf water isotopic compositions are not simply influenced by PAR levels and the evaporation of water out of the leaf. There are a multitude of different interacting climatic, and physiological factors, which can affect the leaf water isotopic composition. A useful tool in elucidating the drivers of the trends in the leaf water δD values observed is to refer to the fractionation of leaf water above xylem water data (ΔD leaf water).

The ΔD leaf water data from July supports the leaf water δD data, where there is a significant negative trend in ΔD leaf water with height of sample, i.e. less evaporative D-enrichment of leaf water is observed with increasing height of sample collection. This suggests that evapotranspiration is being restricted by height of sample collection. As research has indicated coniferous trees, inhabiting the boreal forest zone, can transpire 24-hours a day during the sub-Arctic summer 24-hour photoperiod in July, where transpiration rates are positively correlated with illumination levels (Sen'kina 2002). The data presented here is in direct contrast to these observations. Instead, the data presented here suggest that the leaves in the upper most parts of the trees sampled during the 24-hour photoperiod in July must not be transpiring 24-hours a day. This suggests that although conditions for photosynthesis become increasingly favourable with increasing height from the forest floor (Niinemets, Kull et al. 1999, Niinemets, Sonninen et

al. 2004, Powers, Pregitzer et al. 2008), there must be a plant physiological response that is restricting leaf transpiration in the upper canopy of the taller trees.

Plant physiological studies investigating height related physiological behaviour in tall trees have demonstrated a height related water stress at the tops of tall trees. These studies indicate the effects of extreme irradiance, and the gravitational resistance to water transport through the xylem, result in reduced net photosynthesis and transpiration at the top of tall trees (Niinemets, Sonninen et al. 2004, Duursma and Marshall 2006, Woodruff, Meinzer et al. 2008). Therefore, the July leaf water δD and ΔD leaf water data suggest the foliage in the upper canopy, which is subject to continuous sunlight, along with a 0.01MPa increase in xylem sap tension per meter increase in height (Woodruff, Meinzer et al. 2008), exhibit reduced transpiration. This research suggests the reduction in transpiration is because water supply to these locations cannot keep up with the transpirational demand, and this results in the closure of the stomata to prevent cavitation in the xylem. Therefore, the data within the current study suggests great care needs to be taken in the interpretation of leaf water δD data. As D-depleted leaf water may be a symptom of water stress driven by too favourable conditions for photosynthesis, rather than the complete opposite.

In contrast to the July data, the September ΔD leaf water data highlights a very different process at work. A significant positive correlation between height of sample collection and Sept B ΔD leaf water during September is observed (table 4.10). However, this positive correlation is not being driven by leaf transpiration, and instead appears to be driven by the atmospheric conditions outside the leaf. For example, the total range in ΔD leaf water during September is -23.8 to 42.9 ‰ δD, i.e. it includes both negative, zero, and positive fractionation (figure 4.13). Given that the basic isotopic theory of leaf transpiration dictates leaf water is always D-enriched above xylem water (Leaney, Osmond et al. 1985, Yakir, DeNiro et al. 1990, Wang and Yakir 1995, Farquhar, Cernusak et al. 2007, Kim and Lee 2011), how can leaf water δD values equal, or even be D-depleted with respect to the associated xylem water δD values?

As mentioned previously, two of the key mechanisms which drive leaf water evaporative D-enrichment are RH and the isotopic composition of the water vapour surrounding the leaf. Here, reduced RH and xylem water out of isotopic equilibrium with external water vapour will alter the isotopic composition of the water within the leaf (Farquhar and Cernusak 2005, Farquhar, Cernusak et al. 2007). However, when RH is very high, and the atmospheric water vapour surrounding the leaf very D-depleted (e.g. fog conditions), back

diffusion of light isotopes from the atmosphere into the leaf water has been demonstrated (Dawson 1998, Welp, Lee et al. 2008, Gat 2010, Kim and Lee 2011) (see chapter 2, sections, 2.1.2.1 through to 2.1.4.2 for explanation of this mechanism). This mechanism results in leaf water with δD values that are D-depleted in relation to xylem water δD values.

Research has indicated that conifers can absorb water directly from fog into needles (Dawson 1998, Burgess and Dawson 2004), and this can occur in RH above 50% (Sen'kina 2002, Farquhar and Cernusak 2005). This suggests fog or dew events in coniferous forests have the potential to significantly impact leaf water D-enrichment. Therefore, the observed trend in Sept B ΔD leaf water, where a large proportion of samples collected below 10m height are D-depleted in relation to xylem water, samples collected between 10 and 20m are equal to xylem water δD values, and samples collected above 20m show typical D-enrichment (figure 4.13), suggests the impact of a low lying fog on the sample site in the early morning prior to sample collection.

The data presented here demonstrate that leaf water D-enrichment, as well as ΔD leaf water, significantly vary within and between individuals of Finnish Scots pine, with much of the variation being explained by height of sample collection. The unexpected negative trend in leaf water D-enrichment with increasing height of sample collection observed in July, suggests an increased water stress with increased height induced physiological response of the plant to the 24-hour photoperiod. However, the September data indicates a significant influence of a low-lying fog having been absorbed directly into the leaves. Both these findings could have significant implications for the organic matter subsequently synthesized within these leaves. Furthermore, these data highlight the necessity for paired xylem water - leaf water δD analyses, particularly if the research has a paleoclimate reconstruction application (further discussion chapter 7 section)

4.5.3. Forest water sourcing Scotland

The whole forest isotope hydrology δD versus $\delta^{18}O$ plot (figure 4.2) from the Scottish sample site demonstrates October xylem waters fall directly on the GMWL. This removes any influence of evaporative enrichment on the isotopic composition of the water sourced by the Scots pine at this location (Brandes, Wenninger et al. 2007). However, local lake water exhibits a consistent δD value of -53.9 ‰, and three small streams within the immediate vicinity of sample collection range -56.08 to -59.27 ‰ δD (figure 2.6, chapter 2, section 2.2.1.3). Therefore, the mean xylem water δD value of -56.05±1.41‰ (SEM,

n=23) suggests local ground water is an important water source for the Scottish Scots pine during October. Forest reliance on water sources other than current precipitation is a common observation, previous research has suggested 60% of precipitation falling upon the ground vegetation/litter layer evaporates within 4 days (Reynolds and Knight 1973), and in some cases, precipitation events are not of significant duration and intensity to penetrate the soil profile to any great depth (Hu, Moore et al. 2010). In addition, a thick ground covering of Sphagnum mosses characterizes the Black Wood of Rannoch. As thick ground vegetation has been demonstrated to dramatically reduce the amount of precipitation that can enter the soil (Sachse 2009). The trees at this location must utilize another more reliable water source, i.e. ground water. Unfortunately the consistency of this signal with time in the growth season could not be tested, as April xylem water data is unavailable.

The leaf water δD values from the April 2010 sample collection period exhibit much greater variation across the sample set in comparison to the October data, with a total range of ~100 ‰ δD observed in April, compared to ~30 ‰ δD during October (figure 4.2). Although using leaf water δD values to make inferences regarding the isotopic composition of xylem waters should be approached with caution; a significant level of variation in leaf water δD values is attributed to individual tree size/age, with a clear D-depletion in sapling leaf water, in comparison to the small and large tree-size categories (figure 4.9, table 4.12). It is possible that the observed D-depletion shown within the sapling tree category is simply driven by reduced transpiration as a result of reduced illumination, which is driven by the short stature of these trees (less than 3m). However, it is also possible that the smaller younger trees are tapping into a shallower more D-depleted water source, because of a shallower rooting depth (Dawson and Pate 1996, Dawson and Ehleringer 1998). Nevertheless, complete April xylem water δD analyses would be required to confirm this theory.

4.5.4. Leaf water D-enrichment Scotland

It is clear that the significantly different climatic regimes have very different influences on the isotopic compositions of leaf water between the two geographical sample locations. Although total mean leaf water δD values show no significant difference between April and October, there is a clear difference in trends observed with time in the growth season. For example, as mentioned previously, a much greater range of ~100 ‰ δD is observed in leaf water during April with respect to the ~30 ‰ δD range exhibited in October (figure 4.2). In addition, significant variation due to individual tree size/age is detected during

April, with no similar trend detected during October (figure 4.9, table 4.12). Furthermore, a significant positive correlation of leaf water D-enrichment with height of sample collection during April (figure 4.15), supported by two-way ANOVA, is more in keeping with the increasingly favourable conditions for photosynthesis with increasing height in forest canopies (Niinemets, Kull et al. 1999, Niinemets, Sonninen et al. 2004, Powers, Pregitzer et al. 2008, Woodruff, Meinzer et al. 2008). This suggests the temperate photoperiod is not significant enough to induce similar illumination induced height related water stresses at the tops of tall trees in Scotland, as is observed in the Finnish trees during July.

Although no correlation between height of sample collection and leaf water is observed in October through simple linear regression analysis. Two-way ANOVA (table 4.14) does detect significant variation in leaf water δD values as a result of height of sample collection at this time. As this relationship is not linear, and no significant effect of relative canopy position is also observed, the data indicates PAR is not the dominant driver of this trend, which due to the reduced total photoperiod in Scotland during October, would be anticipated.

4.5.5. Summary

The data presented here demonstrates how Scots pine forest within two distinctly different geographical locations can exhibit significant different isotopic hydrological characteristics. Commonly averaged site values, OIPC values, and MAP values are used to characterise apparent fractionation factors between lipids and source waters for paleo climate reconstructions. The current study supports the MAP approach for characterising the Scottish site, while summer precipitation isotopic compositions characterize the Finnish site. Nevertheless, the significant decrease in ΔD leaf water with height of sample collection observed during July, and the D-depleted leaf water in relation to xylem water data reported in Sept B data from September in Finland are of particular interest. The Scottish sample site however, appears to exhibit more predictable behaviour in its leaf water δD data, with increasing D-enrichment with increasing height of sample collection during the early growing season. Few studies have attempted to fully understand the isotopic heterogeneity that can occur within natural forest ecosystems, or even individual trees. Here it was demonstrated that specific climatic and physiological responses of trees can produce leaf water isotopic compositions, which if imprinted on subsequently synthesized organic matter, could lead to significantly erroneous interpretations of climate within the region of study, discussed in detail in chapters 5 and 7.

4.6. Conclusions

1. Finnish Scots pine (*Pinus Sylvestris L.*) exhibits statistically consistent xylem water δD values across all individuals and time in the growing season.

2. Scottish Scots pines exhibit a statistically consistent xylem water δD composition across all individuals during October.

3. Although there is a lack of April xylem water isotopic data, the significant D-depletion of sapling leaf water δD values in comparison to the other tree-size categories suggests saplings at the Scottish site use a potentially D-depleted water source in April.

4. Finnish Scots pine xylem water δD values are in the region of -80 ‰, which could be indicative of summer precipitation.

5. The Scottish Scots pine mean xylem water δD value of ~-56 ‰ indicates reliance upon MAP.

6. Leaf water isotopic compositions significantly vary within, and between, the different individuals studied in both geographical locations.

7. Height of sample collection exhibits a strong control on leaf water δD values in both geographical locations.

8. Illumination induced water stress with height, due to the 24-hour photoperiod during the early Finnish growth season, produces a significant negative trend of leaf water D-enrichment with height of sample in July.

9. Leaf water D-enrichment significantly positively correlates with height of sample in Scotland during April, which is expected and predicated under the assumptions of increasingly favourable conditions for photosynthesis with height in natural forest canopies.

10. The hydrology of individual forest ecosystems, where meteoric water- xylem water-leaf water isotopic analyses are conducted, is a crucial precursor to the interpretation of any organic matter synthesized within these if paleo-climate proxies are to be calibrated in any reliable capacity.

5. Hydrogen isotopic analysis of *n*-alkanes in Scots pine; variations and fractionations from waters

5.1 A literature review

5.1.1. Introduction

The entire premise of using the compound-specific hydrogen isotopic compositions of *n*-alkanes as a paleo-environmental proxy is that the *δ*D value recorded within these compounds can be related to the original hydrogen isotopic composition of the source regions meteoric water with high accuracy. Issues relating to the compound-specific carbon isotopic compositions, the preservation, transportation, and timing associated with the input of *n*-alkanes to any respective sediment record goes beyond the scope of the current thesis. In this chapter however, the variation in the *δ*D values of *n*-alkanes within and between individuals of Scots pine (*Pinus Sylvestris L.*), of varying size with time in the growth season, is quantified in two different geographical locations. The water isotopic data, presented in chapter 4, is then used to understand how the *δ*D values of the *n*-alkanes relate to leaf and xylem water *δ*D values. This is to better understand which factors are most important in driving the isotopic hydrogen compositions of *n*-alkanes.

5.1.2 Compound-specific hydrogen isotopic compositions of *n*-alkanes

The compound-specific hydrogen isotopic composition of *n*-alkanes (depicted by *δ*D notation and measured in parts per mill, ‰) in any terrestrial modern plant is generally considered to reflect the combination of the original hydrogen isotopic composition of the plants source water, specific conditions present during photosynthesis, and the subsequent biosynthesis of these lipid compounds (Sessions 1999, Chikaraishi, Naraoka et al. 2004, Sachse 2012). Nevertheless, the major drivers influencing the compound specific *δ*D values of *n*-alkanes synthesized by living terrestrial plants are currently a highly debated topic.

The general consensus from current research suggests the *δ*D values observed in *n*-alkanes in various modern terrestrial plant species are highly correlated with the plants

source water δD values (Chikaraishi 2003, Sachse, Radke et al. 2004, Sachse 2006, Hou 2008, Liu and Yang 2008, Rao 2009, Feakins 2010, Sachse 2012). These *n*-alkane isotopic signatures are however offset as the original δD value of the source water becomes D-enriched/depleted as it progresses through the hydrological cycle of a natural ecosystem. Where, evapotranspiration in the leaf generally results in D-enrichment, and then biosynthetic fractionation during *n*-alkane synthesis causes significant D-depletion (Chikaraishi and Naraoka 2001, Sachse 2012). It has been suggested that the δD values of *n*-alkanes can hold information on climatic variables, such as relative humidity (RH), temperature, and incoming photosynthetically active radiation (PAR) (Sachse 2012). Nevertheless, it is becoming increasingly evident that differing plant ecophysiological behaviours, in conjunction with specific environmental characteristics, could be complicating this matter. Until these uncertainties are addressed and resolved, making interpretations from ancient sediments based on our current knowledge may not be accurate.

5.1.3 The D isotopic composition of *n*-alkanes

After water has entered a plant, the hydrogen isotopic compositions expressed by *n*-alkanes are generally the result of three key factors. The D isotopic composition of the biosynthetic precursor (i.e. leaf water), exchange and fractionation as a result of biosynthesis, and hydrogenations at the time of biosynthesis (Sessions 1999). The biosynthesis of *n*-alkanes present in the epicuticular wax of terrestrial higher plants is discussed in chapter 2 sections 2.1.2 and 2.1.2.1. However in brief, research suggests *n*-alkanes are synthesized from leaf water (Sessions 1999, Chikaraishi, Naraoka et al. 2004, Feakins 2010), from C_{16}-C_{18} fatty acid precursors, which themselves are synthesized *de novo* in the plastids via the acetogenic pathway (Post-Beittenmiller 1996, Sessions 1999, Shepherd and Griffiths 2006, Eglinton 2008, Sachse 2012).

These fatty acids are then transported to the endoplasmic reticulum, where further chain elongation processes occur through Fatty Acid Elongases (FAEs). NADPH is the reducing agent throughout this process (Zhang, Gillespie et al. 2009), and research suggests that ~50% of hydrogen in acetogenic lipids is derived from NADPH (Sessions 1999). Each chain elongation cycle produces a two-carbon addition, resulting in multiple elongation cycles to produce fatty acids of longer chain length, termed Very Long Chained Fatty Acids (VLCFA). This process results in the often observed increasing D-depletion with increasing *n*-alkane chain length (Sachse 2006, Eglinton 2008). Typically the VLCFAs lose one carbon through decarbonylation to become *n*-alkanes, a process which is well

established, but not very well understood (von Wettstein-Knowles 1995, Post-Beittenmiller 1996, Samuels, Kunst et al. 2008, von Wettstein-Knowles 2012).

As research suggests plants obtain the majority of the hydrogen required for growth and biosynthesis from water (Dawson, Mambelli et al. 2002), which in most cases is directly absorbed from the soil, it seems reasonable to assume that variations in precipitation hydrogen isotopic compositions could be the driving cause of variations in *n*-alkane hydrogen isotopic compositions (Sachse 2012). Although the current consensus of available literature points to a strong-positive linear relationship between lipid δD values and local precipitation δD values over global scales, these relationships become much more complex when they are investigated over smaller spatial scales (Sachse 2009, Sachse 2012).

It appears from the available literature that significant inter- and intra-specific variations in the δD values of *n*-alkanes have already been reported across both temporal and spatial scales. The same publications reporting significant variations are also the same publications that report a strong linear relationship between the δD values of *n*-alkanes and that of plant source water (Chikaraishi 2003, Sachse 2006, Hou 2007, Yang 2009). Where, large variations in the D isotopic compositions of *n*-alkanes, within and between species, across small temporal and spatial scales, have been previously reported. For example, variability of up to ~90 ‰ δD in *n*C_{29} has been observed between different C_3 angiosperms growing at the same location (Chikaraishi 2003). In addition, variations of up to 25 ‰ δD have been observed within the same *n*-alkane chains between different species of deciduous conifer, which were subjected to the same environmental conditions, and source water δD values, within a controlled growth experiment (Yang 2009).

Even though great advances have been made in understanding the mechanisms that drive δD values of *n*-alkanes, it is becoming increasingly clear that variations in hydrogen isotopic compositions expressed, within and between species, cannot be fully explained by changes in source water δD values. This suggests there are crucial environmental, physiological, and biosynthetic processes, which are currently being overlooked (Kahmen 2011, Sachse 2012). Environmental conditions, as well as individual plant physiological factors, might be playing just as important a role as those of the original source water δD values, with plant species, plant morphology, growth stage, size, and genetic factors influencing lipid synthesis. This is also working in conjunction with environmental temperature, salinity, incoming PAR levels, RH, nutrient availability, and water availability (Sachse 2012).

5.1.3.1 Apparent fractionation (ε_app)

The most widely reported method of describing the relationship between source water D isotopic composition and *n*-alkanes, in both paleoclimate and plant physiological studies, is to calculate the isotopic fractionations of *n*-alkanes above that of Mean Annual Precipitation δD (MAP), this is termed apparent fractionation (ε_app). This can be calculated using equation 2.7, where δ_product is the δD value of the *n*-alkane, and δ_source is the δD value of the water.

$$\varepsilon_{s/p} = 1000 \times \left[\frac{(\delta_p + 1000)}{(\delta_s + 1000)} - 1 \right]$$

(2.7)

In brief, the ε_app of *n*-alkanes above MAP is used to separate variations in the D isotopic composition of *n*-alkanes caused by changes in the precipitation signal of source waters, from those caused by changes in environmental processes and plant physiology. Therefore, ε_app signifies the isotopic fractionation as a result of soil water processes, leaf water D-enrichment, and the isotopic fractionations associated with lipid biosynthesis (Sachse 2012). Under this principle, more negative apparent fractionations indicate little change in the isotopic signature of hydrogen from source water to lipid, while smaller ε_app (e.g. closer to 0), indicate significant change in δD values from source water to lipid (Sachse 2006).

Problems in the relative use of calculating ε_app of *n*-alkanes above MAP arise even before the full heterogeneity of natural ecosystems is considered. As detailed in chapter 4 (section 4.1.3.), due to hydrological processes which occur in the soil, on an ecosystem by ecosystem basis, plants can absorb water into their xylem with an isotopic D composition that is not representative of MAP. Therefore, calculating ε_app of *n*-alkanes above an averaged MAP δD value may not be representative of the true relationship between the water sourced by the plant and the *n*-alkanes. This is because D-enrichment due to soil water processes, leaf water D-enrichment, and biosynthetic isotopic fractionation are not individually characterised within this calculation (Smith 2006, Sachse 2012).

In more recent times, it has become clear that resolving the issues related to constraining ε_app between and within species, to facilitate their use as a paleo-environmental proxy, cannot be achieved without in-depth analyses of xylem water-leaf water-*n*-alkane δD values (Sachse 2012). This is because significant shifts in *n*-alkane δD values have been observed across a large transect in Australia, while the xylem water δD values remained relatively constant (Kahmen, Hoffmann et al. 2013). Therefore, the hydrogen isotopic

fractionation of leaf water above xylem water (ΔD Leaf water), and *n*-alkanes above leaf water (net biosynthetic fractionation, ε_{bio}, both of which are calculated using equation 2.7), give a more accurate representation of how climate and plant physiological aspects could affect the *δ*D values of *n*-alkanes (Kahmen, Hoffmann et al. 2013). This is currently of particular interest, as although research suggests *n*-alkanes are synthesized from leaf water (Chikaraishi and Naraoka 2001, Chikaraishi, Naraoka et al. 2004, Feakins 2010), how often they are synthesized, and the origins of the isotopic *δ*D value of the "biosynthetic water pool" is currently the subject of much debate (Kahmen 2011, McInerney 2011, Sachse 2012, Kahmen, Hoffmann et al. 2013, Kahmen, Schefuß et al. 2013, Tipple 2013).

5.1.3.2. Net biosynthetic isotopic fractionation (ε_{bio})

Net biosynthetic fractionation (ε_{bio}) is defined as the isotopic fractionation of *n*-alkanes above leaf water (usually midday day leaf water) (Kahmen et al., 2011; Sachse et al., 2012). Initial reports suggested ε_{bio} was relatively constant across all plant species (Estep and Hoering 1980), however, more recent publications have indicated that ε_{bio} is believed to be species specific (Sessions 1999, Sachse 2012, Kahmen, Hoffmann et al. 2013, Kahmen, Schefuß et al. 2013). The current problem is identifying how much ε_{bio} can vary, and ascertaining what is driving the observed variations in similar plant types. It has been suggested that variation in plant physiology (Hou et al., 2007; Duursma et al 2006; Nakatsuka et al 2004), variations in micro-climatic factors (Sachse et al., 2012 and references therein), or an undetermined combination of both can influence ε_{bio}. In addition, a major problem is ε_{bio} does not provide any real information regarding the *δ*D values of the theoretical "biosynthetic water pool", i.e. the water source from which *n*-alkanes are synthesized (Kahmen, Hoffmann et al. 2013, Kahmen, Schefuß et al. 2013).

The exact mechanisms for the variation in ε_{bio} between individual species are poorly understood (Sachse et al., 2012). However, it is hypothesized that species-specific variations in leaf morphology and anatomy, along with variations in metabolic networks, may be key in the understanding of this issue. As few investigations have sought to address the potential variation of ε_{bio} between and within individuals under variable environmental parameters, with most investigations assuming a constant ε_{bio}, testing this assumption has been highlighted by a recent review (Sachse et al., 2012).

5.1.4. Factors influencing the *δ*D values of *n*-alkanes

Once water has entered the xylem, it travels to the leaf where photosynthetic assimilation processes take place. The general consensus from available literature reports D-enrichment of leaf water above xylem water as a result of evaporation through the stomata during photosynthesis (Leaney, Osmond et al. 1985, Yakir, DeNiro et al. 1990, Wang and Yakir 1995) (discussed in greater detail in chapter 4, section 4.1.4.). The level of D-enrichment in leaf waters is reported to be affected by the climate in which the leaf resides, with relative humidity (RH), temperature, photosynthetically active radiation levels (PAR), and the isotopic composition of water vapour surrounding the leaf all having influence (Craig and Gordon 1965, Gat 2010, Kahmen, Schefuß et al. 2013). In general terms lower RH, higher PAR levels, and a more dynamic boundary layer is associated with greater leaf water D-enrichment (Smith 2006, Brandes, Wenninger et al. 2007, Shu, Feng et al. 2008). Therefore, if *n*-alkanes are synthesized from leaf water, the same parameters that influence the isotopic compositions of leaf water should in theory affect the hydrogen isotopic composition of *n*-alkanes (Feakins 2010).

Yang et al., (2009) studied the effect of varying light regimes on the *δ*D values of *n*-alkanes synthesized by saplings of 3 deciduous conifer species. These saplings where grown under controlled green house conditions, with half the plants treated with diurnal light conditions, and the other half to continuous light conditions. The continuous light treatment was to simulate the continuous low-level light experienced by the subarctic, and temperature, RH, and source water *δ*D values were kept constant across both light treatments. The subsequent *n*-alkane D isotopic analysis revealed *n*-alkanes synthesized under continuous light conditions had *δ*D values that were up to 40 ‰ D-enriched in relation to *n*-alkanes synthesized under the diurnal light conditions. These significantly D-enriched *n*-alkanes, produced under the continuous light conditions, were attributed to significantly higher rates of transpiration observed during the 24-photoperiod (Yang 2009). However, the suggestion that PAR levels could significantly impact *n*-alkane *δ*D values is not a novel concept, light is reported to be a key stimulus for the expression of many genes involved in *n*-alkane biosynthesis (Shepherd and Griffiths 2006). Furthermore, as it is also suggested leaf transpiration rates are imprinted on the subsequently synthesized *n*-alkanes (Smith 2006, Pedentchouk 2008, Feakins 2010, Sachse 2010, McInerney 2011), it would not be surprising to see a significant influence of PAR on *n*-alkane *δ*D values. Especially as measurements of transpiration rates in pine and spruce, inhabiting natural boreal forest stands of the Komi Republic region of Russia, have demonstrated

transpiration rates of needles are closely positively correlated with illumination levels (Sen'kina 2002).

Another environmental parameter which can be closely linked to PAR is ambient temperature. Although the literature available on the effect of temperature on the hydrogen isotopic fractionations of *n*-alkanes above source waters is somewhat contradictory, the basic principles of isotopic theory dictate that temperature should have an effect. Under these principles, kinetic isotopic fractionation effects are shown to be temperature dependent, therefore, higher temperatures should result in less discrimination against the heavier isotopes (Gat 2010, Zhou, Grice et al. 2011) (see chapter 2 sections 2.1.3 and 2.1.4 for more information). Moreover, as temperature is known to affect rates of photosynthesis, transpiration, and respiration (Gat 2010, Zhou, Grice et al. 2011, Sachse 2012), observing an effect of temperature on the δD values of *n*-alkanes would be anticipated.

Even though isotopic fractionation theory suggests temperature should have an effect on ε_{bio}, greenhouse controlled growth experiments have so far failed to detect this. For example, Zhou et al (2011) suggested ε_{bio} is insensitive to temperature across several C_3 and C_4 species, and Zhang and Sachs (2007) failed to detect an effect of temperature on ε_{bio} in freshwater green algae species subject to a similar experiment. Nevertheless, less discrimination against the heavier isotopes of hydrogen has been reported with increasing temperature for various lipids present in algal species (Zhang, Gillespie et al. 2009), and in White pine (White, Lawrence et al. 1994). In addition, it has so far been difficult to ascertain whether the reported temperature effects on ε_{bio} are influencing isotopic fractionations solely through temperature effects on photosynthesis and respiration, or whether temperature effects on the enzymes involved in *n*-alkane biosynthesis are also contributing. Although it has been suggested that temperature will affect the enzymes involved in photosynthesis and *n*-alkane biosynthesis, research suggests this effect may be too small to influence ε_{app} and ε_{bio} (Kwart 1982, Siebrand and Smedarchina 2004). In addition, aside from climatic parameters, increasing evidence suggests that the physiology of an individual species could have a significant impact on δD values of *n*-alkanes. For example, is has been reported that angiosperm species show greater D-enrichment within their *n*-alkanes when compared to gymnosperm species. This is suggested to be driven by lower levels of stomatal conductance in gymnosperms species in relation to angiosperm species (Hou 2007, Pedentchouk 2008).

In order to establish the hypothesized relationships between *n*-alkane δD values and source water δD values, more recent publications compare the averaged values of one *n*-alkane chain, or the concentration weighted mean *n*-alkane (CWMA) δD value, to an averaged value of either precipitation or meteoric water. CWMA δD values are calculated from equation 5.1 (Kahmen, Schefuß et al. 2013), and give a single δD value for each individual sample investigated, which factors in the relative concentrations of each *n*-alkane chain detected and its respective δD value.

$$\delta D - CWMA = \sum_{k=n} \frac{(\delta D_k * Conc._k)}{Conc._{total}}$$

(5.1)

This is the sum of all the individual δD values, of the individual *n*-alkane chains (δD_k), multiplied by their individual concentrations ($conc._k$), and then divided by the total concentration of *n*-alkanes detected ($conc._{tot}$) within a given sample. This method of calculating a single value for the multiple *n*-alkane chains detected within a single sample is becoming increasingly more common within the literature. This is because it allows isotopic comparison of the dominant *n*-alkane homologues between various species, which could be synthesizing *n*-alkanes of different chain length (Feakins 2010, Kahmen, Schefuß et al. 2013).

Although much research has been conducted on how the D isotopic composition of *n*-alkanes varies, and what could be driving these variations. As mentioned previously, how often they are synthesized, and the origins of the isotopic D composition of the "biosynthetic water pool" is the subject of much debate (Kahmen 2011, McInerney 2011, Sachse 2012, Kahmen, Hoffmann et al. 2013, Kahmen, Schefuß et al. 2013, Tipple 2013).

5.1.5. What D isotopic composition is recorded in *n*-alkanes?

Research suggests *n*-alkanes are continuously synthesised throughout the entire duration of a growing season (Lockheart, Van Bergen et al. 1997). In addition, as the leaf water evapotranspirational D-enrichment is suggested to be imprinted on *n*-alkanes, research also suggests *n*-alkanes record the seasonal changes in precipitation and climate driven variations in leaf water δD values with time (Pedentchouk 2008, Sachse 2009). This is because D-depletion in *n*-alkanes has been observed from the beginning of a growing season in the new spring foliage, to the end of the growing season in autumn (Chikaraishi, Naraoka et al. 2004, Brandes, Wenninger et al. 2007, Pedentchouk 2008).

More recent publications however, suggest that the *n*-alkane *δ*D values are "locked in" at the beginning of the growth season, changing very little once leaf expansion has ceased (Sachse 2010, Kahmen 2011, Tipple 2013). Furthermore, as a result of plant physiological processes that occur during leaf formation, it is also feasible that *n*-alkanes are synthesized from unenriched water in the xylem and/or previously sequestered assimilates. Therefore, they potentially do no record a transpiration, or source water *δ*D value at all (Sachse 2010, McInerney 2011). As can be seen, and despite the vast amount of research conducted within this field, it is currently unknown exactly how important leaf water is in determining *n*-alkane *δ*D values (Feakins 2010, Sachse 2012), and whether they record evaporative D-enrichment of leaf water at all (Hou 2008, McInerney 2011).

To date most studies have examined only one or two periods during the growth season, and/or the variation as a result of strictly controlled greenhouse growth experiments. Although temporal and spatial variation within and between species has been examined and detected, this has typically only been associated with grass species or single-point analysis of trees (Pedentchouk et al., 2008; Sachse et al., 2009). For example, in Sachse et al., (2009), not only were all of the individual samples for each location under investigation averaged prior to comparison with MAP. The initial sample protocol itself could be neglecting potential sources of variation, where pooled leaf samples from shaded leaves at 2-meter height were investigated. This type of protocol, where pooled leaf samples collected from the lower most branches of different trees (Pedentchouk 2008, Sachse 2009, Tipple 2013), is very common within compound-specific D isotopic analyses of *n*-alkanes. Although these studies have provided valuable insights into the basic behaviour of *n*-alkanes within tree species, it would appear that the full heterogeneity of *n*-alkane *δ*D values within individuals, and single species, has not been fully investigated.

As can be seen, the environmental and physiological parameters, which could affect D isotopic compositions of lipids, are very complicated. In most cases it is difficult to disentangle whether metabolic/photosynthetic assimilation processes, or plant structure and growth form process are the major components driving variations observed. One method of attempting to separate variations in physiological performance, from the true impacts of microclimate, would be to conduct an in-depth study of variations in the *δ*D values of *n*-alkanes within a single species, across spatial and temporal scales, in natural field conditions. Where, investigating the variation in *n*-alkane *δ*D values synthesized by a single species, growing in two significantly different climatic environments, will eliminate

the issues associated with variable physiology, while investigating the impact of climatological parameters.

In addition, as the current accepted theory regarding the δD values of *n*-alkanes suggests increasing PAR, temperature, and decreased RH will result in greater leaf water D-enrichment, and therefore more D-enriched *n*-alkanes. Using the well-established gradients of light, temperature, and RH in natural forest canopies (Niinemets, Kull et al. 1999, Woodruff, Meinzer et al. 2008, Woodruff, Meinzer et al. 2009). One could hypothesize that photosynthetic assimilation, and therefore leaf water D-enrichment, would increase with increasing height in the canopy as conditions become more favourable. Therefore, it could be possible to make inferences, through multiple xylem water - leaf water - *n*-alkane δD analysis, about the effect microclimatic variation has on *n*-alkane δD values over very small scales.

The variation in bulk δ^{13}C values in leaves, with height in natural forest stands, has been well established. This has been attributed to variations in microclimate within tree crowns (Farquhar, Hubick et al. 1989, Niinemets, Kull et al. 1999, Le Roux, Bariac et al. 2001, Niinemets, Sonninen et al. 2004, Duursma and Marshall 2006) (see chapter 2, section 2.2.1.4), therefore it may be possible to detect similar variations in the δD values of *n*-alkanes. Although, Hou et al (2007) investigated the variation in *n*-alkane δD values with height for several tree and shrub species and found no significant variation. It is possible, because they tested this hypothesis on samples collected from 6m, 4.5m and 3m, they may not have been examining large enough differences in height (Hou 2007).

Furthermore, by looking at variation at different points in the canopy within single large individuals, the potential influences of variations in physiology, leaf morphology, nutrient status, water status, and genetics will be removed.

5.2. Aims

The current study presents the first in-depth investigation into the potential variation of compound-specific hydrogen isotopic compositions, and associated fractionations above environmental waters, of *n*-alkanes within a single tree species. The study aims to address the following questions;

1. Do *n*-alkane δD values significantly vary within, and between, individuals of the same species grown in natural field conditions?
2. Are the δD values of *n*-alkanes constant with time in the growth season?
3. Are leaf water δD values imprinted on the *n*-alkanes?
4. Is apparent fractionation (ε_{app}) or biosynthetic fractionation (ε_{bio}) constant within the same species?

5.3. Method

5.3.1 Sampling protocol

The data included within the following chapter is the compound-specific δD analysis of the *n*-alkane extracts from the same samples that were previously discussed in chapter 3, for details of sampling protocol please refer to chapter 3 section 3.3 and chapter 2 section 2.2.

5.3.2 Data analysis

Details of the data quality assurance protocols during sample analysis are available in chapter 2, sections 2.2.2 and 2.2.3. However to reiterate, only data where the averaged δD values of duplicate analyses produced an absolute error of less than 5 ‰ δD were included within the following chapter. In addition, due to problems during the cryogenic vacuum distillation procedure, some leaf water and xylem water δD values are not available and as a result the ε_{app} and ε_{bio} data cannot be calculated. This issue results in sample sizes where n= less than 28. The raw δD values of individual *n*-alkanes were displayed in box and whisker plots using R statistical programming software to examine the total variation in signals for individual chains with time in the growth season. Following on from this, the CWMA δD for total, even only, and odd-only were calculated using equation 5.1 and treated in the same manner. To investigate the effect of tree size/age and location within each of the three components, the CWMA δD were presented for each tree category and height within each. Simple linear regression analysis was used to test whether the effect of sample height (m) significantly affects the δD values of *n*-alkanes and whether this relationship varies with time.

To ascertain if the major drivers of δD values observed were related to xylem water or leaf water δD values, fractionation factors were calculated using equation 2.4. In the following study apparent fractionation ε_{app} was calculated using directly measured xylem water δD data.

To estimate the percentage of current leaf water contribution to the theoretical "biosynthetic water pool", along with an estimation of biosynthetic fractionation, a conceptual model devised by Kahmen et al (2013) was applied to the data sets. Within this model, simple linear regressions of the D-enrichment of leaf water above xylem water plotted against ε_{app} for the CWMA δD component was applied. Under this conceptual model, the slope of the linear regression estimates the percentage leaf water contributes

to the "biosynthetic water pool", and the intercept of this relationship is an estimation of biosynthetic fractionation (ε_{bio}) (Kahmen, Hoffmann et al. 2013, Kahmen, Schefuß et al. 2013).

5.4. Results

5.4.1 *δ*D values, Individual *n*-alkane chains

5.4.1.1 Värriö Strict Nature Reserve, Finland

Analysis of the Finnish *n*-alkane extracts provided compound-specific hydrogen isotopic data for individual *n*-alkane chains ranging nC_{21} to nC_{29}. This includes multiple measurements of even-numbered *n*-alkane chains, compounds not typically associated with terrestrial vegetation (discussed in depth in chapter 3). The total range in *δ*D values observed across all samples during both July and September is ~80 ‰ *δ*D; where, the even-numbered *n*-alkanes display a systematic, and significant, D-enriched isotopic composition in relation to the odd-numbered *n*-alkane chains during both July (t-test, t= -5.75, P=1,25E^{-05}) and September (t=-9.60, P=5.54E^{-07}, figure 5.1). In addition, to these different D-enrichments, the odd-numbered *n*-alkanes show a significant D-depletion between the July and September sample collections, while the even-numbered *n*-alkane chains show relatively consistent *δ*D values with time in the growing season (for tables detailing the *δ*D values for each individual *n*-alkane chain, within each individual sample, from the data presented in figure 5, please refer to appendix table 5 for July and table 6 for September).
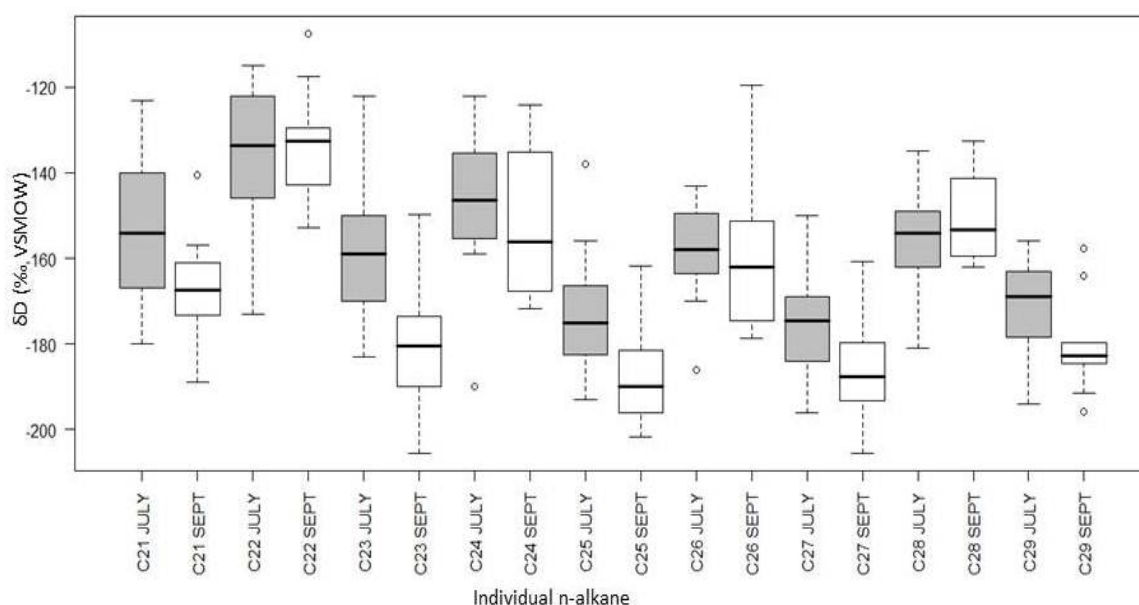
Figure 5.1: Total *δ*D values (measured in ‰, VSMOW) observed for all the individual *n*-alkanes detected within the Finnish samples. Dark boxes represent July 2010 observations, while white boxes depict September 2010.

Utilizing equation 5.1 to calculate the Concentration Weighted Mean *n*-alkane D isotopic composition (CWMA *δ*D), across all samples, confirms the shift in total *n*-alkane *δ*D values between July and September. However, upon examination of the data it was

deemed necessary to devise a new method of CWMA calculation specifically for this data. This was a direct result of the high amount of even-numbered *n*-alkane isotopic measurements. Therefore, the total CWMA, which encompasses both odd- and –even-numbered *n*-alkane chains, was separated into calculation of only the odd-numbered chains (Odd CWMA δD), and then only the even-numbered-*n*-alkane chains (Even CWMA δD).

The Odd CWMA δD values indicate a significant shift to greater levels of D-depletion during September (t-test, t=3.94, P=0.001), with a mean Odd CWMA δD during July of -164.33 ± 2.63 ‰ (SEM, n=26), while -180.30 ± 2.65 ‰ (SEM, n=20) is observed in September. This is a shift in the total mean *n*-alkane δD value of ~ -16 ‰ δD between July and September. The Even CWMA δD values however, reveal very different trends. Not only are all of the observations significantly D-enriched in comparison to the associated odd-numbered *n*-alkane homologues, they also display a much greater total range in the values observed, with a total range of ~60 ‰ δD during July, and ~70 ‰ δD in September. In addition, the total mean Even CWMA δD values show no significant difference over the course of the growing season (t-test, t=0.48, P=0.65), with -143.79 ± 2.99 ‰ δD (SEM, n=22) during July, and -138.72 ± 5.37 ‰ δD (SEM, n=13) during September.

As can be seen, and in agreement with the total individual *n*-alkane chains observations (figure 5.1), the even *n*-alkane chains are not only systematically D-enriched in comparison to the odd-numbered-chains, they also show no significant difference in D isotopic composition between July and September.

5.4.1.2. Black Wood of Rannoch, Scotland

Analysis of *n*-alkanes from the two sampling campaigns conducted in Scotland has revealed both similar, as well as contradictory results to that of the Finnish site. In a similar manner to the Finnish data set, a large range of *n*-alkane chains were detected and isotopically measured. This includes large amounts of even-numbered *n*-alkane chains (figure 5.2). These observed even-numbered *n*-alkane chains display a systematic D-enriched isotopic composition in relation to the odd-numbered *n*-alkane chains, as previously reported in Finland (figure 5.1). However, there are no clear trends in either D-enrichment or D-depletion between the beginning and end of the Scottish growing season in Odd CWMA δD values. Nevertheless, in a similar manner to the Finnish data, the total Scottish data set, for all observed *n*-alkane chains, ranges ~80 ‰ δD. However, the

values are in the region of ~20 ‰ more D-enriched than the Finnish *n*-alkanes; this is expected under latitudinal trends in meteoric waters (Sachse 2006) (see chapter 2 section 2.1.4).

Due to a similarly high abundance of even-numbered *n*-alkanes present within the Scottish samples, it was deemed necessary to separate the total CWMA into Odd CWMA *δ*D values and Even CWMA *δ*D values (figure 5.2). In a similar manner to the Finnish data set, a systematic and significant difference in the D-enrichment of even-numbered *n*-alkane chains is observed in relation to the odd-numbered during both April (t-test, t=8.43, P=7.36E^{-07}) and October (t-test, t=4.48, P=0.0002). For full details of the measured *δ*D values of each individual *n*-alkane chain, within each individual sample, from the data presented in figure 5.2, please refer to appendix table 7 for April and table 8 for October data.
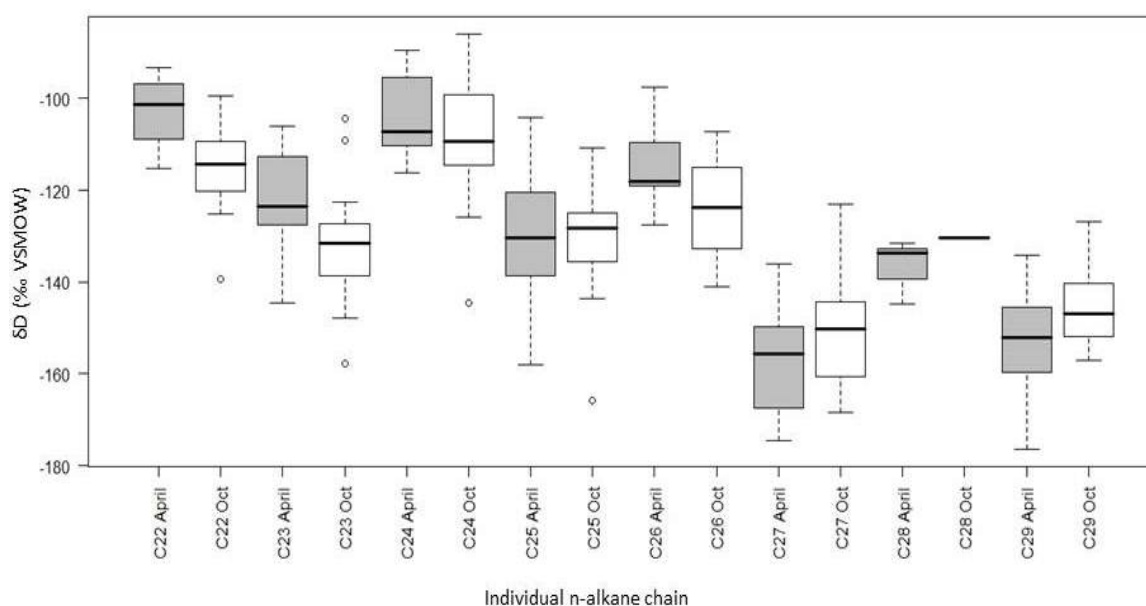
Figure 5.2: The total *δ*D values (measured in ‰, VSMOW) observed for all the individual *n*-alkanes detected within the Scottish samples. Dark boxes represent April 2010 observations, while white boxes depict October 2010.

Furthermore, the total averaged Odd CWMA *δ*D value during April of -140.53± 3.02 ‰ (SEM, n=26) is not significantly different from the -136.96± 2.32 ‰ (SEM, n=27) observed in October 2010. However, the total averaged Even CWMA *δ*D during April of -106.80± 2.75 ‰ (SEM, n=15) is significantly D-enriched (t-test, t=2.33, P=0.04) in comparison to the October *δ*D value of -117.19± 2.99‰ (SEM, n=22).

5.4.2 Variations in *δ*D values within and between individuals

As calculation of the Total CWMA *δ*D value has been deemed inappropriate, due to the high abundances of even-numbered *n*-alkanes chains, the following sections will discuss the Even CWMA and Odd CWMA *δ*D values only.

5.4.2.1. Värriö Strict Nature Reserve, Finland

Examination of mean Odd CWMA *δ*D values, broken down into the respective tree size/age categories, further demonstrates the significant D-depletion in the odd-numbered *n*-alkanes *δ*D values with time in the growing season (figure 5.3). Where, a clear D-depletion in Odd CWMA *δ*D values is observed across all tree size/age categories during September. To test whether tree-size had a significant effect on the Odd CWMA *δ*D values, two-way ANOVAs were applied to the data set (table 5.1), with individual tree size/age and relative height in the canopy as the categorical factors, and Odd CWMA *δ*D values as the continuous factor. Two-way ANOVA indicated significant variation as a result of individual tree size/age category was not observed during July, but is observed during September (F=15.59, P=0.0004). This suggests individual tree size/age has a significant effect on the D isotopic composition of odd-numbered *n*-alkanes in Finnish Scots pine during September only.
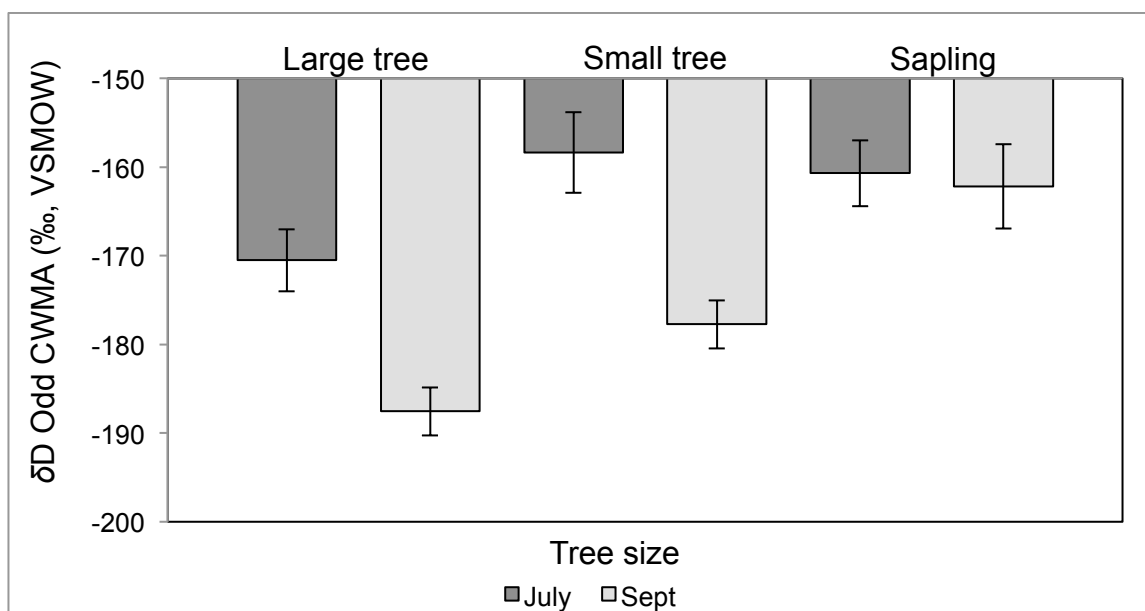
Figure 5.3: Mean Odd CWMA *δ*D for each tree size/age category during the beginning (July) and end (September) of the Finnish growth season. Dark bars represent July 2010 and light grey bars show September 2010, error bars show the standard error of the mean (SEM).

Subsequent testing of the effect of relative position within the crown on mean Odd CWMA *δ*D values (figure 5.4), also demonstrates the clear D-depletion across all samples

between July and September. However, two-way ANOVA (table 5.1) does not detect a significant level of variation in Odd CWMA δD values as a result of relative canopy position during either July or September in the Finnish data set. In addition, during both July and September, no significant variation is also observed as a result of the interaction between relative height in the crown and individual tree size/age during July or September.
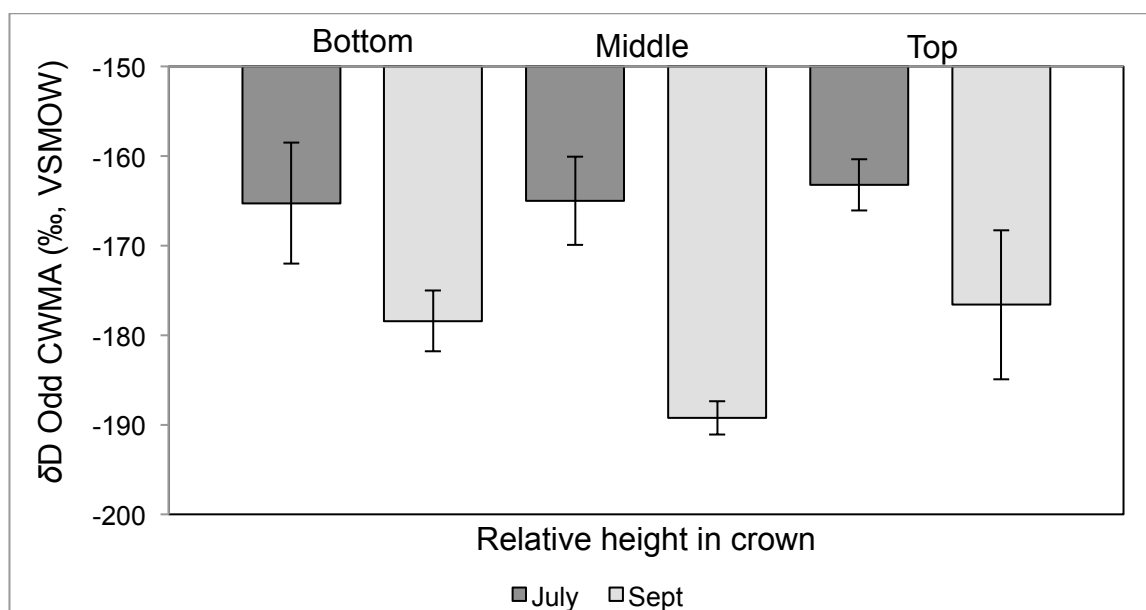
Figure 5.4: Mean Odd CWMA δD for each relative height within the crown for the Finnish data during the beginning (July) and end (September) of the Finnish growth season. Dark bars represent July 2010 and light grey bars show September 2010, error bars show the standard error of the mean (SEM).

Table 5.1: Summary of the two-way ANOVA output of the tested Finnish CWMA δD values, where tree size and height are categorical factors and CWMA δD values are the continuous variables. Statistically significant results are marked "*".

Time	Data tested	Source	DF	F	P
July	Odd CWMA δD	Tree size	2	2.28	0.13
		Relative height	2	0.03	0.97
		Interaction	2	0.24	0.79
		Residuals	21		
July	Even CWMA δD	Tree size	2	0.03	0.97
		Relative height	2	0.02	0.98
		Interaction	2	0.28	0.76
		Residuals	21		
Sept	Odd CWMA δD	Tree size	2	15.59	0.0004*
		Relative height	2	3.75	0.05
		Interaction	2	0.94	0.41
		Residuals	21		
Sept	Even CWMA δD	Tree size	2	0.38	0.70
		Relative height	2	0.92	0.45
		Interaction	2	0.23	0.80
		Residuals	21		

The Even CWMA δD observations for each tree size/age category clearly demonstrate the significantly different results observed in hydrogen isotopic compositions expressed by even-numbered *n*-alkane chains (figure 5.5). Firstly, there are no obvious trends in either

D-enrichment or depletion across the different tree age/size categories between July and September. In support of this, two-way ANOVA with individual tree size/age and relative height in the canopy at categorical factors, and Even CWMA δD values as the continuous factor, does not report significant variation in Even CWMA δD as a result of individual tree size during July or September (table 5.1). This suggests individual tree size/age does not influence the δD values of even-numbered *n*-alkanes at any time in the Finnish growing season (figure 5.5).
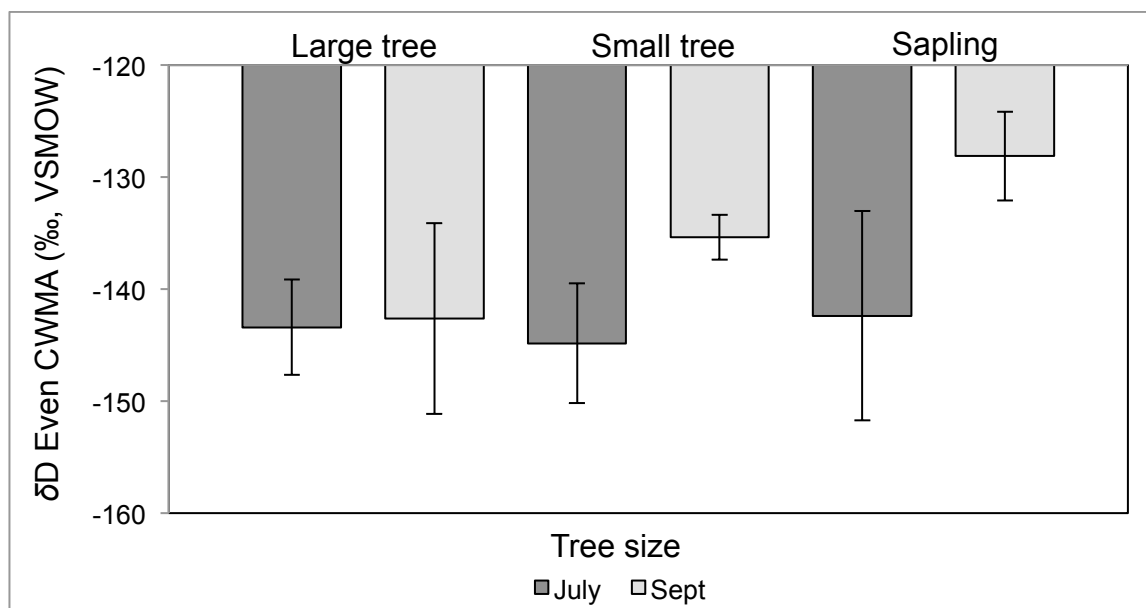
Figure 5.5: Mean Even CWMA δD for each tree size/age category during the beginning (July) and end (September) of the Finnish growth season. Dark bars represent July 2010 and light grey bars show September 2010, error bars show the standard error of the mean (SEM).

In addition, mean Even CWMA δD values by relative height in the crown exhibit no systematic trends in D-depletion or enrichment with time in the growing season (figure 5.6). This is also supported by two-way ANOVA, with no significant variation detected as a result of relative crown position during either July or September (table 5.1). This two-way ANOVA also reported no significant effect of the interaction between individual tree size/age and relative height in the crown during July or September. This suggests Even CWMA δD values do not significantly vary as a result of crown position within individual trees during both July and September.
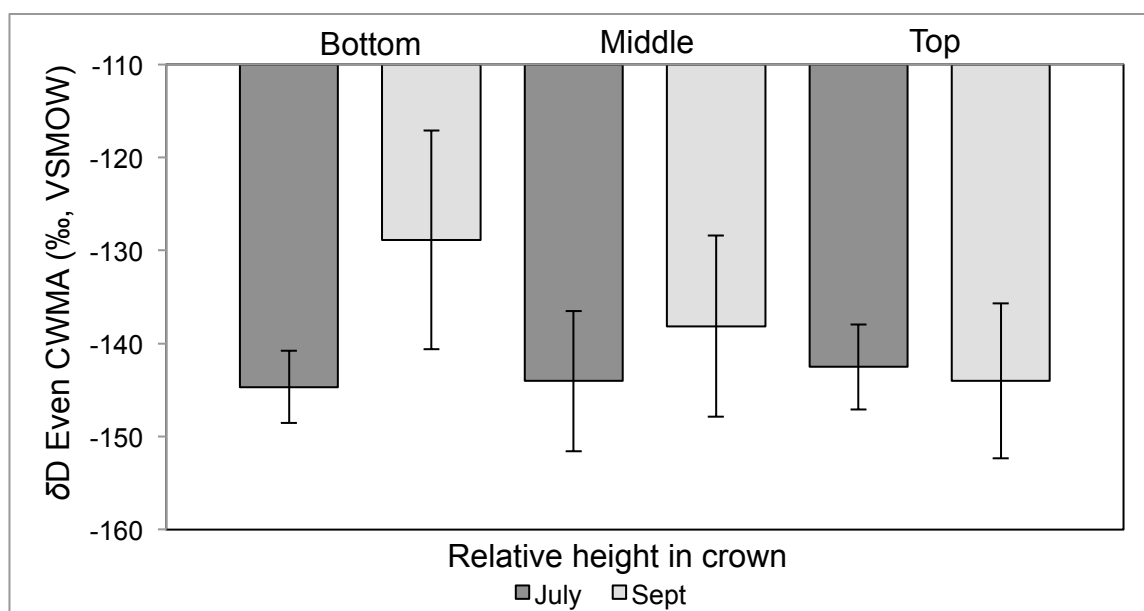
Figure 5.6: Mean Even CWMA δD for each relative height within the crown for the Finnish data during the beginning (July) and end (September) of the Finnish growth season. Dark bars represent July 2010 and light grey bars show September 2010, error bars show the standard error of the mean (SEM).

It should be noted however, that much fewer compound-specific δD measurements of even numbered *n*-alkane chains were possible during September. Where only 3 out of a possible 12 samples from the small tree category contained a high enough abundance of even-numbered *n*-alkanes to facilitate compound-specific δD analysis. This is in comparison to July, where 8 out of a possible 12 samples were measured (see table 10 in the appendix for raw data).

5.4.2.2. Black Wood of Rannoch, Scotland

Mean Odd CWMA δD values for each individual tree size/age category demonstrate no consistent trends in D-enrichment or depletion between April and October in Scotland (figure 5.7). This is supported by two-way ANOVAs (table 5.2), with individual tree size/age and relative height in the canopy as categorical factors, and the δD values of the Even and Odd CWMAs as categorical factors; where, no significant effect of individual tree size/age on the Odd CWMA δD values during April and October is observed.
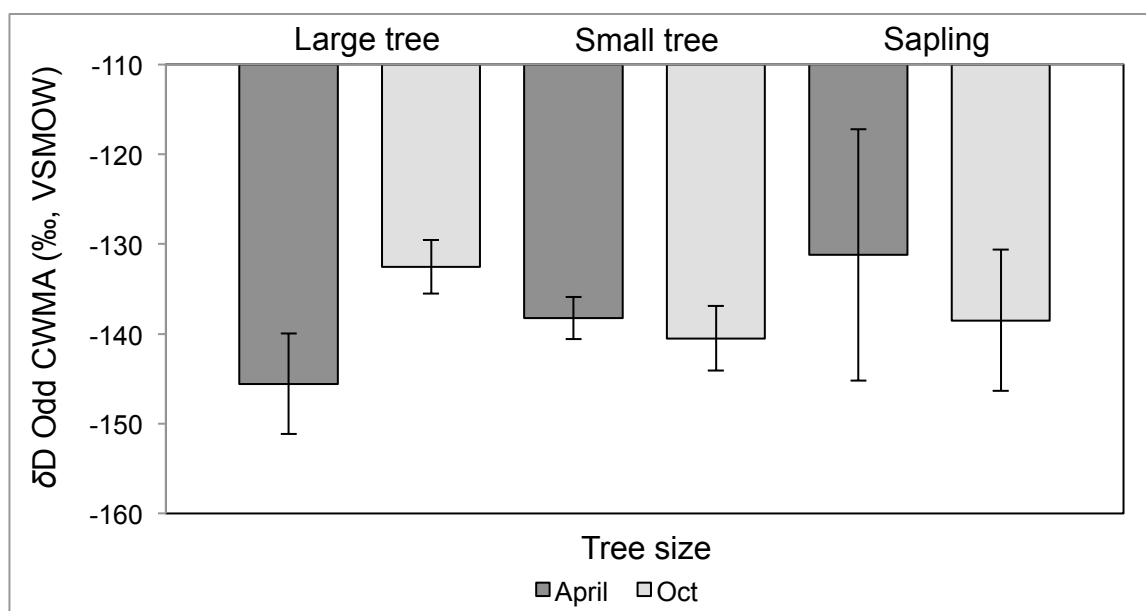
Figure 5.7: Mean Odd CWMA δD for each tree size/age category during the beginning (April) and end (October) of the Scottish growth season. Dark bars represent April 2010 and light grey bars show October 2010, error bars show the standard error of the mean (SEM).

The effect of relative canopy position on mean Odd CWMA δD values in Scotland also reveals no consistent trends across all canopy locations (figure 5.8). Two-way ANOVA (table 5.2) does not detect significant variation in Odd CWMA δD values during either April or October, with no significant variation as a result of the interaction. I.e. variation in Odd CWMA δD within individuals due to relative height in the crown is not detected during April and October. These data suggest that Odd CWMA δD compositions are not influenced by tree size/age, or relative crown position at any time in the Scottish Scots pine.

Table 5.2: Summary table of two-way ANOVA tests of the Scottish CWMA δD values, where tree size and height are the categorical factors and CWMA δD values are the continuous factor.

Time	Data tested	Source	DF	F	P
April	Odd CWMA δD	Tree size	2	1.12	0.35
		Relative height	2	0.25	0.78
		Interaction	2	0.20	0.82
		Residuals	21		
April	Even CWMA δD	Tree size	2	2.49	0.14
		Relative height	2	2.11	0.18
		Interaction	2	0.88	0.37
		Residuals	21		
Oct	Odd CWMA δD	Tree size	2	1.13	0.34
		Relative height	2	0.18	0.84
		Interaction	2	0.13	0.88
		Residuals	21		
Oct	Even CWMA δD	Tree size	2	0.86	0.44
		Relative height	2	0.18	0.21
		Interaction	2	2.04	0.16
		Residuals	21		
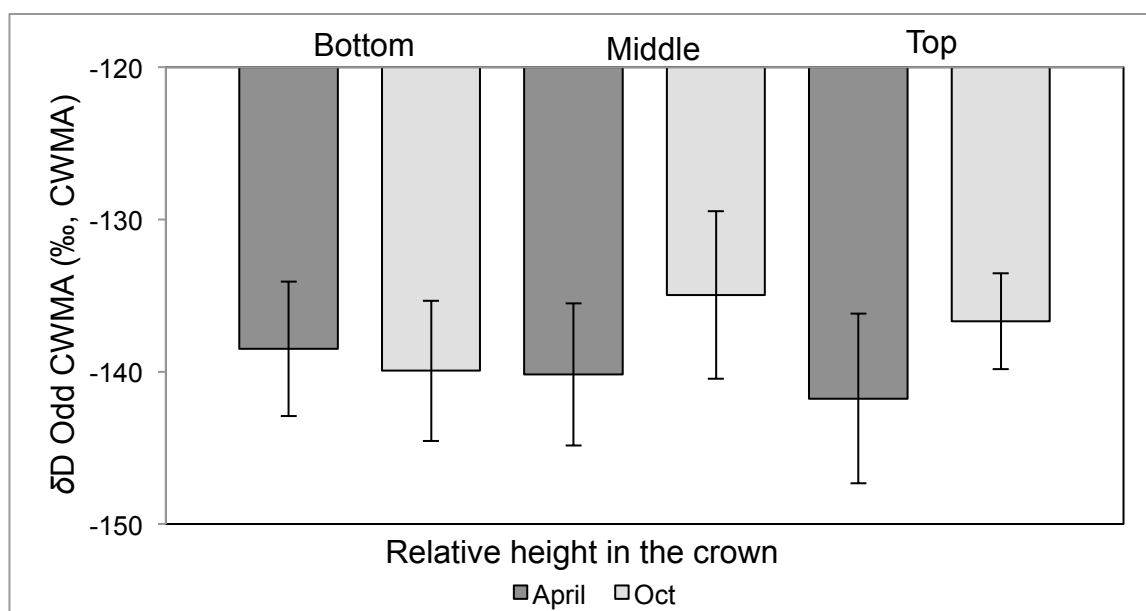
Figure 5.8: Mean Odd CWMA δD for each tree size/age category during the beginning (April) and end (October) of the Scottish growth season. Dark bars represent April 2010 and light grey bars show October 2010, error bars show the standard error of the mean (SEM).

Mean even CWMA δD values show a clear D-depletion across each of the individual tree size/age categories in Scotland (figure 5.9). However,, two-way ANOVA (table 5.2) does not detect significant variation in Even CWMA δD values as a result of tree size/age during April or October.
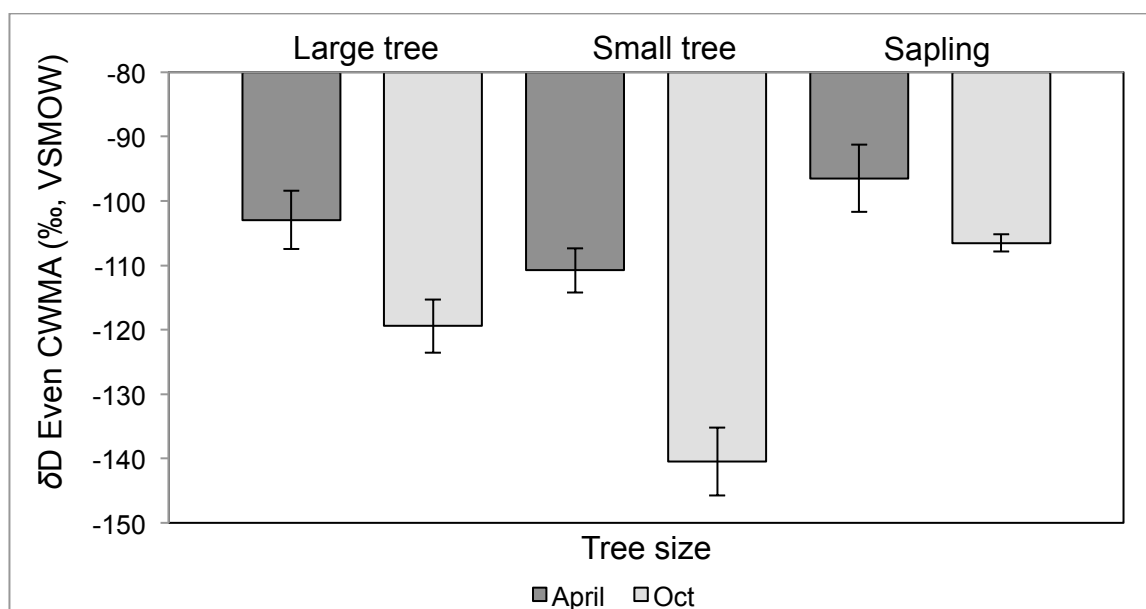
Figure 5.9: Mean Even CWMA δD for each relative height within the crown for the Scottish data during the beginning (April) and end (October) of the Scottish growth season. Dark bars represent April 2010 and light grey bars show October 2010, error bars show the standard error of the mean (SEM).

Furthermore, mean Even CWMA δD values exhibit as clear D-depletion, across all relative heights within the crown, between April and October (figure 5.10). However, two-factor ANOVA (table 5.2) does not attribute significant variations in mean Even CWMA δD values to relative crown positions during April or October,, with no significant variation as

a result of the interaction between relative height in the crown and size/age during April or October . These data suggest, although Even CWMA δD values significantly shift to more D-depleted values over the course of the Scottish growth season, individual tree size/age, as well as relative canopy position, has no significant effect on the δD values observed.
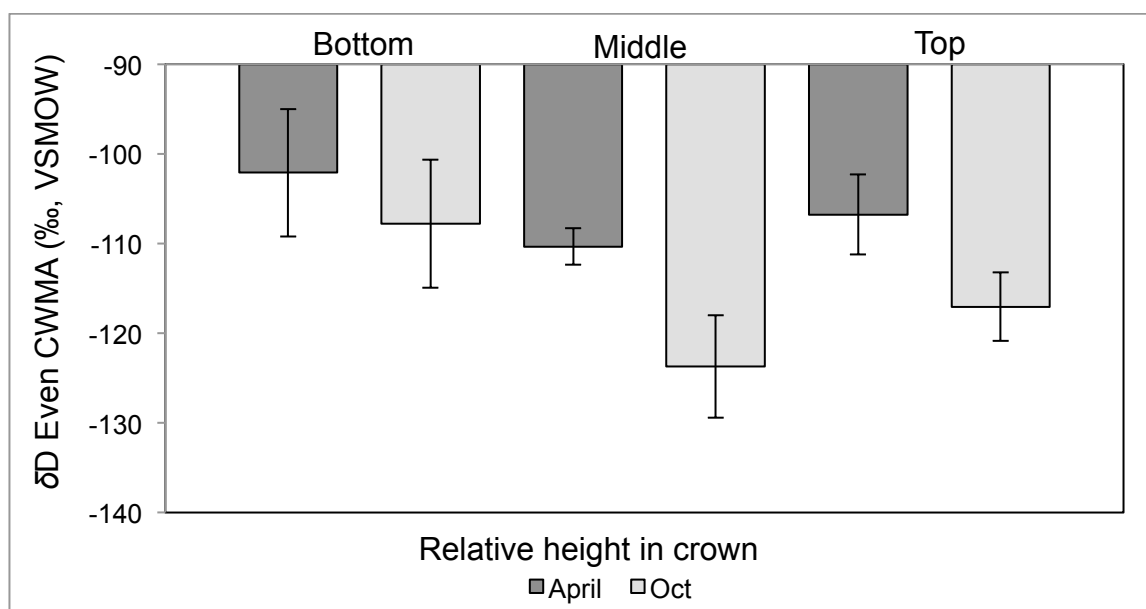
Figure 5.10: Mean Even CWMA δD for each relative height within the crown for the Scottish data during the beginning (April) and end (October) of the Scottish growth season. Dark bars represent April 2010 and light grey bars show October 2010, error bars show the standard error of the mean (SEM).

Nevertheless, it should be noted, even-numbered *n*-alkane chains were not as abundant, or readily measured in the Scottish samples as they were in the Finnish. This is due to the very low total abundances of *n*-alkanes measured in Scotland overall (see chapter 3, section 3.5.1). In addition, the observed mean D-depletion in Even CWMA δD values with time of ~10 ‰ δD in Scotland, which when the large isotopic effects of hydrogen are considered (Bigeleisen 1965), may be statistically significant, but not quantitatively large enough to suggest complete re-synthesis of even-numbered *n*-alkanes with time in the growth season. Instead, and as a result of the demonstrated increasing D-depletion within increasing *n*-alkane chain length; this result may be more indicative of the variability in individual chain length homologues isotopically measured between April and October (i.e. more measurements of longer chains than shorter), rather than a total shift in Even CWMA δD values per se.

5.4.3 Effect of sample position on *n*-alkane *δ*D values

5.4.3.1 Värriö Strict Nature Reserve, Finland

As two-way ANOVAs have suggested individual tree size has a significant effect on the *δ*D values of *n*-alkanes during September in Finland (figure 5.3, table 5.1). The data was statistically analysed for the effect of height of sample collection on the D isotopic compositions.
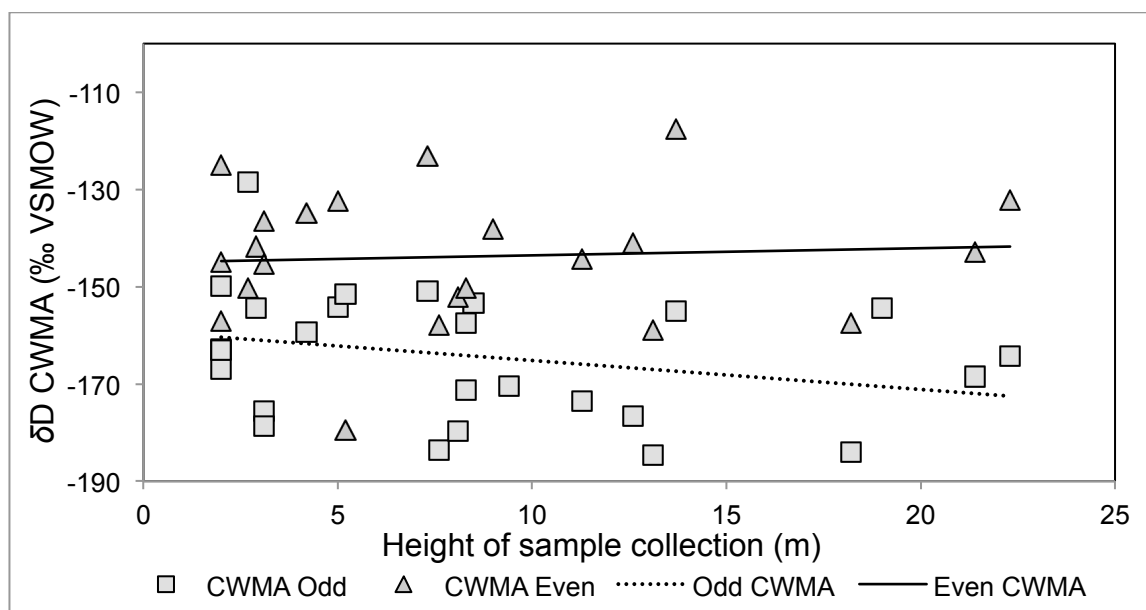
Figure 5.11: Height of sample collection (m) against Odd CWMA and Even CWMA *δ*D (measured in ‰) during July 2010 in Finland. Light squares represent Odd-CWMA; medium triangles depict Even CWMA only. The trend lines depict simple linear regressions applied to the data sets.

Simple linear regression analysis did not detect statistically significant correlations between measured height of sample collection and Odd or Even CWMA *δ*D values across all samples during July 2010 (figure 5.11, table 5.3).

Table 5.3: Summary of the simple linear regression analyses of the Finnish CWMA *δ*D values versus height of sample collection, statistically significant results are marked "*".

Time	y, x	Equation	Adjusted R^2	F	P
July	Odd vs Height	Y=-0.595x-159.27	0.04	1.93	0.16
Sept	Odd vs Height	Y= -1.3919x-168.02	0.45	16.28	0.0008*
July	Even vs Height	Y=0.146x-144.96	-0.06	0.09	0.77
Sept	Even vs Height	Y= -1.6238x-122	0.25	4.97	0.05

This result was further supported by two-way ANOVA (table 5.4), with height of sample and aspect as categorical factors, and *n*-alkane *δ*D values as the continuous factor. No effect of sample collection height or aspect was observed on Odd CWMA or Even CWMA, as well as no effect of the interaction between height of sample collection and aspect. These results suggest that neither even, nor odd-numbered *n*-alkane *δ*D values are affected by sample location during the July sampling period in Finland.

Table 5.4: Summary table of the outputs of two-way ANOVAs tests ran on the Finnish CWMA δD values, where height of sample collection and aspect are the categorical factors and CWMA δD is the continuous factor. Statistically significant results are marked "*".

Time	Data tested	Source	DF	F	P
July	Odd CWMA δD	Height	2	2.05	0.17
		Aspect	2	0.00	0.96
		Interaction	2	3.40	0.08
		Residuals	21		
July	Even CWMA δD	Height	2	0.08	0.78
		Aspect	2	0.23	0.64
		Interaction	2	0.30	0.59
		Residuals	21		
Sept	Odd CWMA δD	Height	2	17.25	0.0007*
		Aspect	2	2.65	0.12
		Interaction	2	0.43	0.52
		Residuals	21	4.58	0.06
Sept	Even CWMA δD	Height	2	0.30	0.60
		Aspect	2	0.30	0.60
		Interaction	2	0.84	0.38
		Residuals	21		

Similar statistical treatments applied to the Finnish September data reveal very different trends. Simple linear regression analyses (table 5.3) indicate significant negative correlations between height of sample collection Odd CWMA δD values (R^2=0.45, F=16.28, P=0.0008) (figure 5.12). However, application of similar two-way ANOVAs (table 5.4) only supports the significant correlation between height of sample collection and *n*-alkane δD values for the Odd CWMA only (F=17.25, P=0.0007), while no similar significant variation in Even CWMA δD is observed with height during September. In addition, no effect of aspect is observed in Odd or Even CWMA δD, as well as no effect of the interaction between height of sample and aspect for Odd and Even CWMA δD (table 5.4).

These data suggest that height of sample collection may be a critical factor in determining the δD values of *n*-alkanes within Finnish Scots pine, but only towards the end of the growing season in September (figure 5.12). In addition, these data further highlight the significant D-depletion exhibited in the Even CWMA δD in relation to that of the Odd CWMA.
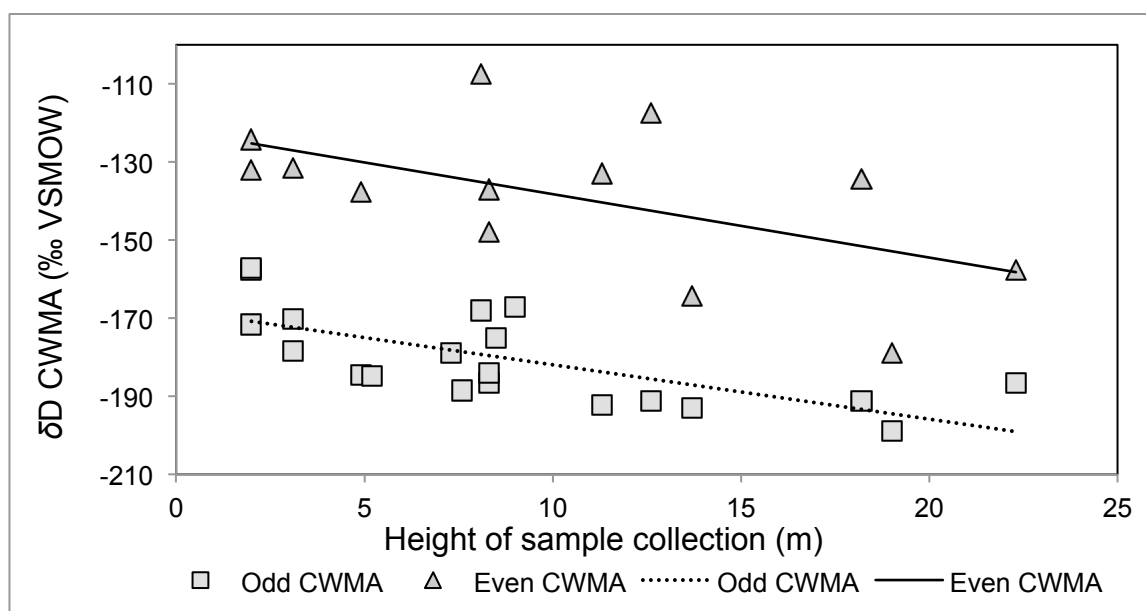
Figure 5.12: Height of sample collection (m) against Even and Odd CWMA δD (measured in ‰) during September 2010 in Finland. Light squares represent Odd-CWMA, medium triangles depict Even CWMA only, and trend lines show results of simple linear regression analysis.

5.4.3.2 Black Wood of Rannoch, Scotland

Although two-way ANOVA failed to report significant variation in *n*-alkane δD values as a result of individual tree size/age, during both April and October in Scotland (table 5.2), the data sets were still tested for the effect of sample collection height on *n*-alkane δD values.

In contrast to the Finnish data, simple linear regression analyses indicate significant negative relationships between height of sample collection and *n*-alkane δD values at the beginning of the growing season in April in Scotland (figure 5.13, table 5.5). Odd CWMA δD values exhibit a weak negative relationship with height of sample during April (R^2=0.18, F=6.57, P=0.02). This is further supported by application of a two-way ANOVA (table 5.6), where a significant level of variation is attributed to height of sample collection (F=5.90, P=0.02), with no effect of aspect, or interaction effect of height of sample and aspect.

Table 5.5: Results of simple linear regressions of each CWMA δD value data set from Scotland, where CWMA δD value is plotted versus height of sample collection and statistically significant results are marked "*".

Time	y, x	Equation	Adjusted R^2	F	P
April	Odd vs Height	Y=-1.343x-122.49	0.18	6.57	0.02*
Oct	Odd vs Height	Y=0.372x-141.85	-0.008	0.8	0.38
April	Even vs Height	Y=1.175x-92.31	0.29	6.83	0.02*
Oct	Even vs Height	Y=-0.936x-103.88	0.07	2.51	0.13

In addition, the Even CWMA δD values show a stronger negative correlation with height of sample collection of (R^2=0.29, F=6.83, P=0.02), this result is also supported by two-way ANOVA where significant levels of variation in Even *n*-alkane D isotopic composition is

attributed to height of sample collection (F=5.36, P=0.04), with no effect of aspect, and no significant interaction between height and aspect.

Table 5.6: Summary of the results of two-way ANOVAs where height of sample collection and aspect are the categorical factors and each Scottish CWMA δD data set is the continuous variable. Statistically significant results are marked "*".

Time	Data tested	Source	DF	F	P
April	Odd CWMA δD	Height	2	5.90	0.02*
		Aspect	2	0.17	0.92
		Interaction	2	1.05	0.32
		Residuals	21		
April	Even CWMA δD	Height	2	5.36	0.04*
		Aspect	2	0.10	0.90
		Interaction	2	0.00	0.95
		Residuals	21		
Oct	Odd CWMA δD	Height	2	0.73	0.40
		Aspect	2	0.50	0.68
		Interaction	2	0.54	0.47
		Residuals	21		
Oct	Even CWMA δD	Height	2	2.21	0.16
		Aspect	2	0.48	0.69
		Interaction	2	0.20	0.66
		Residuals	21		
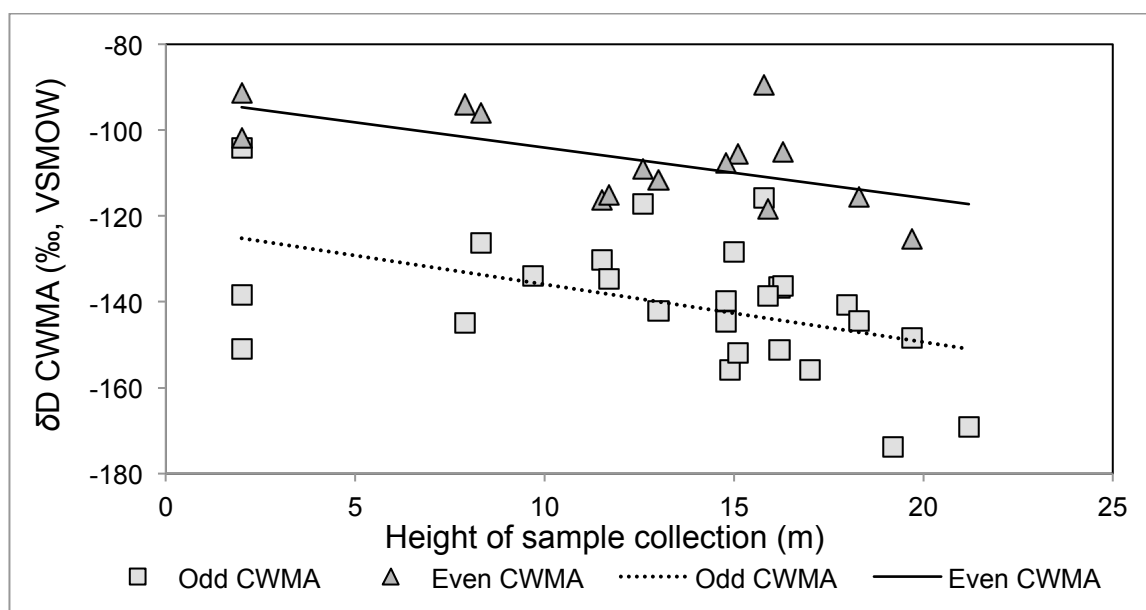
Figure 5.13: Height of sample collection (m) against Odd CWMA and Even CWMA δD (measured in ‰) during April 2010 in Scotland. Light squares represent Odd-CWMA; medium triangles depict Even CWMA only. The trend lines depict simple linear regressions applied to the data sets.

Two-way ANOVA also failed to detect any significant variations in *n*-alkane δD values as a result of height of sample collection or aspect for Odd CWMA and Even CWMA during October (table 5.6). However, these data also further highlight the significantly D-depleted δD values of even *n*-alkanes synthesized within Scots pine.
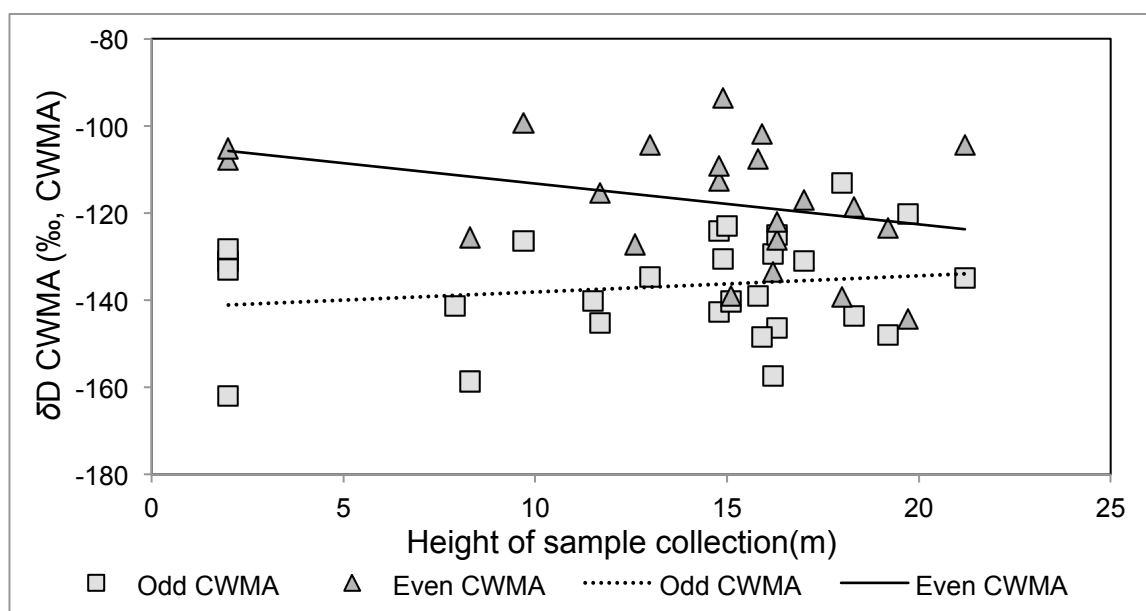
Figure 5.14: Height of sample collection (m) against Even and Odd CWMA δD (measured in ‰) during October 2010 in Scotland. Light squares represent Odd-CWMA, medium triangles depict Even CWMA only, and trend lines show results of simple linear regression analysis.

The results presented here indicate height of sample collection may be a crucial influencing factor on the δD values of *n*-alkanes within Scottish Scots pine during the beginning of the growing season only. This finding is in contrast to the Finnish sample site, where the opposite is observed. As research has indicated *n*-alkanes are closely correlated with source waters δD values and/or leaf water δD values, the fractionation of *n*-alkanes above these environmental water pools should shed further light on what could be driving the discrepancies observed.

5.4.4 Apparent fractionation ($ε_{app}$)

Chapter 4 has already demonstrated xylem water D isotopic compositions do not significantly vary with time in the growth season, within or between individuals, during both July and September in Finland (figures 4.3, 4.4). Therefore, we can rule out any effect of xylem water on the δD values of the *n*-alkanes. Nevertheless, this chapter does indicate significant variation between and within individuals in leaf water δD values and fractionation of leaf water above xylem water (ΔD leaf water). This suggests these may have a significant influence on the δD values of *n*-alkanes.

5.4.5 Biosynthetic fractionation (ε_{bio})

5.4.5.1 Effect of height on ε_{bio}, Värriö Strict Nature Reserve, Finland

Calculation of ε_{bio}, using equation 2.7, for the Finnish Odd and Even CWMA data, provides useful insights into what could be influencing the δD values of *n*-alkanes at the Finnish Sample site. For example, the results of chapter 4 have clearly demonstrated the significant negative trends between height of sample collection and δD leaf water and ΔD leaf water during July (figures 4.12 and 4.13). Where, these results suggest decreased evaporative D-enrichment of leaf water with increasing height of sample collection. This is in contrast to the Odd and Even CWMA δD data, where no significant correlations between height of sample collection and *n*-alkane δD values are observed (figure 5.11, table 5.4). As simple linear regression analysis detects no significant correlation between height of sample collection and Odd CWMA ε_{bio} during July (figure 5.15, table 5.7). These findings are also supported by two-way ANOVA (table 5.8), where height of sample and aspect were categorical factors, and Odd CWMA ε_{bio} was the continuous factor These data suggest the δD values of the *n*-alkanes present during July in Finland are not related to the leaf water present at this time.

Table 5.7: Summary of the results of simple linear regression analyses, where Finnish ε_{bio} data (y) has been plotted against height of sample collection. ε_{bio} was calculated from Odd and Even CWMA ε_{bio} data separately and statistically significant results are marked "*".

Time	y, x	Equation	Adjusted R^2	F	P
July	Odd vs Height	Y=0.292-128.10	-0.03	0.32	0.58
Sept	Odd vs Height	Y=-1.901x-98.103	0.22	5.40	0.035*
July	Even vs Height	Y=0.839x-109.15	0.04	1.70	0.21
Sept	Even vs Height	Y=-2.69x-39.95	0.19	3.53	0.09
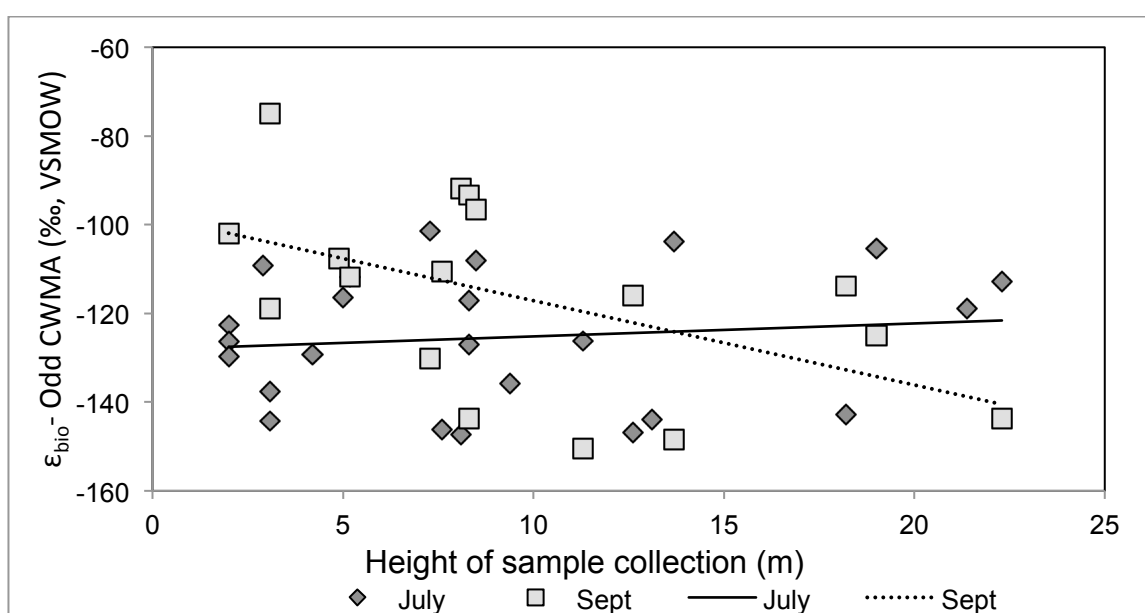
Figure 5.15: Height of sample collection (m) against Odd CWMA ε_{bio} (measured in ‰) during July and September 2010 in Finland. Dark diamonds show July and light squares September and trend lines show results of simple linear regression analysis.

Although a paired t-test did not detect a significant difference in total mean Odd CWMA ε_{bio} between July and September (t-test, t=0.24, P=0.81), with a total mean ε_{bio} of -124.21± 3.24 ‰ (SEM, n=25) observed during July, and -121.62± 6.19 ‰ (SEM, n=18) during September; statistical analysis of the September Odd CWMA ε_{bio} reveals significantly different trends. For example, simple linear regression analysis (table 5.7) indicates a significant negative correlation between height of sample collection and Odd CWMA ε_{bio} during September (R^2= 0.22, F=5.4, P=0.035, figure 5.15). However, this result is not supported by two-way ANOVA (table 5.8); with no effect of height of sample collection, no effect of aspect and no effect of the interaction between height and aspect observed. What is also of interest is, in a similar manner to the July data, the leaf water δD and ΔD leaf water data demonstrate significant positive trends with height of sample collection during September (chapter 4, figures 4.12 and 4.13). This data therefore suggests the September Odd CWMA δD values are not related to the leaf water or xylem water δD values at the time of sampling.

Table 5.8: Summary of two-way ANOVA output of the Finnish ε_{bio} data calculated from the Even and Odd CWMA δD values. Height and aspect are the categorical factors, while ε_{bio} continuous factor.

Time	Data tested	Source	DF	F	P
July	Odd CWMA ε_{bio}	Height	2	0.02	0.90
		Aspect	2	0.02	0.89
		Interaction	2	1.79	0.19
		Residuals	21		
July	Even CWMA ε_{bio}	Height	2	1.37	0.26
		Aspect	2	0.03	0.86
		Interaction	2	0.17	0.69
		Residuals	21		
Sept	Odd CWMA ε_{bio}	Height	2	0.28	0.61
		Aspect	2	0.08	0.78
		Interaction	2	0.06	0.81
		Residuals	21		
Sept	Even CWMA ε_{bio}	Height	2	2.56	0.15
		Aspect	2	0.16	0.70
		Interaction	2	0.44	0.52
		Residuals	21		

Treatment of the Even CWMA ε_{bio} reveals very similar trends; however, the measured mean Even CMWA ε_{bio} is significantly different to the Odd CMWA ε_{bio} during both July (paired t-test, t=7.02, P=1.5E[-06]) and September (paired t-test, t=8.99, P=4.33E[-06]). This demonstrates significantly different biosynthetic fractionation between the even and odd *n*-alkane chains. In addition, and in a similar manner to the Odd CWMA ε_{bio}, there is no significant difference in Even CWMA ε_{bio} between July and September (paired t-test, t=-1.35, P=0.223), even though a mean Even CWMA ε_{bio} of -101.47± 3.82 ‰ (SEM, n=21) is observed during July, and -70.19± 9.81 ‰ (SEM, n=12) during September.
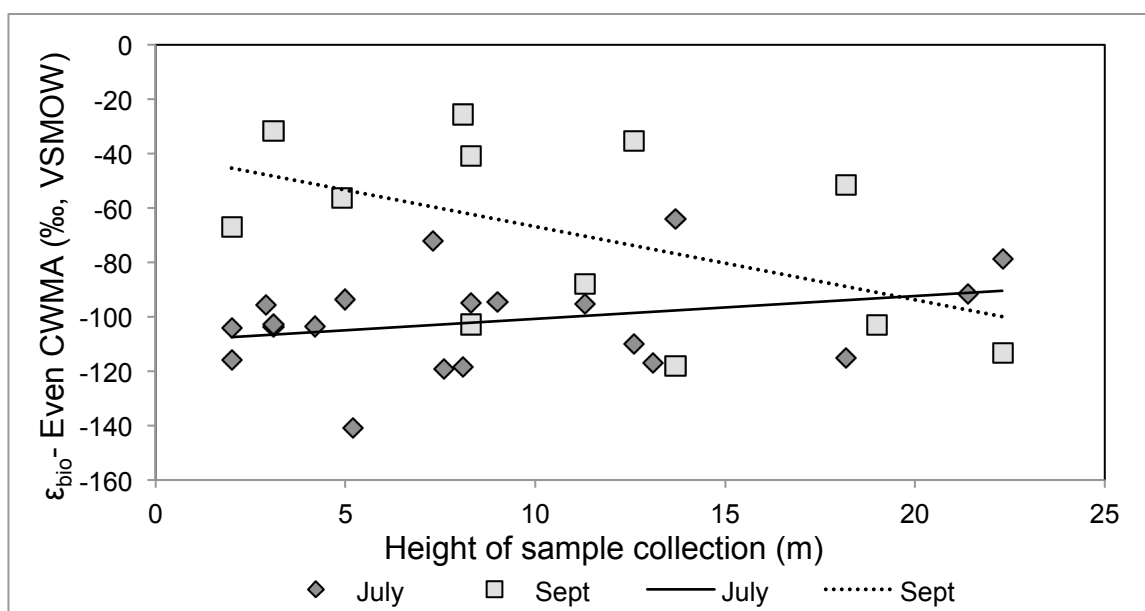
Figure 5.16: Height of sample collection (m) against Even CWMA ε_{bio} (measured in ‰) during July and September 2010 in Finland. Dark diamonds show July and light squares September and trend lines show results of simple linear regression analysis.

Simple linear regression analysis indicates similar trends in Even CWMA ε_{bio} versus height of sample collection as is observed in Odd CWMA ε_{bio} (table 5.7). This is even though significant negative trends in leaf water δD and ΔD leaf water were observed during July, and significantly positive trends were observed in September (chapter 4). Simple linear regression analyses indicate no significant correlation between height of sample collection and Even CWMA ε_{bio} during either July or September (figure 5.16, table 5.7). This is supported by two-way ANOVA (table 5.8), where no effect of sample collection height, aspect, or the interaction of height and aspect during July or September is detected.

The discrepancy observed between the trends in δD leaf water and ΔD leaf water, and those observed in the CWMA ε_{bio} data, for both Even and Odd *n*-alkane chains, suggest that current leaf waters are not the hydrogen source for the *n*-alkanes present during either July or September. These findings present a significant problem in ascertaining what δD source is being recorded in the *n*-alkanes synthesized in the Finnish Scots pine. Furthermore, Even CWMA ε_{bio} is significantly less negative than Odd during both July (t-test, t=5.61, P=2.05E^{-05}) and September (t-test, t=9.02, P=2.04E^{-06}), further highlighting the significantly different isotopic fractionation between even and odd *n*-alkane chains.

5.5.5.2 Effect of height on ε_{bio}, Black Wood of Rannoch, Scotland

Treatment of the Scottish ε_{bio} data, in a similar manner as the Finnish, reveals both similar and contrasting results. As is demonstrated in the Finnish data, the Scottish Even CWMA ε_{bio} is significantly less negative than the Odd CWMA ε_{bio}, during both April (t-test, t=7.92,

P=4.15E^{-06}) and October (t-test, t=-3.60, P=0.001). Nevertheless, a significant difference in total mean Odd CWMA ε_{bio} is observed between April and October in Scotland (t-test, t=-2.08, P=0.05), with a mean Odd CWMA ε_{bio} of -128.97± 3.90 ‰ (SEM, n=22) during April, and -116.41± 3.22 ‰ (SEM, n=23) during October.
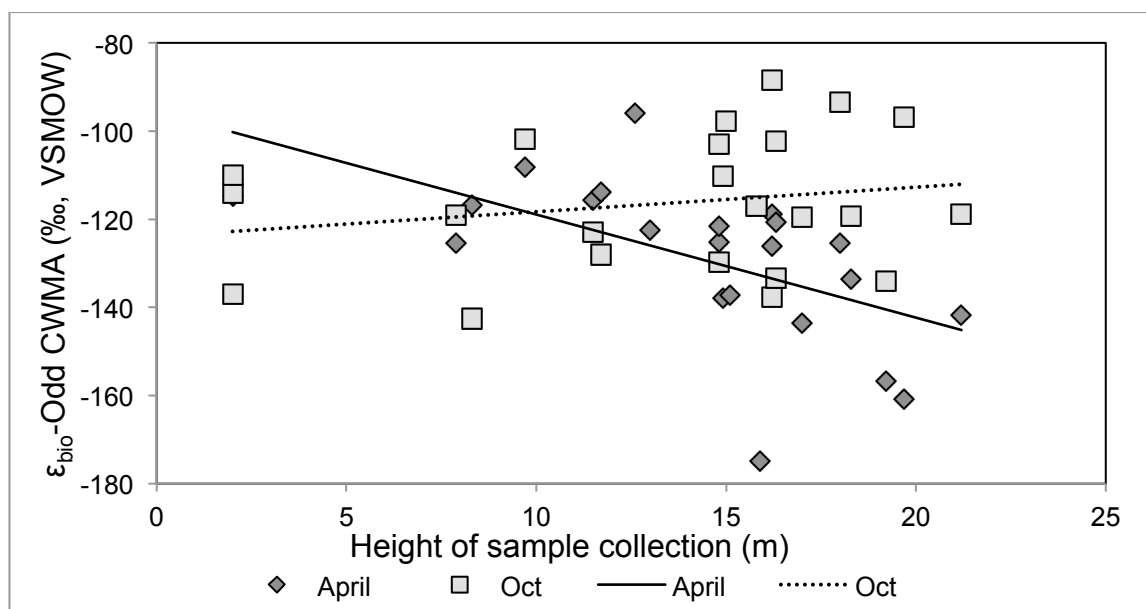
Figure 5.17: Height of sample collection (m) against Odd CWMA ε_{bio} (measured in ‰) during April and October 2010 in Scotland. Dark diamonds show April and light squares October and trend lines show results of simple linear regression analysis.

Although the results of chapter 4 suggest leaf water δD values are significantly positively correlated with height of sample during April (chapter 4, figure 4.15), the Odd CWMA ε_{bio} is significantly negatively correlated with height of sample during April (R^2=0.29, F=9.74, P=0.005, table 5.9).

Table 5.9: Summary of the simple linear regression analyses of ε_{bio} calculated from the Odd and Even CWMA δD values, where ε_{bio} (y) has been plotted against height of sample collection (x). Statistically significant results are marked "*".

Time	y, x	Equation	Adjusted R^2	F	P
April	Odd vs Height	Y=-2.557X+90.11	0.29	9.74	0.005*
Oct	Odd vs Height	Y=0.557X-123.89	-0.40	0.91	0.35
April	Even vs Height	Y=-3.58X-45.51	0.37	8.79	0.01*
Oct	Even vs Height	Y=-0.836X-85.53	0.02	1.37	0.26

This result is further supported by two-way ANOVA (table 5.10), where a significant effect of sample height on Odd CWMA ε_{bio} is observed (F=10.14, P=0.005), with no effect of aspect, and no interaction between height of sample collection and aspect detected. As no xylem water δD data is available for the April sample collection period in Scotland, no information regarding the ΔD leaf water is available. Nevertheless, this data suggests the δD values of April *n*-alkanes are not related to the leaf water measured at the same time.

Table 5.10: Summary of two-way ANOVAs, where height of sample collection and aspect are categorical factors and ε_{bio} calculated from the separated CWMA δD values is the continuous factor. Statistically significant results are marked "*".

Time	Data tested	Source	DF	F	P
April	Odd CWMA ε_{bio}	Height	2	10.14	0.005*
		Aspect	2	0.46	0.50
		Interaction	2	0.02	0.90
		Residuals	21		
April	Even CWMA ε_{bio}	Height	2	10.15	0.009*
		Aspect	2	0.75	0.41
		Interaction	2	1.37	0.27
		Residuals	21		
Oct	Odd CWMA ε_{bio}	Height	2	0.51	0.49
		Aspect	2	0.12	0.73
		Interaction	2	0.26	0.62
		Residuals	21		
Oct	Even CWMA ε_{bio}	Height	2	1.24	0.29
		Aspect	2	0.72	0.41
		Interaction	2	0.21	0.65
		Residuals	21		

The October leaf water δD data however (chapter 4, figure 4.15), does not significantly correlate with height of sample collection, and the October Odd CWMA ε_{bio} data presented here also shows no significant relationship with height of sample collection (table 5.9). This finding is further supported by two-way ANOVA (table 5.10) with no significant effect of height of sample collection, aspect, or interaction of height and aspect detected. As a result, these data make it difficult to speculate which hydrogen source the October 2010 Scottish Odd CWMAs represent.

Examination of the Scottish Even CWMA ε_{bio} data indicates similar correlations with height of sample collection during April and October, to that of the Odd CWMA ε_{bio} data (figure 5.18). However, no significant difference in total mean Even CWMA ε_{bio} is detected between April and October (t-test, t=-1.43, P=0.19), with a total mean Even CWMA ε_{bio} of -90.64$\pm$ 7.37 ‰ (SEM, n=15) during April, and -97.93$\pm$ 3.16 ‰ (SEM, n=18) during October. However, even though the data indicates a positive correlation between leaf water δD values and height of sample collection, simple linear regression analysis suggests a strong negative correlation between height of sample collection and April Even CWMA ε_{bio} exists (table 5.9, R^2=0.43, F=11.5, P=0.005). This result is further supported by two-way ANOVA (table 5.10), where significant variation as a result of sample collection height is observed (F=10.15, P=0.009), with no significant effect of aspect, and no interaction of height and aspect. These data suggest the current leaf water D isotopic composition is not responsible for the δD values of the Even CWMAs during April in Scotland.
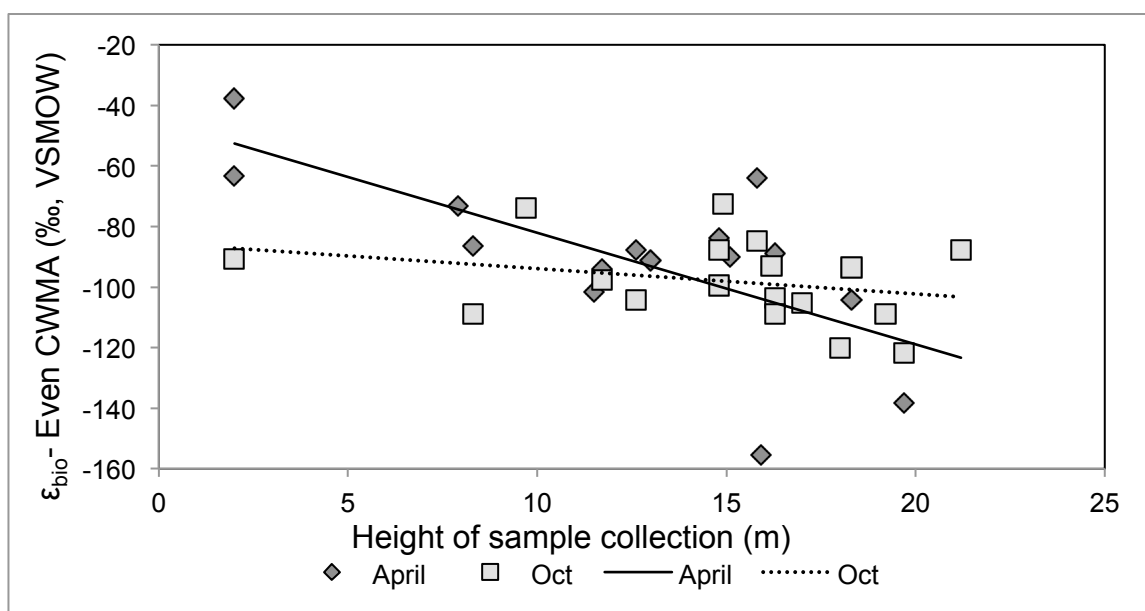
Figure 5.18: Height of sample collection (m) against Even CWMA ε_{bio} (measured in ‰) during April and October 2010 in Scotland. Dark diamonds show April and light squares October and trend lines show results of simple linear regression analysis.

As is also observed in the Odd CWMA ε_{bio} and leaf water δD data, no significant relationship between height of sample collection and Even CWMA ε_{bio} is detected through simple linear regression during October in Scotland (figure 5.18, table 5.9). This result is further supported by two-way ANOVA (table 5.10), where no significant effect of height of sample collection was observed, along with no effect of aspect, and no significant effect of the interaction between height and aspect.

Both the Scottish and Finnish ε_{bio} data exhibit different relationships with height of sample collection than that which was demonstrated by the leaf water δD data presented within the previous chapter. These data therefore suggest that current leaf waters are not the primary hydrogen source for the *n*-alkanes present at the time of sample collection.

5.4.6 Leaf water contribution to biosynthetic water

5.4.6.1 Värriö Strict Nature Reserve, Finland

Application of a conceptual model, which gives an estimation of the percentage contribution of current leaf water to the "biosynthetic water pool", along with an estimation of biosynthetic fractionation (Kahmen, Hoffmann et al. 2013, Kahmen, Schefuß et al. 2013), is applied to the data sets. The application of this conceptual model will provide further insight into the relationships between leaf water and *n*-alkane δD values.

Application of this conceptual model to the Finnish Odd CWMA δD values (figure 5.19) suggests a different, and much more D-enriched, hydrogen isotopic source has been used

during the biosynthesis of the Odd numbered *n*-alkanes in Finland during July. Simple linear regression analysis (table 5.11) indicates a strong positive relationship between ΔD leaf water and Odd CWMA ε_{app} during July (R^2=0.313, F=10.59, P=0.004, figure 5.19). Under the principles of the Kahmen et al (2013) conceptual model, the slope of this linear relationship is an estimation of current leaf waters' contribution to the "biosynthetic water pool" the *n*-alkanes have been synthesized from, while the intercept estimates ε_{bio}. In the case of Odd CWMA *δ*D values during July, an estimated ~112% of current leaf water has contributed to the biosynthetic water pool, with a ε_{bio} of -138 ‰ respectively. As it is impossible to have a contribution of leaf water of over 100%, the conceptual model suggests a more D-enriched hydrogen source must have been used in the synthesis of the *n*-alkanes present during July. Further to this, the ε_{bio} estimation reported from the conceptual model of -138 ‰ is more negative than the empirically derived mean ε_{bio} of -124.21± 3.24‰ (SEM, n=25). This suggests the model has over-estimated the total mean ε_{bio} within the Odd CWMA data set.
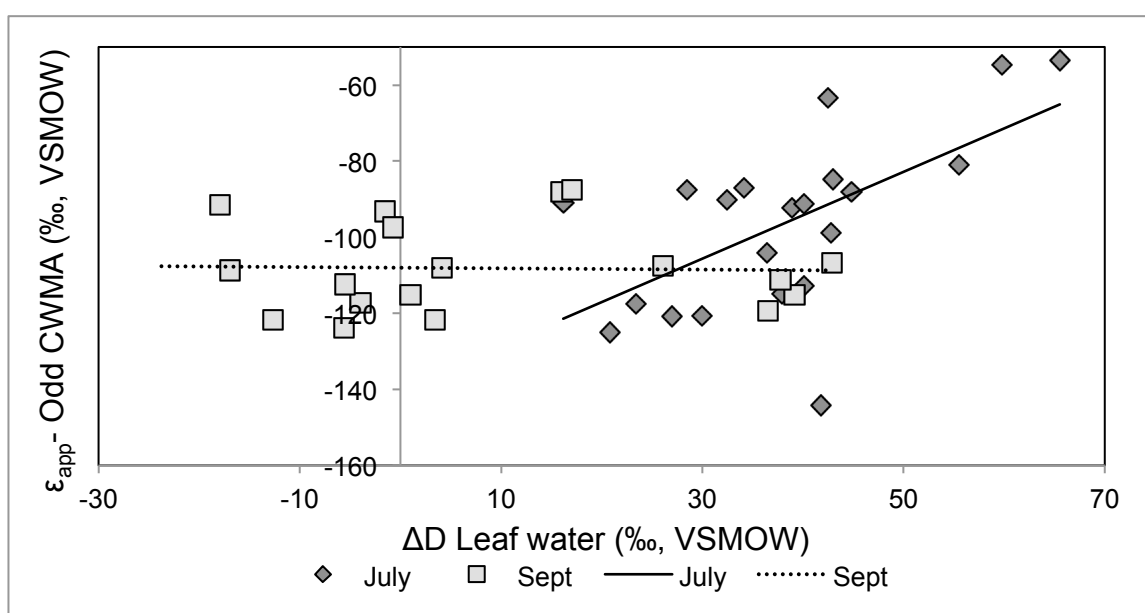
Figure 5.19: The fractionation of leaf water above xylem water (Leaf water ΔD) versus the apparent fractionation between xylem water and Odd CWMA *δ*D (ε_{app}) for both July and September in Finland. Dark diamonds show July data and light squares show September data, the trend lines indicate the results of simple linear regression analyses.

In contrast to July, the conceptual model indicates ~0% of leaf water has contributed to the "biosynthetic water pool" the September Odd CWMAs are synthesized from. Simple linear regression (table 5.11) indicates a non-statistically significant relationship (R^2= -0.062, F=0.012, P=0.91), giving a ε_{bio} estimation of ~-108 ‰, which is much more positive than the empirically derived ε_{bio} of -121.62± 6.19 ‰ (SEM, n=18). However, as detailed in chapter 4 (sections 4.4.4, 4.4.5 and 4.5.2), this result has most likely been driven by the significantly anomalous leaf water *δ*D values reported in Finland during September.

Table 5.11: Summary of simple linear regression analyses of the biosynthetic fractionation of each of the Even and Odd CWMA plotted against their respective apparent fractionations for Finland. Statistically significant results are marked "*".

Time	Data	Equation	Adjusted R^2	F	P
July	Odd CWMA	Y=1.12x-138.43	0.31	10.59	0.004*
Sept	Odd CWMA	Y=-0.016x-108.04	-0.06	0.012	0.91
July	Even CWMA	Y=0.343x-85.93	0.02	0.63	0.44
Sept	Even CWMA	Y=0.0345x-56.02	0.071	1.92	0.19

Application of this conceptual model to the Even CWMA δD values suggests there is no statistically significant relationship between ΔD leaf water and ε_{app}- Even CWMA during July or September in Finland (figure 5.20). Simple linear regression analysis of July Even CWMA data (table 5.11) estimates an Even CWMA ε_{bio} of ~-86 ‰, and a leaf water contribution of ~35%; while the September Even CWMA δD reports an ε_{bio} estimation of ~56 ‰ and a ~-35% leaf water contribution. As neither simple linear regression indicates a statistically significant result, and because it is impossible to have a leaf water contribution of -35% to the "biosynthetic water pool", these data indicate current leaf water is not the dominant source of hydrogen for the Finnish even-numbered *n*-alkanes at any point in the growing season. Furthermore, measured total mean ε_{bio} is consistently more negative than that predicted by the conceptual model, with a total mean Even CWMA ε_{bio} of -101.47± 3.82 ‰ (SEM, n=21) during July and -70.19± 9.81 ‰ (SEM, n=12) during September. Nevertheless, the conceptual model serves to further highlight the significantly different δD values, and fractionations, observed within the even-numbered *n*-alkane chains in relation to that of the odd.
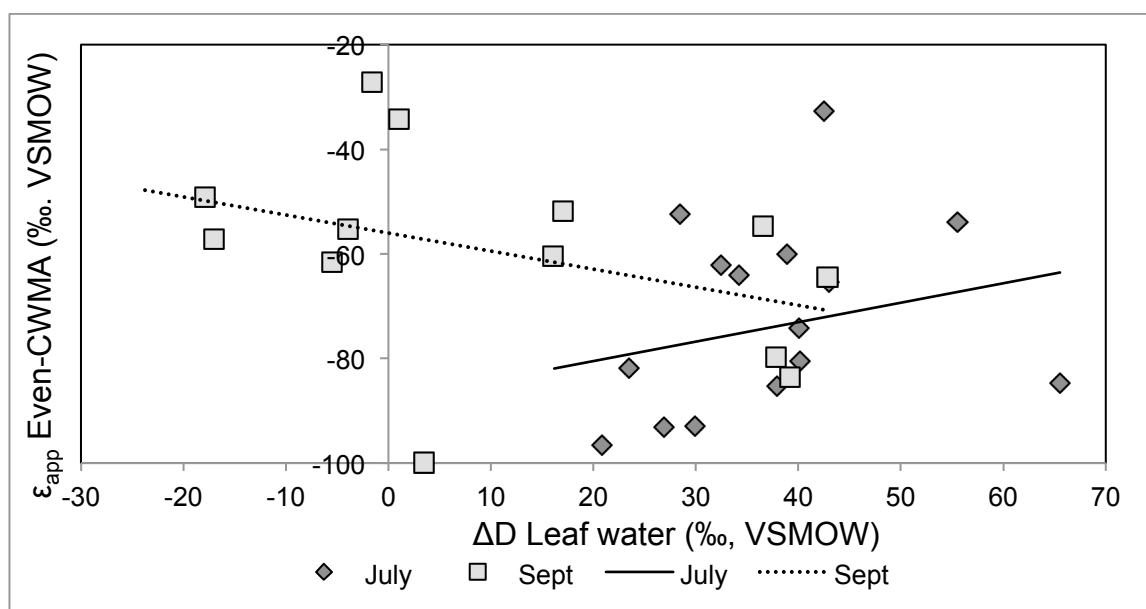
Figure 5.20: The fractionation of leaf water above xylem water (Leaf water ΔD) versus the apparent fractionation between xylem water and Even CWMA δD (ε_{app}) for both July and September in Finland. Dark diamonds show July data and light squares show September data, the trend lines indicate the results of simple linear regression analyses.

5.4.6.2 Blackwood of Rannoch, Scotland

Due to the lack of April xylem water *δ*D data it is only possible to apply the Kahmen (2013) conceptual model to the October Scottish data.
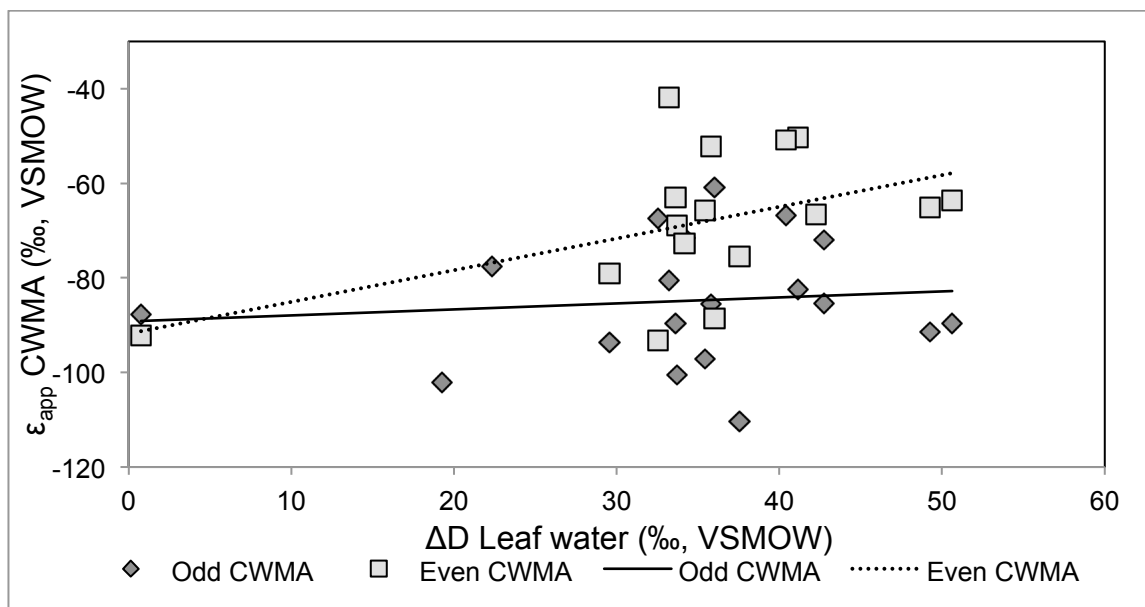
Figure 5.21: The fractionation of leaf water above xylem water (Leaf water ΔD) versus the apparent fractionation between xylem water and CWMA δD (ε_{app}) for October in Scotland. Dark diamonds show Odd CWMA data and light squares show Even CWMA data; the trend lines indicate the results of simple linear regression analyses.

Simple linear regression analysis of the Odd CWMA data from October suggests a relationship of Y=0.1269x-89.206, giving a leaf water contribution to the "biosynthetic water pool" of ~13%, and a ε_{bio} estimation of ~ -89 ‰ (figure 5.21). However, this relationship is not statistically significant (table 5.11). As was previously demonstrated by the Finnish data, the ε_{bio} estimation from the conceptual model has also over-estimated the ε_{bio} in the Scottish October Odd CWMA data; where ~-89 ‰ is estimated, compared to the total mean measured Odd CWMA ε_{bio} of -116.41± 3.22 ‰ (SEM, n=23).

Table 5.12: Summary of simple linear regression analyses of the biosynthetic fractionation of each of the Even and Odd CWMA plotted against their respective apparent fractionations for Scotland.

Time	Data	Equation	Adjusted R^2	F	P
Oct	Odd CWMA	Y=0.127x-89.21	-0.04	0.20	0.66
Oct	Even CMWA	Y=0.67x-91.79	0.18	4.25	0.06

Examination of the October Even CWMA data suggests a leaf water contribution of ~67% and a ε_{bio} estimation of ~-92 ‰, however this relationship is not significant to a 95% C.I (table 5.12). Therefore, the Scottish data also suggest current leaf water does not exert a major influence on the isotopic composition of the *n*-alkanes in Scotland.

5.5. Discussion

5.5.1 δD values of n-alkanes

The samples analysed within the current study provide compound-specific hydrogen isotopic measurements for a whole suite of individual *n*-alkane chains ranging nC_{21} to nC_{31}, including even-numbered *n*-alkane chains. Typically within compound-specific *n*-alkane analyses, especially within tree species, hydrogen isotopic data is usually only available for odd-numbered *n*-alkane chains ranging nC_{27} to nC_{31} (Yang and Huang 2003, Bi, Sheng et al. 2005, Pedentchouk 2008, Sachse 2009). The current study is not the first report of even-numbered-*n*-alkanes present within terrestrial higher plant epicuticular leaf waxes (Chikaraishi 2003, Yang and Huang 2003). However, it is the first report of both even and odd numbered *n*-alkane *δD* data, in conjunction with both leaf water and xylem water *δD* data, making these results entirely novel. Both the Scottish and Finnish data sets show increasing D-depletion with increasing *n*-alkane chain length, across all the individual *n*-alkane chains measured. This trend was expected and has been previously reported (Sachse 2006, Eglinton 2008), however is not always the case (Chikaraishi 2003). Previous research indicates this trend is the result of increasing biosynthetic fractionation with increasing *n*-alkane chain length due chain elongation processes during biosynthesis (von Wettstein-Knowles 1995, Post-Beittenmiller 1996, Shepherd and Griffiths 2006, Eglinton 2008) (see chapter 2, section 2.1.2).

As discussed in chapter 3 (section 3.3.5.), high concentrations of even-numbered *n*-alkanes, identified as of plant origin, were detected across all sample collection campaigns in both Finland and Scotland. As even numbered *n*-alkanes have been detected in high concentrations in sediment records from around the globe, and mainly attributed to bacterial degradation and/or algal inputs (Nishimura and Baker 1986, Elias, Simoneit et al. 1997, Sachse, Radke et al. 2004, Wang, Fang et al. 2010); the even *n*-alkane isotopic data presented within the current study will have significant implications for paleoclimate studies, which is discussed in more detail in chapter 7.

Distinct patterns suggested by the current study indicate the *δD* values of epicuticular leaf wax *n*-alkanes in Scots pine are highly variable. Significant variation across geographical and temporal scales was expected, however significant variation within and between individuals of the same species, inhabiting the same area, sampled at the same time was unexpected. Overall the *δD* values of all the observed *n*-alkanes in Scotland and Finland exhibit similar levels of variation within and between the different *n*-alkane homologues (~80 ‰ *δD*). However, all the measured Scottish *n*-alkanes are on average ~20 ‰ D-

enriched relative to the Finnish *n*-alkanes. Due to the north-south gradient in the isotopic composition of meteoric water, this trend is to be expected (Sachse 2006, Gat 2010). Nevertheless, when comparisons of the Scottish and Finnish data are made over the course of the growing season in each geographical location (between April and October for Scotland, and July and September for Finland), the isotopic behaviour of the two data sets deviates significantly.

The current investigation is the first occurrence where it was deemed necessary to separate the calculated CWMA δD (equation 5.1) into two separate components: 1) the Odd-CWMA, which is calculated from odd-numbered-alkane homologues only, and 2) Even-CWMA, which is calculated from only even-numbered-alkane homologues. These two CWMA δD calculations were required as a direct result of the significant abundance of even-numbered-alkane chains present within all samples analysed in the current study, in conjunction with the significantly different isotopic behaviour of the even-numbered-chains in relation to that of the odd-numbered.

Although the utilization of the CWMA formula in this manner has removed significant amounts of isotopic variation observed within and between the different *n*-alkane homologues. From a paleo-climate interpretation standpoint, this would be a suitable method as it is assumed that the *n*-alkane compounds found in the highest concentration within a particular plant sample (and thus the δD composition it carries) are most likely to be input into a respective sediment archive. However, from a plant physiological perspective, if attempts are made to better constrain *n*-alkane δD values within sediment records, the full extent of δD variations in *n*-alkanes from natural ecosystems need to be reported and hopefully explained. Nevertheless, as such a large suite of *n*-alkanes were isotopically measured, it would be very difficult, and time consuming, to present the data from each individual *n*-alkane chain measured (this raw data is available in tables 5, 6, 7, and 8 in the appendix).

Despite the potential issues in using CWMA δD values, in both geographical locations the even-numbered-alkane chains are systematically, and significantly, D-enriched in relation to the odd-numbered-alkanes (figures 5.1 and 5.2). These findings are consistent with even *n*-alkanes isotopically measured from recent lake sediments in a study of a geographical gradient in Europe (Sachse, Radke et al. 2004). Although only few measurements were permitted due to low concentrations within this investigation, compound-specific δD measurements were possible for some of the sites. Within this study, even-numbered *n*-alkane chains were indicated to be ~10 – 20 ‰ D-enriched in

relation to the odd-numbered homologues from the same samples, which is in agreement with the data presented here. Nevertheless, the high abundance of even-alkanes present within the sediments of this study were attributed to microbial degradation, due to the lack of even-numbered *n*-alkanes in the local terrestrial vegetation (Sachse, Radke et al. 2004). However, as is demonstrated within the current thesis, even numbered *n*-alkanes can be present in high abundances within terrestrial plant epicuticular leaf waxes of Scots pine.

In addition, as the highest concentrations of even *n*-alkanes, from the aforementioned study, were observed in sediment samples collected from Finnish lakes (Sachse, Radke et al. 2004), one of which is in close proximity to the forest sampled within the current study. These findings suggest even-numbered *n*-alkanes within these sediments could have been of terrestrial plant origin, and from Scots pine in particular. There is very little literature available regarding the biosynthesis of even *n*-alkanes in terrestrial vegetation, as a result, finding so many even-*n*-alkane homologues within a terrestrial plant species, especially in two significantly different geographical areas is of high importance.

5.5.2 *n*-alkane *δ*D temporal behaviour

Aside from the significantly different D-enrichments displayed by even-numbered *n*-alkanes in relation to the odd. The two different groups of *n*-alkanes appear to display significantly different isotopic behaviour over the course of the growing season in the two different geographical locations. Total mean Odd CWMA *δ*D values exhibit significant D-depletion with time in the Finnish growing season (figure 5.1), while the Scottish total mean Odd CWMA *δ*D values shows no significant difference with time (figure 5.2). Further to this, the total mean Even CWMA *δ*D values show no significant difference between July and September in Finland, while a significant D-depletion is observed between April and October in Scotland.

All odd-numbered *n*-alkanes analysed in Finland show increased D-depletion in the region of ~40 ‰ *δ*D during September when compared to July values (figure 5.1). This data, in conjunction with the molecular and concentration *n*-alkane data presented in chapter 3, indicates *n*-alkanes have been re-synthesized between July and September. These data therefore suggest that the D isotopic composition of odd-numbered *n*-alkanes is not "locked in" at the beginning of the growth season. The Even CWMA *δ*D values however, display no significant change in *δ*D values with time in the growing season (figure 5.1). Therefore this data, in conjunction with the significant increase in CPI observed in

September from the same data set (chapter 3, section 3.4.6.1), i.e. a reduced abundance of even-numbered *n*-alkane chains. Suggests even-numbered *n*-alkanes are either only synthesized at the beginning of the growth season, or they are synthesized from a δD source with a significant different δD signature, one that remains constant with time in the growing season. Any insight into the mechanisms resulting in the δD values observed in the even *n*-alkanes within the current study is of high importance to the paleoclimate reconstruction application of *n*-alkanes (discussed in more detail in chapter 7).

It is clear from the data presented here that there is a significant difference in the Odd CWMA δD values of *n*-alkanes between July and September, which demonstrates the δD values of *n*-alkanes synthesized by Finnish Scots pine are not "locked in" at the beginning of the growth season. This finding is not surprising, as few studies have investigated the isotopic behaviour of *n*-alkanes from evergreen Conifer species. Despite research from broadleaf tree species suggesting *n*-alkane δD values are "locked in" at the beginning of the growth season after leaf expansion (Kahmen 2011, Tipple 2013). Evergreen Conifer species have significantly different physiology and life strategies, which may explain the discrepancies observed. For example, not only are Scots pines within the Finnish study site subject to extremes of climate, but they have also been shown to retain their needles for up to 8 years. To facilitate this behaviour, and in such a harsh environment, re-synthesis of leaf waxes must occur. In addition, and unlike deciduous species where leaf growth occurs over a short period at the beginning of the growth season (Kahmen 2011, Tipple 2013), pine needle growth has been shown to continue for to up 50-60 days after needle flush (Patov 1985).

The Scottish *n*-alkane data however, is more difficult to interpret. The total concentration and molecular *n*-alkane data presented in chapter 3 suggest *n*-alkanes are not a significant component of the epicuticular leaf waxes of Scots pine at this location (chapter 3, section 3.5.2). This result is in agreement with the compound-specific δD data from the Odd CWMAs, but the significant D-depletion in the Even CWMAs would suggest otherwise. Nevertheless, and as mentioned previously, the significant D-depletion observed in the Even CWMA δD values has been called into question due to the low total concentrations of *n*-alkanes measured at this site. Therefore, it is concluded that not enough data is available to fully investigate the temporal behaviour of the even-numbered-*n*-alkane chains present in Scottish samples at this time. In addition, these data suggest that the Odd CWMA δD values could be "locked in" at the beginning of the growing season in Scotland. However, this finding is more likely representative of the conclusions from chapter 3 (section 3.5.1), i.e. *n*-alkanes are not a significant component

of the epicuticular waxes of Scots pine in Scotland, and therefore are not synthesized in great abundances or activity regulated.

As re-synthesis of odd-numbered *n*-alkane chains is demonstrated within the Finnish data with time during the growth season, this presents a problem in ascertaining what is driving the significantly different δD values observed. A controlled greenhouse growth experiment, testing the effect of a continuous sub-Arctic 24-hour photoperiod on *n*-alkane δD values, has suggested deciduous conifer *n*-alkanes are up to ~40 ‰ D-enriched due to enhanced transpiration, when compared to those synthesized under temperate light conditions (Yang 2009). As measured xylem water δD values shows no significant variation within or between individuals with time in the growing season (chapter 4, figure 4.11). The *n*-alkane δD values alone would indicate D-enrichment of July *n*-alkanes is the result of significant leaf water D-enrichment, due to enhanced transpiration from the 24 hour photoperiod that the Finnish forest experiences during July. However, examination of δD values within and between the different individual Scots pine studied, during both July and September, has highlighted more complex processes are at work. The δD values of *n*-alkanes in Finnish Scots pine, across the whole Finnish data set, provide insights into the behaviour of Scots pine on an entire forest-stand-level over time. For example, the Odd and Even CWMA δD values show no statistically significant trends within or between individuals during July, and yet repetition of the same sample collection towards the end of the Finnish growing season in September demonstrates significant variation within and between the same individuals studied.

Moreover, the Odd CWMA δD values exhibit significant variation as a result of individual tree size during September, and show strong significant negative correlations with height of sample collection (figure 5.12). This relationship indicates increasing D-depletion with increasing height of sample collection, and a similar but less significant relationship is observed for Even CWMA δD values. Therefore, if *n*-alkanes are synthesized from water within the leaf (Chikaraishi and Naraoka 2001, Chikaraishi, Naraoka et al. 2004), constantly recording the δD values of leaf waters (Smith 2006, Pedentchouk 2008, Feakins 2010, Sachse 2010); one would anticipate the trends in leaf water δD, and ΔD leaf water, to exhibit similar trends with height. However, as is demonstrated by chapter 4 (section 4.4.7, figure 4.12 and figure 4.13), leaf water δD and ΔD leaf water exhibit significantly positive correlations with height of sample collection during September. This suggests that current leaf water is not the primary δD source for *n*-alkanes sampled at this time.

5.5.3 Variations within and between individuals, Finland

To shed light on the temporal behaviour of *n*-alkane δD values with time in the Finnish data, the data presented here must be examined in conjunction with the leaf water δD and ΔD leaf water data presented in the preceding chapter 4.

The Odd and Even CWMA δD values from July show no significant variations within or between individuals, as well as no significant variation as a result of sample collection height. However, the leaf water δD (figure 4.12) and ΔD leaf water (figure 4.13) exhibit significant negative correlations with height of sample collection. As xylem water δD values do not significantly vary with height of sample collection during July (figure 4.11), and leaf water δD values suggest a significant negative relationship with height of sample collection. While the September Odd CWMA δD values show a significant negative correlation with height of sample collection (figure 5.12), and leaf water δD and ΔD leaf water (chapter 4, figures 4.12 and 4.12) are significantly positively correlated with height of sample collection. This presents a problem, if the *n*-alkanes are not representative of current leaf waters, what δD signal do the *n*-alkanes represent during each sample collection period?

As demonstrated and discussed in chapter 4, the leaf water δD and ΔD leaf water data produced unexpected results. Leaf water D-enrichment and ΔD leaf water were shown to be significantly negatively correlated with height of sample collection during July, while repetition of the sample collection in September showed significantly positive correlations with height of sample collection. Where, the July data suggest a physiological response of trees with height to the 24-hour photoperiod (Mencuccini and Grace 1996, Niinemets, Kull et al. 1999, Niinemets, Sonninen et al. 2004, Woodruff, Meinzer et al. 2008, Woodruff, Meinzer et al. 2009), resulting in reduced evapotranspiration, and therefore leaf water D-enrichment. While the September leaf water δD and ΔD leaf water suggests the impact of a low lying fog, which has affected the isotopic composition of leaf waters (Dawson 1998, Sen'kina 2002, Farquhar and Cernusak 2005, Welp, Lee et al. 2008, Kim and Lee 2011), the mechanisms of which are explained in greater detail in chapter 4 (section 4.5.2).

Taking into account the problematic leaf water data observed during September, if the trend with height in leaf water δD and ΔD leaf water data observed during July, is compared with the Odd CWMA δD data from September. One could cautiously hypothesize: 1) the July leaf water δD and ΔD leaf water data is more representative of the general trends in leaf water δD values observed within the forest under investigation

during the height of productivity in the growing season. 2) This general trend is represented within the secondary leaf waxes synthesized with time in the growing season, which is indicated by the δD values of *n*-alkanes analysed during September. This finding would therefore suggest gradients in micro-climatic variables within natural forest canopies are of significant magnitude to impact the δD values of *n*-alkanes in secondary leaf waxes. Nevertheless, this suggestion does not explain the δD values of the Finnish *n*-alkanes analysed during July.

5.5.4 Source of hydrogen for *n*-alkanes in Finland

As these results indicate the level of leaf water D-enrichment is only imprinted on the secondary Odd-*n*-alkanes. This raises the issue of which δD signal the Odd-*n*-alkanes represent in July. As mentioned previously, the leaf water δD and ΔD leaf water show a statistically significant negative correlation with height, and no such trend is reflected in the *n*-alkanes. This would suggest that the δD values of *n*-alkanes observed in July are representative of either earlier leaf water, which shows no significant trends with height of sample collection, or they are representative of some other physiological processes.

Spring D-enrichment of *n*-alkanes is a commonly reported phenomenon (Chikaraishi, Naraoka et al. 2004, Brandes, Wenninger et al. 2007, Pedentchouk 2008), however the reasons for this observed D-enrichment is the subject of debate. D-enriched *n*-alkanes at the beginning of growing seasons have been suggested to be the result of *n*-alkane synthesis from D-enriched metabolic water, and/or stored assimilates generated towards the end of the previous growing season (Sachse 2009, Sachse 2012, Tipple 2013). Recent research conducted by Tipple et al (2013) attributed the δD values of *n*-alkanes from *Populus angustifolia* trees growing in a natural riparian environment, to the combination of the evaporative D-enrichment of xylem water over winter, and the utilization of stored sugars in *n*-alkane biosynthesis. Although xylem water pre needle flush was not measured in the current study, the xylem water δD values do not significantly vary with time in the Finnish growing season. In addition, as winter temperatures at the sample site can reach as low as -40 °C, and remain below freezing until May, extensive transpirational D-enrichment of xylem water over winter is unlikely. However, future studies should test for this possibility.

Instead, the data presented here suggest the *n*-alkanes present during July could be synthesized from stored assimilates generated towards the end of the previous growth season (Sachse 2009), rather than D-enriched xylem waters. Previous research has

suggested more D-enriched *n*-alkane isotopic values, and/or deviations from a linear relationship between plant source water and *n*-alkanes, is the result of plants relying upon stored carbohydrates during biosynthesis (Sachse et al., 2012). Therefore, the D-enriched signal of the *n*-alkanes may be the result of differing origins of NADPH (Schimmelmann 2006, Sachse 2012), the reducing agent used in *n*-alkane biosynthesis (Zhang, Gillespie et al. 2009). Where, NADPH sourced directly from the light reactions of photosynthesis has been indicated to be very D-depleted (Luo, Steinberg et al. 1991, Schmidt 2003). While NADPH derived via the oxidative pentose phosphate pathway (PPP) from stored glucose, is significantly D-enriched by comparison (Schmidt 2003, Schimmelmann 2006, Feakins 2010). As NADPH is the reducing agent used during *n*-alkane biosynthesis, it would seem a reasonable assumption that NADPH used at this time would more likely originate via PPP from glucose, than via the light reactions in photosynthesis. This is because the leaves will not have reached full metabolic activity, especially when they are still undergoing growth and expansion (Sessions 1999, Kahmen 2011, Tipple 2013).

The utilization of stored assimilates for the growth of new plant tissues in spring is a widely reported concept in plant physiology. Where carbon isotopic analysis of tree rings, cellulose, and bulk foliar material, have linked spring growth to ^{13}C-enriched carbohydrates and sugars generated toward the end of the previous growth season (Damesin and Lelarge 2003, Niinemets, Sonninen et al. 2004). However, as needle retention of the Finnish trees would suggest the ability to begin photosynthesis prior to the current years' needle flush; the isotopic analysis of tree rings from Scots pine inhabiting the same study forest have indicated it is possible to observe a switch from reliance on stored assimilates to current assimilates through ^{13}C isotopic analyses of the wood that is laid down over the course of the growth season in tree rings (Hilasvuori, Berninger et al. 2009).

This suggests, despite the significantly different life strategy of evergreen conifer species in relation to deciduous species, pre-acquired assimilates from the end of the previous growth season still dictate the isotopic composition of the new plant organic matter growing the following spring. Unfortunately, due to too little sample remaining after *δ*D analysis, as well as time constraints, compound-specific carbon isotopic analyses of the *n*-alkanes could not be conducted. This is a significant recommendation for future studies in this area. Nevertheless, these data suggest that the D-enriched *n*-alkanes observed in Finland during spring are the result of significant D-enriched NADPH used in biosynthesis.

Further evidence in support of this hypothesis is demonstrated through the application of the Kahmen et al., (2013) conceptual model, where, the gradient of the linear correlation between ΔD leaf water and ε_{app} gives an estimation of the current leaf waters' contribution to the "biosynthetic water pool" the *n*-alkanes were synthesized from, and the intercept an estimate of ε_{bio}. Application of this conceptual model to the July Odd CWMA data set reveals ~112% of the current leaf water has contributed to the "biosynthetic water pool" of the odd-numbered *n*-alkanes (figure 5.19). For obvious reasons, a leaf water contribution to the "biosynthetic water pool" of over 100% is impossible. In addition, and unlike the findings of Kahmen et al., (2013), where they attribute their findings of over 100% leaf water contribution to the "biosynthetic water pool" to an under-estimated leaf water D-enrichment from their model calculations. The current investigation measured leaf water δD values directly, and it can be concluded that the value of ~112% leaf water contribution is representative of the samples collected, and not a leaf water D-enrichment estimation error. This further supports the hypothesis of July odd-numbered-*n*-alkane δD values representing D-enriched stored assimilates, rather than current leaf waters.

In addition, further evidence in support of this hypothesis can be found if the Kahmen et al., (2013) conceptual model is applied using the Odd CWMA δD values from September, and the leaf water and xylem water δD values from July. Simple linear regression suggests, with high statistical significance, that ~90% of the July leaf water contributes to the September Odd-CWMA "biosynthetic water pool" (Y=0.909x-144.64, adjusted R^2=0.36, F=10.1, P=0.006, figure 5.22).
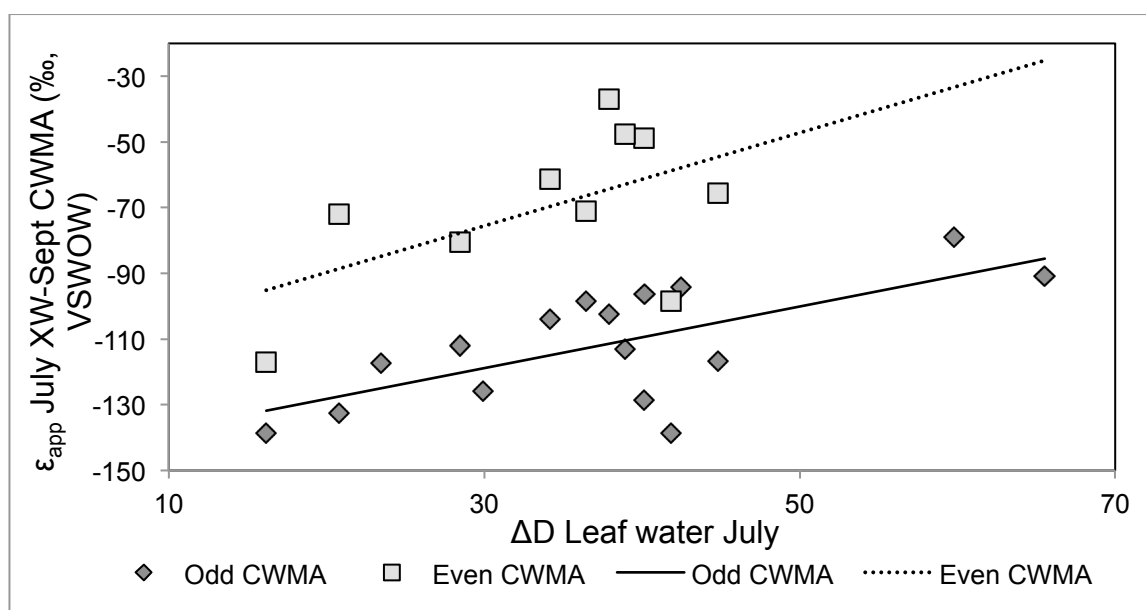
Figure 5.22: The fractionation of leaf water above xylem water (Leaf water ΔD) for July 2010 versus the apparent fractionation between July 2010 xylem water and September 2010 CWMA δD for all data measured in Finnish Lapland. Dark diamonds depict Odd-CWMA data; light squares show Even-CWMA. The trend lines represent simple linear regression analyses.

Working under the assumption that the leaf water δD values from July are more representative of the leaf water D-enrichment trends within the forest under investigation; application of this conceptual model in this manner further corroborates the suggestion that microclimate driven leaf water D-enrichment could impact the δD values of secondary *n*-alkanes. Further to this, as conifers are well adapted to absorbing water directly from the atmosphere into the leaf (Dawson 1998), and as D-depletion of leaf water in relation to xylem water can occur in dew or fog conditions (Welp, Lee et al. 2008, Kim and Lee 2011); if the unusually D-depleted leaf water δD values observed during September occurred relatively regularly during the course of the growing season, this could explain why the correlations within the current study are not stronger. As is always the case with in-depth studies of natural environments, significant levels of variation are always to be expected.

The Even CWMA δD values are unfortunately more difficult to interpret. When the even *n*-alkane data is subjected to the same statistical analyses as the odd-numbered-*n*-alkane data, they appear to follow similar trends, but are always off-set with a significant D-enriched signal and a much more positive ε_{bio}. Unfortunately, application of the Kahmen et al., (2013) conceptual model using July leaf and xylem water δD values (figure 5.22) does not provide any additional information regarding the hydrogen source of these compounds, as no significant relationship is found (Y=1.415x-116.93, adjusted R^2= 0.21, F=3.71, P=0.09). The conceptual model suggests an estimated leaf water contribution of 34% during July and -35% during September, neither of which is statistically significant. Nevertheless, these results do highlight the need to separate the current data set into the odd-numbered and even-numbered *n*-alkane components. They also suggest even number *n*-alkanes are synthesized from a significantly different, and D-enriched hydrogen source, which cannot be identified at this time. Future studies must try to elucidate the origins of these even numbered *n*-alkanes, for both plant physiological and paleoclimate studies.

5.5.5 Biosynthetic fractionation (ε_{bio})

Biosynthetic fractionation (ε_{bio}), has been reported to be genus specific (Liu, Yang et al. 2006, Hou 2007, Sachse 2012, Kahmen, Hoffmann et al. 2013, Kahmen, Schefuß et al. 2013) and insensitive to environmental conditions (Zhang and Sachs 2007, Zhou, Grice et al. 2011). As the vast majority of publications, especially those utilizing the paleoclimate reconstruction applications of *n*-alkane hydrogen isotopic composition, assume ε_{bio} is

always constant within a single species, the current study suggests this is not always the case.

In the current study, ε_{bio} increases with increasing chain length and this relationship is expected under the theory of increased isotopic fractionation with increasing chain length (Figures 5.14 and 5.16) (Sachse 2006, Eglinton 2008). However, significant levels of variation are reported between individual chains sampled at the same time. This would suggest ε_{bio} is not constant within the same species, and as shown (figure 5.15), ε_{bio} can significantly vary with height within the same individual. Furthermore, the biosynthetic fractionation estimates, generated through the application of the Kahmen et al., (2013) conceptual model support this hypothesis. Not only are several different values for ε_{bio} reported with time (figures 5.19, 5.20 and 5.22), if ε_{bio} was constant, one could expect a significantly greater correlation. To the author's knowledge, this is the first time such a large data set has been subjected to this conceptual model; granted natural ecosystems are very complex, and data generated from these cannot be expected to display perfect correlations, nevertheless one would anticipate a stronger correlation if ε_{bio} was constant.

It is however important to note,, testing the consistency of ε_{bio} within the current data set is complex because there are so many variables and uncertainties involved. The results from the current investigation do however suggest that either the "biosynthetic water pool" from which odd-numbered *n*-alkanes are synthesized from is extremely variable within and between individuals of the same species at the same time. Alternatively, the results suggest ε_{bio} is not constant either within Scots pine, within natural forest ecosystems', or within plants as a whole. It is strongly recommended that the consistency of ε_{bio} within individuals, in natural environments, be fully investigated before the assumption of a constant ε_{bio} is applied to either plant physiological studies or paleoclimate reconstructions.

5.5.6 Summary

The current study represents the first in-depth investigation into the variation in *n*-alkane δD values within an evergreen conifer species in natural forest conditions (Sachse 2009). It is also the first study where highly detailed xylem water- leaf water-lipid δD analyses were conducted (Sachse 2012) in conjunction with *n*-alkane δD analyses. Significant variations in the δD values of *n*-alkanes, and their associated fractionations from environmental waters have been previously reported. However, significant levels of variation with height within single individuals, in the same species, inhabiting the same

location, have not been reported previously. Variations between different species are readily explained by differences in physiology, leaf growth, development and phenology (Kahmen 2011, Kahmen, Schefuß et al. 2013), or differences in biosynthesis and metabolism (Sachse 2012). Nevertheless, as the current study focusses on one single species, these differences can be ruled out, along with potential variation due to genetics, soil water status, and nutrient status.

Finding some degree of variation with time in the growth season was expected due to the natural heterogeneity in natural ecosystems. In addition, variations in fractionations and the δD values of *n*-alkanes within individuals was expected as a result of the differing levels of exposure of different parts of the tree to the environment. However, to report statistically significant trends with height across an entire forest stand, suggests environmental/physiological influences on the hydrogen isotopic composition, and fractionations from environmental waters, of *n*-alkanes within the Sub-Arctic Finnish Scots pine forest under investigation. These findings could have significant impacts for the paleoclimate application of *n*-alkanes, which will be discussed in detail in the following chapter 7.

5.7 Conclusions

1. Xylem water δD value has little control on the δD values of *n*-alkanes within this study.

2. *n*-alkane δD values are not "locked in" at the beginning of the growth season in Finnish Scots pine.

3. *n*-alkanes present in Finnish Scots pine during July are mainly synthesized from D-enriched stored assimilates, which are generated toward the end of the previous growth season.

4. Even number *n*-alkanes may be synthesized via a completely different biosynthetic pathway and/or use a different hydrogen source to the odd-numbered *n*-alkanes.

5. Leaf water D isotopic composition during July significantly contributes to the isotopic signature of secondary leaf waxes present during September.

6. The ε_{app} should not be used in plant physiological studies involving *n*-alkanes, as this does not provide information on leaf water evaporative D-enrichment.

7. Either Biosynthetic fractionation (ε_{bio}) is not constant within single species or individual, or the theoretical "biosynthetic water pool" is highly dynamic. This issue requires immediate investigation if the application of *n*-alkanes as a paleo-climate proxy are to have any validity.

8. This study highlights the need for complete xylem water- leaf water –*n*-alkane δD data in understanding the D isotopic behaviour of *n*-alkanes, both spatially and temporally.

6. Change in the δD values of *n*-alkanes in Salix with time in the growth season

6.1. Temporal studies of deciduous species; a literature review

6.1.1. Introduction

As the aim of the current thesis is to better understand the variation in the δD values of *n*-alkanes in natural ecosystems, as well as constrain the environmental and physiological drivers of these. Using a multi-isotope approach, a small study composing of a chronological sequence of the bulk foliar carbon isotopic composition, the compound-specific hydrogen isotopic composition of *n*-alkanes, and the fractionations of leaf waters above xylem water, was conducted on 3 Salix individuals located around the University Broad, at UEA, Norwich, during the growth season of 2012.

Many of the same principles, hypotheses, and theory discussed in chapters 3, 4 and 5 also apply within the current chapter. However, as the tree species under investigation is deciduous, they exhibit a significantly different physiology and life strategy in comparison to the conifer species previously investigated. Furthermore, current research suggests species-specific biosynthetic fractionation, along with species-specific responses to environmental conditions. Therefore, the Salix under investigation could exhibit significantly different *n*-alkane hydrogen isotopic compositions, with significantly different relationships to source waters.

6.1.2. The *n*-alkanes of deciduous tree species

Evergreen Conifer and deciduous tree species exhibit very different life strategies. Conifers can retain their foliage for multiple years, while deciduous species will completely replace all of their foliage at the beginning of each growing season. Chapters 3 and 5 demonstrate the *n*-alkanes of Scots pine inhabiting North-Eastern Finnish Lapland are continuously synthesized as part of their leaf waxes throughout the growing season. Despite this, it has become increasingly clear that both the molecular and compound-specific isotopic hydrogen compositions of *n*-alkanes are not only species specific, but they may also be environment specific.

6.1.2.1. Concentrations and molecular distributions of *n*-alkanes

Within Paleo-climate reconstructions, one of the major assumptions suggests *n*-alkanes of terrestrial origin can be easily distinguished from other sources because of two quantitative calculated values. The first, Average Chain Length (ACL), describes the weighted-average number of carbon atoms per molecule (Poynter 1991) (calculated using equation 2.2) and the second, Carbon Preference Index (CPI), describes the odd/even predominance of carbon number range (Allan 1977) (calculated using equation 2.1).

Both of these quantitative values have been used in determining what has contributed most to *n*-alkanes extracted from sediments, and shifts detected in ACL in sediment archives are increasingly applied as paleo-vegetation proxies. For example, an ACL of less than nC$_{23}$ is reported to indicate greater inputs from algae and submerged aquatic plants (Sachse 2006), CPI values closer to 1.0 are suggested to indicate contamination from petrogenic sources, and CPI values of 5-10 are suggested as diagnostic of terrestrial vegetation inputs (Jeng 2006). Shifts in ACL of around 1.5 units are considered statistically significant (Jeng 2006), and shifts in CPI of a similar magnitude are also considered statistically significant (Vogts, Schefuß et al. 2012). More recently, shifts in both CPI and ACL have been linked to aspects of climate such as moisture levels, temperature, and RH (Eglinton 2008, Vogts, Schefuß et al. 2012), which in turn are being used to infer shifts in vegetation (Jeng 2006, Sachse 2006, Vogts, Schefuß et al. 2012).

As these two descriptive values appear crucial in the interpretation of sediments in paleo-environmental reconstructions, it is of crucial importance to fully investigate whether the signals produced by terrestrial vegetation stay within the diagnostic values indicated above, or whether they change over time. For example, if a shift of 1.0 ACL units with depth in a sediment core is considered important, it is absolutely necessary to determine whether ACLs between and within individuals show less variation than this. Otherwise, variation within and/or between individuals will overwhelm this signal and may bring the use of CPI and ACL values as a diagnostic tool into dispute.

Recent research specifically addressing the molecular composition and concentrations of the *n*-alkanes in deciduous tree species has produced contradictory results. A controlled greenhouse growth experiment on *Populus trichocarpa* seedlings observed relatively stable *n*-alkane total concentrations, and molecular compositions, throughout the duration of a 50 day experiment (Kahmen 2011). Similar results were observed from an investigation into the *n*-alkanes of Barley (Sachse 2010), and field grown *Populus* trees

(Tipple 2013), with both studies suggesting *n*-alkanes are not significantly altered after the initial period of leaf expansion. In contrast, several other studies have documented continuous *n*-alkane synthesis with time in the growing season for deciduous natural forest ecosystems (Piasentier 2000, Pedentchouk 2008, Sachse 2009, Gao, Burnier et al. 2012, Gao, Tsai et al. 2012). Despite these findings, it has become increasingly apparent, as valuable as controlled greenhouse growth experiments are, they are not representative of natural field conditions. This is because wax removal, through natural processes such as wind abrasion, is not represented within these experiments (Shepherd and Griffiths 2006, Gao, Burnier et al. 2012, Gao, Tsai et al. 2012).

This suggests research from natural forest ecosystems, which indicate progressive increases in ACL with time in the growth season, as well as changes in the isotopic compositions of *n*-alkanes with time (Eglinton 1967, Piasentier 2000, Sachse 2009), are perhaps more representative of natural field conditions. These natural field investigations have suggested a temporal trend of highest *n*-alkane concentrations during spring, with a relatively constant concentration with time thereafter, until a sharp decrease immediately prior to leaf senescence (Sachse 2009, Gao, Tsai et al. 2012). These reports of varying *n*-alkane concentrations, and molecular compositions, introduce further issues into the interpretation of *n*-alkane molecular distributions. This is because increasing *n*-alkane chain length distributions over time can indicate either the preferential removal of shorter *n*-alkane chains, or an increase in the abundance of longer chain *n*-alkanes.

The preferential removal of shorter chain-length *n*-alkanes can arise with time in the growth season because wax morphological studies suggest longer *n*-alkane chains have a higher melting point (Riederer and Schneider 1990, Gao, Tsai et al. 2012). Where, these higher melting points result in greater resistances to wax-removal caused by high summer temperatures. Therefore, if *n*-alkanes are synthesized primarily during the period of leaf expansion, it is impossible to confirm from *n*-alkane total concentration and molecular distribution data alone, whether preferential erosion or continued synthesis of longer chains has occurred. This is why it is crucial to conduct *n*-alkane concentration and molecular distribution analyses in conjunction with compound-specific isotopic hydrogen analyses. Nevertheless, in terms of the applications of *n*-alkanes as a paleo-environmental proxy, how these parameters vary over the course of a whole growth season, what drives this variation, and which signal is ultimately imparted to the sediment record is of greater importance.

6.1.3. *δ*D values of *n*-alkanes

As the crux of current research is in understanding the *δ*D values produced by living plants in to order to understand the *δ*D values of *n*-alkanes in ancient sediments. Establishing the main drivers of the *δ*D values produced, as well as the timing of these, is of critical importance (Rao 2009, Zech 2009, Hren 2010). The general consensus of current research suggests the *δ*D values of *n*-alkanes in terrestrial modern vegetation are highly positively correlated with mean annual precipitation (MAP) over global and catchment level scales (figure 2.1, Chapter 2, section 2.1.1) (Chikaraishi 2003, Sachse 2006, Eglinton 2008, Hou 2008, Liu 2008, Rao 2009, Feakins 2010, Sachse 2012). However, investigation into this correlation on a forest-by-forest, or even individual tree-by-tree basis, increasingly suggests a simple positive linear correlation between *n*-alkane and source water *δ*D values does not always hold. This suggests the relationship between source water and *n*-alkane D isotopic composition is much more complex than previously thought (Sachse 2012).

Once the temporal behaviour of the molecular and isotopic characteristics exhibited by *n*-alkanes is identified. The next, and most crucial, step will be in identifying which physiological and/or environmental parameters are most important for driving the signals observed. Despite much research in this area, investigations directly addressing the importance of environmental and physiological drivers of both the molecular and isotopic compositions of *n*-alkanes are still lacking, particularly in natural ecosystems (Smith 2006, Feakins 2010, Sachse 2012). Recent research investigating exactly when and from where the *n*-alkanes of living vegetation gain their hydrogen isotopic composition has produced conflicting results. Until recently, it was assumed the hydrogen isotopic composition of *n*-alkanes represent D-enriched leaf water, which is constantly altered over the course of the growth season as wax is removed and *de novo* synthesis takes place (Sachse 2006, Pedentchouk 2008, Sachse 2009). Nevertheless, several controlled growth experiments on grasses (McInerney 2011), Barley (Sachse 2010), Poplar seedlings (Kahmen 2011), along with field Poplar studies (Tipple 2013), indicate the hydrogen isotopic composition of *n*-alkanes are "locked in" at the beginning of the growth season, changing very little once leaf expansion has ceased.

Despite the conclusions from the previous chapter, where the results suggest *n*-alkane synthesis occurs continuously throughout the growing season in Finnish Scots pine (*Pinus sylvestris L.*). As mentioned previously, the current study focuses on a deciduous tree species with a completely different life strategy. Therefore, it is very possible that the *δ*D

values of deciduous *n*-alkanes are indeed "locked in" for Salix. However, ascertaining which hydrogen isotopic signal is recorded at this time is the subject of much debate (Sachse 2010, Sachse 2012, Tipple 2013). Studies conducted on annual grass species suggest the "locked in" *n*-alkane isotopic compositions are representative of un-enriched leaf/ xylem water from the base of the expanding leaf (Sachse 2010, McInerney 2011). While, studies conducted on perennial species indicate the "locked in" signal could be more representative of D-enriched metabolic water and/or previously synthesized D-enriched carbohydrate stores (Sachse 2009, Sachse 2010, McInerney 2011, Tipple 2013). Despite these discrepancies, no studies exist where a direct comparison of the isotopic compositions of xylem water - leaf water - *n*-alkanes between an annual and a perennial species is made.

Although several studies have addressed which hydrogen isotopic signal is recorded in the δD values of *n*-alkanes (Sachse 2010, Kahmen 2011, Kahmen 2012, Tipple 2013). Only one of these studies was conducted in natural field conditions, on a tree species, and with complete measured sets of xylem water-leaf water-alkane δD values (Tipple 2013). The findings of this investigation indicate only *n*-alkanes formed during the period of leaf flush can be affected by environmental conditions (Tipple 2013) (while a similar study conducted on Scots pine (see chapter 5) concluded the opposite). As can be seen, although many recent publications have come to the same conclusion that *n*-alkane δD values are "locked in" at the beginning of the growth season, questions still remain regarding the origins of this signal.

6.1.4. Determining the origins of *n*-alkane δD values

As fractionation factors of *n*-alkanes above source waters are applied in paleo-climate reconstructions, it is a necessary prerequisite to fully understand how these fractionations vary spatially and temporarily. The current accepted theory suggests averaged values of apparent fractionations (ϵ_{app}) of *n*-alkanes above source waters can be utilized effectively over large scales (Sachse 2006, Sachse 2012). It is also suggested that biosynthetic fractionation (ϵ_{bio}) is constant within a given species (Sessions 1999, Zhou, Grice et al. 2011, Kahmen 2012, Kahmen 2012, Sachse 2012). Nevertheless, applications of fractionation factors, in any capacity, cannot be applied with high fidelity until we resolve how much source water δD, leaf water D-enrichment (Smith 2006, Sachse 2010, Kahmen 2012, Sachse 2012), and D-enriched stored assimilates (Sessions 1999, Sachse 2009, Gao, Tsai et al. 2012), influence the δD values of *n*-alkanes observed in field studies.

To this end, a small investigation was conducted on Salix trees, where xylem water- leaf water- alkane δD data was collected continuously from leaf flush through to immediately prior to leaf senescence. However, in order to make further inferences regarding the potential sources of hydrogen, a multi-isotope approach was applied. Where oxygen isotopic analysis of bulk leaf water was conducted in conjunction with bulk ^{13}C isotopic analysis of the corresponding leaf material. To the authors' knowledge, this is the first instance where the oxygen versus carbon isotopic conceptual model (Saurer 1997, Farquhar, Barbour et al. 1998, Scheidegger 2000) has been applied to aid in the interpretation of *n*-alkane δD values.

Under this conceptual model, it is theoretically possible to ascertain whether the driving cause of the isotopic signals observed in leaf waters is the result of climatic influences or that of photosynthetic capacity. For example, bulk leaf water δD and δ^{18}O values are related, this is because both are governed by the same processes that influence the evapotranspiration of water out of the leaf (see chapter 2 section 2.1.4 and Chapter 4 for further discussion). However, δ^{18}O and δ^{13}C leaf values share a different relationship, where both are affected by stomatal aperture, but δ^{13}C can also be influenced by photosynthetic capacity. As a result, if the stomata are closed, the leaf must fix all CO_2 available, this results in more ^{13}C-enriched isotopic compositions in organic matter (Farquhar 1980, Sharkey 1982, Farquhar 1989). Essentially, utilization of the δ^{13}C versus δ^{18}O conceptual model provides additional information regarding what is causing an enriched carbon isotopic signal. I.e. whether an enriched carbon isotopic composition is the result of low rates of photosynthesis or reduced stomatal conductance (Scheidegger 2000). Although this model was devised for the study of bulk foliar δ^{18}O versus bulk foliar δ^{13}C, using leaf water δ^{18}O measurements represents a more dynamic oxygen isotopic source than bulk foliar δ^{18}O, which is a time-integrated measurement of oxygen composition (Farquhar and Lloyd 1993, Farquhar, Barbour et al. 1998, Barbour 2007). Despite leaf water δ^{18}O values being more dynamic, restrictions on analysis time and cost prevented the analysis of bulk foliar material δ^{18}O. Additionally, as research suggests the *n*-alkanes of broadleaved tree species may be highly dynamic (Gao, Tsai et al. 2012), a dynamic δ^{18}O source pool should not be a problem in current study.

Therefore, if the bulk foliar δ^{13}C and leaf water δ^{18}O values are negatively correlated, it is suggested stomatal aperture, and potentially RH, are driving any signals observed. However, if there is no correlation between these two, then the signal is driven by some aspect of photosynthetic capacity (Yakir and Israeli 1995, Saurer 1997, Farquhar, Barbour et al. 1998, Barbour and Farquhar 2000, Scheidegger 2000). As a result, if the oxygen-

carbon isotopic conceptual model indicates low photosynthetic capacity we can speculate that the organic matter produced within the leaf at the time of sampling will not be generated by current photosynthesis.

6.2 Aims

The current study focuses on the variation in *n*-alkane compositions and the potential drivers of these with time, rather than variations within and between individuals of the same species. Therefore, samples were collected at the same height, at the same location, on 6 different days throughout the 2012 growing season, with the aim of addressing the following questions:

1. Can significant variation in *n*-alkane molecular distributions, and concentrations, be found with time during the growth season?
2. Are *n*-alkanes "locked in" at the beginning of the growth season?
3. What hydrogen isotopic signal is incorporated into the *n*-alkanes synthesized at the start of the growth season, does this remain constant with time?
4. Are any trends found a plant physiological or a climatic response?

6.3 Methodology

6.3.1. Sample collection

3 Salix individuals, 5m in height, and in close proximity, were randomly selected and marked with yellow string. Leaf and xylem material was collected from each tree on 6 occasions throughout the course of the 2012-growing season. Three leaf samples, one for *n*-alkane analysis, a second for leaf water analysis, and a third for bulk foliar carbon isotopic analysis, along with a small section of xylem supplying each leaf with water, were collected. Material was collected twice during the period of leaf flush April when the leaves were still undergoing expansion, and then collected once a month until the end of September immediately prior to leaf senescence (please see chapter 2, section 2.2.1.5).

Full sample preparation, sample analysis, data processing and quality control are detailed within chapter 2, sections 2.2.2 and 2.2.3.

6.3.2. Data analysis

Molecular distribution data was calculated using equation 2.2 (chapter 2, section 2.1.2.2) for ACL (Poynter 1991) and equation 2.1 for CPI (Allan 1977, Marzi, Torkelson et al. 1993) (See chapter 2 sections 2.1.2.2 and chapter 3 for more information). Concentration weighted mean alkane δD values were calculated from equation 5.1, chapter 5 (Kahmen 2012), and fractionations of the *n*-alkanes above various measured waters were calculated using equation 5.2, chapter 5 (Sachse 2006). Statistical analyses were conducted using Microsoft Excel and R statistical programming package, full details of which are described in Chapter 2 section 2.2.3.5.

6.4 Results

6.4.1. *n*-alkane molecular data

The total concentration of *n*-alkanes during leaf expansion is relatively low in the beginning of April with 1.81± 0.28 mg/g DM (SEM, n=3) and increases quickly thereafter (figure 6.1). Total *n*-alkane concentrations peak at 4.11± 0.48 mg/g DM (SEM, n=3) during May, gradually decreasing with time until leaf senescence, where a total concentration of 2.48 ± 0.4 mg/g DM (SEM, n=3), is reported at the end of September. These data suggest the total concentration of *n*-alkanes synthesized by Salix starts to decrease during early May and continues to decrease thereafter.
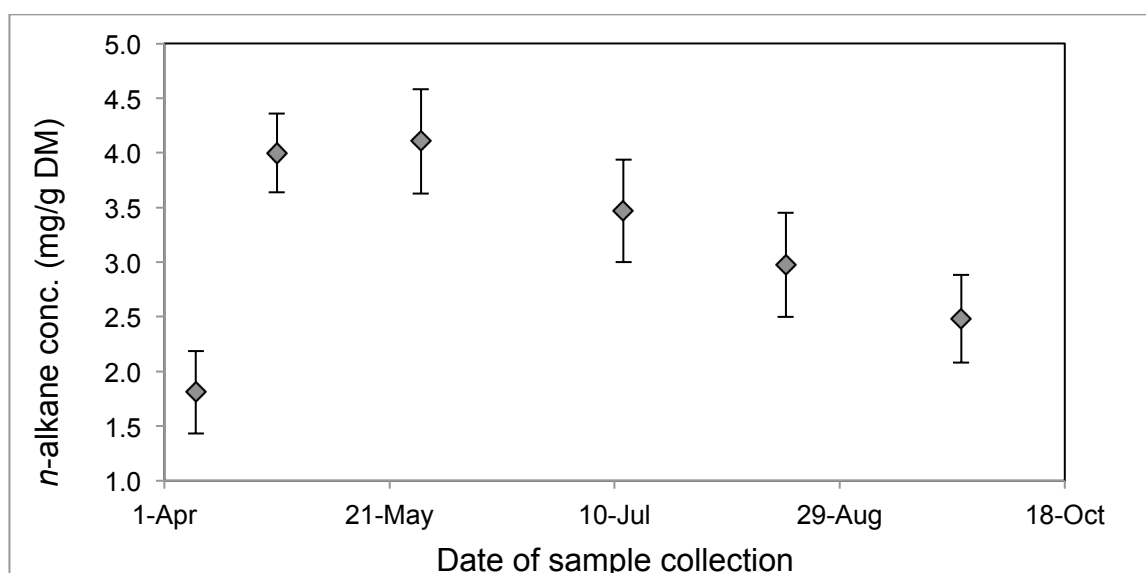
Figure 6.1: The total concetration of *n*-alkanes per mg/g DM for Salix against time in the growth season. Error bars represent SEM n=3 for each sample collection time.

The Average Chain Length (ACL) data of Salix also exhibit change with time in the growth season (figure 6.2), showing increases with time. ACL during the 2-3 weeks of leaf flush in April is relatively low, but very uniform among the three individual Salix trees investigated at 27.4 ± 0.01 (SEM, n=3). ACLs continue to increase gradually with time, and peak at 28.27 ± 0.26 (SEM, n=3) during the end of September.
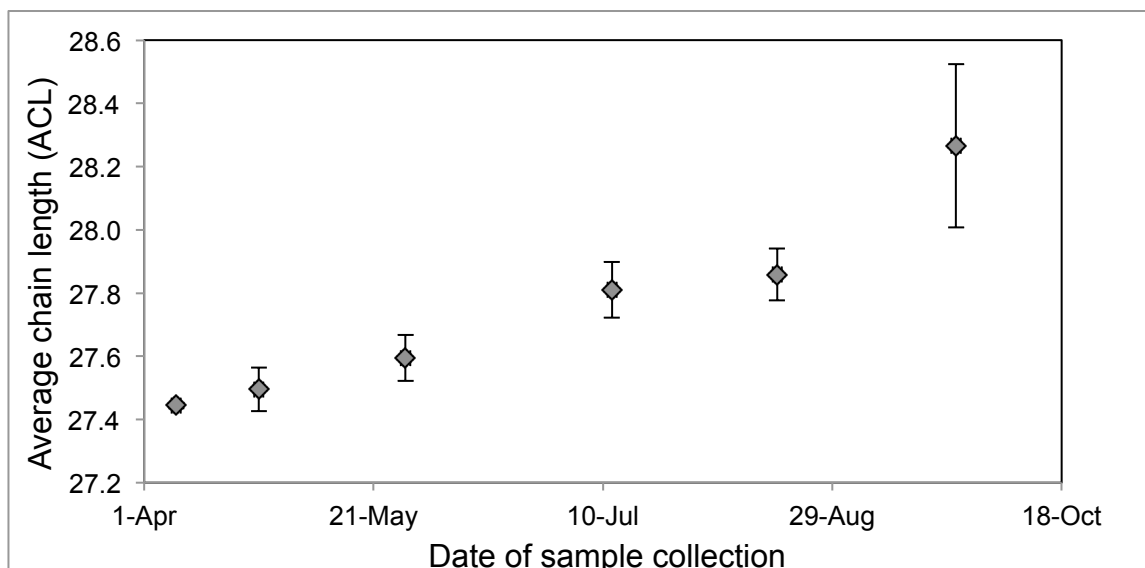
Figure 6.2: Average Chain Length (ACL) against time in the growth season for Salix. Error bars represent SEM, n=3 for each sample collection time.

The Carbon preference Index (CPI) is also relatively low during leaf flush, peaking during May at 27.93 ± 4.52 (SEM, n=3), this is then gradually reduced back down to CPI values similar to those reported during leaf flush of 17.96 ± 2.8 (SEM, n=3) (figure 6.3).
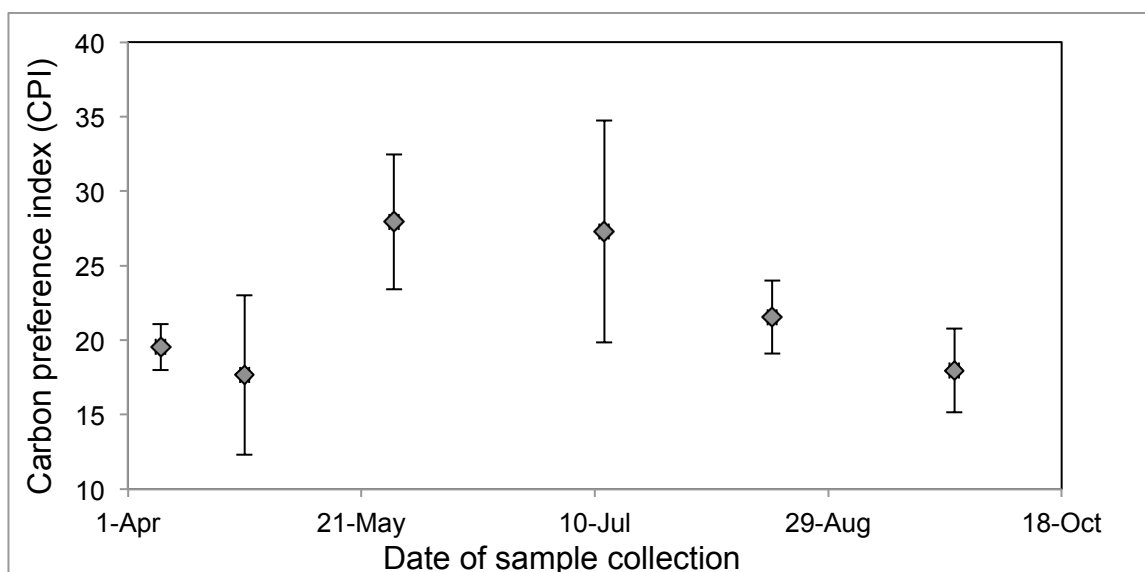
Figure 6.3: Carbon Preference Index (CPI) against time in the growth season for Salix. Error bars represent SEM (n=3) for each sample collection period.

6.4.3. δD values of *n*-alkanes

The nC$_{27}$ and nC$_{29}$ *n*-alkane homologues were the major constituents of the leaf wax *n*-alkanes in the Salix under investigation, with δD measurements possible for both of these *n*-alkane chains during every sample collection over the course of the growing season. However, as is commonplace in compound-specific hydrogen isotopic analysis of *n*-

alkanes, the concentration-weighted mean alkane (CWMA) *δ*D value was calculated using equation 5.1 (chapter 5, section 5.1.4) (figure 6.4).
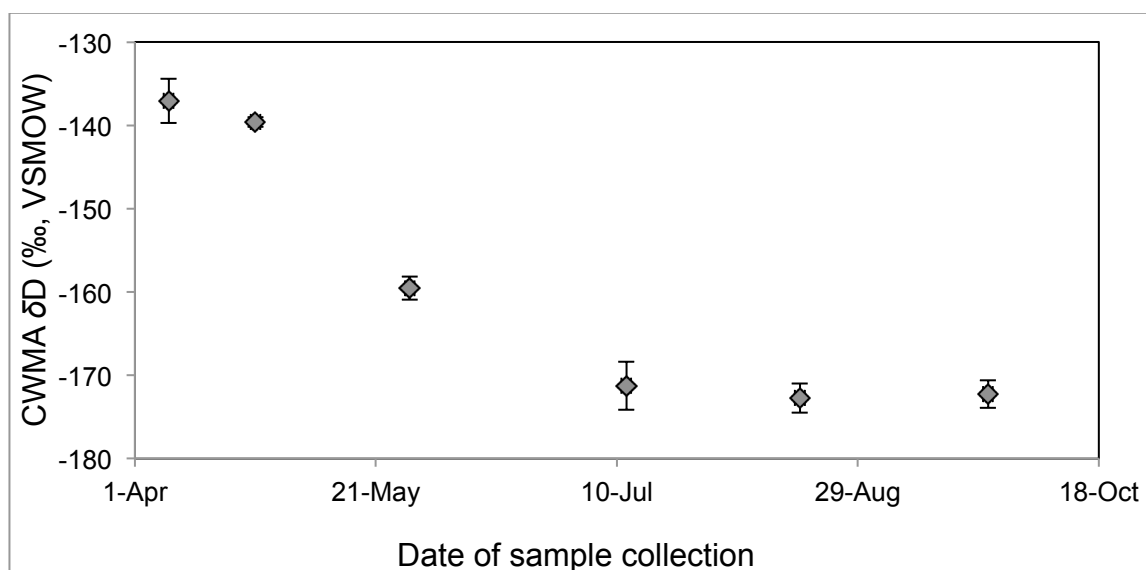
Figure 6.4: Scatter plot showing CWMA hydrogen isotopic data (*δ*D, ‰ VSMOW) against time in the growing season. Error bars depict the standard error of the mean (SEM, N=3).

CWMA *δ*D values exhibit D-enriched compositions during the period of leaf flush in April, with *δ*D values of -137.1± 2.65 ‰ (SEM, n=3) on the 8th of April and -139.6± 0.57 ‰ *δ*D (SEM, n=3) on the 26th of April (figure 6.4). From April to July, the CWMA *δ*D value experiences a D-depletion of ~35 ‰ to -171.3± 2.88 ‰ (SEM, n=3), where the composition remains relatively consistent until leaf senescence.
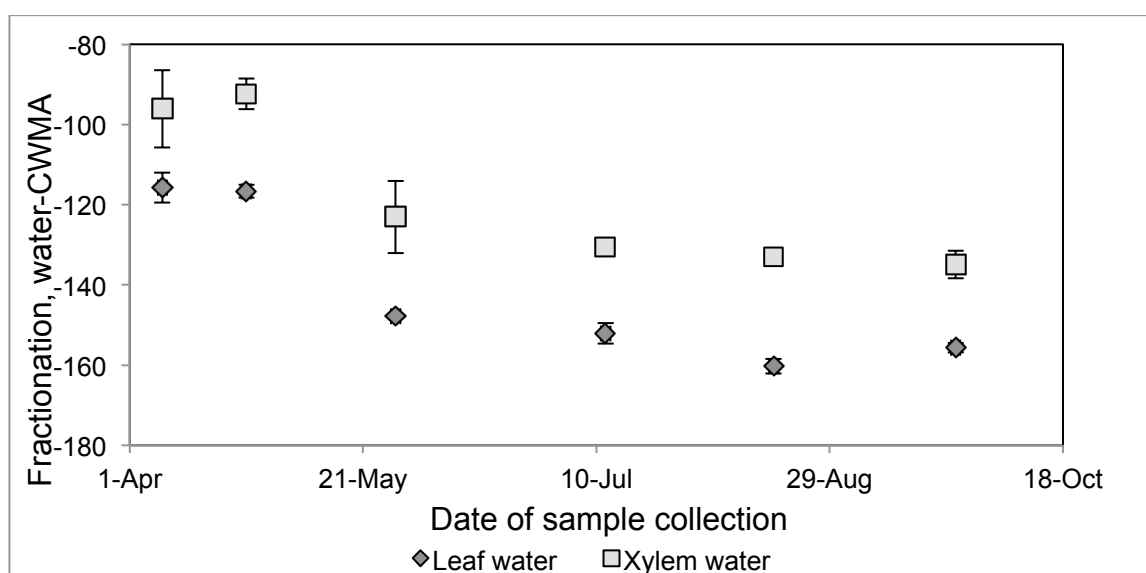
Figure 6.5: Fractionation between CWMA *δ*D data and environmental waters. Dark diamonds represent fractionation between leaf water and CWMA and light grey squared depict apparent fractionation between xylem waters and CWMA. Error bars show standard error of the mean (SEM), n=3.

During the growth season, fractionation of the CWMA *δ*D values above leaf water *δ*D values (ε_{bio}) became increasingly negative by ~50 ‰ from April 8th to September 25th

2012. With the *n*-alkanes during leaf flush exhibiting a small fractionation of -115.75 ± 3.75‰ (SEM, n=3), which peaks during August at -160.25 ± 1.85 ‰ (SEM, n=3).

The apparent fractionation of CWMA *δ*D values above xylem water *δ*D values (ε_{app}) exhibits similar behaviour to the ε_{bio} data. However, and as expected, the values are overall considerably less negative, along with a smaller total range of ~30 ‰ observed throughout the sample period (figure 6.5). A mean ε_{app} of -105.77 ±11.14 ‰ (SEM, n=3) is observed during leaf flush in April, with ε_{app} becoming increasingly negative with time and peaking at -134.94 ±3.45 ‰ (SEM, n=3) immediately prior to leaf senescence at the end of September.
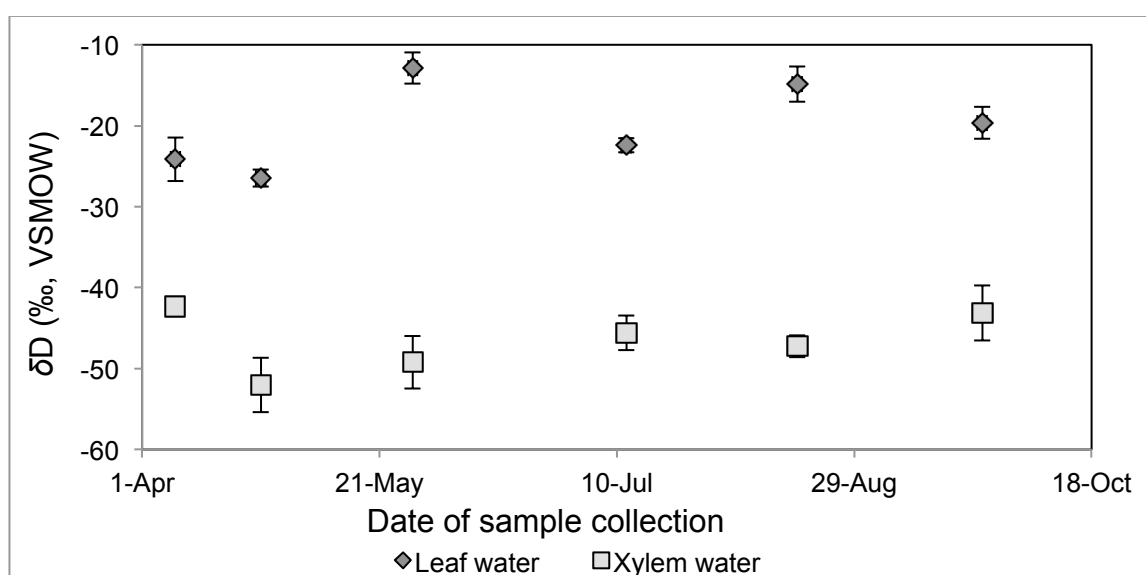
Figure 6.6: The mean leaf water and xylem water *δ*D against time in the growing season 2012. Dark diamonds represent mean leaf water *δ*D and light grey squared depict xylem waters *δ*D. Error bars represent the standard error of the mean (SEM), n=3.

The xylem water and leaf water *δ*D data alone (figure 6.6) does not appear to track the temporal trends observed in CWMA *δ*D values (figure 6.4). Xylem water does not vary by more than ~10 ‰ *δ*D during the whole growth season, while leaf water varies by ~14 ‰ *δ*D. In terms of the isotopes of hydrogen, where the fractionation effects are large (Bigeleisen 1965), these reported variations in leaf water and xylem water *δ*D values are relatively small.

Further to this, the fractionation of leaf water above xylem water (ΔD leaf water) does not display the same temporal trend as the ε_{app} and ε_{bio} data. Where the smallest ΔD leaf water is observed at the beginning of leaf flush (8th of April, figure 6.7), indicating the least amount of evaporative D-enrichment of leaf water above xylem water. ΔD leaf water then peaks on the 28th of May at 41.22± 5.49 ‰ (SEM, n=3), where it does not vary by more than ~10 ‰ until leaf senescence.
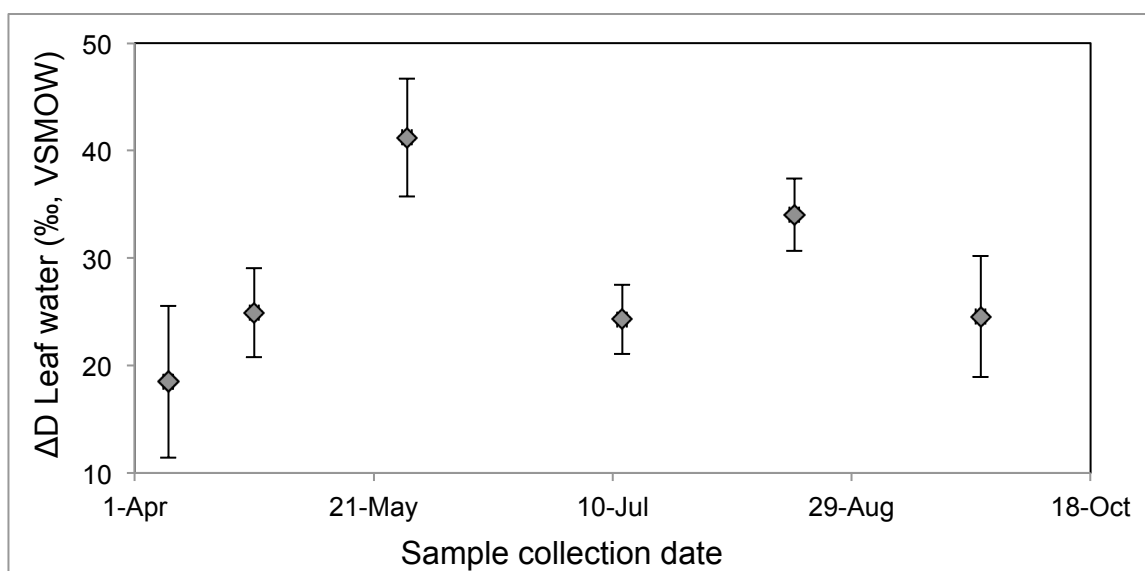
Figure 6.7: Fractionation of leaf water above xylem water ΔD leaf water against time for the 2012-growing season. The error bars show the standard error of the mean (SEM), n=3.

6.4.4. Separations of leaf flush versus rest of the growth season

Upon inspection of the data sets, and in keeping with the hypothesis of significantly different physiological behaviour during leaf flush, the data is separated in two: April leaf flush data and May to September data (representing the remainder of the growth season). From here onward, leaf flush refers to the two sampling periods in April (8/04/12 - 26/04/12), and the remainder of the growth season refers to the four-sample collection periods thereafter (28/05/12 - 25/9/12). One is aware of the potential bias the deliberate separation of data sets in this manner can produce; however, due to the nature of the hypotheses under investigation within the current study, this approach is deemed appropriate.

6.4.4.1. Drivers of *n*-alkane *δ*D values, April versus May-Sept

Simple linear regression analysis, applied to the separated data (figure 6.8), indicate significantly different correlations between CWMA *δ*D values and xylem water *δ*D values between leaf flush and the remainder of the growth season. The simple linear regressions reveal no statistically significant correlation between xylem water *δ*D and CWMA *δ*D during leaf flush. While a strong negative statistically significant correlation is observed between xylem water *δ*D and CWMA *δ*D for the remainder of the growth season with a correlation of y= -0.8706x-210.2 (adjusted R^2= 0.332, F= 5.465, P= 0.0476) (figure 6.8).
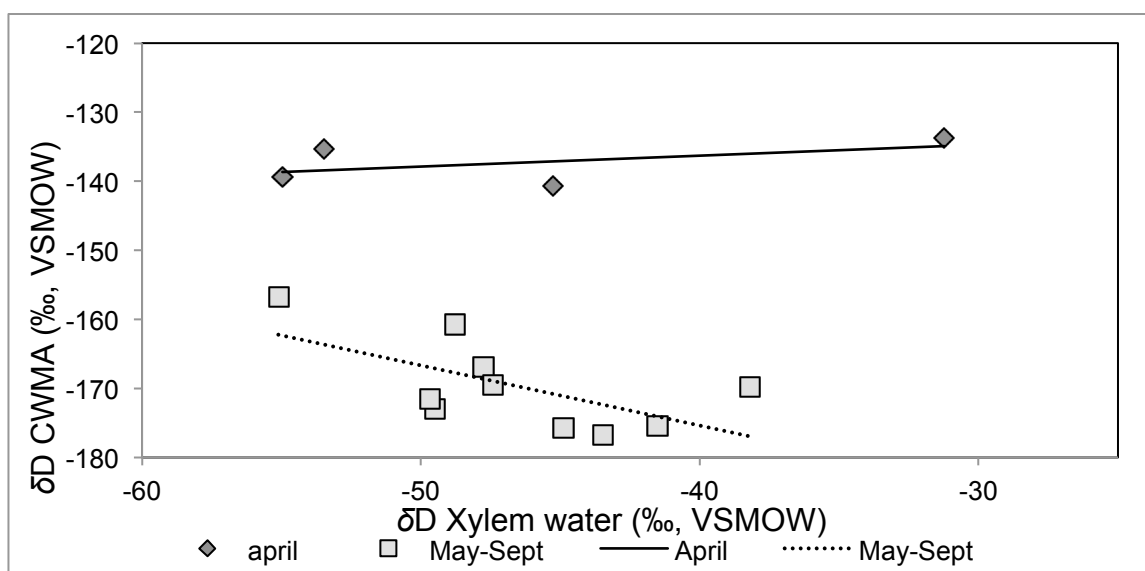
Figure 6.8: Concentration weighted mean n-alkane (CWMA) δD against the δD signal of the corresponding xylem water for leaf flush (dark diamonds, April) and May-September 2012 (Light grey squares). The trend line represents simple linear regressions applied to the data set, where the dark line is April and the dash line the rest of the growth season.

Applications of simple linear regression analysis to leaf water δD versus CWMA δD value for the separated data suggest similar trends, where leaf flush data behaves in a significantly different manner to the rest of the growth season (figure 6.9). No statistically significant correlation is reported for leaf flush between leaf water δD and CWMA δD values. While a different relationship is observed between leaf water δD and CWMA δD values during remainder of the growth season of Y=0.7812x-156 (figure 6.9), however this correlation is not statistically significant to a 95% C.I. (adjusted R^2= 0.2076, F=3.358, P= 0.104).
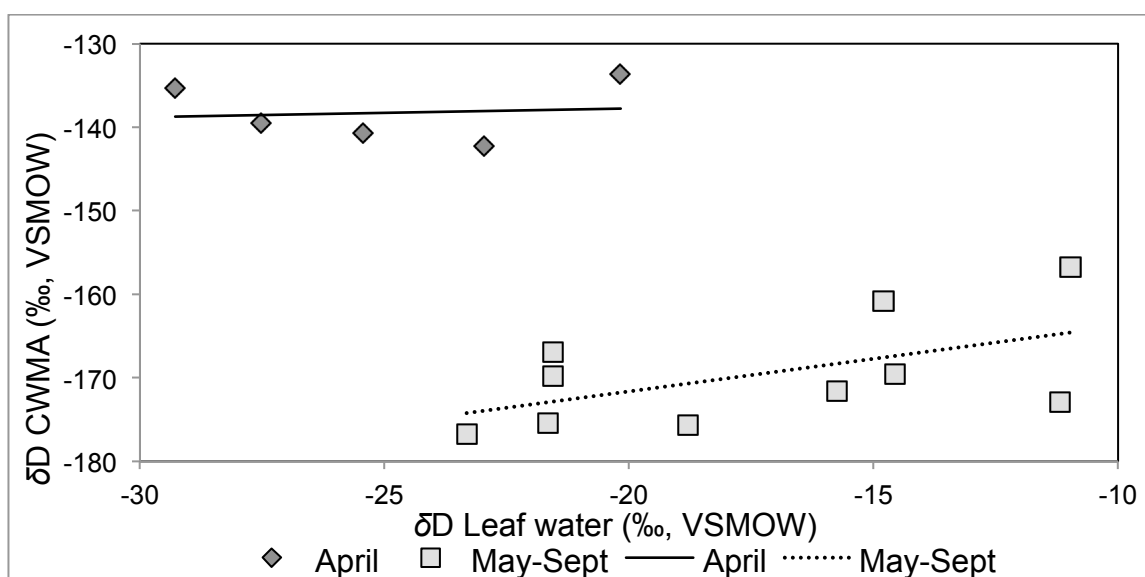
Figure 6.9: Concentration weighted mean n-alkane (CWMA) δD against the δD signal of the corresponding leaf water for leaf flush (dark diamonds, April) and May-September 2012 (Light grey squares). The trend lines represent simple linear regressions applied to the data set, where the dark line depicts April and the dashed the rest of the growth season.

Utilization of the relationship between bulk foliar $\delta^{13}C$ and leaf water $\delta^{18}O$ values shows no statistically significant correlation during leaf flush, with a relationship of y= 0.0485x-29.113 (adjusted R^2= -0.1932, F= 0.1904, P= 0.685). While the remainder of the growth season exhibits a moderate-strong statically significant relationship of y= 0.4927x-33.19 (adjusted R^2= 0.27, F= 5.06, P= 0.048) (figure 6.10).
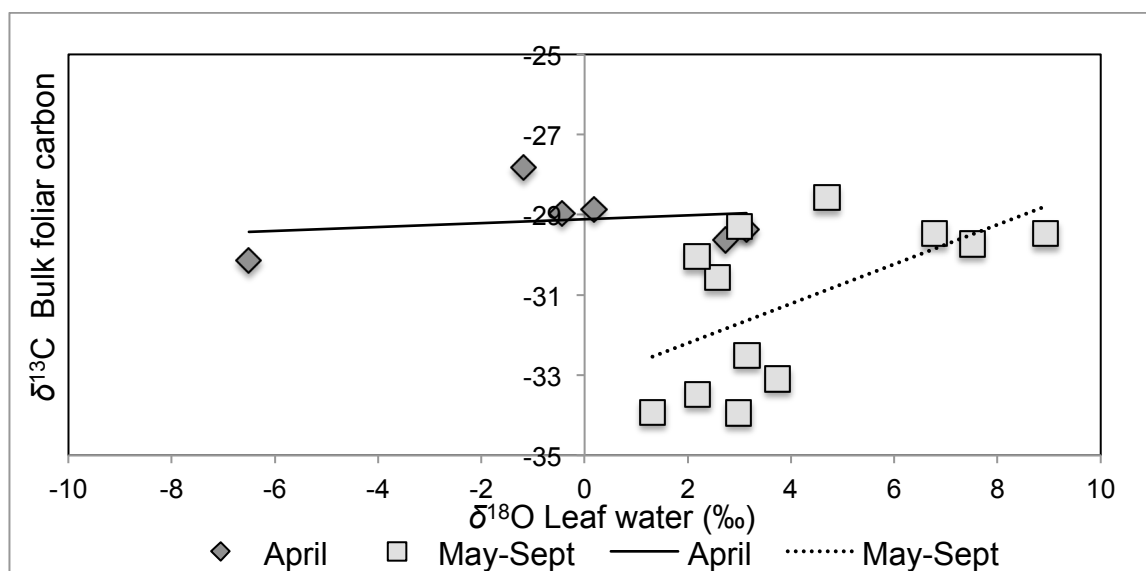
Figure 6.10: Bulk foliar $\delta^{13}C$ versus bulk $\delta^{18}O$ of the corresponding leaf water for the separated data set, dark diamonds depict leaf flush data (April) and light grey squares show the remainder of the growth season data (May – Sept). The trendlines represent simple linear regression, with the black line showing April and the dashed line the rest of the growth season.

Under the Kahmen et al., (2013) conceptual model, ~116% of the current leaf water has contributed to the "biosynthetic water-pool" the leaf flush CWMA were synthesized from, with an estimated ε_{bio} of -121 ‰ (y= 1.1579x-120.65, adjusted R^2= 0.943, F= 66.73,P= 0.00384), with very high statistical significance (figure 6.10). After leaf flush, the conceptual model suggests ~92% of the current leaf water has contributed to the "biosynthetic water pool", with an estimated ε_{bio} of ~-157 ‰ for the period of May to September. This strong positive relationship of adjusted R^2= 0.673, has similarly very high statistical significance (F= 19.529, P= 0.00223).
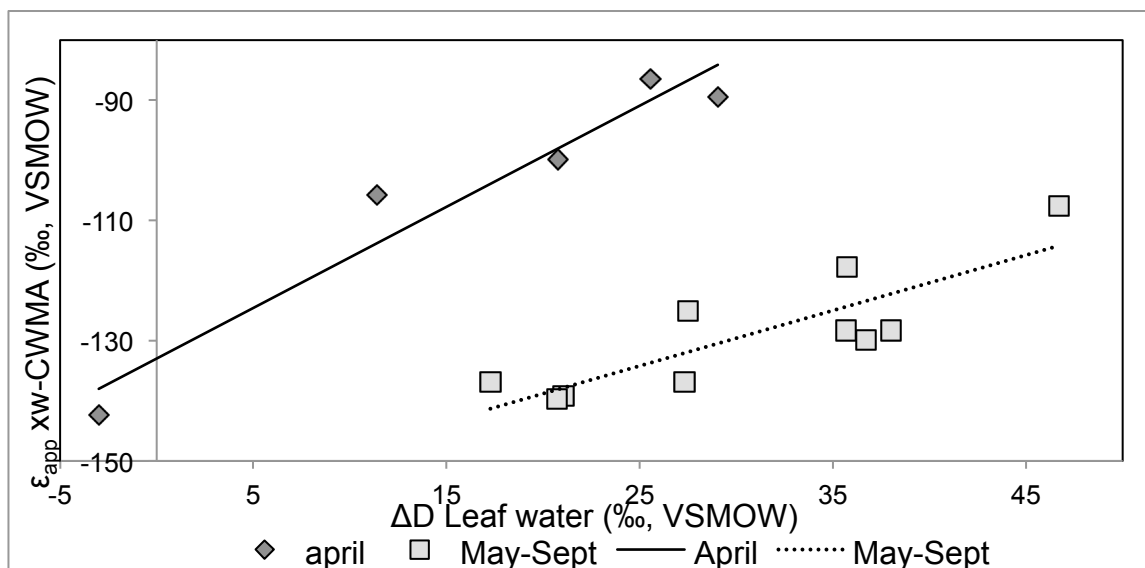
Figure 6.11: The Kahmen et al., (2012a) conceptual model, the fractionation between xylem water and leaf water (ΔD leaf water) against apparent fractionation between xylem water and CWMA (εapp XW-CWMA) through simple linear regression gives an estimation of the percentage contribution of current leaf water to the biosynthetic water pool the CWMA were synthesised from. Dark diamonds show leaf flush data (April) and light grey squares show the remainder of the growth season (May-Sept). The black trend line is the April simple linear regression and the dashed the rest of the growth season.

6.5 Discussion

6.5.1. *n*-alkane molecular data

The total range in the *n*-alkane concentrations of Salix during the course of the 2012 growth season of 1.10-4.92 mg/g DM, is similar to previous reports from other *Salicaceae* species studied (Kahmen 2011). Despite this, the total *n*-alkane concentration is not constant with time during the growth season in Salix, unlike previous reports from the *Salicaceae* family (Kahmen 2011). *n*-alkane concentrations are lowest on the first sample collection date during leaf flush (1.81±0.38 mg/g DM, SEM, n=3, 08/04/12, figure 6.1), when the leaves are only approximately 2cm in length. However, within 18 days total *n*-alkane concentrations are over double this amount at 4.00± 0.36 mg/g DM (SEM, n=3, 26/04/12 figure 6.1). Peak concentrations are observed during May, after which they gradually decrease until senescence. This is consistent with previous observations of deciduous species in natural environments (Sachse 2009) and the data suggests *n*-alkanes are not synthesized after May.

The most common *n*-alkane homologue observed in the current investigation is nC$_{29}$, this is consistent with previous reports for deciduous tree species (Sachse 2009), and for other members of the *Salicaceae* family (Kahmen 2011). However, despite the concentration observations, ACL is shown to increase with time during the growth season (figure 6.2). The ACL data alone would suggest synthesis of longer *n*-alkanes with time in the growth season, which is consistent with previous investigations of deciduous species (Eglinton 1967, Piasentier 2000). However, combination of the total *n*-alkane concentration and ACL data (figure 6.12), which is separated between leaf flush and rest of the growth season, shows a very strong, and very statistically significant, negative correlation between ACL and concentration during May-September (Y= -0.3076x+28.884, adjusted R^2= 0.69, F= 25.95, P=0.0005). These data suggests either the preferential removal of shorter *n*-alkanes with time in the growth season (Gao, Burnier et al. 2012), or lower amounts of longer chained *n*-alkanes are synthesized as the growth season progresses.
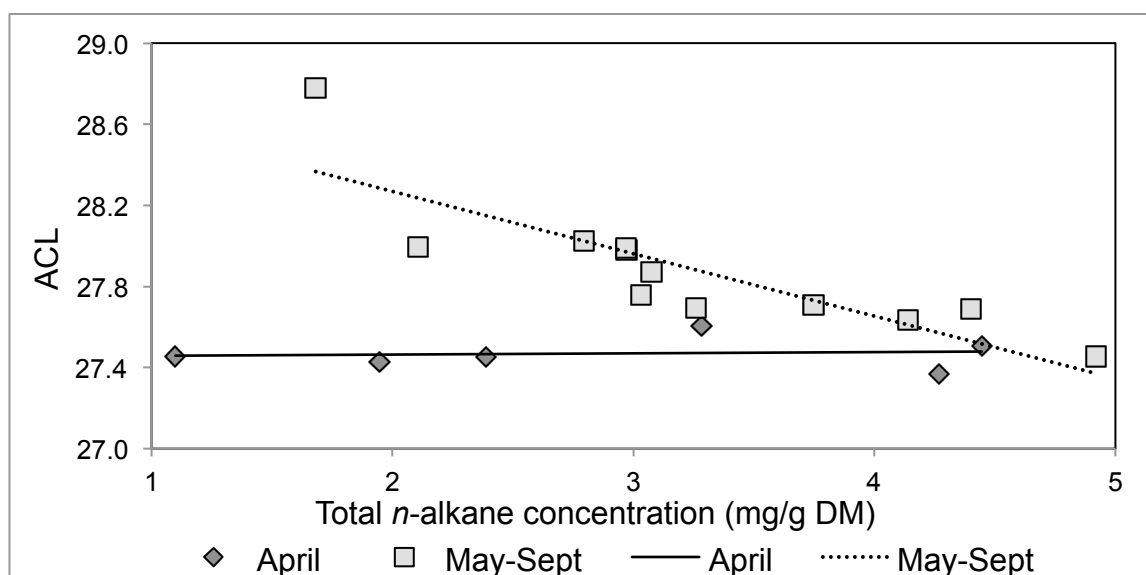
Figure 6.12: ACL against total *n*-alkane concentration (mg/g DM) during leaf flush (April) and the rest of the growing season (May-Sept). Dark diamonds show April leaf flush data while light grey squares show May- Sept data for the rest of the growth season. The trend lines depict simple linear regressions applied to the data sets where the relationship of Y= 0.0061x+27.451, adjusted R^2= -0.24, F=0.04, P= 0.85 is reported for April (black trend line) and Y= -0.3076x+28.884, adjusted R^2= 0.69, F= 25.95, P=0.0005 reported for May-Sept (dashed trend line).

The CPI values observed within the current investigation range 12.29 - 40.83 CPI units, and are within the range of those previously reported for a modern terrestrial tree species (Bi, Sheng et al. 2005). However, the CPI data displays a different temporal trend to both total *n*-alkane concentration and ACL data (figure 6.3). CPI values are lowest on the second sampling date (17.66± 5.37 CPI units, SEM, n=3, 26/04/12), which coincides with a period of rapid increase in *n*-alkane concentration (figure 6.2). This suggests the rapid biosynthesis of *n*-alkane homologues with both even and odd-numbered carbon predominance. CPI values then peak at 27.93± 4.52 (SEM, n=3) during May, as does the total concentration, then gradually decrease again to similar values observed on the second sampling date. As the ACL and total concentration data together suggest *n*-alkanes synthesis decreases after May, and as contamination from plastics and human skin lipids can be ruled out. The data presented here suggests the gradual decrease in CPI value from May to September could be indicative of the degradation of odd-numbered *n*-alkanes by bacteria (Nishimura and Baker 1986, Elias, Simoneit et al. 1997, Sachse, Radke et al. 2004, Wang, Fang et al. 2010) as the leaves begin to senesce towards the end of the growth season.

Unlike recent studies where large variations in *n*-alkane concentrations and ACL were observed over time scales as short as 25 hours (Gao, Burnier et al. 2012, Gao, Tsai et al. 2012). The molecular data within the current investigation suggests the *n*-alkanes in Salix are relatively stable once full leaf expansion is complete (estimated to be late May in Norwich). Despite these findings, molecular and total *n*-alkane concentration data alone

cannot prove either way whether *n*-alkanes are continuously synthesized with time in the growth season (Baker and Hunt 1986, Shepherd and Griffiths 2006).

6.5.2. Compound-specific *δ*D values of *n*-alkanes in Salix

The CWMA *δ*D values in the current investigation show D-depletion in the region of 35 ‰ from the first sample date (08/04/12) to the last (25/09/12) (figure 6.4). However, this observed D-depletion only occurs between the 08/04/12 and the 12/07/12 sample dates, after which the *δ*D value appears to stabilize and does not exhibit significant variation for the rest of the growth season (less than 10‰, figure 6.4). As the sampling and analytical techniques are destructive, and the isotopic effects of hydrogen so large (Bigeleisen, 1965), this variation of less than 10 ‰ indicates relatively stable *δ*D values, as a certain level of variation from one sample to the next in a natural environment is anticipated. This would suggest, unlike the molecular *n*-alkane distributional and total concentration data, that *n*-alkane synthesis decreases around July, rather than May. These results therefore suggest it takes approximately 13 weeks for the *n*-alkane *δ*D values to be "locked in", and in agreement with recent research, deciduous trees exhibit different *n*-alkane molecular and isotopic behaviour during the period leaf flush (Tipple 2013).

The apparent fractionation (ε_{app}) and biosynthetic fractionation (ε_{bio}) data (figure 6.5) also agree with the hypothesis of significantly different physiological behaviour in Salix during leaf flush. As can be seen, both ε_{app} and ε_{bio} show more positive values during the leaf flush period in April, which gradually become more negative until after the 12th of July, when they both stabilize and show less than ~15 ‰ variation. Although these findings do conclude that the *δ*D values of *n*-alkanes are "locked in" after 13 weeks in the Norwich investigated. These results are in stark contrast to previous reports from field grown deciduous *Populus angustifolia* trees, where the *n*-alkanes showed stable *n*-alkane *δ*D values after just a 2 week period of leaf flush (Tipple 2013).

Studies conducted on perennial species have suggested the "locked in" *δ*D values could be more representative of D-enriched metabolic water and/or previously synthesized D-enriched carbohydrate stores (Sachse 2009, Sachse 2010, McInerney 2011, Tipple 2013). While studies conducted on annual plant species suggest that un-enriched xylem water at the base of the expanding leaf may be the predominant hydrogen source for *n*-alkanes synthesized during leaf flush (Sachse 2010, McInerney 2011). Despite this, no study has directly compared the leaf flush D isotopic compositions of annual and perennial

species within a controlled growth experiment environment, this would be a major recommendation for future research.

6.5.3. D-enriched spring *n*-alkanes

D-enriched spring *n*-alkane values are a commonly reported phenomenon (Pedentchouk 2008, Sachse 2009, Tipple 2013), however the cause of this D-enrichment is the subject of much debate. Simple linear regression analysis failed to detect any correlation between CWMA δD and xylem water δD values during the period of leaf flush (figure 6.8). In addition, despite indications that leaf waxes derive from leaf water pools (Kahmen 2011), there is also no correlation observed between leaf water δD and CWMA δD values during leaf flush (figure 6.9).

In both cases, leaf water and xylem water δD values exhibit much greater variation than the CWMA δD values, which during April 2012 do not vary by more than ~10 ‰ δD (figure 6.4). This suggests the isotopic hydrogen source of the *n*-alkanes synthesized during leaf flush is not current leaf waters or current xylem waters. Further to this, the ε_{app} and ε_{bio} data from the period of leaf flush exhibit very positive values in comparison to the rest of the growth season (figure 6.5). Despite this, these values are being driven by the D-enriched *n*-alkanes (figure 6.4), not by D-enriched leaf or xylem waters (figure 6.6).

Although xylem water δD values were not measured prior to leaf flush, xylem water δD values measured at the beginning of leaf flush have δD values that are not significantly D-enriched in comparison to those observed during the rest of the growth season. This is in disagreement with reports of D-enriched xylem waters driving D enriched *n*-alkanes during leaf flush (Tipple 2013). Furthermore, ΔD leaf water does not appear to correlate well with the temporal trends in the CWMA δD values observed during the growing season. Where, the smallest ΔD leaf water is observed during the beginning of leaf flush (8th of April, figure 6.7), indicating the least amount of evaporative D-enrichment of leaf water above xylem water. This also coincides with the most D-enriched CWMA signal (figure 6.4), but the most D-depleted leaf water δD values (figure 6.6). As research suggests *n*-alkanes are synthesized from leaf water (Chikaraishi 2003, Chikaraishi, Naraoka et al. 2004), D-depleted *n*-alkane δD values would be expected at this time. As a result of this, the *n*-alkanes present during April must be synthesized from a different, significantly D-enriched, hydrogen source.

As *n*-alkanes are synthesized via the acetogenic pathway (Eglinton 2008), with a precursor that originates in the carbohydrate metabolism, with NADPH as the major reducing agent (Zhang, Gillespie et al. 2009) (Chapter 5, section 5.5.8), where NADPH can originate from two completely different sources (Sessions 2006, Sachse 2012). Research suggests NADPH sourced directly from current photosynthesis is much more D-depleted in relation to NADPH originating from glucose via the Pentose Phosphate Pathway (PPP) (Luo, Steinberg et al. 1991, Schmidt 2003, Sessions 2006, Sachse 2012). This would then suggest the *n*-alkanes present during April are synthesized from stored assimilates. In addition, further support for the D-enriched stored NADPH origin is demonstrated by applying the Kahmen et al., (2013) conceptual model to the April leaf flush data (figure 6.11, black trend line). Where, this reports a contribution of current leaf water to the "biosynthetic water pool" of 116± 14% (SEM, n=6), along with a considerably positive ε_{bio} estimation of -121± 2.88 ‰ (SEM, n=6). As it is impossible to have a leaf water contribution of more than 100% this, along with the uncharacteristically positive ε_{bio} estimation, points to a substantially D-enriched hydrogen source from which leaf flush *n*-alkanes are synthesized.

Further to this, utilization of the inherent relationship between bulk foliar $\delta^{13}C$ and $\delta^{18}O$ of the associated leaf water (Scheidegger 2000), supports the stored assimilate origin of NADPH during leaf flush. As no correlation between $\delta^{13}C$ and $\delta^{18}O$ values is observed during leaf flush (figure 6.10), where bulk $\delta^{13}C$ is relatively stable, but leaf water $\delta^{18}O$ water variable. This indicates evaporative enrichment of leaf water is occurring, yet a physiological response of the plant is producing a ^{13}C-enriched, and relatively stable, carbon source for the synthesis of the organic material within the leaf (Saurer 1997, Scheidegger 2000). Under this conceptual model, the data suggests the trees are reacting more strongly on the biochemical side of photosynthesis, i.e. there is reduced photosynthetic capacity. Therefore, the trees must be utilizing a different carbon source in the biosynthesis of organic matter, rather than current photosynthates (Barbour and Farquhar 2000, Scheidegger 2000). These findings also indicate that during the period of leaf expansion, the leaves have not reached full metabolic activity (Kahmen 2011, Tipple 2013), and therefore the D-enriched *n*-alkanes must be sourcing their hydrogen from somewhere outside the leaf.

As NADPH used in *n*-alkane biosynthesis, directly sourced from current photosynthesis, is very D-depleted (Luo, Steinberg et al. 1991, Schmidt 2003), while NADPH generated from stored assimilates is much more D-enriched (Schmidt 2003). These results, in combination with the oxygen-carbon isotope conceptual model, suggest a ^{13}C-enriched

organic matter source in conjunction with a significantly D-enriched *n*-alkane source. It would thus appear that *n*-alkanes present during the period of leaf flush are synthesized from stored carbohydrates, which have been generated toward the end of the previous growth season, rather than from current leaf or xylem waters.

This conclusion is in agreement with the findings of chapter 5, and other physiological studies conducted on tree species, where the utilization of previously acquired assimilates for spring growth is a widely accepted concept (Damesin and Lelarge 2003, Niinemets, Sonninen et al. 2004). Nevertheless, due to small sample amounts compound-specific carbon isotopic data for the *n*-alkanes was not obtained, this is a major recommendation for future research. In addition, as the current study was conducted at only one sample height, variations within individuals was not quantified, therefore an in-depth investigation into the δD values of Salix is a significant recommendation for future research.

6.5.4. *n*-alkane *δ*D values after leaf flush

The *n*-alkanes present within the current study appear to stabilize and remain relatively constant from the 12th of July sample period up until leaf senescence (figure 6.4). As total *n*-alkane concentration peaks in May (figure 6.1), but the isotopic hydrogen composition of the *n*-alkanes does not stabilize until July (figure 6.4). This suggests the δD values of current photosynthesis could have been used in the biosynthesis of *n*-alkanes during May and June. This indicates the period immediately after leaf flush is when *n*-alkanes can be affected by climatic variables, rather than the period of leaf flush itself (Tipple 2013). Nevertheless, due to the temporal separation of the sample collection periods, the exact timing and δD signal, which is incorporated in the *n*-alkanes at this time, can only be speculated. Future investigations should focus attention on the transition of *n*-alkane δD values from leaf flush to the "locked in" phase, and whether the hydrogen source and timing of synthesis can be elucidated.

The ε_{app} and ε_{bio} values also display the same trends shown by the *n*-alkane δD data. Where, the values are relatively stable from the 12th of July onward (figure 6.5), with variation of ~11 ‰ and ~15 ‰ respectively, which is in agreement with previous studies (Kahmen 2011, Tipple 2013). However, as mentioned previously, this observation is being driven primarily by the δD values of the CWMAs, rather than the δD values of the leaf water or xylem water. Further to this, after the CWMA δD value stabilizes from July onward, ΔD leaf water values exhibit variation in the range of ~20 ‰. This suggests the *n*-alkanes after July are not influenced by leaf water either. Close inspection of the entire

data set indicates, although the *n*-alkane molecular data suggests synthesis appears to cease after May, the CWMA *δ*D values does not stabilize until July. Furthermore, the May samples exhibit the most D-enriched leaf water of -12.89± 1.91 ‰ *δ*D (SEM, n=3, figure 6.6), as well as the highest ΔD leaf water of 41.22± 5.49 ‰ (SEM, n=3, figure 6.7). However, it is the next sample collection period (July) that then displays the very D-depleted CWMA *δ*D values (figure 6.4). These data indicate that the very D-enriched leaf water observed during May, which has also been indicated as a period of rapid growth due to the doubling of the total *n*-alkane concentration (figure 6.1), is the major contributor to the signals observed in July. Further to this, it is during the same time period that a clear shift in the relationship between bulk foliar $δ^{13}C$ and leaf water $δ^{18}O$ values is observed (figure 6.9). Where, the correlation shifts from no relationship, to a significant moderately positive correlation (adjusted R^2=0.27, F=5.06, P=0.048), which under the carbon versus oxygen isotopic conceptual model, indicates the trees are not water limited and photosynthetic capacity is constant (Saurer 1997, Barbour and Farquhar 2000, Scheidegger 2000). In addition, the bulk foliar $δ^{13}C$ values from May onward show much more ^{13}C-depleted isotopic compositions in agreement with the more D-depleted *n*-alkanes. As a result, these data further support a switch from an isotopically enriched stored organic source, to a much more depleted current photosynthates source.

Application of the Kahmen et al., (2013) conceptual model estimated a current leaf water contribution to the "biosynthetic water pool" of 92± 21 % (SEM, n=10), with an estimated $ε_{bio}$ of -157± 6.7 ‰ (SEM, n=10, figure 6.11). Interestingly, the Kahmen et al., 2013 conceptual model estimation of $ε_{bio}$ is very close to the mean $ε_{bio}$ calculated from the data set after leaf flush of -156± 1.53 ‰ (SEM, n=10). These $ε_{bio}$ values are very close to $ε_{bio}$ estimations reported from other investigations of tree *n*-alkanes (Chikaraishi 2003, Huang, Shuman et al. 2004, Sachse, Radke et al. 2004, Hou 2008, Pedentchouk 2008), and support the validity of this conceptual model in estimating biosynthetic fraction. However, as can be seen from chapter 5, only if *n*-alkane *δ*D values are stable spatially and temporally. Therefore, the findings from the period after leaf flush agree with the previous suggestion of a constant $ε_{bio}$ for individual species (Sessions 1999, Sachse 2012, Kahmen, Hoffmann et al. 2013, Tipple 2013). Despite this, the constant $ε_{bio}$ indicated, appears to be the result of stable *n*-alkane *δ*D values after leaf flush, rather than a completely constant $ε_{bio}$ during the entire life of the leaf. This result will have both positive and negative implications for the application of *n*-alkanes as a paleo-climate proxy; this will be discussed in greater detail in chapter 7.

The results presented here may explain why averaged δD values of *n*-alkanes have a suggested strong positive correlation with mean annual precipitation (MAP) over global scales (Sachse 2012). This is because the vast majority of publications have used single point in time analyses of *n*-alkane δD values, which have not demonstrated the very different physiological behaviour the trees showed during the period of leaf flush. However, the reason the previously reported strong positive linear correlation between MAP δD and *n*-alkane δD becomes much more complex over smaller spatial scales. May be because on an individual tree level, the δD values of xylem water and leaf water may not exert much control over the δD values of *n*-alkanes on a leaf-by-leaf basis. This is clear from the lack of any correlation between xylem and leaf water δD values and *n*-alkane δD values during leaf flush, but also from the lack of a correlation between xylem water and *n*-alkanes during the remainder of the growth season.
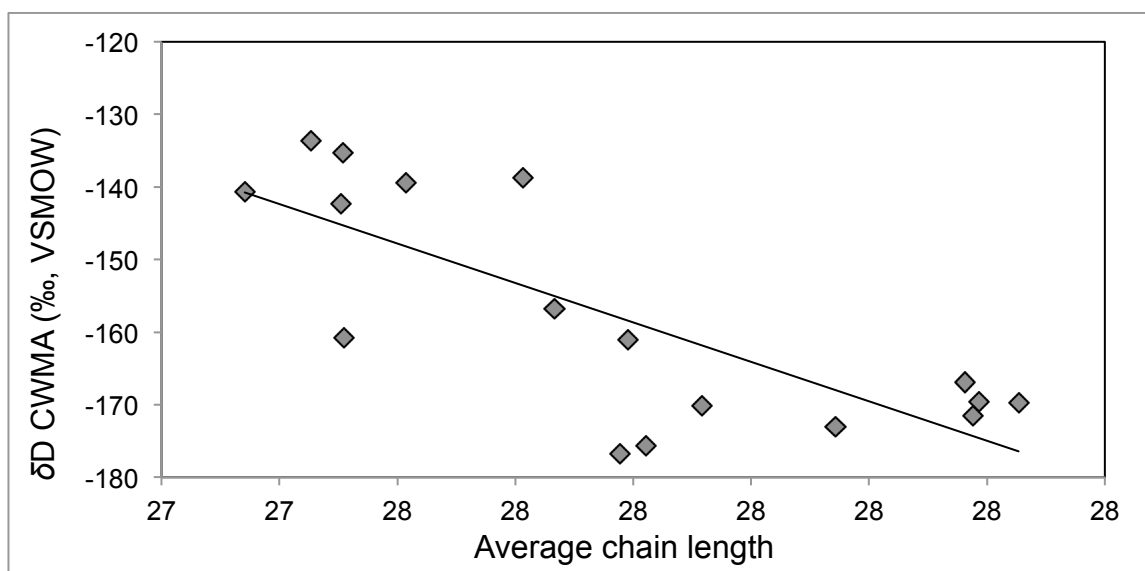
Figure 6.13: Scatter plot of the relationship between the concentration weighted mean *n*-alkane (CWMA) δD and the average chain length (ACL) of the n-alkanes detected within the total data set. Simple linear regression reports a correlation of Y=-54.354x+1346.9, adjusted R^2=0.57, F= 22.24, P= 0.0003.

In addition, a statistically significant negative correlation between xylem water δD and *n*-alkane δD was observed for the remainder of the growth season (figure 6.8). Although this finding is highly controversial, examination of the ACL and *n*-alkane δD values (figure 6.13) has revealed this trend is caused by the increased abundance of longer *n*-alkane chains/ preferential removal of shorter chains. Which through normal biosynthetic fractionation processes are more D-depleted than shorter chains (von Wettstein-Knowles 1995, Post-Beittenmiller 1996, Shepherd and Griffiths 2006, Eglinton 2008).

Further to this, although a positive correlation between leaf water δD and *n*-alkane δD is reported for the remainder of the growth season, this relationship is not statistically significant (figure 6.9). These findings support the hypothesized minimal *n*-alkane re-

synthesis after leaf flush (Kahmen 2011, Gao, Tsai et al. 2012). Despite this, it does introduce significant issues with regard to our current understanding of how much the leaf water D-evaporation signal contributes the *n*-alkane D-signal (Smith and Freeman 2006, Sachse 2012), when *n*-alkanes are synthesized from leaf water, and how often (Feakins 2010).

6.6 Conclusions

1. n-alkane molecular and concentration data show clear variability with time in the growth season, which is in response to the ontogeny of the leaf, as well as removal processes driven by the environment.

2. The δD values of Salix n-alkanes do become "locked in" however, it takes approximately 13 weeks for this to occur.

3. The δD values of the n-alkanes during leaf flush appears to originate from significantly isotopically enriched stored assimilates, while the n-alkanes present after July originate from current photosynthates generated between May and July 2012.

4. Plant physiological behaviour may be a more important factor in determining the isotopic δD values of n-alkanes than source water δD values, this behaviour appears to be both species and ecosystem specific.

7. *n*-alkanes *δ*D values; applications for paleoclimate studies and conclusions

7.1 Part 1: *n*-alkanes *δ*D values; applications for paleoclimate studies

7.1.1 Introduction

The common theme throughout this entire thesis is in investigating the variations in *n*-alkane concentrations, molecular distributions, and compound-specific hydrogen isotopic compositions in modern living trees; then applying this new information to the current accepted interpretations of *n*-alkanes preserved in sediment archives. Since the seminal works detailing the potential of *n*-alkanes as a new paleoclimate proxy (Sessions 1999, Sauer, Eglinton et al. 2001), research within this area has intensified. There are now a plethora of publications utilizing the molecular distributions and *δ*D values of *n*-alkanes to reconstruct a multitude of different environmental characteristics of the past. These include temperature (Schefuß, Schouten et al. 2005, Eglinton 2008, Castañeda, Werne et al. 2009, Zech 2009, Hren 2010), vegetation composition (Schwark, Zink et al. 2002, Jansen, Haussmann et al. 2008, Castañeda, Werne et al. 2009, Russell, McCoy et al. 2009), and even altitude (Jia, Wei et al. 2008, Jahren, Byrne et al. 2009, Polissar, Freeman et al. 2009). This is despite a complete understanding of how important climatic or plant physiological parameters are in influencing *n*-alkane compositions (Sachse 2012).

As mentioned throughout this thesis, the use of the D isotopic compositions of *n*-alkanes as a paleoclimate proxy is based upon several critical assumptions. 1) The compound-specific D isotopic composition of *n*-alkanes synthesized by terrestrial plant species are highly correlated to the study regions meteoric water (Sachse 2012), and 2) the *δ*D values presented by *n*-alkanes within a single site must show little variation (Hou 2007). Most publications to date suggest the *δ*D values of *n*-alkanes generally mirror those expressed by the regions meteoric water and mean annual precipitation (MAP) *δ*D values, with a strong linear positive correlation (chapter 2, figure 2.1) (Sachse 2006, Smith 2006, Eglinton 2008, Hou 2008, Liu and Yang 2008, Rao 2009, Sachse 2012). In addition, the general consensus suggests that the dominant source of *n*-alkanes within sediment

archives can be elucidated from the *n*-alkane chain length distributions, mainly CPI (carbon preference index) and ACL (average chain length) (Seki, Nakatsuka et al. 2010).

However, as has become increasingly apparent as a result of the current investigation, there are significant issues with these assumptions that require urgent investigation if paleo-environmental reconstructions are to be made using *n*-alkanes with any degree of accuracy. Therefore, in this chapter I discuss the general methods used in paleo-environmental reconstructions using *n*-alkanes from sediment archives, and then discuss the results of the data chapters (chapters 3 through 6) in the context of these current accepted hypotheses.

7.1.2 Paleo-climate interpretations to date

After terrestrial higher plant senesce and decomposition, *n*-alkanes may persist in surface soils over relatively large geological timescales (Jansen, Haussmann et al. 2008). Alternatively, depending upon the prevailing climatic and environmental conditions within the area of synthesis, these compounds may be transported, in some cases great distances, as aerosols from vegetation fires, abrasion by wind, or water flow (Bird, Summons et al. 1995, Conte and Weber 2002, Eglinton 2008). Although the exact timescales and mechanisms of how these compounds are transported, and which vegetation types contribute most within a single sediment, are still highly contentious issues (Seki, Nakatsuka et al. 2010), *n*-alkanes may eventually become incorporated into river, lake (lacustrine), peat, or marine sediment archives. Over time these sediments will accumulate and provided there is no geothermal or tectonic disturbances, vast chronological/geological sediment archives can develop (Vogts, Moossen et al. 2009).

The most commonly used application has been measurement of *n*-alkanes extracted from marine (Huang, Dupont et al. 2000, Jeng 2006, Handley, Pearson et al. 2008) or lake sediment cores (Polissar, Freeman et al. 2009, Russell, McCoy et al. 2009, Castañeda and Schouten 2011), however increasing research is being applied to soil surface sediments (Hou 2008, Rao 2009, Seki, Nakatsuka et al. 2010), fossils (Yang 2009, Hren 2010) and peat cores (Seki, Meyers et al. 2009). Nevertheless, in brief, the general method for using *n*-alkanes extracted from sediment archives from marine and lacustrine environments is as follows. A sediment core is collected from a sediment archive of interest, the core is then analysed using radiocarbon dating to establish a chronostratigraphy. Provided time estimations can be placed throughout the core with an associated modest error, a calendar date in years is then estimated (Galy, François et al. 2008, Castañeda, Werne et al. 2009, Seki, Meyers et al. 2009). The core is then cut into

appropriately thick sections depending on the sedimentation rate of the region under study, and any particular time periods the investigator wishes to examine (Eglinton 2008, Zech 2009). The *n*-alkanes are then extracted using similar wet chemistry techniques, and analysed using similar equipment and methodologies, as was used in the current thesis (see chapter 2, sections 2.2.2 and 2.2.3). In some cases, where possible, pollen, leaf fossils or other paleo-botanical indicators are also used to try to identify the major contributors to that sediment archive (Sachse, Radke et al. 2004, Polissar, Freeman et al. 2009, Polissar and Freeman 2010).

Once data has been generated, the molecular chain length distribution data is mainly used to infer the dominant source of *n*-alkanes (Polissar and Freeman 2010, Seki, Nakatsuka et al. 2010), and the level of maturity/petrogenic contamination. For example, as previously discussed, carbon preference index (CPI) values (calculated using equation 2.1 (Allan 1977, Marzi, Torkelson et al. 1993)) are used to determine the OEP (Odd to Even predominance). Where, CPIs greater than 5 indicate significant terrestrial plant contribution (Rielley, Collier et al. 1991, J.I. Hedges 1993, Bi, Sheng et al. 2005, Vogts, Moossen et al. 2009, Vogts, Schefuß et al. 2012), and CPIs less than 3 indicate significant petrogenic/bacterial/algal input (Farrington and Tripp 1977, Nishimura and Baker 1986, Jeng 2006, Eglinton 2008).

Similar principles apply to the use of ACL (average chain length, calculated from equation 2.2 (Poynter 1991)), where the dominant source of *n*-alkanes in the sediment is inferred based upon diagnostic ranges in ACL (Schwark, Zink et al. 2002, Seki, Nakatsuka et al. 2010). As discussed previously, typically ACLs below nC$_{20}$ are indicative of significant bacterial and algal input (Polissar and Freeman 2010), ACLs between nC$_{20}$ and nC$_{23}$ suggest significant submerged aquatic plant input (Ficken, Li et al. 2000, Zech 2009), while nC$_{27}$ to nC$_{29}$ indicate trees and shrubs, and nC$_{31}$ and above suggest grass inputs (Cranwell 1973, Michener and Lajtha 2008, Zech 2009). Aside from this, shifts in ACL have also been linked to shifts in climatic parameters such as aridity, temperature, photosynthetically active radition (PAR) and relative humidity (RH) (Riederer and Schneider 1990, Shepherd, Robertson et al. 1995, Rommerskirchen, Eglinton et al. 2003, Castañeda and Schouten 2011), however these will discussed in more detail in following sections.

As these two descriptive values appear crucial in the interpretation of sediments as a paleo-environmental proxy, it is of crucial importance to investigate whether the signals produced by modern terrestrial vegetation is within the diagnostic values indicated previously, and/or whether they change over time. For example, if a shift of 1.0 ACL with

depth in a sediment core is considered important, it is necessary to determine whether ACLs between and within individuals show less variation than this. Otherwise variation within and/or between individuals will overwhelm signals in sediment archives and may bring the use of CPI and ACL values as a diagnostic tool into dispute.

After *n*-alkane chain length distribution calculations, the compound-specific *δ*D values are used to make quantitative reconstructions of meteoric waters, temperatures, and other environmental aspects. Typically, the most widely reported method of describing the relationship between source waters and *n*-alkanes, in both paleoclimate and plant physiological studies, is to calculate the mean fractionation of *n*-alkanes above current MAP *δ*D values (apparent fractionation, ε_{app}). This is usually calculated for the dominant plant species near the region of sedimentation, estimated from previous studies (Sachse, Radke et al. 2004, Sachse 2006, Yang 2009), or determined as a minimum ε_{app} from living counterparts of those identified in paleo-botanical analyses (Polissar, Freeman et al. 2009, Polissar and Freeman 2010). ε_{app} is then assumed as constant (Tierney, Russell et al. 2008, Polissar, Freeman et al. 2009, Hren 2010, Castañeda and Schouten 2011), and the value of this is used to provide an estimate of the regions ancient meteoric water hydrogen isotopic composition, during which the *n*-alkanes preserved where synthesized (Castañeda and Schouten 2011).

In principle, this method should give a good estimate of ancient precipitation isotopic composition from which temperature, latitude, aridity, RH, and other environmental characteristics can be reconstructed (Eglinton 2008, Rao 2009, Castañeda and Schouten 2011, Sachse 2012). However, the entire premise of this approach is based on the tight correlations between MAP and *n*-alkane *δ*D values (Sachse 2012), and the little variation in *n*-alkanes *δ*D values within a single site (i.e. fractionations are constant) (Hou 2007, Castañeda and Schouten 2011). It is becoming increasingly evident that despite the vast amount of literature already available, were different aspects of paleo-environmental characteristics have been reconstructed, *n*-alkane *δ*D values can be highly variable at a single site (Chikaraishi 2003), and ε_{app} is certainly not constant across all plant species (Chikaraishi 2003, Liu, Yang et al. 2006, Smith 2006, Liu and Yang 2008, Feakins 2010, Sachse 2012) as previously thought. The current problem is identifying how much ε_{app} can vary, and ascertaining what is driving the observed variations in similar plant types. Therefore, if the *δ*D values of *n*-alkanes exhibit significant variation for a single species, at a single site, and ε_{app} is neither constant nor easily explained, this could cause significant problems for the use of *n*-alkane *δ*D values as a paleo-climate proxy.

7.1.3 Implications of the current study's molecular results for future paleoclimate research

7.1.3.1 Total *n*-alkane abundances

The results of the current study have provided some interesting insights into *n*-alkane concentrations and molecular characteristics in Scots pine (*Pinus sylvestris*), which may have significant implications for paleoclimate research. However, the Salix investigation conducted at UEA in Norwich did not produce any findings relating to total *n*-alkane abundances that were unexpected in a deciduous species with time during the growing season.

The total *n*-alkane concentration data from Finnish Scots pine during September is in contrast to previous research conducted on evergreen Coniferous species, and Scots pine as a species itself. As detailed in chapter 3 sections 3.4.1 and 3.5.1, Finnish Scots pine contain a total mean *n*-alkane concentration of 25.14 ± 4.58 µg/g DM (SEM, n=28), with a maximum measured concentration of 76.76 µg/g DM during September 2010. This finding suggests Finnish Scots pine contain appreciable concentrations of *n*-alkanes within their epicuticular leaf waxes towards the end of the growing season. However, this trend cannot be seen within the epicuticular leaf waxes of the Scots pine analysed in Scotland.

The discrepancy between the findings of the current thesis and those of previous studies on evergreen conifer species is attributed to the extremely harsh climatic regime of the Finnish forest site, in conjunction with the timing of sample collection. As discussed in previous sections, one study investigating the *n*-alkane concentrations of Scots pine inhabiting Siberia, where climate conditions are very similar to study site in Finland, suggest Scots pine contains very low total concentrations of *n*-alkanes within its leaf waxes (Tarasov, Müller et al. 2013). However as discussed, the Tarasov et al., (2013) investigation collected material for analysis during the summer, which as was demonstrated in the current study, is the period during the growth season when Scots pine contain low total *n*-alkane concentrations. In addition, as the needles of Scots pine in Värriö Strict Nature Reserve demonstrated up to 8 years retention, when compared to the maximum observation of 3-4 in the Black Wood of Rannoch. The higher *n*-alkane abundances in Finland are consistent with the theory of higher total *n*-alkane abundances in linger lived leaves (Diefendorf, Freeman et al. 2011).

Even though finding appreciable concentrations of *n*-alkanes within the epicuticular leaf waxes of an evergreen conifer species is a result of high importance. The significant

variation observed in total *n*-alkane concentrations within and between individuals of the same species, sampled at the same time, is also of high importance. These results suggest, as previously indicated, *n*-alkanes can be dynamic (Gao, Burnier et al. 2012, Gao, Tsai et al. 2012), and may be continuously synthesised over the course of the growing season in response to natural environmental cues. This is in agreement with previous research in controlled growth experiments (Gao, Burnier et al. 2012, Gao, Tsai et al. 2012), as well as field investigations (Pedentchouk 2008, Sachse 2009). These findings therefore suggest that *n*-alkane synthesis and total abundances are ecosystem specific and not species specific.

7.1.3.2 Average Chain Length

Although the Finnish total *n*-alkane abundance data from September may not seem a significant issue for paleoclimate reconstructions, the Average Chain Length (ACL) molecular distributional data could cause significant issues in two different ways.

Firstly, the ACL data observed in Scots pine from the current study demonstrates uncharacteristic ACLs for a tree species (see figure 7.1). As is discussed throughout the current thesis, ACLs are commonly used as a diagnostic tool to make inferences regarding the original source of *n*-alkanes input into the sediment record (Seki, Nakatsuka et al. 2010). Furthermore, as demonstrated in figure 7.1, both the Scottish and Finnish Scots pine studied exhibit a wide range in ACLs. However, the ACLs produced, if detected in a sediment archive, would suggest significant input from either aquatic plants (Ficken, Li et al. 2000, Zech 2009) or sphagnum moss species (Pancost, Baas et al. 2002, Bush and McInerney 2013). The suggestion ACLs may not be a good diagnostic tool of *n*-alkane source has been highlighted by recent publications (Castañeda and Schouten 2011, Bush and McInerney 2013), where it is suggested that the original basis of using ACLs as a diagnostic tool for characterising *n*-alkane source is based on few original studies. Further to this, several studies have come light where plant species studied exhibited ACLs outside their diagnostic range (Castañeda and Schouten 2011). For example *Betula*, a deciduous tree species, was found to contain high concentrations of nC$_{23}$ (Sachse 2006), while certain species of algae have been reported to produce long chain *n*-alkanes (Lichtfouse, Derenne et al. 1994). The Salix study however, indicates that this deciduous angiosperm species still falls within its diagnostic ACL range (figure 7.1), with nC$_{29}$ as the most common *n*-alkane homologue.
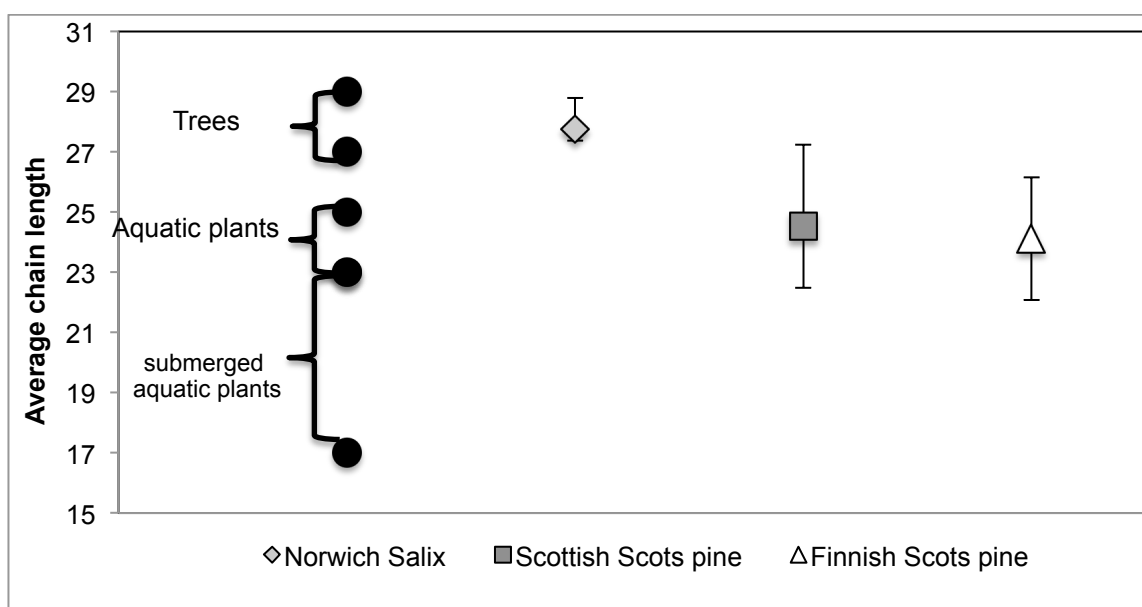
Figure 7.1: Comparison of the average chain length (ACL) data from Scots pine studied in Finland and Scotland, and Salix studied in Norwich, to the accepted diagnostic ranges in ACL applied to interpret *n*-alkane source in studies from sediment archives.

The second issue with regard to the Scots pine ACL data is the significant variations observed in the ACL data within and between individuals sampled at the same site. In an area of research where shifts in ACL of ~0.5 are considered significant (Vogts, Moossen et al. 2009, Gao, Burnier et al. 2012, Vogts, Schefuß et al. 2012), the total range of 5.15 ACLs observed in the current study, for the same species of tree, is quite dramatic. Shifts in ACL of this magnitude have been previously documented (Bi, Sheng et al. 2005, Sachse 2006) and attributed to either latitude, with lower latitudes associated with higher ACLs (Poynter, Farrimond et al. 1989, Poynter 1991, Jeng 2006), or differences in plant type (Cranwell 1973, Ficken, Li et al. 2000, Zech 2009). However, a variation of 3.44 ACL is observed at different heights and aspects in the crown of the same individual tree, sampled at the same time, in the same geographical location (VLT Finland, September appendix Table1). This is a greater variation than those commonly observed in paleoclimate studies. This finding alone is highly significant as it shows how extensive the variation in ACL can be within a single individual. Furthermore, this is particularly significant when vegetation type, which has long been suggested as the greatest influence on ACLs (Cranwell 1973), is the same. Moreover, these variations are occurring when differences in species, water availability, nutrient status, and genetics are completely removed.

This finding is also in contrast to recent reports that suggest *n*-alkanes do not significantly vary within individual trees as a result of canopy position (Bush and McInerney 2013). However, as the current study is the first to investigate variation in ACLs over height gradients of up to almost 20m in natural field conditions, while others have examined

variation over only a few meters (Hou 2007, Bush and McInerney 2013); a discrepancy between the findings presented here, and that of other studies, could be expected.

The data presented in chapter 3 also suggests different sample position parameters can affect different aspects of *n*-alkane molecular composition in different ways, at different times in the growth season. This is in contrast to suggestions from recent research, where *n*-alkane abundance and composition was indicated to be consistent in different crown positions of individual large trees (Bush and McInerney 2013). Further to this, the significant variations observed in ACL, as a result of sample collection height in Finnish Scots pine during September, support the hypothesis that ACLs can be influenced by climatic factors.

As ACLs within the current study significantly positively correlate with height of sample collection, this suggests longer chain lengths are synthesized in response to increasing PAR and temperatures, which is in agreement other studies (Poynter, Farrimond et al. 1989, Eglinton 2008, Castañeda, Werne et al. 2009, Vogts, Schefuß et al. 2012). However, as this shift occurs within a single species, it will make it difficult to ascertain whether a dramatic shift in ACL within a sediment archive is the result of a change in climate, a change in species, or a change in which part of a tree has input most to sediments. Therefore, the data presented within the current thesis suggests the natural heterogeneity observed in ACLs within a single species (5.15 ACLs), and even as a single individual (3.44 ACLs), is far too high to reliably use ACLs as a diagnostic tool of changes in either vegetation type or climate.

7.1.3.3 Carbon Preference Index

The Carbon Preference Index (CPI) data from the Salix study conducted at UEA did not present any findings that were unexpected from a deciduous angiosperm species. However, the CPI data from Scots pine has produced results that may have significant impacts for the use of CPIs in paleoclimate reconstructions.

As can be seen in figure 7.2, Scots pine from both Scotland and Finland exhibit CPI values which are below the diagnostic thresholds for significant marine organism and/or petrogenic contamination (less than 3) (Farrington and Tripp 1977, Nishimura and Baker 1986, Elias, Simoneit et al. 1997, Jeng 2006, Eglinton 2008). The total range of CPI values observed for Scots pine in both locations of 0.35 – 6.32 is very low, and as contamination is ruled out, this data therefore indicates high abundances of even *n*-alkanes within the epicuticular leaf waxes of Scots pine as a species. This finding is not

entirely novel as *n*-alkanes extracted from *Pinus strobes* and *P. taeda* species showed highly variable *n*-alkane compositions, displaying both odd and even *n*-alkane chains, within their leaf waxes (Tipple 2012). In addition, Serbian spruce (*Picea omorika*) has also shown uncharacteristically low CPI values for terrestrial vegetation, with a range of 0.34 - 4.78 and a mean of 2.48, with significant contributions from nC$_{26}$, nC$_{28}$, and nC$_{30}$ (Nikolic, Tesevic et al. 2009), in agreement with the data presented here.
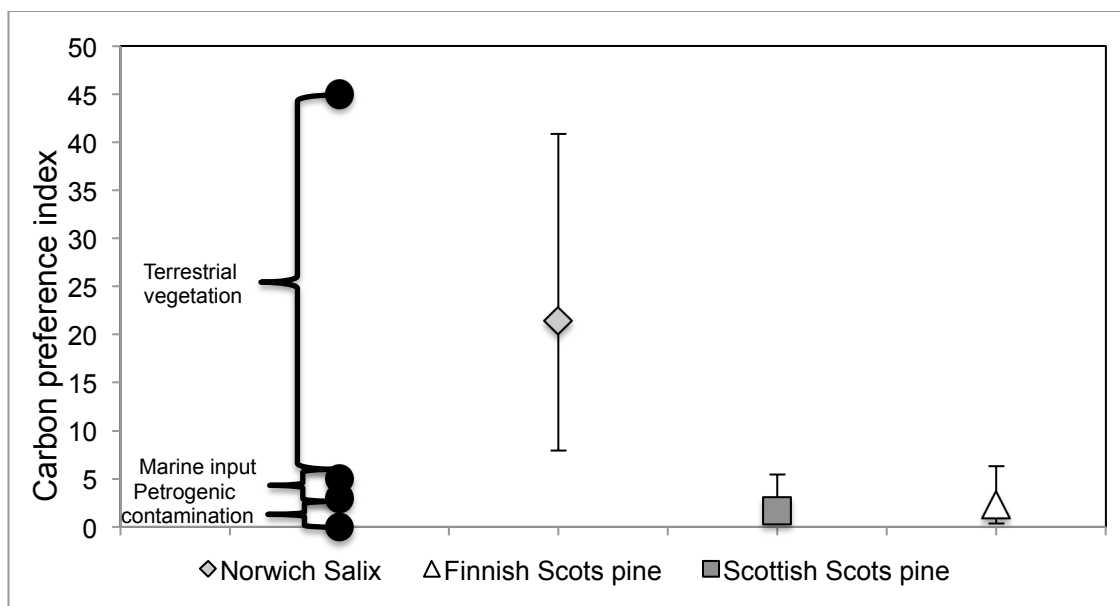
Figure 7.2: Comparison of the Carbon Preference Index (CPI) data from Scots pine studied in Finland and Scotland and Salix studied in Norwich to the accepted diagnostic ranges in CPI applied to interpret n-alkane source in n-alkane studies from sediment archives.

All this evidence suggests evergreen conifer species may synthesize different distributions of *n*-alkanes to deciduous species, with high abundances of even chain length *n*-alkanes as a large component of their waxes. This poses a significant problem for paleo-climate reconstructions because even numbered *n*-alkanes have been detected in appreciable amounts in both lacustrine (Sachse, Radke et al. 2004, Wang, Fang et al. 2010, Tarasov, Müller et al. 2013) and marine (Nishimura and Baker 1986, Elias, Simoneit et al. 1997) sediment archives globally. Within these studies, the predominance of even *n*-alkanes in sediments has been attributed to algal inputs and/or bacterial degradation, which as is demonstrated here, may not always be the case.

In addition to the uncharacteristically low CPI values demonstrated by Scots pine, significant variations in CPI within and between individuals were detected. CPI showed significant variations as a result of height of sample collection, tree size/age, and aspect, at different times in the Finnish growing season. Attempting to correlate CPIs to changes in climatic factors as a result of biosynthesis is a new concept, as most studies link changes in CPI to changes in climate-linked degradation (Rao 2009, Vogts, Schefuß et al. 2012). Although the current study could not draw any concrete conclusions on which

climatic parameters appear to influence CPIs the most. The findings point to a strong influence of PAR levels, with CPIs positively significantly correlating with increasing sample collection height during the 24-hour photoperiod in Finland.

7.1.3.4 Molecular distribution summary

The *n*-alkane total abundance and molecular distributions data presented for the deciduous angiosperm Salix trees studied did not produce results that were unexpected, or in contrast to previous publications. However, it should be highlighted that this study was not concerned within variation within large individuals, a study of this nature is strongly recommended for future research. However, in contrast to this, the data from studies conducted on Scots pine have produced results that are contradictory to previous publications.

The total *n*-alkane abundance, ACL and CPI data from Scots pine suggests that all three of these *n*-alkane molecular characteristics can significantly vary within, and between, different individuals of the same species, sampled at the same time, in the same location. The strong positive correlations between height of sample collection and CPI, ACL, and *n*-alkane abundance, at different times during the Finnish growth season, suggest PAR levels could have a significant influence on the molecular compositions of *n*-alkanes in leaf waxes; a climatic parameter which plant physiological studies have already linked to the *de novo* synthesis of leaf wax lipids (Shepherd and Griffiths 2006). Furthermore, the overall variation observed in ACLs within this single species is much larger than ACLs commonly reported within sediment archives. It is therefore strongly suggested that ACLs are not used a diagnostic tool to identify *n*-alkane source until further investigations can ascertain if this is species-specific, or common among all plants. Finally, even though recent research has suggested that a CPI threshold of 2 could be used to separate petrogenic contamination from terrestrial plant input (Bush and McInerney 2013), the current thesis demonstrates even this threshold is not appropriate, and CPIs should not be applied.

7.1.4 Implications of the current study's *n*-alkane *δ*D results for future paleoclimate research

As is detailed extensively throughout this thesis, to use *n*-alkanes reliably as a paleo-environmental proxy, the *δ*D values of *n*-alkanes must record the region of synthesis' meteoric water with high fidelity, and the variation at a single site must be small. However, as is demonstrated in the three different sampling locations studied in the current thesis,

n-alkane *δ*D values do not reflect source water *δ*D values at each of the individual sites studied (figures 7.4 and 7.5). In addition significant levels of variation in *δ*D values of *n*-alkanes have been demonstrated within and between individual trees, as well as temporally and geographically.

7.1.4.1 Variations in *n*-alkane *δ*D values

Although the Scottish Scots pine investigation did not reveal any noteworthy information due to the lack of *n*-alkanes within their epicuticular leaf waxes. The Norwich Salix and Finnish Scots pine studies have provided useful insights into the temporal behaviour of the trees studied in these locations.

Recent research suggests the *n*-alkanes of deciduous angiosperm species are "locked in" once the period of leaf expansion has ceased (Kahmen 2011, Tipple 2013). However, the Salix temporal study, detailed in chapter 6, demonstrates that it took approximately 13 weeks for the *δ*D values of the *n*-alkanes to become "locked in". In addition, the *n*-alkanes of Finnish Scots pine exhibited a statistically significant D-depletion in mean *n*-alkane *δ*D values of ~40 ‰ between July and September, also demonstrating the *n*-alkanes are not "locked in" after leaf flush. The breakdown of these results, from both locations, discussed in more detail in following sections, also has significant connotations for the use of *n*-alkanes as a paleoclimate proxy.

Schefuß et al. (2005) used a ~20 ‰ D-enrichment of nC$_{29}$ in marine sediments to infer a period of greater aridity in equatorial Africa during the Younger Dryas. Yet the current study has shown the Odd-CWMA *δ*D values of *n*-alkanes sampled from Finnish Scots pine vary by ~70 ‰ *δ*D, and by ~40‰ *δ*D in Salix over the course of a growing season in Norwich. This presents a significant problem for paleo-environmental reconstructions as the level of variation reported at individual locations, within the same species, is greater than which is often used to infer shifts in climate within sediment archives (e.g. Schefuß et al. (2005) used a ~20‰ *δ*D shift).

Further to this, when the total range in *n*-alkane *δ*D values, from the three sample locations, is compared (figure 7.3), their *δ*D values overlap. What is of even greater concern is the total mean *n*-alkane *δ*D values of the Finnish Scots pine and Norwich Salix are very similar; sub-arctic Finnish Lapland and Norwich, Norfolk, UK, have significantly different climate regimes.
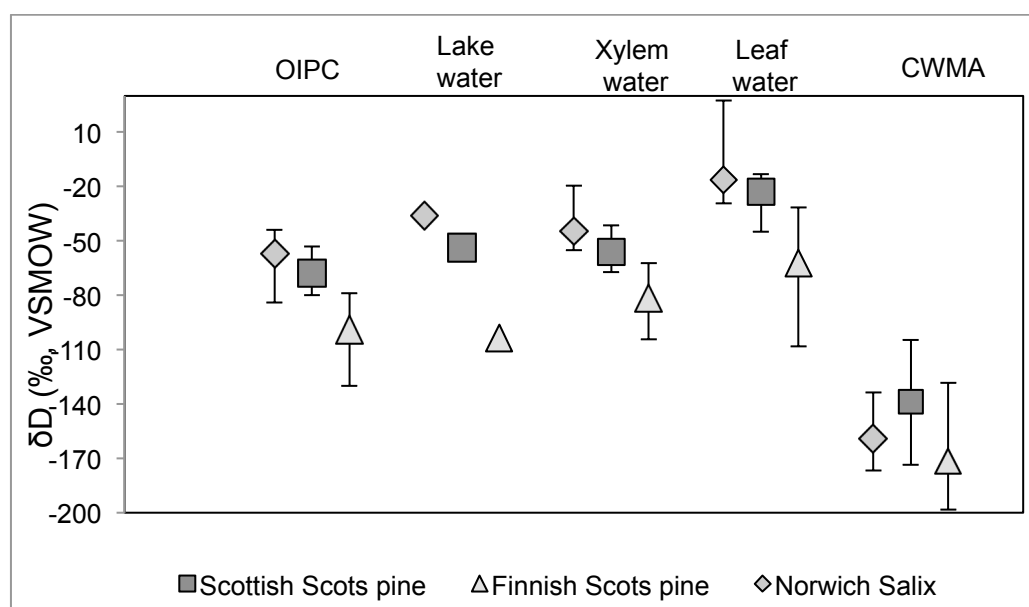
Figure 7.3: Comparisons of the total ranges in *δ*D compositions of OIPC estimated precipitation, measured lake water, xylem water and leaf water and how these relate to the total ranges observed in CWMA *δ*D compositions for the three different sites investigated.

Some could argue that the apparent fractionation factors (ε_{app}), which are applied to a respective sedimentary archive, would eliminate the problem of overlapping *n*-alkane *δ*D values. However, as is demonstrated in figure 7.4, all three sites also overlap in their respective total ε_{app} ranges.
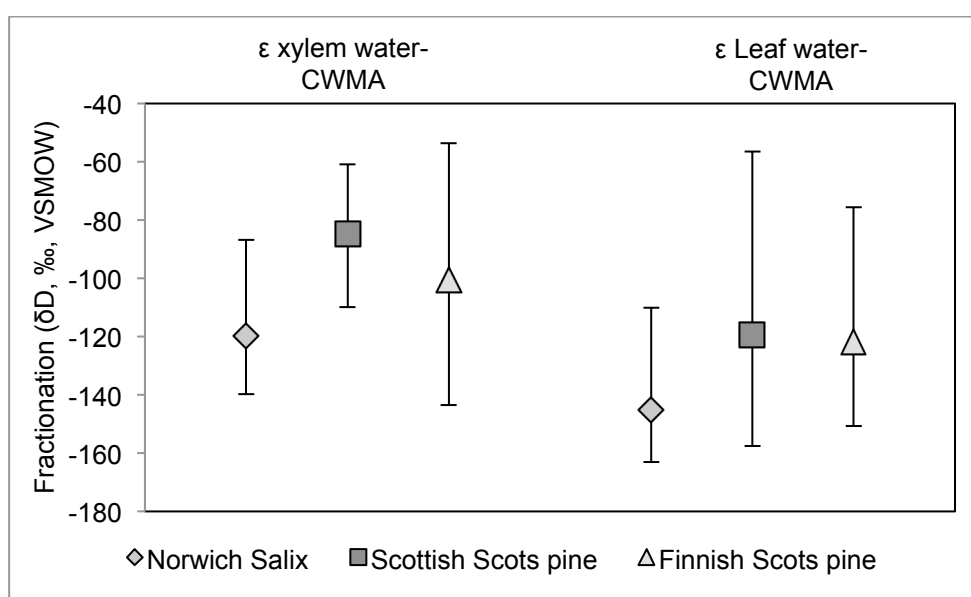
Figure 7.4: Comparisons of the total ranges in fractionation of CWMA above xylem water and CWMA above leaf water for the three different sites investigated.

Moreover, seeing as the consensus from the available literature points to a strong positive linear correlation between *n*-alkane *δ*D values and source water *δ*D values (Sachse 2006, Eglinton 2008, Hou 2008, Liu and Yang 2008, Rao 2009, Sachse 2012), as is demonstrated from figure 7.5 and 7.6, xylem water *δ*D values exert little control over the *δ*D values of *n*-alkanes in the current study.
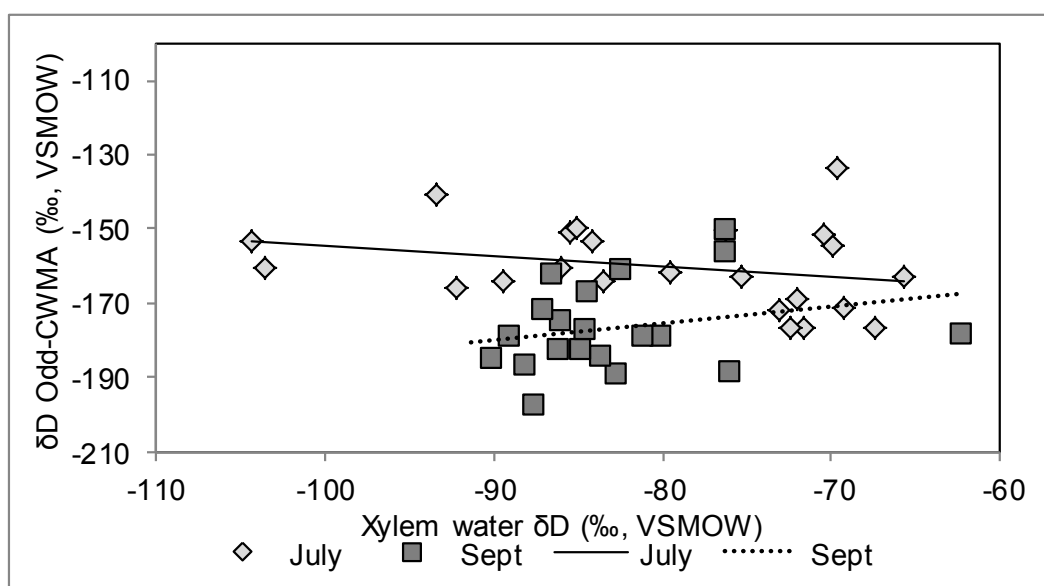
Figure 7.5: Simple linear regression analyses of Odd-CWMA δD composition versus xylem water δD composition during July and September in Finnish Lapland, light diamonds are July, dark squares are September. July: Y=-0.2794x-182.56, adjusted R^2=0.03, F=1.76, P=0.20. September: Y=0.4652x-138.23, adjusted R^2=0.01, F=1.17, P=0.2.
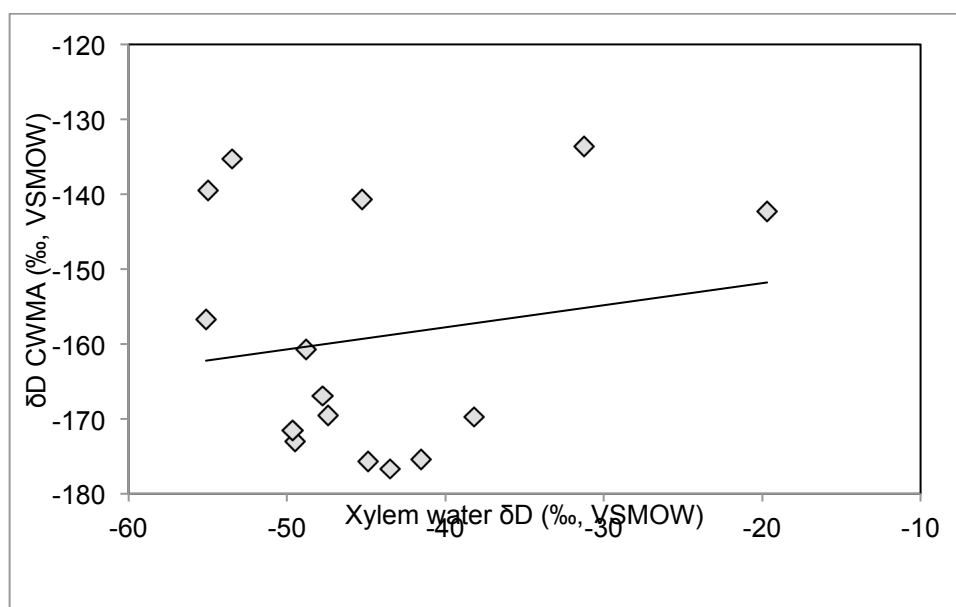
Figure 7.6: Simple linear regression analyses of Odd-CWMA δD composition versus xylem water δD composition for Salix studied with time during the 2012 growing season in Norwich, Norfolk, UK. y=0.2948x-145.98, adjusted R^2=-0.05, F=0.39, P=0.54

These results therefore suggest xylem water δD values have little control over the δD values of *n*-alkanes synthesised by Scots pine in Finland, and Salix in Norwich.

Another issue associated with the investigation of links between xylem water and *n*-alkane D-signals is the definition of plant source water is not strictly defined in the vast majority of literature. This is particularly prevalent in earlier publications, where Online Isotopes in Precipitation Calculator (OIPC (Bowen 2013)) calculated meteoric waters are used to calculate ε_{app}, instead of direct δD measurement of the xylem waters of the plant under study. The OIPC is unquestionably a useful tool for estimating MAP δD values at a particular site. However, using these values has the potential to introduce further error into

correlations between *n*-alkane and source water D-values. In addition, ε_{app} completely neglects leaf water evaporative D-enrichment (Smith 2006), which, as is discussed in the following sections, is a significant influencing factor of the *δ*D values of secondary *n*-alkanes in Finland.

7.1.4.2 Drivers of variation in *n*-alkane *δ*D values

If observed variations in *n*-alkane *δ*D values are not linked to variations in xylem water *δ*D values, this raises the issue of ascertaining what exactly is driving the *δ*D values of *n*-alkanes observed in both Norwich Salix and Finnish Scots pine.

One of the issues in understanding the variations observed in *n*-alkane hydrogen isotopic compositions, is whether leaf water evaporative D-enrichment is recorded in the *δ*D values of the *n*-alkanes (Sachse 2009, Castañeda and Schouten 2011). This is because research to date has provided conflicting results, with several publications suggesting the evapotranspirational D-signal is recorded (Leaney, Osmond et al. 1985, Lockheart, Van Bergen et al. 1997, Chikaraishi and Naraoka 2001, Marshall, Brooks et al. 2007), while others have suggested it is not (Hou 2008, Sachse 2010, McInerney 2011). The results of the Finnish Scots pine investigation however, suggest the level of evapotranspirational D-enrichment is recorded in the leaf wax *n*-alkanes, but only in the secondary *n*-alkanes. This is indicated by the significant strong negative correlation between leaf water D-enrichment and height of sample collection during July, and the significant strong negative correlation between *n*-alkane D-enrichment and height of sample collection reported during September.

Although the *n*-alkane *δ*D data from September demonstrates variation in leaf water evapotranspirational D-enrichment can be reflected in *n*-alkane hydrogen isotopic compositions. This finding also produces a significant issue for paleoclimate reconstructions. This is because the July leaf water *δ*D data indicates a strong physiological response of the trees with height to the 24-hour photo-period, where height related trends in water stress (Mencuccini and Grace 1996, Niinemets, Kull et al. 1999, Niinemets, Sonninen et al. 2004, Woodruff, Meinzer et al. 2008, Woodruff, Meinzer et al. 2009) suggest reduced evapotranspiration, and therefore leaf water D-enrichment. Therefore, these data suggest great care needs to be taken in the interpretation of leaf water *δ*D data, as D-depleted leaf water may be a symptom of water stress driven by too favourable conditions for photosynthesis, rather than the complete opposite. Moreover, this phenomenon could result in under-estimations of climate during paleo-climate

reconstructions because the high temperature and extreme irradiance conditions have reduced evapotranspirational D-enrichment, rather than increasing it.

These results are in contrast to greenhouse controlled growth studies, where no significant effects of RH and leaf water D-enrichment were detected in *n*-alkane *δ*D values (Hou 2008, McInerney 2011). However, it is clear that there may be three fundamental flaws in the current methodologies applied in controlled greenhouse growth experiments. Two of these have already been recently highlighted; the issue of static boundary layers, and no natural stressors for wax removal (Gao, Burnier et al. 2012, Gao, Tsai et al. 2012); the third, and potentially most important, is none of these studies appear to have considered the natural climatic ranges of the species they are using. For example, field transpiration studies conducted on boreal tree species of Russia have shown the transpiration rates of pine and spruce species, growing in natural forest stands, are markedly reduced at RH greater than 50 and 70% respectively (Sen'kina 2002). Therefore, if you were to subject a pine species to RH above 50% in a controlled growth experiment, you would see no effect of the RH treatments because these plant species cannot function properly under these conditions.

7.1.5 Hydrogen source for *n*-alkanes

How often *n*-alkanes are synthesized and the origins of the *δ*D value of the "biosynthetic water pool" they are synthesized from is the subject of much debate (Kahmen 2011, McInerney 2011, Sachse 2012, Kahmen, Hoffmann et al. 2013, Kahmen, Schefuß et al. 2013, Tipple 2013). However, the current study suggests *n*-alkane *δ*D values are not constant with time within single species, and xylem water isotopic compositions are not driving this.

Both the Finnish Scots pine and Norwich Salix investigations indicate spring D-enrichment of *n*-alkanes, which is a commonly reported phenomenon (Chikaraishi, Naraoka et al. 2004, Brandes, Wenninger et al. 2007, Pedentchouk 2008). The results of the application of the Kahmen et al., (2013) conceptual model to the Norwich and Finnish data suggest significant leaf water contributions to the conceptual "*n*-alkane biosynthetic water-pool" of ~116% and ~112% respectively, during the early growing season at each location. As a leaf water contribution of over 100% is not possible, this suggests a much more D-enriched source of hydrogen is used during the biosynthesis of spring *n*-alkanes. This data, in combination with the oxygen-carbon isotopic conceptual model applied to the Norwich Salix, indicates D-enriched stored assimilates are a large source for spring D-enriched *n*-alkanes.

Although it has been previously suggested *n*-alkanes may source hydrogen from D-enriched stored assimilates (Sachse 2009, Sachse 2012), and this is a widely reported concept in plant physiology, especially for carbon. In the case of *n*-alkanes, it appears NADPH sourced via the oxidative PPP from stored glucose is significantly D-enriched (Schmidt 2003, Sessions 2006, Feakins 2010) when compared to that sourced directly from the light reaction of photosynthesis (Luo, Steinberg et al. 1991, Schmidt 2003). As NADPH is the reducing agent used in *n*-alkane biosynthesis, this presents a significant issue for paleoclimate reconstructions because the timing of sample collection for the calibration and interpretation of *n*-alkane *δ*D values from sediment archives will produce erroneous results if samples are collected during spring.

In addition, the results of the current investigation suggest either the conceptual "biosynthetic water-pool" from which odd-numbered *n*-alkanes are synthesized from is extremely variable within and between individuals of the same species at the same time; or, ε_{bio} is not constant within single species, within natural forest ecosystems' or within plants as a whole (as shown in figure 7.4). It is therefore strongly recommended that the consistency of ε_{bio} within individuals, in natural environments, be fully investigated before the assumption of a constant ε_{bio} can be applied to either plant physiological studies or paleoclimate reconstructions.

7.1.6 Additional noteworthy points for discussion

Although it has already been highlighted by previous publications (Sachse 2009, Kahmen 2011, Kahmen, Hoffmann et al. 2013), it is imperative to further highlight that using single point in time measurements of leaf water *δ*D values will not give a full and accurate representation of leaf water *δ*D behaviour. In addition, these must be conducted in conjunction with the associated xylem water *δ*D values, otherwise it is impossible to gain any insight into what is driving variations in *n*-alkane *δ*D values.

7.2 Part 2: Conclusions and future research

7.2.1 Conclusions

1. Evergreen Coniferous species can significantly contribute to sedimentary archives, synthesizing both odd-and-even *n*-alkanes chain lengths in sub-arctic Finland.

2. *n*-alkane concentrations, ACLs and CPIs are highly variable within and between individuals of the same species, inhabiting the same region, sampled at the same time, pointing to a significant influence of PAR levels.

3. ACLs and CPIs should not be used as diagnostic tools of *n*-alkane source in paleoclimate studies until further research can better constrain values between different species.

4. Xylem water *δ*D values exert little control on the *δ*D values of *n*-alkanes on a leaf-by-leaf basis.

5. *n*-alkanes are not "locked in" immediately after leaf flush in Finnish Scots pine or Norwich Salix.

6. Leaf water evaporative D-enrichment is recorded in the secondary *n*-alkanes synthesized by Finnish Scots pine, while spring *n*-alkanes reflect stored assimilates.

7. Too favourable conditions for photosynthesis can reduce evapotranspirational D-enrichment of leaf waters, resulting in reduced *n*-alkane D-enrichment and potentially erroneous interpretations in sedimentary archives.

8. The hydrology of individual forest ecosystems, where meteoric water- xylem water-leaf water isotopic analyses are conducted, is a crucial precursor to the interpretation of any organic matter synthesized if paleo-climate proxies are to be calibrated in any reliable capacity.

9. Plant physiological behaviour may be a more important factor in determining the isotopic *δ*D values of *n*-alkanes than source water *δ*D values, and this behaviour appears to be both species and ecosystem specific.

7.2.2 Future directions

Although the current study has provided useful insights into the paleoclimate applications of *n*-alkanes, it is clear a great deal of research still needs to be conducted within this area.

As this study is the first investigating variation within large individual trees over gradients in height of up to 20m, it suggested that similar studies are conducted on other tree species, especially deciduous angiosperms. In addition, any investigations examining the compound-specific hydrogen isotopic compositions of *n*-alkanes from modern vegetation should also calculate ACLs and CPIs. *n*-alkane quantification and molecular distribution data is not difficult or time consuming if *n*-alkanes are already being studied for their *δ*D values. Moreover, this will also aid in ascertaining whether ACLs and CPIs could be used in the future to infer *n*-alkane source in sediments, if values can be better constrained. In addition, it is strongly recommended the September Finnish sampling campaign is repeated to ensure the high concentrations of *n*-alkanes can be repeated.

To shed further light on which hydrogen isotopic sources contribute most to *n*-alkane *δ*D values and when, a multi-isotope approach is recommended. Hydrogen and oxygen analyses of MAP, xylem waters, leaf waters, along with carbon and hydrogen isotopic analysis of *n*-alkanes, would facilitate the use of the oxygen-carbon conceptual model, and help to fully understand how MAP is related to *n*-alkane *δ*D values. The lack of any control of xylem water D isotopic composition on *n*-alkane *δ*D values within the current study is a cause for concern. Especially as this is one of the major assumptions applied to the use of *n*-alkanes as a paleoclimate proxy. Nevertheless, future research should attempt to address how important this is in terms of what is input into a sediment archive. For example, if an average season-integrated signal is input, we can only estimate an average climate, and the heterogeneity observed within the current study may not be so important. This suggests that a large investigation, detailing every aspect of the use of *n*-alkanes as a paleoclimate proxy is undertaken; E.g. full investigation into the relationship between meteoric water *δ*D and *n*-alkane *δ*D, and then how this is related to a sediment archive in close proximity.

If I were given the opportunity to repeat the investigations detailed within the current thesis, I would ensure there was enough *n*-alkane extract and time to complete compound-specific carbon isotopic analyses of the *n*-alkanes in conjunction with the hydrogen. I would also have collected samples from a greater number of individual trees, and tried to combine the sample methodology applied to the Norwich Salix with that of the Finnish and

Scottish Scots pine. I.e. Regular sampling from leaf flush, up until leaf senescence, as in the Norwich Salix, however with variation within individuals also incorporated.

I believe greenhouse controlled growth experiments are very valuable in understanding which processes are key in driving *n*-alkane *δ*D values. However, these must be conducted with great care, ensuring only the natural range of environmental conditions that a particular species inhabits is applied, otherwise conclusions drawn from these will be erroneous.

The current study has highlighted several issues associated with the use of *n*-alkanes as a paleoclimate proxy; mainly the relationship between MAP *δ*D and *n*-alkane *δ*D is not a simple one. Nevertheless, it is clear that we can make great strives to understand the level of heterogeneity in *n*-alkane *δ*D values in modern terrestrial vegetation, yet this will be of little use until we can understand how what is produced by a living plant relates to what is found within a sediment archive.

Table 1: A complete breakdown of all of the *n*-alkane total concentration, Carbon Preference Index (CPI), and Average Chain Length (ACL) data collected dur September in Finnish Lapland, detailing the exact location of the samples within each individual tree studied. Gaps within the table represent sample lost during preparation or analysis.

Sample code	Tree size	Aspect	Height (m)	Relative height	ACL_{21-36} July	ACL_{21-36} Sept	CPI JULY	CPI Sept	µg/g Conc. July	µg/g Conc. Sept
LT2 NT	LT	North	18.2	Top	23.73	23.65	2.53	2.14	3.02	11.35
LT2 SB	LT	North	8.1	Bottom	23.81	24.26	2.38	2.12	2.03	8.91
LT2 NB	LT	North	7.6	Bottom	24.17	24.32	2.36	2.46	4.01	17.70
LT2 NM	LT	South	13.1	Middle	23.63	26.03	2.14	3.49	3.91	9.63
LT2 SM	LT	South	12.6	Middle	24.10	25.65	2.48	3.44	13.34	9.03
LT2 ST	LT	South	19	Top	23.54	25.77		4.09	13.25	22.05
MT1 SMR MN	ST	North	4.2	Middle	22.62	23.18	1.49	1.62	9.66	9.63
MT1 SMR MS	ST	South	5	Middle		23.41	1.57	2.29	7.98	2.62
MT1 SMR NB	ST	North	2.9	Bottom	23.10	23.75	1.75	1.82	1.63	9.41
MT1 SMR NT	ST	North	8.3	Top	23.69	23.78	1.86	1.76	5.24	14.06
MT1 SMR SB	ST	South	3.1	Bottom	22.76	24.65	0.76	3.51	5.34	5.52
MT1 SMR ST	ST	South	9.4	Top	22.58	24.96	1.64	4.02	1.52	14.59
MT2 SMR NB	ST	North	2.7	Bottom	23.63		1.74		3.58	52.84
MT2 SMR NM	ST	North	4.9	Middle	24.08	25.84	1.64	4.02	7.17	7.70
MT2 SMR NT	ST	North	9	Top	24.31		1.78		1.57	5.64
MT2 SMR SB	ST	South	3.1	Bottom	23.54		2.19	2.07	2.79	24.26
MT2 SMR SM	ST	South	5.2	Middle		26.03		3.49	6.63	6.63
MT2 SMR ST	ST	South	8.5	Top	24.24		1.81		2.07	76.76
Sap1	SAP	South	2	Top	23.48	24.95	1.52	2.16	2.75	33.39
SAP1SMR	SAP	South	2	Top	23.12	23.11	0.35	1.45	6.79	13.49
Sap2	SAP	South	2	Top	23.49	25.43	1.67	2.71	7.98	33.39
Sap2 SMR	SAP	South	2	Top	24.06	24.07	2.10	1.29	8.71	11.44
VLT NB	LT	North	8.3	Middle	22.94	22.08	1.78	0.50	5.74	5.64
VLT MN	LT	South	13.7	Middle	23.72	24.81	1.71	3.43	8.57	67.83
VLT SB	LT	North	7.3	Bottom	22.88	25.25	1.60	3.45	4.52	52.84
VLT NT	LT	North	21.4	Top	23.03	25.52	1.91	4.06	12.99	76.59
VLT ST	LT	South	22.3	Bottom	24.89	25.83	1.88	6.32	8.92	76.76
VLT MS	LT	South	11.3	Top	24.34	26.15	1.95	5.54	2.84	24.26

Table 2: A complete breakdown of all of the *n*-alkane total concentration, Carbon Preference Index (CPI), and Average Chain Length (ACL) data collected during April and October in the Black Wood of Rannoch, Scotland. Detailing the exact location of the samples within each individual tree studied, gaps within the table represent sample lost during preparation or analysis.

Sample code	Tree size	Aspect	Height (m)	Relative height	ACL$_{21-33}$ April	ACL$_{21-33}$ Oct	CPI APR	CPI OCT	µg/g Conc. April	µg/g Conc. Oct
LTS17	LT	North	14.90	Bottom	24.52	23.78	2.04	1.43	9.59	3.18
LTN18	LT	South	14.80	Bottom	25.18	24.45	1.85	1.67	4.42	9.62
LTN14.9	LT	South	17.00	Middle	24.02	23.57	2.10	0.51	6.88	7.40
LTN21.2	LT	North	18.00	Middle	24.96	22.48	2.26	0.62	6.99	
LTS14.8	LT	North	21.20	Top	24.33	24.09	2.26	1.59	10.47	6.36
LTS19.2	LT	South	19.20	Top	23.50	24.69	0.87	2.03	3.19	6.36
MTTN	LT	South	12.60	Middle	24.19	22.84	1.22	0.71	6.31	3.61
MTW	LT	North	15.10	Middle	26.31	24.39	4.29	1.56	6.85	3.53
MTE	LT	North	16.30	Top	23.85	23.10	1.22	0.51	8.44	2.86
MTSM	LT	West	16.20	Top	24.12	23.47	0.47	0.54	4.09	5.25
MT ST	LT	East	14.80	Top	25.36	23.50	1.92	0.60	3.62	6.55
MTN15.1	LT	South	15.80	Top	26.50	23.96	2.93	1.43	5.83	5.71
MT2 N11.7	MT	South	11.50	Bottom	25.36	24.41	1.62	1.72	9.37	7.31
MT2S13	MT	North	8.30	Bottom	25.08	25.88	1.50	2.26	7.77	8.77
MT2N16.3	MT	North	11.70	Middle	24.81	24.21	0.44	1.30	10.34	8.24
MT2 S11.5	MT	South	13.00	Middle	24.94	23.80	1.43	1.55	6.85	7.03
MT2 S15.9	MT	North	16.30	Top	25.39	24.26	1.64	1.59	8.91	5.73
MT2 N8.3	MT	South	15.90	Top	25.87	24.00	1.20	1.75	15.95	7.62
STS7.9	MT	South	7.90	Bottom	25.64	23.32	2.27	1.42	5.73	5.11
STN9.7	MT	North	9.70	Bottom	25.13	23.61	1.73	1.43	5.95	4.72
ST S15	MT	South	15.00	Middle	24.02	23.90	1.63	1.44	2.69	3.65
ST N18.3	MT	North	16.20	Middle	23.63	25.63	0.63	2.30	2.72	12.14
STN16.2	MT	North	18.30	Top	25.38	25.22	1.83	2.00	6.99	14.27
ST S19.4	MT	South	19.40	Top	25.07	25.14	2.10	2.72	6.20	12.17
SAP1	Sap	South	2.00	Top	24.70	24.71	1.82	1.53	6.99	2.96
SAP2	Sap	South	2.00	Top	24.15	24.74	2.42	1.68	5.25	2.61
SAP3	Sap	South	2.00	Top	23.95	25.47	1.30	1.93	6.85	6.01
SAP4	Sap	South	2.00	Top	27.23	24.09	2.67	1.55	8.38	8.38

Table 3: The complete ^{18}O and D isotopic compositions of the analysed data (‰, VSMOW) for leaf water and xylem water. The calculated fractionation of leaf water above xylem water (ΔD Leaf Water) for July and September in Finland are shown with full details of the sample locational variables.

Sample code	Tree	Aspect	Relative height	July Leaf water δD	July Leaf water δ18O	July Xylem Water δD	July Xylem Water δ18O	ΔD Leaf water July	Sept Leaf Water δD	Sept Leaf Water δ18O	Sept Xylem Water δD	Sept Xylem Water δ18O	ΔD Leaf water Sept
LT2 NB	MT	North	Bottom	-43.80	-0.23	-71.59	-10.24	29.9	-87.66	-4.69	-75.95	-8.64	-13
LT2 NM	MT	North	Middle	-47.42	-1.37	-72.42	-9.38	34.1	-80.07	-6.49	-78.43	-10.22	43
LT2 NT	MT	North	Top	-47.95	0.25	-67.37	-8.65	26.9	-87.34	-5.56	-83.71	-10.71	-2
LT2 SM	MT	South	Middle	-34.88	0.09	-72.09	-10.65		-85.24	-5.56	-86.18	-9.10	39
LT2 ST	MT	South	Top	-54.90	-3.04	-69.95	-9.59	20.8	-84.51	-5.84	-87.65	-9.60	-4
LT2 SB	MT	South	Bottom	-37.94	1.26	-73.07	-8.68	32.5	-83.84	-6.42	-82.43	-10.33	38
MT1 SMR MN	ST	North	Middle	-34.67	6.34	-85.47	-11.31		-103.84	-12.56	-82.04	-11.01	-22
MT1 SMR MS	ST	South	Middle	-42.75	5.16		-11.79		-102.62	-12.12	-90.06	-11.79	
MT1 SMR NB	ST	North	Bottom		-4.82	-70.45	-11.02	55.5	-108.24	-12.15	-88.35	-9.88	-24
MT1 SMR NT	ST	North	Top	-34.92	-4.40	-76.32	-10.65		-100.14	-11.77	-84.61	-10.81	-5
MT1 SMR SB	ST	South	Bottom	-36.64	6.04	-75.31	-10.38	44.8	-102.82	-11.67	-86.48	-10.78	-17
MT1 SMR ST	ST	South	Top	-40.17	-5.59	-79.57	-10.48		-101.87	-11.65	-81.32	-10.67	
MT2 SMR NM	ST	North	Middle	-47.30	-4.74		-9.50	37.9	-86.20	-10.36	-81.17	-10.66	-2
MT2 SMR SM	ST	South	Middle	-44.76	-5.62	-103.51	-11.45	42.5	-82.35	-9.29	-86.12	-11.34	26
MT2 SMR SB	ST	South	Bottom	-47.45	-4.82	-69.28	-9.54	40.1	-67.53	2.61	-62.27	-11.65	1
MT2 SMR NB	ST	North	Bottom	-50.71				38.9		-12.25	-69.45	-8.27	37
MT2 SMR ST	ST	South	Top	-50.83	-6.14	-104.37	-10.52	16.2	-86.72	-10.52	-86.04	-12.16	3
MT2 SMR NT	ST	North	Top	-47.95				28.5		-11.01	-84.48	-11.65	38
SAP1SMR	SAP	South	Top	-45.81	2.02	-85.12	-10.49	41.8	-103.86	-11.20	-91.37	-12.09	-18
Sap2 SMR	SAP	South	Top	-46.68	0.85	-83.47	-10.69	23.5			-87.06	-11.55	-6
Sap1	SAP	South	Top	-31.63	1.76	-65.69	-7.61		-61.43	-5.16	-76.24	-9.70	-14
Sap2	SAP	South	Top	-38.30	0.48	-69.73	-8.37	65.5			-76.29	-6.45	4
VLT ,MN	LT	North	Middle	-57.38	-3.79		-12.04	42.8	-52.36	-2.16	-88.09	-11.51	-22
VLT MS	LT	South	Middle	-54.08	-1.41	-89.50	-12.23	59.8	-49.28	-2.07	-82.78	-11.02	-1
VLT NB	LT	North	Bottom	-61.17	-4.42	-92.17	-12.07	43.0	-50.05	-2.24	-89.09	-10.26	-14
VLT NT	LT	North	Top	-56.37	-3.86	-86.07	-11.79	40.1	-52.32	-1.94	-87.09	-9.97	
VLT SB	LT	South	Bottom	-54.94	-2.15	-93.45	-12.40	36.5	-56.06	-3.20	-80.04	-9.73	16
VLT ST	LT	South	Top	-58.11	-2.53	-84.18	-12.59		-50.25	-1.44	-84.83	-11.30	17

Table 4: The complete ^{18}O and D isotopic compositions of the analysed data (‰, VSMOW) for leaf water and xylem water, complete with the calculated fractionation of leaf water above xylem water (ΔD Leaf Water) for April and October in the Black Wood of Rannoch, Scotland. Full details of the sample locational variables are also provided.

Sample code	Tree size	Aspect	Height	Relative height	April Leaf Water δD	April Leaf Water δ18O	Oct Leaf Water δD	Oct Leaf Water δ^{18}O	Oct Xylem water δD	Oct Xylem Water δ^{18}O	ΔD Leaf water Oct
LTN14.9	LT	North	14.90	Bottom	-20.73	1.01	-22.69	-2.75	-54.12	-8.43	33.22
LTN18	LT	North	18.00	Middle	-17.27	0.79	-21.67	-2.12	-55.68	-8.86	36.01
LTN21.2	LT	North	21.20	Top	-32.10	-4.88	-18.27	-1.54	-57.06	-7.90	41.14
LTS14.8	LT	South	14.80	Bottom	-16.81	0.38	-14.70	0.06	-46.85	-6.84	33.73
LTS17	LT	South	17.00	Middle	-14.36	1.00	-13.02	0.28	-41.36	-6.05	29.56
LTS19.2	LT	South	19.20	Top	-20.24	0.67	-16.30	1.71	-62.45	-8.37	49.22
MTE	LT	East	14.80	Top	-26.07	-1.14	-23.52		-61.43		40.39
MT ST	LT	South	15.80	Top	-27.42	-1.97	-24.92	-0.27	-58.59	-8.84	41.09
MTN15.1	LT	North	15.10	Middle	-17.01	6.47		-2.62	-58.50	-8.52	
MTSM	LT	South	12.60	Middle	-23.40	-1.80	-25.44	-0.08	-64.92	-8.65	42.19
MTTN	LT	North	16.30	Top	-23.65	-1.88	-25.29	0.14	-57.50	-7.95	34.18
MTW	LT	West	16.20	Top	-20.18	-0.79	-44.93		-45.66		0.77
MT2N16.3	MT	North	16.30	Top	-17.69	3.31	-15.03	-2.02	-62.49	-8.81	36.26
MT2S13	MT	South	13.00	Middle	-22.35	12.77		-2.04	-58.05	-8.36	
MT2 S11.5	MT	South	11.50	Bottom	-16.37	4.05	-19.66	-2.53	-59.86	-8.33	42.76
MT2 N11.7	MT	North	11.70	Middle	-23.47	2.54	-19.73	-2.04	-53.28	-7.81	35.44
MT2 N8.3	MT	North	8.30	Bottom	-10.75	4.70	-18.76	-3.21	-54.28	-7.93	37.56
MT2 S15.9	MT	South	15.90	Top	44.08	14.92		-1.73	-67.34	-9.15	
STN16.2	MT	North	16.20	Middle	-28.62	-0.27	-19.01	-1.10			
STN9.7	MT	North	9.70	Bottom	-28.90	-0.24	-20.43	-1.19	-60.59	-8.19	39.84
STS7.9	MT	South	7.90	Bottom	-22.36	11.17	-28.74	-3.39			
ST S15	MT	South	15.00	Middle	-5.75	4.81					
ST S19.4	MT	South	19.40	Top	14.77	8.66	-22.76	-1.11		-8.96	
ST N18.3	MT	North	18.30	Top	-12.50	10.00	-27.36	-1.83		-8.96	
SAP1	Sap	South	2.00	Top	-40.66	-6.29	-25.34		-43.74	-6.69	45.74
SAP2	Sap	South	2.00	Top	-6.79	5.31	-28.01	-4.89	-49.29	-7.96	22.38
SAP3	Sap	South	2.00	Top	-55.70	-1.22	-25.88	-4.41	-56.58	-7.89	32.54
SAP4	Sap	South	2.00	Top	-40.89	0.46	-27.73	-4.64	-59.34	-8.81	33.60

Table 5: Compound –specific *δ*D values of all the individual *n*-alkane chain homologues analysed in Finland during July 2010 (‰, VSMOW), showing the multiple chains analysed per sample and the different locational variables of each tree studied.

Sample	Tree size	Aspect	Relative height	Height (m)	nC_{21}	nC_{22}	nC_{23}	nC_{24}	nC_{25}	nC_{26}	nC_{27}	nC_{28}	nC_{29}	nC_{30}	nC_{31}
LT2 NB	LT	North	Bottom	7.6	-175	-146	-179	-159	-191	-168	-191	-162	-182		
LT2 NM	LT	North	Middle	13.1	-180	-160	-180	-153	-193	-170	-196	-166	-180		-175
LT2 NT	LT	North	Top	18.2	-176	-156	-183	-159	-188	-158	-187	-154			
LT2 SM	LT	South	Middle	12.6	-174	-145	-171	-139	-182		-184		-167		
LT2 ST	LT	South	Top			-165		-159	-156		-150				
LT2 SB	LT	South	Bottom	8.1	-173	-148	-174	-148	-188	-168	-187		-177		
MT1 SMR MN	MT	North	Middle	4.2	-137	-124	-152	-131	-169	-152	-173	-146	-169		
MT1 SMR MS	MT	South	Middle	5.0	-145	-122	-150	-133		-149	-178		-164		
MT1 SMR NB	MT	North	Bottom	2.9	-138	-130	-157	-145	-183		-182				
MT1 SMR NT	MT	North	Top	8.3	-136	-129	-150	-138	-167	-148	-171		-160		
MT1 SMR SB	MT	South	Bottom	3.1	-165	-137	-170		-183	-159	-185	-156	-175		
MT1 SMR ST	MT	South	Top	9.4	-123	-115	-141	-122	-162		-168		-181		
MT2 SMR NM	MT	North	Middle	4.9	-169	-143	-172	-158	-191		-186		-177		
MT2 SMR SM	MT	South	Middle	5.2	-145	-173	-154	-190	-163	-186	-160	-181	-194		
MT2 SMR SB	MT	South	Bottom	3.1		-127	-170	-155	-182	-158					
MT2 SMR NB	MT	North	Bottom	2.7				-122		-138					-174
MT2 SMR ST	MT	South	Top	8.5				-144		-169		-169		-158	
MT2 SMR NT	MT	North	Top	9.0	-145			-148		-169		-167			
SAP1SMR	Sap	South	Top	2.0	-162	-146	-159	-142	-171	-149	-162		-156		
Sap2 SMR	Sap	South	Top	2.0	-157	-158	-160	-156	-175	-159	-176	-152	-169		-157
Sap1	Sap	South	Top	2.0					-162		-164				
Sap2	Sap	South	Top	2.0	-141	-125	-141		-161		-172				
VLT ,MN	LT	North	Middle	13.7	-135	-118	-151		-166		-171				
VLT MS	LT	South	Middle	11.3	-158	-118	-167	-152	-182	-156	-183	-149	-168		
VLT NB	LT	North	Bottom	8.3	-158		-167	-150	-182		-177				
VLT NT	LT	North	Top	21.4	-151	-141	-170	-145	-180	-150	-179				
VLT SB	LT	South	Bottom	7.3	-140	-120	-149	-127	-171		-169				
VLT ST	LT	South	Top	22.3	-140	-120	-153	-131	-177	-143	-171	-135	-162		

Table 6: Compound –specific *δD* values of all the individual *n*-alkane chain homologues analysed in Finland during September 2010 (‰ VSMOW), showing the multiple chains analysed per sample and the different locational variables of each tree studied.

Sample code	Tree size	Aspect	Relative height	Height (m)	nC_{21}	nC_{22}	nC_{23}	nC_{24}	nC_{25}	nC_{26}	nC_{27}	nC_{28}	nC_{29}
LT2 NB	LT	North	Bottom	7.60	-165.28		-181.74		-194.73		-202.49		
LT2 SB	LT	South	Bottom	8.10	-140.37	-107.38	-154.52		-181.38		-193.24		
VLT NB	LT	North	Bottom	8.30	-168.48	-132.47	-180.31	-148.87	-191.76	-162.14	-190.38		
VLT SB	LT	South	Bottom	7.30	-156.78		-173.49		-185.27		-182.29		
LT2 NM	LT	North	Middle	13.10					-201.83		-192.88		
LT2 SM	LT	South	Middle	12.60	-161.14	-117.51			-192.74		-195.66		
VLT ,MN	LT	North	Middle	13.70	-172.50	-152.74	-190.41	-171.66	-198.37	-175.56	-198.08	-162.13	-191.55
VLT MS	LT	South	Middle	11.30	-173.15	-127.55	-189.85	-163.62	-196.71		-198.59		-184.53
LT2 NT	LT	North	Top	18.20	-168.39	-134.36	-188.69		-195.36		-198.63		
LT2 ST	LT	South	Top	19.00	-171.51		-191.41		-201.76	-178.77	-205.62		-195.93
VLT NT	LT	North	Top	21.40	-176.28		-196.20	-170.54	-198.80	-173.71	-192.42	-156.66	-183.55
VLT ST	LT	South	Top	22.30	-175.00	-152.57	-187.04	-164.90	-191.08	-161.27	-187.71	-149.76	-179.75
MT1 SMR NB	MT	North	Bottom	2.90							-177.52		
MT1 SMR SB	MT	South	Bottom	3.10	-160.51	-131.38	-170.13		-180.20		-182.52		-164.15
MT2 SMR NB	MT	North	Bottom	2.70									
MT2 SMR SB	MT	South	Bottom	3.10	-167.45		-174.94		-186.52		-179.72		
MT1 SMR MN	MT	North	Middle	4.20									
MT1 SMR MS	MT	South	Middle	5.00	-157.01		-173.72		-181.50		-176.50		-157.56
MT2 SMR NM	MT	North	Middle	4.90	-161.58	-131.32	-186.84	-143.88	-195.05		-189.41		-183.86
MT2 SMR SM	MT	South	Middle	5.20	-173.46		-180.48		-188.79		-187.55		-182.11
MT1 SMR NT	MT	North	Top	8.30	-174.17	-136.05	-193.19		-184.95	-141.00	-182.87	-132.70	-180.38
MT1 SMR ST	MT	South	Top	9.40	-164.30		-176.27		-185.26		-175.04		
MT2 SMR NT	MT	North	Top	9.00			-205.48		-197.75		-190.17		
MT2 SMR ST	MT	South	Top	8.50	-188.77		-166.82		-177.87		-178.84		
Sap1	SAP	South	Top	2.00	-166.80	-149.82	-149.71	-126.35	-161.85	-119.44	-160.80		
SAP1SMR	SAP	South	Top	2.00									
Sap2	SAP	South	Top	2.00				-124.17	-164.68		-174.38		
Sap2 SMR	SAP	South	Top	2.00	-160.09		-169.63		-177.25		-181.84		

Table 7: Compound –specific δD values of all the individual n-alkane chain homologues analysed in Scotland during April 2010 (‰ VSMOW), showing the multiple chains analysed per sample and the different locational variables of each tree studied.

Sample	Tree size	Aspect	Relative height	Height (m)	nC_{22}	nC_{23}	nC_{24}	nC_{25}	nC_{26}	nC_{27}	nC_{28}	nC_{29}	nC_{30}	nC_{31}
LT	LT	North	Bottom	14.90								-155.83		-145.25
LT	LT	North	Middle	18.00		-133.48		-138.60		-148.11		-151.46		
LT	LT	North	Top	21.20						-165.36		-176.48		-163.11
LT	LT	South	Bottom	14.80								-139.80		
LT	LT	South	Middle	17.00		-144.47		-158.08		-169.42		-172.95		-163.58
LT	LT	South	Top	19.20								-173.75		-159.57
LT 2	LT	East	Top	14.80		-112.63		-115.49		-174.50		-144.71		-123.35
LT 2	LT	North	Middle	15.10		-124.56	-105.58	-134.96		-150.30		-151.56		-184.80
LT 2	LT	North	Top	16.30										
LT 2	LT	South	Middle	12.60		-112.34	-109.03	-114.62		-135.95		-134.27		
LT 2	LT	South	Top	15.80	-100.18	-127.55	-110.30	-139.63	-109.57	-151.38		-154.47		-128.82
LT 2	LT	West	Top	16.20		-110.42	-89.59	-111.90		-158.45		-150.21		
MT 2	MT	North	Bottom	8.30		-106.15	-95.45	-109.02	-97.67	-155.71		-151.41		
MT 2	MT	North	Middle	11.70	-115.21	-129.46		-136.45		-149.01		-152.62		
MT 2	MT	North	Top	16.30		-122.69	-104.99	-127.24		-154.81		-145.52		-132.01
MT 2	MT	South	Bottom	11.50			-116.27	-130.20						
MT 2	MT	South	Middle	13.00		-116.66	-108.94	-125.71	-117.05	-173.44		-163.76		
MT 2	MT	South	Top	15.90		-127.50	-113.65	-124.73	-119.05	-151.42	-133.79	-151.42	-122.62	-134.12
MT 3	MT	North	Bottom	9.70		-118.97		-120.36		-149.74		-145.62		
MT 3	MT	North	Middle	16.20				-144.91		-162.29		-162.49		
MT 3	MT	North	Top	18.30	-102.48	-125.25	-109.09	-140.80	-118.96	-170.65	-131.54	-165.87		-155.27
MT 3	MT	South	Bottom	7.90	-93.30	-111.39	-94.56	-130.39		-167.40		-157.06		
MT 3	MT	South	Middle	15.00				-122.81		-140.09		-139.57		
MT 3	MT	South	Top	19.70		-127.54	-114.77	-147.31	-127.57	-156.81	-144.79	-155.20		-131.68
SAP1	SAP	South	Top	2.00										
SAP2	SAP	South	Top	2.00		-123.53		-138.75		-148.78		-144.64		
SAP3	SAP	South	Top	2.00			-91.28	-104.15						
SAP4	SAP	South	Top	2.00		-123.32	-101.71	-134.76		-172.47		-153.38		-144.29

Table 8: Compound –specific δD values of all the individual *n*-alkane chain homologues analysed in Scotland during October 2010 (‰, VSMOW), showing the multiple chains analysed per sample and the different locational variables of each tree studied.

Tree Size	Aspect	Relative height	Height (m)	nC_{21}	nC_{22}	nC_{23}	nC_{24}	nC_{25}	nC_{26}	nC_{27}	nC_{28}	nC_{29}	nC_{30}	nC_{31}
LT	North	Bottom	14.9		-99.5	-134.0	-85.9	-116.2		-144.2		-139.8		
LT	North	Middle	18.0	-119.7	-139.3	-104.3		-131.6		-144.6		-147.4		
LT	North	Top	21.2		-109.3	-131.3	-99.4	-124.4		-157.0		-145.9		
LT	South	Bottom	14.8		-114.3	-137.2	-111.4	-129.5		-166.9		-151.8		
LT	South	Middle	17.0		-118.4	-128.2	-114.8	-133.6		-150.5		-148.4		
LT	South	Top	19.2		-124.6	-147.8	-121.0	-137.0	-124.5	-159.5	-130.3	-155.0	-125.2	-145.2
LT	East	Middle	14.8			-109.1		-124.1						
LT	South	Bottom	15.8		-107.2	-131.6	-108.1	-126.8		-164.3		-140.4		
LT	North	Middle	15.1			-139.0		-137.7		-143.7				
LT	South	Top	12.6			-138.3	-110.7					-157.1		
LT	North	Bottom	16.3			-126.1		-125.0						
LT	West	Bottom	16.2			-133.6		-124.9						
MT	North	Bottom	16.3		-113.0		-125.8	-142.3	-123.1	-151.4		-148.7		-128.5
MT	South	Middle	13.0			-132.7	-104.2	-124.2		-155.3				
MT	South	Top	11.5			-122.5				-162.7				
MT	North	Bottom	11.7		-115.2	-140.7	-112.7	-132.7		-168.4		-152.0		
MT	North	Middle	8.3	-231.4	-120.2	-139.4		-135.5		-149.9		-146.4		
MT	South	Top	15.9	-210.6	-106.6	-127.8	-97.4	-125.2		-149.8				
Sap	South	Top	2.0			-128.5	-107.8	-125.8		-141.0				
Sap	South	Top	2.0			-128.2								
Sap	South	Top	2.0							-161.9				
Sap	South	Top	2.0		-112.7	-126.8	-98.7	-132.5		-145.2		-130.4		
MT	North	Middle	16.2	-140.5		-157.7		-165.8						
MT	North	Bottom	9.7			-122.7	-99.2	-125.5		-138.9		-126.9		
MT	South	Bottom	7.9	-141.4										
MT	South	Middle	15.0							-123.0				
MT	South	Top	19.4			-128.3	-144.5	-110.9	-141.1					
MT	North	Top	18.3		-125.3	-139.9	-114.1	-143.7	-107.2	-149.0		-146.0		

Table 9: Breakdown of Concentration Weighted Mean Alkane (CWMA) δD values (measured in ‰, VSMOW), and the fractionation of CWMA δD values above leaf water (biosynthetic fractionation, ε_{bio}) during July in Finnish Lapland.

Tree size	Aspect	Relative height	Height (m)	July Total CWMA δD	July Odd CWMA δD	July Even CWMA δD	July Leaf Water δD	July ε_{bio}- Total CWMA	July ε_{bio}- Odd CWMA	July ε_{bio}- Even CWMA
LT	North	Bottom	7.6	-176	-184	-158	-43.8	-138.75	-146.16	-119.28
LT	South	Bottom	8.1	-172	-180	-152	-37.9	-139.20	-147.34	-118.67
LT	North	Bottom	8.3	-166	-171	-150	-61.2	-111.82	-117.20	-95.00
LT	South	Bottom	7.3	-141	-151	-123	-54.9	-91.18	-101.41	-72.10
LT	North	Middle	13.1	-177	-185	-159	-47.4	-135.79	-143.94	-117.01
LT	South	Middle	12.6	-169	-177	-141	-34.9	-138.96	-146.93	-109.89
LT	North	Middle	13.7	-149	-155	-118	-57.4	-97.47	-103.67	-63.92
LT	South	Middle	11.3	-164	-173	-144	-54.1	-116.32	-126.21	-95.33
LT	North	Top	18.2	-177	-184	-157	-48.0	-135.35	-142.87	-115.02
LT	South	Top	19.0	-154	-154		-54.9	-105.29	-105.29	
LT	North	Top	21.4	-160	-169	-143	-56.4	-110.16	-118.83	-91.57
LT	South	Top	22.3	-154	-164	-132	-58.1	-101.40	-112.74	-78.63
MT	North	Bottom	2.9	-152	-154	-142	-50.7	-106.46	-109.23	-95.84
MT	South	Bottom	3.1	-163	-176	-137	-36.6	-131.11	-144.21	-103.66
MT	South	Bottom	3.1	-171	-179	-145	-47.5	-129.79	-137.64	-102.84
MT	North	Bottom	2.7	-128	-128	-150				
MT	North	Middle	4.2	-151	-159	-135	-34.7	-120.64	-129.23	-103.64
MT	South	Middle	5.0	-145	-154	-132	-42.7	-107.24	-116.46	-93.67
MT	North	Middle	4.9				-47.3			
MT	South	Middle	5.2	-161	-152	-179	-44.8	-121.34	-111.76	-140.99
MT	North	Top	8.3	-151	-158		-34.9	-119.85	-127.10	
MT	South	Top	9.4	-162	-171		-40.2	-126.68	-135.79	
MT	South	Top	8.5	-153	-153		-50.8	-108.03	-108.03	
MT	North	Top	9.0			-138	-48.0			-94.69
SAP	South	Top	2.0	-150	-163	-145	-45.8	-109.19	-122.58	-103.90
SAP	South	Top	2.0	-164	-167	-157	-46.7	-123.09	-126.30	-115.89
SAP	South	Top	2.0	-163	-163		-38.3	-129.63	-129.63	
SAP	South	Top	2.0	-134	-150	-125				

Table 10: Breakdown of the Concentration Weighted Mean Alkane (CWMA) δD values (measured in ‰, VSMOW), and the fractionation of CWMA δD values above leaf water (biosynthetic fractionation, ε_{bio}) during September in Finnish Lapland.

Tree size	Aspect	Relative height	Height (m)	Sept Total CWMA δD	Sept Odd CWMA δD	Sept Even CWMA δD	Sept Leaf Water δD	Sept ε_{bio}-Total CWMA	Sept ε_{bio}-Odd CWMA	Sept ε_{bio}-Even CWMA
LT	North	Bottom	7.6	-188	-188.50		-87.7	-110.53	-110.53	
LT	South	Bottom	8.1	-161	-168.05	-107.38	-83.8	-84.37	-91.92	-25.69
LT	North	Bottom	8.3	-179	-186.50	-147.83	-50.0	-135.97	-143.64	-102.93
LT	South	Bottom	7.3	-179	-178.91		-56.1	-130.14	-130.14	
LT	North	Middle	13.1				-80.1			
LT	South	Middle	12.6	-183	-191.32	-117.51	-85.2	-106.51	-115.96	-35.28
LT	North	Middle	13.7	-187	-193.10	-164.35	-52.4	-141.86	-148.52	-118.18
LT	South	Middle	11.3	-189	-192.35	-132.96	-49.3	-147.30	-150.49	-88.02
LT	North	Top	18.2	-185	-191.16	-134.36	-87.3	-106.52	-113.75	-51.52
LT	South	Top	19.0	-197	-198.84	-178.77	-84.5	-123.41	-124.88	-102.96
LT	North	Top	21.4				-52.3			
LT	South	Top	22.3	-183	-186.70	-157.77	-50.3	-139.77	-143.67	-113.20
MT	North	Bottom	2.9				-108.2			
MT	South	Bottom	3.1	-162	-170.11	-131.38	-102.8	-66.25	-75.00	-31.83
MT	South	Bottom	3.1	-178	-178.40		-67.5	-118.90	-118.90	
MT	North	Bottom	2.7							
MT	North	Middle	4.2				-103.8			
MT	South	Middle	5.0	-185			-102.6	-91.67		
MT	North	Middle	4.9	-179	-184.51	-137.76	-86.2	-101.77	-107.58	-56.43
MT	South	Middle	5.2		-184.89		-82.3		-111.74	
MT	North	Top	8.3	-178	-184.10	-137.00	-100.1	-86.02	-93.31	-40.96
MT	South	Top	9.4				-101.9			
MT	South	Top	8.5	-175	-175.04		-86.7	-96.71	-96.71	
MT	North	Top	9.0	-167	-167.13					
SAP	South	Top	2.0				-103.9			
SAP	South	Top	2.0	-172	-171.69					
SAP	South	Top	2.0	-150	-157.66	-132.09				
SAP	South	Top	2.0	-157	-157.12	-124.17	-61.4	-101.42	-101.95	-66.84

Table 11: Breakdown of the Concentration Weighted Mean Alkanes (CWMA) δD values (measured in ‰, VSMOW), and the fractionation of CWMA δD above leaf water (biosynthetic fractionation, ε_{bio}) during April in the Black Wood of Rannoch, Scotland.

Tree size	Aspect	Relative height	Height (m)	April Leaf water δD	Total CWMA δD	Odd CWMA δD	Even CWMA δD	ε_{bio} Total CWMA	ε_{bio} Odd CWMA	ε_{bio} Even CWMA
LT	North	Bottom	14.90	-20.73	-155.83	-155.83		-137.96	-137.96	
LT	North	Middle	18.00	-17.27	-140.61	-140.61		-125.50	-125.50	
LT	North	Top	21.20	-32.10	-169.20	-169.20		-141.65	-141.65	
LT	South	Bottom	14.80	-16.81	-139.80	-139.80		-125.09	-125.09	
LT	South	Middle	17.00	-14.36	-155.86	-155.86		-143.57	-143.57	
LT	South	Top	19.20	-18.83	-173.75	-173.75		-157.88	-157.88	
LT	East	Top	14.80	-29.85	-136.66	-136.66		-110.10	-110.10	
LT	North	Middle	15.10	-17.01	-147.53	-151.93	-105.58	-132.78	-137.25	-90.11
LT	North	Top	16.30	-23.65						
LT	South	Middle	12.60	-25.51	-114.52	-117.08	-109.03	-91.34	-93.96	-85.70
LT	South	Top	15.80	-23.40	-137.00	-144.58	-107.70	-116.32	-124.08	-86.32
LT	West	Top	16.20	-20.18	-105.35	-115.80	-89.59	-86.93	-97.60	-70.84
MT	North	Bottom	8.30	-7.99	-116.42	-126.19	-96.10	-109.30	-119.15	-88.82
MT	North	Middle	11.70	-22.09	-127.71	-134.56	-115.21	-108.00	-115.01	-95.23
MT	North	Top	16.30	-17.69	-129.49	-136.19	-104.99	-113.81	-120.64	-88.87
MT	South	Bottom	11.50	-12.82	-123.71	-130.20	-116.27	-112.33	-118.91	-104.80
MT	South	Middle	13.00	-22.35	-131.93	-141.95	-111.54	-112.08	-122.33	-91.23
MT	South	Top	15.90		-130.99	-138.63	-118.26			
MT	North	Bottom	9.70	-28.90	-133.97	-133.97		-108.19	-108.19	
MT	North	Middle	16.20	-28.62	-151.24	-151.24		-126.23	-126.23	
MT	North	Top	18.30	-12.78	-125.53	-144.34	-115.46	-114.20	-133.26	-104.01
MT	South	Bottom	7.90	-22.36	-132.42	-145.06	-93.97	-112.58	-125.51	-73.25
MT	South	Middle	15.00	-3.32	-128.28	-128.28		-125.37	-125.37	
MT	South	Top	19.70	-13.52	-142.27	-148.45	-125.30	-130.51	-136.77	-113.31
SAP	South	Top	2.00							
SAP	South	Top	2.00	-9.27	-138.42	-138.42		-130.36	-130.36	
SAP	South	Top	2.00	-50.81	-98.24	-104.15	-91.28	-49.98	-56.20	-42.64
SAP	South	Top	2.00	-41.01	-146.61	-151.03	-101.71	-110.12	-114.73	-63.30

Table 12: Breakdown of the Concentration Weighted Mean Alkanes (CWMA) *δD* values (measured in ‰, VSMOW), and the fractionation of CWMA *δD* above leaf water (biosynthetic fractionation, ε_{bio}) during October in the Black Wood of Rannoch, Scotland.

Tree size	Aspect	Relative height	Height (m)	Oct Leaf water δD	Oct xylem water δD	Total CWMA δD	Odd CWMA δD	Even CWMA δD	ε_{bio} Total CWMA	ε_{bio} Odd CWMA	ε_{bio} Even CWMA	ε_{app} Total CWMA	ε_{app} Odd CWMA	ε_{app} Even CWMA
LT	North	Bottom	14.90	-22.69	-54.12	-116.19	-130.40	-93.64	-95.67	-110.21	-72.60	-65.63	-80.65	-41.79
LT	North	Middle	18.00	-21.67	-55.68	-125.74	-113.14	-139.32	-106.37	-93.49	-120.25	-74.19	-60.85	-88.57
LT	North	Top	21.20	-18.27	-57.06	-124.01	-134.81	-104.44	-107.71	-118.71	-87.77	-71.00	-82.46	-50.24
LT	South	Bottom	14.80	-14.70	-46.85	-132.35	-142.61	-112.65	-119.40	-129.81	-99.41	-89.70	-100.46	-69.03
LT	South	Middle	17.00	-13.02	-41.36	-122.28	-131.04	-117.07	-110.70	-119.58	-105.42	-84.41	-93.55	-78.98
LT	South	Top	19.20	-16.30	-62.45	-140.99	-148.15	-123.39	-126.75	-134.03	-108.86	-83.77	-91.41	-65.00
LT	North	Middle	15.10		-58.50	-139.93	-140.26	-138.99				-86.48	-86.83	-85.49
LT	West	Top	16.20	-44.93	-45.66	-131.44	-129.44	-133.59	-90.57	-88.48	-92.83	-89.88	-87.79	-92.14
LT	North	Top	16.30	-25.29	-57.50	-125.94	-125.00	-126.15	-103.27	-102.29	-103.47	-72.62	-71.61	-72.83
LT	East	Top	14.80	-23.52	-61.43	-111.82	-124.09	-109.14	-90.43	-102.99	-87.68	-53.69	-66.77	-50.84
LT	South	Middle	12.60	-25.44	-64.92	-127.18		-127.18	-104.40		-104.40	-66.58		-66.58
LT	South	Top	15.80	-24.92	-58.59	-121.91	-139.04	-107.72	-99.47	-117.04	-84.91	-67.26	-85.46	-52.18
MT	North	Bottom	8.30	-18.76	-54.28	-151.82	-158.72	-125.64	-135.61	-142.63	-108.92	-103.14	-110.43	-75.45
MT	North	Middle	11.70	-19.73	-53.28	-131.96	-145.22	-115.52	-114.49	-128.02	-97.71	-83.11	-97.11	-65.74
MT	North	Top	16.30	-15.03	-62.49	-134.15	-146.47	-122.06	-120.93	-133.44	-108.66	-76.43	-89.58	-63.54
MT	South	Bottom	11.50	-19.66	-59.86	-140.16	-140.16		-122.92	-122.92		-85.41	-85.41	
MT	South	Middle	13.00		-58.05	-127.00	-134.67	-104.23				-73.20	-81.34	-49.03
MT	South	Top	15.90		-67.34	-134.40	-148.59	-102.01				-71.90	-87.12	-37.18
SAP	South	Top	2.00	-19.01		-125.01	-130.97	-107.85	-108.06	-114.14	-90.56			
SAP	South	Top	2.00	-20.43	-60.59	-128.20	-128.20		-110.02	-110.02		-71.96	-71.96	
SAP	South	Top	2.00	-28.74		-161.86	-161.86		-137.05	-137.05				
SAP	South	Top	2.00			-123.07	-132.97	-105.21	-123.07	-132.97	-105.21			
MT	North	Bottom	9.70	-27.36		-119.35	-126.36	-99.24	-94.58	-101.79	-73.91			
MT	North	Middle	16.20	-22.76		-157.39	-157.39		-137.76	-137.76				
MT	North	Top	18.30	-27.73	-59.34	-137.40	-143.75	-118.67	-112.79	-119.33	-93.53	-82.98	-89.73	-63.07
MT	South	Bottom	7.90	-25.34	-43.74	-141.38	-141.38		-119.05	-119.05		-102.10	-102.10	
MT	South	Middle	15.00	-28.01	-49.29	-122.99	-122.99		-97.71	-97.71		-77.52	-77.52	
MT	South	Top	19.70	-25.88	-56.58	-126.52	-120.25	-144.48	-103.31	-96.87	-121.75	-74.13	-67.49	-93.17

Table 13: The fractionation of the different Concentration Weighted Mean N-alkane (CWMA) δD compositions above xylem water (ε_{app} , measured in ‰) sampled in both July and September during the 2010-growth season in Finnish Lapland.

Tree	Aspect	Relative height	Height (m)	July Xylem Water δD	July ε_{app} Total CWMA	July ε_{app} Odd CWMA	July ε_{app} Even CWMA	Sept Xylem Water $\delta^2 H$	Sept ε_{app} Total CWMA	Sept ε_{app} Odd CWMA	Sept ε_{app} Even CWMA
LT	North	Bottom	7.60	-71.59	-112.96	-120.60	-92.91	-75.95	-121.79	-121.79	
LT	South	Bottom	8.10	-73.07	-106.58	-115.02	-85.27	-89.09	-85.78	-93.32	-27.20
LT	North	Bottom	8.30	-92.17	-81.49	-87.05	-64.10	-78.43	-98.93	-106.93	-64.48
LT	South	Bottom	7.30	-93.45	-52.57	-63.24	-32.68	-88.09	-107.47	-107.47	
LT	North	Middle	13.10	-72.42	-112.50	-120.87	-93.21	-83.71			
LT	South	Middle	12.60	-72.09	-104.43	-112.72	-74.19	-87.09	-105.60	-115.06	-34.29
LT	North	Middle	13.70		-149.26			-88.35	-108.23	-115.15	-83.62
LT	South	Middle	11.30	-89.50	-81.94	-92.22	-60.13	-69.45	-116.16	-119.46	-54.71
LT	North	Top	18.20	-67.37	-117.35	-125.03	-96.59	-82.04	-110.06	-117.26	-55.28
LT	South	Top	19.00	-69.95	-90.81	-90.81		-81.17	-120.39	-121.87	-99.87
LT	North	Top	21.40	-86.07	-81.24	-90.19	-62.04	-84.61			
LT	South	Top	22.30	-84.18	-75.83	-87.48	-52.41	-84.48	-107.27	-111.31	-79.70
MT	North	Bottom	2.90	-70.45	-87.49	-90.32	-76.65	-82.43			
MT	South	Bottom	3.10	-36.64	-131.11	-144.21	-103.66	-80.04	-82.95	-91.54	-49.15
MT	South	Bottom	3.10	-69.28	-109.38	-117.42	-81.80	-86.18	-123.85	-123.85	
MT	North	Bottom	2.70		-128.41			-82.78			
MT	North	Middle	4.20	-85.47	-71.80	-80.87	-53.85	-87.65			
MT	South	Middle	5.00		-145.41			-84.83	-104.21		
MT	North	Middle	4.90					-86.48	-106.69	-112.47	-61.59
MT	South	Middle	5.20	-103.51	-63.76	-53.55	-84.69	-62.27		-108.07	
MT	North	Top	8.30	-76.32	-80.40	-87.98		-90.06	-101.53	-108.69	-57.24
MT	South	Top	9.40	-79.57	-89.30	-98.79		-86.12			
MT	South	Top	8.50	-104.37	-54.70	-54.70		-81.32	-98.92	-98.92	
MT	North	Top	9.00					-86.04	-88.73	-88.73	
SAP	South	Top	2.00	-85.12	-70.91	-84.88	-65.40	-91.37			
SAP	South	Top	2.00	-83.47	-87.89	-91.23	-80.40	-87.06	-103.28	-103.28	
SAP	South	Top	2.00	-65.69	-104.11	-104.11		-76.24	-64.76	-72.96	-44.81
SAP	South	Top	2.00		-68.91	-86.24	-59.47	-76.29	-87.02	-87.56	-51.88

Table 14: Total raw data of *n*-alkane abundance, average chain length (ACL), Carbon Preference Index (CPI), hydrogen and oxygen isotopic analysis of leaf water and xylem waters (‰, VSMOW), the Concentration Weighted Mean Alkane δD compositions and the fractionation of these above xylem water (ε_{app}) and leaf water (ε_{bio}) for Salix trees sampled at The University of East Anglia, Norwich.

Salix	Date	mg/g n-alkane concentration	ACL	CPI	Leaf water δD	Leaf water δ^{18}O	Xylem water δD	Xylem water δ^{18}O	CWMA δD	ε_{bio}-Total CWMA	ε_{app} Total CWMA	Bulk Foliar δ^{13}C
S1	08 April 2012	1.95	27.43	17.00	-20.17	0.18	-31.23	-1.88	-133.66	-115.83	-105.73	-28.87
S2	08 April 2012	2.39	27.45	19.27	-22.96	-0.44	0.00	-0.50	-142.31	-122.16		-28.96
S3	08 April 2012	1.10	27.45	22.33	-29.28	-1.18	-53.48	-6.04	-135.34	-109.25	-86.48	-27.82
S1	26 April 2012	3.28	27.61	7.94		-6.50	-55.78	-5.93	-138.71		-87.83	-30.14
S2	26 April 2012	4.45	27.51	12.29	-27.52	3.14	-54.97	-6.00	-139.46	-115.11	-89.40	-29.36
S3	26 April 2012	4.27	27.37	23.03	-25.44	2.72	-45.28	-3.92	-140.67	-118.23	-99.91	-29.63
S1	28 May 2012	4.14	27.63	19.39	-10.98	7.51	-55.11	-5.21	-156.77	-147.41	-107.59	-29.73
S2	28 May 2012	3.26	27.70	34.76		8.94	-43.78	-4.41	-161.07		-122.66	-29.47
S3	28 May 2012	4.92	27.45	29.65	-14.80	6.78	-48.78	-4.28	-160.77	-148.16	-138.85	-29.47
S1	12 July 2012	3.03	27.76	25.92		3.00		2.02	-170.21	-150.64	-128.61	-29.30
S2	12 July 2012	2.97	27.98	15.14	-21.55	2.57	-47.74	-5.33	-166.89	-148.54	-129.04	-30.57
S3	12 July 2012	4.40	27.69	40.83	-23.32	4.69	-43.46	-5.42	-176.71	-157.05	-133.85	-28.57
S1	17 August 2012	3.07	27.87	16.64	-14.56	3.15	-49.48	-5.41	-172.97	-163.61	-134.11	-32.51
S2	17 August 2012	2.11	27.99	24.24	-11.19	3.74	-47.41	-5.47	-169.58	-157.31	-130.25	-33.09
S3	17 August 2012	3.75	27.71	23.73	-18.79	2.18	-44.88	-4.86	-175.63	-159.84	-134.60	-30.05
S1	25 September 2012	1.68		13.61	-21.65	2.19	-41.51	-4.73	-175.43	-157.18	-139.72	-33.48
S2	25 September 2012	2.79	28.03	23.20	-21.56	1.32	-38.17	-5.96	-169.79	-156.50	-136.84	-33.93
S3	25 September 2012	2.97	27.99	17.07	-15.75	2.98	-49.66	-5.45	-171.54	-153.28	-128.25	-33.95

References

Allan, J., Douglas, A.G. (1977). "Variation in the content and distribution of n-alkanes in a series of carboniferous vitrinites and sporinites of bituminous rank." Geochimica et Cosmochimica Acta **41**: 1223-1230.

Allison, G., J. R. Gat and F. W. Leaney (1985). "The relationship between deuterium and oxygen-18 delta values in leaf water." Chemical Geology: Isotope Geoscience section **58**(1): 145-156.

Baker, E. A. and G. M. Hunt (1986). "Erosion of waxes from leaf surfaces by simulated rain. ." New Phytologist **102**(1): 161-173.

Barbour, M. M. (2007). "Stable oxygen isotope composition of plant tissue: a review." Functional Plant Biology **34**(2): 83-94.

Barbour, M. M. and G. D. Farquhar (2000). "Relative humidity- and ABA-induced variation in carbon and oxygen isotope ratios of cotton leaves." Plant, Cell & Environment **23**(5): 473-485.

Barnes, J. D., K. E. Percy, N. D. Paul, P. Jones, C. K. McLaughlin, P. M. Mullineaux, G. Creissen and A. R. Wellburn (1996). "The influence of UV-B radiation on the physicochemical nature of tobacco (Nicotiana tabacum L.) leaf surfaces." Journal of Experimental Botany **47**(1): 99-109.

Barthlott, W. (1990). "Scanning electron microscopy of the epidermal surface in plants." Scanning electron microscopy in taxonomy and functional morphology.. Systematics association special volume(41): 69-94.

Bi, X., G. Sheng, X. Liu, C. Li and J. Fu (2005). "Molecular and carbon and hydrogen isotopic composition of n-alkanes in plant leaf waxes." Organic Geochemistry **36**(10): 1405-1417.

Bigeleisen, J. (1965). "Chemistry of isotopes, isotope chemistry has opened new areas of chemical physics, geochemistry, and molecular biology." Science **147**(3657): 463-471.

Bigeleisen, J., M. W. Lee and F. Mandel (1973). "Equilibrium isotope effects." Annual Review of Physical Chemistry **24**(1): 407-440.

Bird, M. I., R. E. Summons, M. K. Gagan, Z. Roksandic, L. Dowling, J. Head, L. Keith Fifield, R. G. Cresswell and D. P. Johnson (1995). "Terrestrial vegetation change

inferred from n-alkane σ13C analysis in the marine environment." <u>Geochimica et Cosmochimica Acta</u> **59**(13): 2853-2857.

Bonan, G. B., H.H. Shugart (1989). "Environmental factors and ecological processes in boreal forests." <u>Annu. REV. ecol. System</u> **20**: 1-28.

Bowen, G. J. (2013). The Online Isotopes in Precipitation Calculator.

Bowen, G. J. and J. Revenaugh (2003). "Interpolating the isotopic composition of modern meteoric precipitation." <u>Water Resources Research</u> **39**(10): 1299.

Brandes, E., J. Wenninger, P. Koeniger, D. Schindler, H. Rennenberg, C. Leibundgut, H. Mayer and A. Gessler (2007). "Assessing environmental and physiological controls over water relations in a Scots pine (Pinus sylvestris L.) stand through analyses of stable isotope composition of water and organic matter." <u>Plant, Cell & Environment</u> **30**(1): 113-127.

Broadmeadow, M. S., Griffiths, H. (1993). Carbon isotope discrimination and the coupling of CO_2 fluxes within forest canopies. <u>Stable Isotopes and Plant Carbon-Water Relations</u>. J. R. Ehleringer, Hall, AE., Farquhar, GD. San Diego, ACADEMIC PRESS INC.

Brooks, J. R., Barnard, H.R., Coulombe, R., McDonnell, J.J. (2010). "Ecohydrologic separation of water between trees and streams in a Mediterranean climate." <u>Nature Geoscience</u> **3**: 100-104.

Brugnoli, E., G.D. Farquhar (1998). Photosynthetic fractionation of carbon isotopes, . <u>Photosynthesis: physiology and metabolism, advances in photosynthesis</u>. T. D. S. R.C. Leegood, S. Von Caemmerer, Kluwer Academic Publishers.

Burgess, S. and T. Dawson (2004). "The contribution of fog to the water relations of Sequoia sempervirens (D. Don): foliar uptake and prevention of dehydration." <u>Plant, Cell & Environment</u> **27**(8): 1023-1034.

Bush, R. T. and F. A. McInerney (2013). "Leaf wax n-alkane distributions in and across modern plants: Implications for paleoecology and chemotaxonomy." <u>Geochimica et Cosmochimica Acta</u> **117**(0): 161-179.

Cappa, C. D., M. B. Hendricks, D. J. DePaolo and R. C. Cohen (2003). "Isotopic fractionation of water during evaporation." <u>Journal of Geophysical Research</u> **108**(D16): 4525.

Castañeda, I. S. and S. Schouten (2011). "A review of molecular organic proxies for examining modern and ancient lacustrine environments." Quaternary Science Reviews **30**(21): 2851-2891.

Castañeda, I. S., J. P. Werne, T. C. Johnson and T. R. Filley (2009). "Late Quaternary vegetation history of southeast Africa: The molecular isotopic record from Lake Malawi." Palaeogeography, Palaeoclimatology, Palaeoecology **275**(1): 100-112.

Cernusak, L., J. Pate and G. Farquhar (2002). "Diurnal variation in the stable isotope composition of water and dry matter in fruiting Lupinus angustifolius under field conditions." Plant, Cell & Environment **25**(7): 893-907.

Cernusak, L. A., G. D. Farquhar and J. S. Pate (2005). "Environmental and physiological controls over oxygen and carbon isotope composition of Tasmanian blue gum, Eucalyptus globulus." Tree Physiology **25**(2): 129-146.

Chikaraishi, Y. and H. Naraoka (2001). "Organic hydrogen-carbon isotope signatures of terrestrial higher plants during biosynthesis for distinctive photosynthetic pathways." Geochemical Journal Japan **35**(6): 451-458.

Chikaraishi, Y., H. Naraoka and S. R. Poulson (2004). "Carbon and hydrogen isotopic fractionation during lipid biosynthesis in a higher plant (*Cryptomeria japonica*)." Phytochemistry **65**(3): 323-330.

Chikaraishi, Y., Naraoka, H. (2003). "Compound-specific δD-$\delta^{13}C$ analyses of n-alkanes extracted from terrestrial and aquatic plants." Phytochemistry **63**: 361-371.

Connelly, N. G., Damhus, T., Hartshorn, R.M., Hutton, A.T. (2005). Nomenclature of Inorganic Chemistry - IUPAC Recommendations 2005, RSC Publishing.

Conte, M. H. and J. Weber (2002). "Long–range atmospheric transport of terrestrial biomarkers to the western North Atlantic." Global Biogeochemical Cycles **16**(4): 89-81-89-17.

Coplen, T. B. (2011). "Guidelines and recommended terms for expression of stable-isotope-ratio and gas-ratio measurement results." Rapid Communications in Mass Spectrometry **25**: 2538 - 2560.

Craig, H. (1961). "Isotopic variations in meteoric waters." Science **133**(3465): 1702-1703.

Craig, H. (1961). "Standard for reporting concentrations of deuterium and oxygen-18 in natural waters." Science **133**(3467): 1833-1834.

Craig, H. and L. I. Gordon (1965). "Deuterium and oxygen 18 variations in the ocean and the marine atmosphere."

Cranwell, P. (1973). "Chain−length distribution of n−alkanes from lake sediments in relation to post−glacial environmental change." Freshwater Biology **3**(3): 259-265.

Cranwell, P. (1982). "Lipids of aquatic sediments and sedimenting particulates." Progress in Lipid Research **21**(4): 271-308.

Cranwell, P., G. Eglinton and N. Robinson (1987). "Lipids of aquatic organisms as potential contributors to lacustrine sediments—II." Organic Geochemistry **11**(6): 513-527.

Cromier, M. A., Kahmen, A (In prep). "A robust methodology for the extraction of epicuticular leaf waxes for GC-IRMS analysis." In Prep.

Damesin, C. and C. Lelarge (2003). "Carbon isotope composition of current−year shoots from Fagus sylvatica in relation to growth, respiration and use of reserves." Plant, Cell & Environment **26**(2): 207-219.

Dansgaard, W. (1964). "Stable isotopes in precipitation." Tellus **16**(4): 436-468.

Dawson, T. E. (1998). "Fog in the California redwood forest: ecosystem inputs and use by plants." Oecologia **117**(4): 476-485.

Dawson, T. E. and J. R. Ehleringer (1998). "Plants, isotopes and water use: a catchment-scale perspective." Isotope tracers in catchment hydrology: 165-202.

Dawson, T. E., S. Mambelli, A. H. Plamboeck, P. H. Templer and K. P. Tu (2002). "Stable Isotopes in Plant Ecology." Annual Review of Ecology and Systematics **33**: 507-559.

Dawson, T. E. and J. S. Pate (1996). "Seasonal water uptake and movement in root systems of Australian phraeatophytic plants of dimorphic root morphology: a stable isotope investigation." Oecologia **107**(1): 13-20.

Dawson, T. E. and R. Siegwolf (2011). Stable isotopes as indicators of ecological change, Access Online via Elsevier.

Diebel, J. N. J. (2013). "Average weather for Norwich, United Kingdom."   Retrieved 20th August1, 2013, from http://weatherspark.com/averages/28767/Norwich-England-United-Kingdom.

Diefendorf, A. F., K. H. Freeman, S. L. Wing and H. V. Graham (2011). "Production of *n*-alkyl lipids in living plants and implications for the geologic past." Geochimica et Cosmochimica Acta **75**(23): 7472-7485.

Dodd, R. S. and Z. Afzal-Rafii (2000). "Habitat-related adaptive properties of plant cuticular lipids." Evolution **54**(4): 1438-1444.

Dodd, R. S., Z. A. Rafii and A. B. Power (1998). "Ecotypic adaptation in Austrocedrus chilensis in cuticular hydrocarbon composition." New Phytologist **138**(4): 699-708.

Dongmann, G., H. Nürnberg, H. Förstel and K. Wagener (1974). "On the enrichment of H2 18O in the leaves of transpiring plants." Radiation and environmental biophysics **11**(1): 41-52.

Dove, H., R. Mayes and M. Freer (1996). "Effects of species, plant part, and plant age on the n-alkane concentrations in the cuticular wax of pasture plants." Crop and Pasture Science **47**(8): 1333-1347.

Duursma, R. and J. Marshall (2006). "Vertical canopy gradients in δ13C correspond with leaf nitrogen content in a mixed-species conifer forest." Trees **20**(4): 496-506.

Eglinton, G., Hamilton, R.J. (1967). "Leaf epicuticular waxes." Science **156**: 1322-1334.

Eglinton, T. I., Eglinton, G. (2008). "Molecular proxies for paleoclimatology." Earth and Planetary Science Letter **275**: 1-16.

Ehleringer, J. and T. Dawson (1992). "Water uptake by plants: perspectives from stable isotope composition." Plant, Cell & Environment **15**(9): 1073-1082.

Ehleringer, J. R., J.C. Vogel (1993). Historical aspects of stable isotopes in plant carbon and water relations. Stable isotopes and plant carbon-water relations. A. E. H. a. G. D. F. J.R. Ehleringer, Academic Press Inc**:** 9-18.

Ehleringer, J. R., S. L. Phillips, W. S. Schuster and D. R. Sandquist (1991). "Differential utilization of summer rains by desert plants." Oecologia **88**(3): 430-434.

Elias, V. O., B. R. Simoneit and J. N. Cardoso (1997). "Even n-alkane predominances on the Amazon shelf and a Northeast Pacific hydrothermal system." Naturwissenschaften **84**(9): 415-420.

Eliassen, A. (2012). "Weather statistics for Ardtalnaig, Scotland (United Kingdom)." Retrieved 20th August, 2013, from http://www.yr.no/place/United_Kingdom/Scotland/Ardtalnaig/statistics.html.

Epstein, S., C. J. Yapp and J. H. Hall (1976). "The determination of the D/H ratio of non-exchangeable hydrogen in cellulose extracted from aquatic and land plants." Earth and Planetary Science Letters **30**(2): 241-251.

Estep, M. F. and T. C. Hoering (1980). "Biogeochemistry of the stable hydrogen isotopes." Geochimica et Cosmochimica Acta **44**(8): 1197-1206.

Farquhar, G., M. Barbour and B. Henry (1998). "Interpretation of oxygen isotope composition of leaf material." Stable Isotopes: Integration of Biological, Ecological, and Geochemical Processes: 27-48.

Farquhar, G., K. Hubick, A. Condon and R. Richards (1989). Carbon isotope fractionation and plant water-use efficiency. Stable isotopes in ecological research, Springer**:** 21-40.

Farquhar, G. and J. Lloyd (1993). "Carbon and oxygen isotope effects in the exchange of carbon dioxide between terrestrial plants and the atmosphere." Stable isotopes and plant carbon-water relations **40**: 47-70.

Farquhar, G. and R. Richards (1984). "Isotopic composition of plant carbon correlates with water-use efficiency of wheat genotypes." Functional Plant Biology **11**(6): 539-552.

Farquhar, G. D. (1980). Carbon isotope discrimination by plants: effects of carbon dioxide concentrations and temperature via the ratio of intercellular and atmospheric CO_2 concentration. Carbon Dioxide and Climate: Australian Research. G. I. Pearman, Austrailian Academy of Science**:** 105-110.

Farquhar, G. D. and L. A. Cernusak (2005). "On the isotopic composition of leaf water in the non-steady state." Functional Plant Biology **32**(4): 293-303.

Farquhar, G. D., L. A. Cernusak and B. Barnes (2007). "Heavy Water Fractionation during Transpiration." Plant Physiology **143**(1): 11-18.

Farquhar, G. D., J.R. Ehleringer, K.T. Hubick (1989). "Carbon Isotope Discrimination and Photosynthesis." Plant Physiology **40**: 503-537.

Farquhar, G. D., M.H. O'Leary, J.A. Berry (1982). "On the relationship between carbon isotope discrimination and the intercellular carbon dioxide concentration is leaves." Austrailian Journal of Plant Physiology **9**: 121-137.

Farrington, J. W. and B. W. Tripp (1977). "Hydrocarbons in western North Atlantic surface sediments." Geochimica et Cosmochimica Acta **41**(11): 1627-1641.

Faure, G. and T. M. Mensing (2005). Isotopes: principles and applications, Wiley Hoboken, NJ.

Feakins, S. J., Sessions, A.L. (2010). "Controls on the D/H ratios of plant leaf waxes in an aird ecosystem." Geochimica et Cosmochimica Acta **74**: 2128-2141.

Feakins, S. J., Sessions, A.L. (2010). "Controls on the D/H ratios of plant leaf waxes in an arid ecosystem." Geochimica et Cosmochimica Acta **74**: 2128-2141.

Ficken, K., B. Li, D. Swain and G. Eglinton (2000). "An *n*-alkane proxy for the sedimentary input of submerged/floating freshwater aquatic macrophytes." Organic Geochemistry **31**(7): 745-749.

Flanagan, L. B., J. P. Comstock and J. R. Ehleringer (1991). "Comparison of modeled and observed environmental influences on the stable oxygen and hydrogen isotope composition of leaf water in Phaseolus vulgaris L." Plant Physiology **96**(2): 588-596.

Fogel, M. and L. Cifuentes (1993). Isotope fractionation during primary production. Organic Geochemistry**:** 73-98.

Galy, V., L. François, C. France-Lanord, P. Faure, H. Kudrass, F. Palhol and S. K. Singh (2008). "C4 plants decline in the Himalayan basin since the Last Glacial Maximum." Quaternary Science Reviews **27**(13): 1396-1409.

Gao, L., A. Burnier and Y. Huang (2012). "Quantifying instantaneous regeneration rates of plant leaf waxes using stable hydrogen isotope labeling." Rapid Communications in Mass Spectrometry **26**(2): 115-122.

Gao, L., Y.-J. Tsai and Y. Huang (2012). "Assessing the rate and timing of leaf wax regeneration in Fraxinus americana using stable hydrogen isotope labeling." Rapid Communications in Mass Spectrometry **26**(19): 2241-2250.

Garten Jr, C. T. and G. Taylor Jr (1992). "Foliar δ13C within a temperate deciduous forest: spatial, temporal, and species sources of variation." Oecologia **90**(1): 1-7.

Gat, J. (1998). Stable isotopes, the hydrological cycle and the terrestrial biosphere**:** 397-407.

Gat, J. (2010). Isotope hydrology: A study of the water cycle, World Scientific.

Gat, J. and H. Craig (1965). "Characteristics of the air–sea interface determined from isotope transfer studies." Trans. Am. Geophys. Union **47**: 115.

Gat, J. R. (1996). "Oxygen and hydrogen isotopes in the hydrologic cycle." <u>Annual Review of Earth and Planetary Sciences</u> **24**(1): 225-262.

Gearing, P., J. N. Gearing, T. F. Lytle and J. S. Lytle (1976). "Hydrocarbons in 60 northeast Gulf of Mexico shelf sediments: a preliminary survey." <u>Geochimica et Cosmochimica Acta</u> **40**(9): 1005-1017.

Gonfiantini, R., S. Gratziu and E. Tongiorgi (1965). "Oxygen isotopic composition of water in leaves." <u>Isotopes and radiation in soil-plant nutrition studies</u>: 405-410.

Grace, J., F. Berninger, L. Nagy (2002). "Impacts of climate change on the tree line." <u>Annals of Botany</u> **90**: 537-544.

Handley, L., P. N. Pearson, I. K. McMillan and R. D. Pancost (2008). "Large terrestrial and marine carbon and hydrogen isotope excursions in a new Paleocene/Eocene boundary section from Tanzania." <u>Earth and Planetary Science Letters</u> **275**(1): 17-25.

Hari, P., M. Kulmala, T. Pohja, T. Lahti, E. Siivola, L. Plva, P. Aalto, K. Hameri, T. Vesala, S. Luoma, E. Pulliainen (1994). "Air pollution in Eastern Lapland: challenge for an environmental measurement station." <u>Silva Fennica</u> **28**: 23-39.

Harwood, J. L. and N. J. Russell (1984). <u>Lipids in plants and microbes</u>, George Allen & Unwin.

Helliker, B. R. and H. Griffiths (2007). "Toward a plant–based proxy for the isotope ratio of atmospheric water vapor." <u>Global Change Biology</u> **13**(4): 723-733.

Hietala, T., N. Mozes, M. J. Genet, H. Rosenqvist and S. Laakso (1997). "Surface lipids and their distribution on willow (*Salix*) leaves: a combined chemical, morphological and physicochemical study." <u>Colloids and Surfaces B: Biointerfaces</u> **8**(4): 205-215.

Hilasvuori, E., F. Berninger, E. Sonninen, H. Tuomenvirta and H. Jungner (2009). "Stability of climate signal in carbon and oxygen isotope records and ring width from Scots pine (Pinus sylvestris L.) in Finland." <u>Journal of Quaternary Science</u> **24**(5): 469-480.

Hou, J., D'Andrea, W.J., MacDonald, D., Huang, Y. (2007). "Hydrogen isotopic variability in leaf waxes among terrestrial and aquatic plants around Blond Pond, Massachusetts (USA)." <u>Organic Geochemistry</u> **38**: 977-984.

Hou, J., D'Andrea, W.J., MacDonald, D., Huang, Y. (2007). "Hydrogen isotopic variability in leaf waxes amoung terrestrial and aquatic plants around Blond Pond, Massachusetts (USA)." <u>Organic Geochemistry</u> **38**: 977-984.

Hou, J., D'Andrea, W.J., MacDonald, D., Huang, Y. (2008). "Can sedimentary leaf waxes record D/H ratios of continental precipitation? Field, model and experimental assessments." Geochimica et Cosmochimica Acta **72**: 3503-3517.

Hren, M., Pagani, M., Brandon, M. (2010). "Biomarker reconstruction of the early Eocene paleotopography and palaeoclimate of the norther Sierra Nevada." Geology **38**: 7-11.

Hu, J., D. J. Moore, S. P. Burns and R. K. Monson (2010). "Longer growing seasons lead to less carbon sequestration by a subalpine forest." Global Change Biology **16**(2): 771-783.

Huang, Y., L. Dupont, M. Sarnthein, J. M. Hayes and G. Eglinton (2000). "Mapping of C_4 plant input from North West Africa into North East Atlantic sediments." Geochimica et Cosmochimica Acta **64**(20): 3505-3513.

Huang, Y., B. Shuman, Y. Wang and T. Webb (2004). "Hydrogen isotope ratios of individual lipids in lake sediments as novel tracers of climatic and environmental change: a surface sediment test." Journal of Paleolimnology **31**(3): 363-375.

Ingraham, N. L. (1998). Isotopic variations in precipitation. Isotope tracers in catchment hydrology**:** 87-118.

Ingraham, N. L. and B. E. Taylor (1991). "Light stable isotope systematics of large–scale hydrologic regimes in California and Nevada." Water Resources Research **27**(1): 77-90.

Institute, F. M. (2009). "The seasons."   Retrieved 28 March 2009, 2009, from http://www.fmi.fi/weather/climate_4.html.

J.I. Hedges, F. G. P. (1993). Early diagenesis: consequences for applications of molecular biomarkers. Organic Geochemistry. S. A. M. M.H. Engel. New York, Plenum Press**:** 237–253.

Jahren, A. H., M. C. Byrne, H. V. Graham, L. S. Sternberg and R. E. Summons (2009). "The environmental water of the middle Eocene Arctic: Evidence from δD, $\delta^{18}O$ and $\delta^{13}C$ within specific compounds." Palaeogeography, Palaeoclimatology, Palaeoecology **271**(1): 96-103.

Jansen, B., N. S. Haussmann, F. H. Tonneijck, J. M. Verstraten and P. de Voogt (2008). "Characteristic straight-chain lipid ratios as a quick method to assess past forest–páramo transitions in the Ecuadorian Andes." Palaeogeography, Palaeoclimatology, Palaeoecology **262**(3): 129-139.

Jeng, W.-L. (2006). "Higher plant *n*-alkane average chain length as an indicator of petrogenic hydrocarbon contamination in marine sediments." Marine Chemistry **102**(3): 242-251.

Jeng, W. L. (2006). "Higher plant n-alkane average chain length as an indicator of petrogenic hydrocarbon contamination in marine sediments." Marine Chemistry **102**: 242-251.

Jia, G., K. Wei, F. Chen and P. a. Peng (2008). "Soil *n*-alkane δD vs. altitude gradients along Mount Gongga, China." Geochimica et Cosmochimica Acta **72**(21): 5165-5174.

Kahmen, A., Dawson, T.E., Vieth, A., Sachse, D. (2011). "Leaf wax n-alkane δD values are determined early in the ontongeny of *Populus trichocarpa* Leaves when grown under controlled environmental conditions." Plant, Cell and Environment **34**(10): 1639-1651.

Kahmen, A., B. Hoffmann, E. Schefuß, S. K. Arndt, L. A. Cernusak, J. B. West and D. Sachse (2013). "Leaf water deuterium enrichment shapes leaf wax n-alkane δD values of angiosperm plants II: Observational evidence and global implications." Geochimica et Cosmochimica Acta **111**(0): 50-63.

Kahmen, A., Hoffmann, B., SchefuB, E., Arndt, S.K., Cernusak, L.A., West, J.B., Sachse, D. (2012). "Leaf water deuterium enrichment shapes leaf wax n-alkane δD values of angiosperm plants II: Observational evidence and global implications." Geochimica et Cosmochimica Acta **111**: 50-63.

Kahmen, A., SchefuB, E., Sachse, D. (2012). "Leaf water deuterium enrichment shapes leaf wax n-alkane δD values of angiosperm plants I: Experimental evidence and mechanistic insights." Geochimica et Cosmochimica Acta **111**: 39-40.

Kahmen, A., E. Schefuß and D. Sachse (2013). "Leaf water deuterium enrichment shapes leaf wax n-alkane δD values of angiosperm plants I: Experimental evidence and mechanistic insights." Geochimica et Cosmochimica Acta **111**(0): 39-49.

Kahmen, A., K. Simonin, K. P. Tu, A. Merchant, A. Callister, R. Siegwolf, T. E. Dawson and S. K. Arndt (2008). "Effects of environmental parameters, leaf physiological properties and leaf water relations on leaf water δ18O enrichment in different Eucalyptus species." Plant, Cell & Environment **31**(6): 738-751.

Kendall, C. and J. J. MacDonnell (1998). Isotope tracers in catchment hydrology, Access Online via Elsevier.

Kim, K. and X. Lee (2011). "Transition of stable isotope ratios of leaf water under simulated dew formation." Plant, Cell & Environment **34**(10): 1790-1801.

Kolattukudy, P. (1980). Cutin, suberin, and waxes. The biochemistry of plants (eds. Stumpf, PK & Conn. EE) **4:** 571-645.

Kulmala, M., U. Rannik, L. Pirjola, M.D. Maso, J. Karimak, A. Asmi, A. Jappinen, V. Karhu, H. Korhonen, S. Malvikko, A. Puustinen, J. Raittila, S. Romakkaniemi, T. Suni, S. Yli-Koivisto, J. Paatero, P. Hari, T. Vesala (2000). "Characterization of atmospheric trace gas and aerosol concentrations at forest sites in southern and northern Finland using back trajectories." Boreal Environment Research **5**: 315-336.

Kunst, L. and A. Samuels (2003). "Biosynthesis and secretion of plant cuticular wax." Progress in Lipid Research **42**(1): 51-80.

Kwart, H. (1982). "Temperature dependence of the primary kinetic hydrogen isotope effect as a mechanistic criterion." Accounts of Chemical Research **15**(12): 401-408.

Le Roux, X., T. Bariac, H. Sinoquet, B. Genty, C. Piel, A. Mariotti, C. Girardin and P. Richard (2001). "Spatial distribution of leaf water–use efficiency and carbon isotope discrimination within an isolated tree crown." Plant, Cell & Environment **24**(10): 1021-1032.

Leaney, F., C. Osmond, G. Allison and H. Ziegler (1985). "Hydrogen-isotope composition of leaf water in C3 and C4 plants: its relationship to the hydrogen-isotope composition of dry matter." Planta **164**(2): 215-220.

Lichtfouse, E., S. Derenne, A. Mariotti and C. Largeau (1994). "Possible algal origin of long chain odd *n*-alkanes in immature sediments as revealed by distributions and carbon isotope ratios." Organic Geochemistry **22**(6): 1023-1027.

Liu, W. and H. Yang (2008). "Multiple controls for the variability of hydrogen isotopic compositions in higher plant n–alkanes from modern ecosystems." Global Change Biology **14**(9): 2166-2177.

Liu, W., H. Yang and L. Li (2006). "Hydrogen isotopic compositions of n-alkanes from terrestrial plants correlate with their ecological life forms." Oecologia **150**(2): 330-338.

Liu, W., Yang, H. (2008). "Multiple controls for the variability of hydrogen isotopic compositions in higher plant n-alkanes from modern ecosystems." Global Change Biology **14**: 2166-2177.

Lockheart, M. J., P. F. Van Bergen and R. P. Evershed (1997). "Variations in the stable carbon isotope compositions of individual lipids from the leaves of modern angiosperms: implications for the study of higher land plant-derived sedimentary organic matter." Organic Geochemistry **26**(1): 137-153.

Luo, Y.-H., L. Steinberg, S. Suda, S. Kumazawa and A. Mitsui (1991). "Extremely low D/H ratios of photoproduced hydrogen by cyanobacteria." Plant and cell physiology **32**(6): 897-900.

Luz, B. and E. Barkan (2010). "Variations of 17 O/16 O and 18 O/16 O in meteoric waters." Geochim. Cosmochim. Acta **74**(22): 6276-6286.

Majoube, M. (1971). "Oxygen-18 and deuterium fractionation between water and steam." J. Chim. Phys. Phys. Chim. Biol **68**(10): 1423-1436.

Marshall, J. D., J. R. Brooks and K. Lajtha (2007). "Sources of variation in the stable isotopic composition of plants." Stable isotopes in ecology and environmental science: 22-60.

Marshall, J. D., J. Zhang (1993). Altitudinal variation in carbon isotope discrimination by conifers. Stable isotopes and plant carbon-water relations. A. E. H. a. G. D. F. J.R. Ehleringer, Academic Press Inc**:** 187-199.

Martin, G. J. and M. L. Martin (2003). "Climatic significance of isotope ratios." Phytochemistry Reviews **2**(1-2): 179-190.

Marzi, R., B. E. Torkelson and R. K. Olson (1993). "A revised carbon preference index." Organic Geochemistry **20**(8): 1303-1306.

McDowell, N. G., J. Licata and B. J. Bond (2005). "Environmental sensitivity of gas exchange in different-sized trees." Oecologia **145**(1): 9-20.

McGuire, K., McDonnell (2007). Stable Isotopes in Ecology and Environmental Science. Stable Isotopes as Indicators of Ecological Change. J. Marshall, Lajtha, K. Oxford, Black Well.

McGuire, K., J. McDonnell, R. Michener and K. Lajtha (2007). Stable isotope tracers in watershed hydrology, Blackwell Publishing: Oxford.

McInerney, F. A., Helliker, B.R., Freeman, K.H. (2011). "Hydrogen isotope ratios of leaf wax n-alkanes in grasses are insensitive to transpiration." Geochimica et Cosmochimica Acta **75**: 541-554.

McLeod, C., Yeo, M. Brown, AE, Burn, AJ, Hopkins, JJ and Way SF. (2013, 25th July 2013). "Black Wood of Rannoch." The Habitats Directive:selection of Special Areas of Conservation in the UK Retrieved 20th August, 2013, from jncc.defra.gov.uk/protectedsites/sacselection/sac.asp?EUCode=UK0012758.

Mencuccini, M. and J. Grace (1996). "Hydraulic conductance, light interception and needle nutrient concentration in Scots pine stands and their relations with net primary productivity." Tree Physiology **16**(5): 459-468.

Merlivat, L. and J. Jouzel (1979). "Global climatic interpretation of the deuterium–oxygen 18 relationship for precipitation." Journal of Geophysical Research: Oceans (1978–2012) **84**(C8): 5029-5033.

Meyers, P. and R. Ishiwatari (1995). Organic matter accumulation records in lake sediments. Physics and chemistry of lakes, Springer**:** 279-328.

Michener, R. and K. Lajtha (2008). Stable isotopes in ecology and environmental science, Wiley-Blackwell.

Niinemets, Ü., O. Kull and J. D. Tenhunen (1999). "Variability in leaf morphology and chemical composition as a function of canopy light environment in coexisting deciduous trees." International Journal of Plant Sciences **160**(5): 837-848.

Niinemets, Ü., E. Sonninen and M. Tobias (2004). "Canopy gradients in leaf intercellular CO_2 mole fractions revisited: interactions between leaf irradiance and water stress need consideration." Plant, Cell & Environment **27**(5): 569-583.

Nikolic, B., V. Tesevic, I. Djordjevic, M. Jadranin, S. Bojovic and P. Marin (2009). "n-Alkanes in needle waxes of Picea omorika var. vukomanii." Chemistry of Natural Compounds **45**(5): 697-699.

Nishimura, M. and E. W. Baker (1986). "Possible origin of n-alkanes with a remarkable even-to-odd predominance in recent marine sediments." Geochimica et Cosmochimica Acta **50**(2): 299-305.

Nødskov Giese, B. (1975). "Effects of light and temperature on the composition of epicuticular wax of barley leaves." Phytochemistry **14**(4): 921-929.

O'Leary, M., J. Ehleringer, A. Hall and G. Farquhar (1993). Biochemical basis of carbon isotope fractionation. Stable isotopes and plant carbon-water relations., Academic Press Inc.

O'Leary, M. H. (1981). "Carbon Isotope Fractionation in Plants." Phytochemistry **20**(4): 553-567.

O'Leary, M. H. (1988). "Carbon isotopes in photosynthesis." Bioscience **38**(5): 328-336.

Ohlrogge, J. B. and J. G. Jaworski (1997). "Regulation of fatty acid synthesis." Annual review of plant biology **48**(1): 109-136.

Ometto, J. P., L. B. Flanagan, L. A. Martinelli, M. Z. Moreira, N. Higuchi and J. R. Ehleringer (2002). "Carbon isotope discrimination in forest and pasture ecosystems of the Amazon Basin, Brazil." Global Biogeochemical Cycles **16**(4): 1109.

Oros, D. R., L. J. Standley, X. Chen and B. SIMONEIT (1999). "Epicuticular wax compositions of predominant conifers of Western North America." Zeitschrift Fur Natureforschung C **54**(12): 17-24.

Pancost, R. D., M. Baas, B. van Geel and J. S. Sinninghe Damsté (2002). "Biomarkers as proxies for plant inputs to peats: an example from a sub-boreal ombrotrophic bog." Organic Geochemistry **33**(7): 675-690.

Patov, A. I. (1985). "Seasonal Dynamics of Aboveground Organ Growth in Pine and Spruce." Comprehensive Biogeocenological Studies on Coniferous Forests in Northeastern Europe **73**: 15-25.

Paul, D., Skrzypek, G., Forizs, I. (2007). "Normalization of measured stable isotopic compositions to isotope reference scales- a review." Rapid Communications in Mass Spectrometry **21**: 3006-3014.

Pedentchouk, N., Sumner, W., Tipple, B., Pagani, M. (2008). "δ^{13} and δD compositions of n-alkanes from modern angiosperms and conifers: An experimental set up in central Washington State, USA." Organic Geochemistry **39**: 1066-1071.

Percy, K. E., J. Cape, R. Jagels and C. Simpson (1994). Air pollutants and the leaf cuticle, Springer-Verlag.

Piasentier, E., Bovolenta, S., Malossini, F. (2000). "The n-alkane concentrations in buds and leaves of browsed broadleaf trees." Journal of Agricultural Science **135**: 311-320.

Polissar, P. J. and K. H. Freeman (2010). "Effects of aridity and vegetation on plant-wax δD in modern lake sediments." Geochimica et Cosmochimica Acta **74**(20): 5785-5797.

Polissar, P. J., K. H. Freeman, D. B. Rowley, F. A. McInerney and B. S. Currie (2009). "Paleoaltimetry of the Tibetan Plateau from D/H ratios of lipid biomarkers." Earth and Planetary Science Letters **287**(1): 64-76.

Post-Beittenmiller, D. (1996). "Biochemistry and molecular biology of wax production in plants." Annual review of plant biology **47**(1): 405-430.

Powers, M. D., K. S. Pregitzer and B. J. Palik (2008). "δ^{13}C and δ^{18}O Trends Across Overstory Environments in Whole Foliage and Cellulose of Three *Pinus* Species." Journal of the American Society for Mass Spectrometry **19**(9): 1330-1335.

Poynter, J., Eglinton, G. (1991). "The biomarker concept- strengths and weaknesses." Fresenius' Journal of Analytical Chemistry **339**: 725-731.

Poynter, J., P. Farrimond, N. Robinson and G. Eglinton (1989). Aeolian-derived higher plant lipids in the marine sedimentary record: Links with palaeoclimate. Paleoclimatology and Paleometeorology: Modern and Past Patterns of Global Atmospheric Transport, Springer**:** 435-462.

Prügel, B. and G. Lognay (1996). "Composition of the Cuticular Waxes of Picea abies and P. sitchensis." Phytochemical Analysis **7**(1): 29-36.

Prügel, B., P. Loosveldt and J.-P. Garrec (1994). "Changes in the content and constituents of the cuticular wax of Picea abies (L.) Karst. in relation to needle ageing and tree decline in five European forest areas." Trees **9**(2): 80-87.

Rao, Z., Zhu, Z., Jia, G., Henderson, A., Xue, Q., Wang, S. (2009). "Compound specific δD values of long chain n-alkanes derived from terrestrial higher plants are indicative of the δD of meteoric waters: Evidence from surface soils in eastern China." Organic Geochemistry **40**: 992-930.

Reye-GarcÍa, C., M. Mejia-Chang, G. D. Jones and H. Griffiths (2008). "Water vapour isotopic exchange by epiphytic bromeliads in tropical dry forests reflects niche differentiation and climatic signals." Plant, Cell & Environment **31**(6): 828-841.

Reynolds, J. F. and D. H. Knight (1973). "The magnitude of snowmelt and rainfall interception by litter in lodgepole pine and spruce-fir forests in Wyoming."

Rhodes, A. (2012). "Trail 3: UEA Broad." University of East Anglia Wildlife Trail Retrieved 20th August, 2013, from http://www.uea.ac.uk/documents/3067737/3071262/ueawildlifetrail.pdf/2c52c873-af2a-471b-94c3-f504dad9e180.

Riederer, M. (1989). The cuticles of conifers: structure, composition and transport properties. Forest decline and air pollution, Springer: 157-192.

Riederer, M. and G. Schneider (1990). "The effect of the environment on the permeability and composition of Citrus leaf cuticles." Planta **180**(2): 154-165.

Rielley, G., R. Collier, D. Jones and G. Eglinton (1991). "The biogeochemistry of Ellesmere Lake, UK—I: source correlation of leaf wax inputs to the sedimentary lipid record." Organic Geochemistry **17**(6): 901-912.

Riley, W., C. Still, M. Torn and J. Berry (2002). "A mechanistic model of H218O and C18OO fluxes between ecosystems and the atmosphere: Model description and sensitivity analyses." Global Biogeochemical Cycles **16**(4): 1095.

Rommerskirchen, F., G. Eglinton, L. Dupont, U. Güntner, C. Wenzel and J. Rullkötter (2003). "A north to south transect of Holocene southeast Atlantic continental margin sediments: Relationship between aerosol transport and compound−specific δ13C land plant biomarker and pollen records." Geochemistry, Geophysics, Geosystems **4**(12).

Rozanski, K., L. Araguás-Araguás and R. Gonfiantini (1993). "Isotopic patterns in modern global precipitation." Geophysical Monograph Series **78**: 1-36.

Russell, J. M., S. McCoy, D. Verschuren, I. Bessems and Y. Huang (2009). "Human impacts, climate change, and aquatic ecosystem response during the past 2000 yr at Lake Wandakara, Uganda." Quaternary Research **72**(3): 315-324.

Ruuskanen, T. M., A. Reissell, P. Keronen, P.P. Aaltp, L. Laakso, T. Gronholm, P. Hari, M. Kulmala (2003). "Atmospheric trace gas and aersosol particle concentration measurements in Eastern Lapland, Finalnd 1992-2001." Boreal Environment Research **8**: 335-349.

Sachse, D., Billault, I., Bowen, G.J., Chikaraishi, Y., Dawson, T.E., Feakins, A.J., Freeman, K.H., Magill, C.R., McInerney, F.A., van ser Meer, M.T.J., Polissar, P., Robins, R.J., Sachs, J.P., Schmidt, H.L., Sessions, A.L., White, W.C., West, J.B., Kahmen, A. (2012). "Molecular Paleohydrology: Interpreting the Hydrogen-Isotopic Composition of Lipid Biomarkers from Photosynthesizing Organisms." The Annual Review of Earth and Planetary Sciences **40**: 221-249.

Sachse, D., Gleixner, G., Wilkes, H., Kahmen, A. (2010). "Leaf wax n-alkane δD values of field-grown barley reflect leaf water δD values at the time of leaf formation." Geochimica et Cosmochimica Acta **74**(23): 6741-6750.

Sachse, D., Kahmen, A., Gleixner, G. (2009). "Significant seasonal variation in the hydrogen isotopic composition of leaf-wax lipids of two deciduous tree ecosystems (*Fagus sylvatica* and *Acer pseudoplatanus*)." Organic Geochemistry **40**: 732-742.

Sachse, D., J. Radke and G. Gleixner (2004). "Hydrogen isotope ratios of recent lacustrine sedimentary n-alkanes record modern climate variability." Geochimica et Cosmochimica Acta **68**(23): 4877-4889.

Sachse, D., Radke, J., Gleixner, G. (2006). "δD values of invidual n-alkanes from terrestrial plants along a climatic gradient- Implications for the sedimentary biomarker record." Organic Geochemistry **37**: 469-483.

Samuels, L., L. Kunst and R. Jetter (2008). "Sealing plant surfaces: cuticular wax formation by epidermal cells." Plant Biology **59**(1): 683.

Sauer, P. E., T. I. Eglinton, J. M. Hayes, A. Schimmelmann and A. L. Sessions (2001). "Compound-specific D/H ratios of lipid biomarkers from sediments as a proxy for environmental and climatic conditions." Geochimica et Cosmochimica Acta **65**(2): 213-222.

Saurer, M., Aellen, K., Siegwolf, R. (1997). "Correlating δ^{13} and $\delta^{18}O$ in cellulose of trees." Plant, Cell and Environment **20**: 1543-1550.

Scartazza, A. L., M. Guido, M. Brugnoli, C E. (1998). "Carbon isotope discrimination in leaf and stem sugars, water-use efficiency and mesophyll conductance during different developmental stages in raice subjected to drought." Austrailian Journal of Plant Physiology **25**: 489-498.

Schefuß, E., V. Ratmeyer, J.-B. W. Stuut, J. Jansen and J. S. Sinninghe Damsté (2003). "Carbon isotope analyses of *n*-alkanes in dust from the lower atmosphere over the central eastern Atlantic." Geochimica et Cosmochimica Acta **67**(10): 1757-1767.

Schefuß, E., S. Schouten and R. R. Schneider (2005). "Climatic controls on central African hydrology during the past 20,000[thinsp]years." Nature **437**(7061): 1003-1006.

Scheidegger, M., Saurer, M., Bahn, M.,Siegwolf, R. (2000). "Linking stable oxygen and carbon isotopes with stomatal conductance and photosynthetic capacity: a conceptual model." Oecologia(125): 350-357.

Schimmelmann, A., M. D. Lewan and R. P. Wintsch (1999). "D/H isotope ratios of kerogen, bitumen, oil, and water in hydrous pyrolysis of source rocks containing kerogen types I, II, IIS, and III." Geochimica et Cosmochimica Acta **63**(22): 3751-3766.

Schimmelmann, A., Sessions, A.L., Mastalerz, M. (2006). "Hydrogen isotopic (D/H) composition of organic matter during diagenesis and thermal maturation." Annual Review of Earth and Planetary Sciences **34**: 501-533.

Schleucher, J. (1998). "Intramolecular deuterium distributions and plant growth conditions." Stable Isotopes, integration of biological, ecological and geochemical processes. BIOS Scientific Publishers Ltd., Oxford: 63-73.

Schmidt, H.-L. (2003). "Fundamentals and systematics of the non-statistical distributions of isotopes in natural compounds." Naturwissenschaften **90**(12): 537-552.

Schwark, L., K. Zink and J. Lechterbeck (2002). "Reconstruction of postglacial to early Holocene vegetation history in terrestrial Central Europe via cuticular lipid biomarkers and pollen records from lake sediments." Geology **30**(5): 463-466.

Seki, O., P. A. Meyers, K. Kawamura, Y. Zheng and W. Zhou (2009). "Hydrogen isotopic ratios of plant wax *n*-alkanes in a peat bog deposited in northeast China during the last 16kyr." Organic Geochemistry **40**(6): 671-677.

Seki, O., T. Nakatsuka, H. Shibata and K. Kawamura (2010). "A compound-specific *n*-alkane δ^{13} C and δD approach for assessing source and delivery processes of terrestrial organic matter within a forested watershed in northern Japan." Geochimica et Cosmochimica Acta **74**(2): 599-613.

Sen'kina, S. (2002). "Ecophysiological parameters of transpiration in coniferous woody plants in phytocenoses of the north." Russian Journal of Ecology **33**(4): 235-241.

Sessions, A. L. (2006). "Seasonal changes in D/H fractionation accompanying lipid biosynthesis in *Spartina alterniflora*." Geochimica et Cosmochimica Acta **70**(9): 2153-2162.

Sessions, A. L., Burgoyne, T.W., Schimmelmann, A., Hayes, J.M. (1999). "Fractionations of hydrogen isotopes in lipid biosynthesis." Organic Geochemistry **30**: 1193-1200.

Sharkey, T. D., G.D. Farquhar (1982). "Stomatal conductance and photosynthesis." Plant Physiology **33**: 317-345.

Sharp, Z. (2007). Principles of stable isotope geochemistry. Upper Saddle River, NJ, Pearson education.

Shepherd, T. and D. Griffiths (2006). "The effects of stress on plant cuticular waxes." New Phytologist **171**(3): 469-499.

Shepherd, T., G. W. Robertson, D. W. Griffiths, A. N. Birch and G. Duncan (1995). "Effects of environment on the composition of epicuticular wax from kale and swede." Phytochemistry **40**(2): 407-417.

Shepherd, T., G. W. Robertson, D. W. Griffiths and A. N. E. Birch (1997). "Effects of environment on the composition of epicuticular wax esters from kale and swede." Phytochemistry **46**(1): 83-96.

Shu, Y., X. Feng, E. S. Posmentier, A. M. Faiia, M. P. Ayres, L. E. Conkey and L. J. Sonder (2008). "Isotopic studies of leaf water. Part 2: between-age isotopic variations in pine needles." Geochimica et Cosmochimica Acta **72**(21): 5189-5200.

Shu, Y., X. Feng, E. S. Posmentier, L. J. Sonder, A. M. Faiia and D. Yakir (2008). "Isotopic studies of leaf water. Part 1: a physically based two-dimensional model for pine needles." Geochimica et Cosmochimica Acta **72**(21): 5175-5188.

Siebrand, W. and Z. Smedarchina (2004). "Temperature dependence of kinetic isotope effects for enzymatic carbon-hydrogen bond cleavage." The Journal of Physical Chemistry B **108**(13): 4185-4195.

Smith, F. A. and K. H. Freeman (2006). "Influence of physiology and climate on δD of leaf wax n-alkanes from C3 and C4 grasses." Geochimica et Cosmochimica Acta **70**(5): 1172-1187.

Smith, F. A., Freeman, K.H. (2006). "Influence of physiology and climate on the δD of leaf wax n-alkanes from C_3 and C_4 grasses." Geochimica et Cosmochimica Acta **70**: 1172-1187.

Ste-Marie, C., D. Pare (1999). "Soil, pH and N availability effects on net nitrification in the forest floors of a range of boreal forest stands." Soil Biology and Biochemistry **31**: 1579-1589.

Sternberg, L. d. S. L. (1988). "D/H ratios of environmental water recorded by D/H ratios of plant lipids." Nature **333**(6168): 59-61.

Tang, K. and X. Feng (2001). "The effect of soil hydrology on the oxygen and hydrogen isotopic compositions of plants' source water." Earth and Planetary Science Letters **185**(3–4): 355-367.

Tarasov, P. E., S. Müller, M. Zech, D. Andreeva, B. Diekmann and C. Leipe (2013). "Last glacial vegetation reconstructions in the extreme-continental eastern Asia: Potentials of pollen and *n*-alkane biomarker analyses." Quaternary International **290**: 253-263.

Tierney, J. E., J. M. Russell, Y. Huang, J. S. S. Damsté, E. C. Hopmans and A. S. Cohen (2008). "Northern hemisphere controls on tropical southeast African climate during the past 60,000 years." Science **322**(5899): 252-255.

Tipple, B. J., Berke, M.A., Donman, C.E., Khachaturyan, S., Ehleringer, J.R. (2013). "Leaf-wax n-alkanes record the plant-water environment at leaf flush." PNAS **110**(7): 2659-2664.

Tipple, B. J., Pagani, M. (2012). "Environmental control on eastern broadleaf forest species' leaf wax distributions and D/H ratios." Geochimica et Cosmochimica Acta **111**: 64-77.

Van Gardingen, P. R. and J. Grace (1991). Plants and wind, Academic Press.

Vogel, J. C. (1993). Variability of carbon isotope fractionation during photosynthesis. Stable isotopes and plant carbon-water relations. A. E. H. a. G. D. F. J.R. Ehleringer, Academic Press Inc**: 29-46.

Vogts, A., H. Moossen, F. Rommerskirchen and J. Rullkötter (2009). "Distribution patterns and stable carbon isotopic composition of alkanes and alkan-1-ols from plant waxes of African rain forest and savanna C_3 species." Organic Geochemistry **40**(10): 1037-1054.

Vogts, A., E. Schefuß, T. Badewien and J. Rullkötter (2012). "n-Alkane parameters from a deep sea sediment transect off southwest Africa reflect continental vegetation and climate conditions." Organic Geochemistry **47**(0): 109-119.

von Wettstein-Knowles, P. (1995). "Biosynthesis and genetics of waxes." Waxes: Chemistry, Molecular Biology and Functions. Oily Press, Dundee, Scotland: 91-130.

von Wettstein-Knowles, P. (2012). "Plant Waxes."

Walton, T. J. (1990). Waxes, cutin and suberin. Methods in plant biochemistry. **4:** 5-158.

Wang, J. H., C. V. Robinson and I. Edelman (1953). "Self-diffusion and Structure of Liquid Water. III. Measurement of the Self-diffusion of Liquid Water with H2, H3 and O18 as Tracers1." Journal of the American Chemical Society **75**(2): 466-470.

Wang, X. F. and D. Yakir (1995). "Temporal and spatial variations in the oxygen−18 content of leaf water in different plant species." Plant, Cell & Environment **18**(12): 1377-1385.

Wang, Y., X. Fang, T. Zhang, Y. Li, Y. Wu, D. He and Y. Wang (2010). "Predominance of even carbon-numbered *n*-alkanes from lacustrine sediments in Linxia Basin, NE Tibetan Plateau: Implications for climate change." Applied Geochemistry **25**(10): 1478-1486.

Weete, J. D. (1976). "Algal and fungal waxes." Chemistry and Biochemistry of Natural Waxes, Elsevier, Amsterdam: 349-418.

Welp, L. R., X. Lee, K. Kim, T. J. Griffis, K. A. Billmark and J. M. Baker (2008). "δ18O of water vapour, evapotranspiration and the sites of leaf water evaporation in a soybean canopy." Plant, Cell & Environment **31**(9): 1214-1228.

Wershaw, R., I. Friedman, S. Heller and P. Frank (1966). Hydrogen isotopic fractionation of water passing through trees.

West, A. G., S. J. Patrickson and J. R. Ehleringer (2006). "Water extraction times for plant and soil materials used in stable isotope analysis." Rapid Communications in Mass Spectrometry **20**(8): 1317-1321.

White, J. W. C., J. R. Lawrence and W. S. Broecker (1994). "Modeling and interpreting DH ratios in tree rings: A test case of white pine in the northeastern United States." Geochimica et Cosmochimica Acta **58**(2): 851-862.

Woodruff, D., F. Meinzer and B. Lachenbruch (2008). "Height–related trends in leaf xylem anatomy and shoot hydraulic characteristics in a tall conifer: safety versus efficiency in water transport." New Phytologist **180**(1): 90-99.

Woodruff, D., F. Meinzer, B. Lachenbruch and D. Johnson (2009). "Coordination of leaf structure and gas exchange along a height gradient in a tall conifer." Tree Physiology **29**(2): 261-272.

Yakir, D., J. Berry, L. Giles and C. B. Osmond (1994). "Isotopic heterogeneity of water in transpiring leaves: identification of the component that controls the δ18O of atmospheric O2 and CO2." Plant, Cell & Environment **17**(1): 73-80.

Yakir, D., M. DeNiro and J. Gat (1990). "Natural deuterium and oxygen–18 enrichment in leaf water of cotton plants grown under wet and dry conditions: evidence for water compartmentation and its dynamics." Plant, Cell & Environment **13**(1): 49-56.

Yakir, D. and Y. Israeli (1995). "Reduced solar irradiance effects on net primary productivity (NPP) and the 13 C and 18 O values in plantations of Musa sp., Musaceae." Geochimica et Cosmochimica Acta **59**: 2149-2151.

Yakir, D. and X.-F. Wang (1996). "Fluxes of CO2 and water between terrestrial vegetation and the atmosphere estimated from isotope measurements."

Yang, H. and Y. Huang (2003). "Preservation of lipid hydrogen isotope ratios in Miocene lacustrine sediments and plant fossils at Clarkia, northern Idaho, USA." Organic Geochemistry **34**(3): 413-423.

Yang, H., Pagani, M., Briggs, D.E.G., Equiza, M.A., Jagels, R., Leng, Q., LePage, B.A. (2009). "Carbon and hydrogen isotope fractionation under continuous light: implications for paleoenvironmental interpretations of the High Arctic during Paleogene warming." Oecologia **160**: 461-470.

Yurtsever, Y. G., JR (1981). Atmospheric Waters. In: Stable Isotopes Hydrology D and 0-18 in the Water Cycle. IAEA. J. G. Gat, R. Vienna, Tech. Rep. Ser. . **No. 210:** 103-142.

Zech, M., Zech, R., Morras, H., Moreti, L., Glaser, B., Zech, w. (2009). "Late Quaternary environmental changes in Misiones, subtropical NE Argentina, deduced from multi-proxy geochemical analyses in a palaeosol-sediment sequence." Quaternary International **196**: 121-136.

Zhang, X., A. L. Gillespie and A. L. Sessions (2009). "Large D/H variations in bacterial lipids reflect central metabolic pathways." Proceedings of the National Academy of Sciences **106**(31): 12580-12586.

Zhang, Z. and J. P. Sachs (2007). "Hydrogen isotope fractionation in freshwater algae: I. Variations among lipids and species." Organic Geochemistry **38**(4): 582-608.

Zhou, Y., K. Grice, Y. Chikaraishi, H. Stuart-Williams, G. D. Farquhar and N. Ohkouchi (2011). "Temperature effect on leaf water deuterium enrichment and isotopic fractionation during leaf lipid biosynthesis: Results from controlled growth of C3 and C4 land plants." Phytochemistry **72**(2–3): 207-213.

Zimmermann, U., D. Ehhalt and K. Münnich (1968). Soil-water movement and evapotranspiration: Change in the isotopic composition of the water, Univ., Heidelberg.